

**INVESTIGATION INTO THE MIGRATION  
OF *LEISHMANIA* WITHIN PHLEBOTOMINE  
SAND FLIES**



**Yasmine Precious Kumordzi**

**Lancaster University  
Division of Biology and Life Sciences  
Faculty of Health and Medicine**

**A thesis submitted in partial fulfilment of the requirements  
for the degree of  
MSc (by Research) in Biomedical Sciences**

**January 2019**

## **DECLARATION**

I declare that the submitted work presented in this thesis is my own work and has not previously been submitted for a degree at this university or any other institution.

## **ACKNOWLEDGMENT**

First and foremost, I would like to thank Dr Rod Dillon and Dr Alexandre Benedetto, my Masters of Research supervisors for giving me this opportunity to work with their group and for their guidance and support during this work. I would like to thank Dr Rod Dillon, for his patience and useful discussions throughout this project. I would also like to thank Dr Alexandre Benedetto for teaching me about microfluidics. I am grateful to all the members of Dr Rod Dillon's group especially Dr Raquel Vionette and Ms Monica Staniek, for teaching me everything I know about sandfly rearing and dissection.

## TABLE OF CONTENTS

<b>DECLARATION.....</b>	<b>1</b>
<b>ACKNOWLEDGMENT.....</b>	<b>2</b>
<b>TABLE OF CONTENTS.....</b>	<b>3</b>
<b>List of Figures .....</b>	<b>6</b>
<b>List of Tables.....</b>	<b>8</b>
<b>List of Images .....</b>	<b>8</b>
<b>List of Abbreviations.....</b>	<b>9</b>
<b>Abstract.....</b>	<b>11</b>
<b>CHAPTER ONE: GENERAL INTRODUCTION .....</b>	<b>13</b>
<b>1.1 Leishmaniasis .....</b>	<b>13</b>
1.1.1 Epidemiology.....	13
1.1.2 Clinical Presentation.....	14
1.1.3 Causative Agent and Vector .....	18
1.1.4 Interventions .....	18
<b>1.2 Sandfly – The vector .....</b>	<b>21</b>
1.2.1 Life cycle.....	22
1.2.2 Structure.....	23
1.2.3 Feeding .....	26
1.2.4 Microbiota.....	30
<b>1.3 Leishmania protozoa - The parasite .....</b>	<b>35</b>
1.3.1 Flagellum .....	36
1.3.2 Kinetoplast .....	38
1.3.3 Plasma membrane.....	43
<b>CHAPTER TWO: LITERATURE REVIEW.....</b>	<b>49</b>
<b>2.1 Leishmania Sand fly Interactions .....</b>	<b>49</b>
2.1.1 Metacyclogenesis of suprapylaria <i>Leishmania</i> .....	49
2.1.2 Developmental cycles in the sand fly .....	53
2.1.3 <i>Leishmania</i> manipulation of the Phlebotomine host interaction.....	55
2.1.4 Important features of <i>Leishmania</i> for transmission.....	56
2.1.5 Transmission.....	58
<b>2.2 Chemotaxis .....</b>	<b>59</b>
2.2.1 <i>Leishmania</i> chemotaxic assay methods .....	62
2.2.2 Microfluidics for studying <i>Leishmania</i> migration .....	68
<b>2.3 Aims of the project.....</b>	<b>70</b>
<b>CHAPTER THREE: MATERIALS AND METHODS .....</b>	<b>72</b>
<b>3.1 General Methods.....</b>	<b>72</b>
3.1.1 Insect rearing.....	72
3.1.2 Parasites .....	73
3.1.3 Preparation of culture medium.....	73
3.1.4 Growth of parasites.....	74

<b>3.2</b>	<b>Part A: <i>Leishmania</i> morphological studies of <i>Leishmania tarentolae</i> and <i>Leishmania mexicana</i> in axenic culture .....</b>	<b>74</b>
3.2.1	Slide preparation .....	74
3.2.2	Morphological configuration and classification of promastigotes .....	75
<b>3.3</b>	<b>Part B: Capillary assays of <i>Leishmania</i> challenged with an array of chemical compounds.....</b>	<b>75</b>
3.3.1	Preparation of Washing and Incubation Solution (WIS) buffer and promastigote suspension .....	75
3.3.2	Preparation of capillary tube solution.....	76
3.3.3	Collecting results .....	77
3.3.4	Experimental conditions.....	78
<b>3.4</b>	<b>Part C: Development of a microfluidic method to analysing <i>Leishmania</i> chemotaxis .....</b>	<b>79</b>
3.4.1	Microfabrication .....	79
3.4.2	Cell migration in microfluidic device .....	80
<b>3.5</b>	<b>Part D: Experimental infections of the <i>Lutzomyia longipalpis</i> with <i>Leishmania tarentolae</i> and <i>Crithidia fasciculata</i>, and <i>Aedes aegypti</i> with <i>Crithidia fasciculata</i> .....</b>	<b>81</b>
3.5.1	Heat treatment of sheep blood .....	81
3.5.2	Infection protocol .....	81
3.5.3	Dissection .....	82
<b>CHAPTER FOUR: RESULTS.....</b>		<b>83</b>
<b>4.1</b>	<b><i>Leishmania mexicana</i> morphometric analysis <i>in vitro</i> .....</b>	<b>83</b>
<b>4.2</b>	<b><i>Leishmania tarentolae</i> morphometric analysis <i>in vitro</i> .....</b>	<b>88</b>
4.2.1	Bulgtomonad promastigotes .....	94
4.2.2	Kinetoplast Nucleus swapping promastigotes .....	96
<b>4.3</b>	<b>Analysing chemotactic migration .....</b>	<b>98</b>
4.3.1	Capillary assay .....	98
4.3.2	Capillary assay morphometrics .....	100
<b>4.4</b>	<b>Microfluidic Chip design .....</b>	<b>113</b>
4.4.1	Design and operations of the microdevice.....	113
	.....	<b>114</b>
4.4.2	Initial testing of microfluidic device .....	116
<b>4.5</b>	<b>Preliminary study of hypopylarian status of <i>L. tarentolae</i> .....</b>	<b>116</b>
<b>CHAPTER FIVE: DISCUSSION .....</b>		<b>118</b>
<b>5.1</b>	<b>Is <i>Leishmania tarentolae</i> hypopylarian? .....</b>	<b>118</b>
<b>5.2</b>	<b>Morphometric analysis and comparison between <i>L. mexicana</i> and <i>L. tarentolae</i> .....</b>	<b>119</b>
5.2.1	<i>Leishmania mexicana</i> .....	120
5.2.2	<i>Leishmania tarentolae</i> .....	121
<b>5.3</b>	<b>Traditional Capillary Chemotactic Assays .....</b>	<b>122</b>
<b>5.4</b>	<b><i>Leishmania</i> promastigote taxis .....</b>	<b>124</b>
5.4.1	Migration of <i>Leishmania</i> within the sand fly alimentary canal .....	125
5.4.2	Morphology of migrated promastigotes .....	127
<b>5.5</b>	<b>Understanding the taxis of hypopylarian and suprapylarian and parasites. ....</b>	<b>129</b>
<b>5.6</b>	<b>Development of a microfluidic device for the screening of chemoattractants .</b>	<b>132</b>

5.7 Future .....	135
<b>CHAPTER SIX: CONCLUSION .....</b>	<b>137</b>
<b>REFERENCES .....</b>	<b>139</b>
<b>APPENDICES .....</b>	<b>161</b>

## List of Figures

- Figure 1.** Leishmaniasis life cycle
- Figure 2.** Reported distribution of cutaneous (A) and visceral (B) leishmaniasis in the New World.
- Figure 3.** Reported distribution of cutaneous (A) and visceral (B) leishmaniasis in the Old World
- Figure 4.** Sandfly life cycle
- Figure 5.** The anatomy of the alimentary canal of sandflies
- Figure 6.** Illustration of the 3 cell types in the Malpighian tubules (MT)
- Figure 7.** The digestion of the blood meal within the sandfly midgut
- Figure 8.** The anatomy of *Lu. longipalpis* gut and the pH of the midgut during the first 10h (a) and 24 hours (b) after blood ingestion
- Figure 9.** Network analysis showing the shared bacteria species between sandflies species
- Figure 10.** *Lutzomyia longipalpis* gut microbiota
- Figure 11.** The two main morphological forms of *Leishmania spp*
- Figure 12.** Schematic representation of the main intracellular organelles from *Leishmania* promastigote (left) and amastigote (right) forms
- Figure 13.** Kinetoplast repositioning in relation to other organelles during the life cycle of a flagellate
- Figure 14.** The cell cycle of promastigote *L. mexicana* by light microscopy
- Figure 15.** Illustrations showing the properties of each cell measurement
- Figure 16.** Illustration of promastigote morphologies categorisation
- Figure 17.** A electron micrograph through the flagellar pocket of a kinetoplastid
- Figure 18.** Metacyclogenesis of suprapylarian *Leishmania*
- Figure 19.** Diagrammatic representation of *Leishmania* development sections within a sandfly
- Figure 20.** Schematic diagram of LPGs from representative procyclic and metacyclic *Leishmania* species
- Figure 21.** Apparatus used in early chemotaxis assay. A) Illustration of the chemotaxis assay set up of Adler B) Illustration of a Boyden chamber assay
- Figure 22.** Illustration of the experimental set up used by Oliveira et al, 2000
- Figure 23.** Illustration of the alimentary canal of the sandfly showing areas containing sugars (yellow) and urea (red)
- Figure 24.** Diagrammatic representation of experimental apparatus used for capillary assay
- Figure 25.** Development of a microfluidic device for *Leishmania* taxis assay
- Figure 26:** Growth curve of *Leishmania mexicana* in vitro
- Figure 27:** Scatter plot showing *L. mexicana* cell body length against cell body width
- Figure 28:** Scatter plot showing *L. mexicana* cell body length against cell flagella length measured

**Figure 29:** Scatter plot showing *L. mexicana* cell body width against cell flagella length measured

**Figure 30:** Scatter plot showing *L. mexicana* cell body length against distance from kinetoplast to nucleus

**Figure 31:** *L. mexicana* morphological changes of promastigotes in culture

**Figure 32:** Growth curve of *Leishmania tarentolae* in vitro

**Figure 33:** Scatter plot showing *L. tarentolae* cell body length against cell body width

**Figure 34:** Scatter plot showing *L. tarentolae* cell body length against cell flagella length measured

**Figure 35:** Scatter plot showing *L. tarentolae a* cell body width against cell flagella length measured

**Figure 36:** Scatter plot showing *L. tarentolae a* cell body length against distance from kinetoplast to nucleus

**Figure 37:** *L. tarentolae* morphological changes of promastigotes in culture

**Figure 38:** Morphology criteria for *L. tarentolae* Bulgtomonad promastigotes

**Figure 39:** Movement of *Leishmania* promastigotes in the presence of potential chemoeffectors

**Figure 40a:** The percentage of migrated categorised promastigotes of day 3 and 5 old culture of *L. mexicana* towards potential chemoeffectors of fructose 0.5M

**Figure 40b:** The percentage of migrated categorised promastigotes of day 3 and 5 old culture of *L. tarentolae* towards potential chemoeffectors of fructose 0.5M

**Figure 41a:** The percentage of migrated categorised promastigotes of day 3 and 5 old culture of *L. mexicana* towards potential chemoeffectors of sucrose 0.5M.

**Figure 41b:** The percentage of migrated categorised promastigotes of day 3 and 5 old culture of *L. tarentolae* towards potential chemoeffectors of sucrose 0.5M.

**Figure 42a:** The percentage of migrated categorised promastigotes of day 3 and 5 old culture of *L. mexicana* towards potential chemoeffectors of mannose 0.5M.

**Figure 42b:** The percentage of migrated categorised promastigotes of day 3 and 5 old culture of *L. tarentolae* towards potential chemoeffectors of mannose 0.5M

**Figure 43a:** The percentage of migrated categorised promastigotes of day 3 and 5 old culture of *L. mexicana* towards potential chemoeffectors of urea 0.5M.

**Figure 44a:** The percentage of migrated categorised promastigotes of day 3 and 5 old culture of *L. tarentolae* towards potential chemoeffectors of urea0.5M.

**Figure 45a:** The percentage of migrated categorised promastigotes of day 3 and 5 old culture of *L. mexicana* towards potential chemoeffectors of crude PSG

**Figure 45b:** The percentage of migrated categorised promastigotes of day 3 and 5 old culture of *L. tarentolae* towards potential chemoeffectors of crude PSG

**Figure 46:** Movement of *Leishmania tarentolae* promastigotes in the presence of chemoeffectors

**Figure 47:** Movement of *Leishmania mexicana* promastigotes in the presence of chemoeffectors

**Figure 48:** Microfluidic device design

**Figure 50:** Schematic of the integrated microfluidic device for cell-based High content screening

## List of Tables

**Table 1.** Transporters in *Leishmania* species and the nutrients they provide

**Table 2.** All the agents that have been showed to have positive chemotaxic responses from literature

**Table 3.** Summary of test substances and concentrations as used for the capillary assay.

## List of Images

**Image 1:** Image shows Bulgtomonad promastigotes from *Leishmania tarentolae* axenic culture day 4

**Image 2:** Image shows kinetoplast and nucleus swapping promastigotes from *Leishmania tarentolae* axenic culture day 7

**Image 3:** Image shows *L. tarentolae* promastigotes found in the hindgut on day 10 of infection in *Lu. longipalpis*

## List of Abbreviations

A	Anterior
AIs	Autoinducers
ABC transporters	ATP-binding cassette transporters
BSA	Bovine serum albumin
CL	Cutaneous leishmaniasis
CPV	Cytoplasmic polyhedrosis virus
DMSO	Dimethylsulfoxide
DALYs	Disability-adjusted life years
DAPI	4',6-diamidino-2-phenylindole
DNA	Deoxyribonucleic acid
DKN	Distance from kinetoplast to nucleus
DDT	Dichlorodiphenyltrichloroethane
<i>E. coli</i>	<i>Escherichia coli</i>
ELISA	Enzyme-linked immunosorbent assay
FPPG	Filamentous proteophosphoglycan
F	Flagella
Fe <sup>2+</sup>	Ferrous iron
Fe <sup>3+</sup>	Ferric iron
GLUT	Glucose transporter
G Phase	Growth phase
IFT	Intraflagellar transport
K	Kinetoplast
kDNA	Kinetoplast DNA
<i>L. braziliensis</i>	<i>Leishmania braziliensis</i>
<i>L. panamensis</i>	<i>Leishmania panamensis</i>
<i>L. guyanensis</i>	<i>Leishmania guyanensis</i>
<i>L. infantum</i>	<i>Leishmania infantum</i>
<i>L. donovani</i>	<i>Leishmania donovani</i>
<i>L. chagasi</i>	<i>Leishmania chagasi</i>
<i>L. tropica</i>	<i>Leishmania tropica</i>
<i>L. mexicana</i>	<i>Leishmania mexicana</i>
<i>Leishmania spp</i>	<i>Leishmania species</i>
LPG	Lipophosphoglycans

Lu. longipalpis	Lutzomyia longipalpis
LPRV1	Lutzomyia Piaui reovirus 1
LPRV2	Lutzomyia Piaui reovirus 2
LPNV	Lutzomyia Piaui nodavirus
mL	Milliliter
MCI	Migrated Chemotaxic Index
MAP kinases	Mitogen-activated protein kinases
N	Nucleus
Nd:YAG	Neodymium-doped yttrium aluminium garnet
NTD	Neglected tropical disease
NADPH	Nicotinamide adenine dinucleotide phosphate oxidase
PCR	Polymerase chain reaction
PM	Peritrophic membrane
PV	Parasitophorous vacuole
PFR	Paraflagellar rod
SFSV	Sand fly fever Sicilian Viruses
S Phase	Synthesis phase
sAP	Filamentous acid phosphatase
TOSV	Toscana viruses
TSLM	Time of straight line movement
VL	Visceral leishmaniasis
WIS	Washing and incubating solution
WHO	World Health Organisation

## Abstract

Protozoan parasites of the genus *Leishmania* are the causative agents of a wide spectrum of diseases from self-healing cutaneous leishmaniasis to visceral leishmaniasis. The parasites undergo a complex life cycle including motile and non-motile cell types within the insect vector and vertebrate host. Within the insect vector, promastigotes generally migrate anteriorly along the gut as they undergo morphological changes from procyclic to nectomonad and later to metacyclic form of promastigotes. In order for the insect vector to transmit infective stage *Leishmania* promastigotes to the mammalian host via a blood feed, metacyclic promastigotes need to be located within the foregut. The study of the elicitors of migration within the sand fly alimentary canal have to date been fragmentary with no exploration of the different promastigote forms and the effects of the vast array of potential chemoeffectors present. Two *Leishmania* species were selected based on their migration properties in the sand fly gut. This study focussed on understanding the chemotaxis of different morphotypes of posterior migrating reptilian- pathogenic *Leishmania tarentolae* compared to the anterior migrating human pathogenic *Leishmania mexicana* within the biochemical gradients of the sand fly alimentary canal.

This study explored the movement of both *L. mexicana* and *L. tarentolae* promastigotes towards a gradient of urea that may be found emitting from Malpighian tubules in the hindgut, the novel morphologies of *L. tarentolae*, the migration of procyclics, neptomonads, leptomonads and metacyclics, and the development of a novel microfluidic device for the study of chemotaxis in *Leishmania*.

The results from the chemotaxic assays suggested that the migration of promastigotes occurred through the attraction towards cues such as the urea gradient from the Malpighian tubules and hindgut, and the sugars gradient from the diverticulum. These assays showed that *L. tarentolae* had a significantly higher attraction to urea and *L. mexicana* to sugars; confirming the species-specific differences between suprapylarian and hypopylarian parasites. Using different populations of *L. mexicana* and *L. tarentolae* promastigotes, a significant difference in migration between population based on age was observed. The results also suggested that a population rich in leptomonads and nectomonads had a higher migration and therefore a higher attraction towards the chemical cues. The results shed light on parasite migration that

Yasmine Precious Kumordzi

is dependent on the developmental stage of promastigotes as well as the species-specific cues. The role that the cues play in determining which *Leishmania* species can be transmitted via the bite of a sandfly are discussed.

## CHAPTER ONE: GENERAL INTRODUCTION

### 1.1 Leishmaniasis

Leishmaniasis are a group of vector-borne (Gillespie et al, 2016) neglected tropical disease (NTD) with a wide geographical distribution globally (Spotin et al, 2015; Alvar et al, 2012) and great impact in magnitude of morbidity and mortality (Alvar et al, 2012). It is transmitted by the bite of an infected sandfly with the protozoan parasite *Leishmania* (Figure 1).

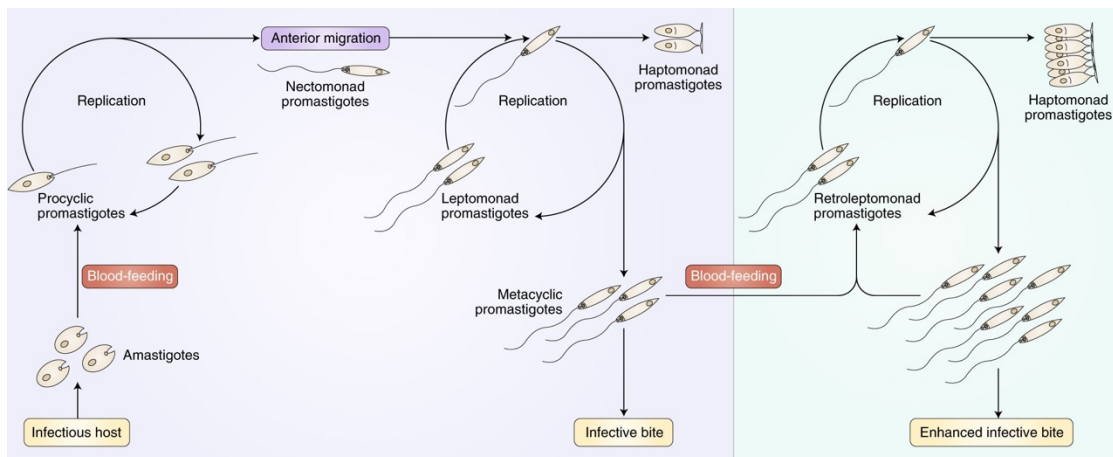


**Figure 1.** *Leishmania* life cycle within a sandfly. Amastigotes are taken up in a bloodmeal by female sandflies. Within the midgut, the amastigotes transform into the procyclic promastigotes which can further replicate into more procyclics or differentiate into nectomonad promastigotes which migrate anteriorly and replicate into leptomonad promastigotes and further into haptomonad or metacyclic promastigotes. Image from Bates, 2018

#### 1.1.1 Epidemiology

Leishmaniasis is endemic in 88 countries (Alvar et al, 2013; Alawieh et al, 2014) and is prevalent in areas in tropical and subtropical regions, and the Mediterranean Basin (Alawieh et al, 2014; Gillespie et al, 2016). It has an estimated incidence of 1.6 million new cases annually (Rezvan, Nourain and Navard, 2017); causing over 50 thousand deaths annually (Gillespie et al, 2016; Rezvan, Nourain and Navard, 2017), 3.3 million disability-adjusted life years (DALYs) lost annually (Gillespie et al, 2016) and 350 million people at risk of infection worldwide (Rezvan, Nourain and Navard, 2017). These factors have led to leishmaniasis to be considered a public health problem worldwide (Costa et al, 2013) and categorized as a class I

disease (emerging and uncontrolled) by the World Health Organisation (WHO) (**Rezvan, Nourain and Navard, 2017**).

Leishmaniasis is known to have strong associations with poverty (**Alvar et al, 2013**) and environmental changes (**Rezvan, Nourain and Navard, 2017**), leading to the burden of this NTD falling disproportionately on the poorest global population. Poverty is associated with poor nutrition, housing conditions and sanitation, as well as migration; all of which brings nonimmune hosts into close proximity to domestic animals (potential reservoir), other infected persons and sandflies. This in addition to the lack of access to healthcare, delays in diagnosis and treatment increases the risk of disease progression, leading to an increase of the clinical manifested disease (**Alvar et al, 2013**). The costly diagnosis and treatment of leishmaniasis leads to further hardship for the families involved, reinforcing the cycle of the disease and poverty. In the poverty stricken prevalent areas, periodic epidemics are known to occur (Ethiopia (2005, 2006), Kenya (2008) and Sudan (2009-2011) (**Gillespie et al, 2016**).

Epidemics have also emerged due to conflicts and war where public health has broken down and housing conditions have fallen, leading to the proximity to untreated patients decreasing and the migration of immunologically naive migrants from nonendemic to endemic areas (**Alvar et al, 2013; Alawieh et al, 2014**). An example of this was seen in 2013 when an outbreak of Leishmaniasis in Lebanon occurred following the migration of Syrian refugees from endemic Syria (**Alawieh et al, 2014**).

The high burden of leishmaniasis is linked to the great impact in magnitude of morbidity and mortality that it has (**Alvar et al, 2013**). However, with symptomatic cases taking months to show clinical manifestations after exposure (**Alawieh et al, 2014**) representing 5-16% of all cases and the lack of proper reporting, the actual burden of leishmaniasis could be exceeding its estimations.

### **1.1.2 Clinical Presentation**

The various species of *Leishmania* parasites and the wide distribution of insect vectors allows for numerous interplay leading to various clinical manifestations of the

disease (**Rezvan, Nourain and Navard, 2017**). The clinical manifestations have been classified into three (3) main forms of leishmaniasis dependent on characteristics and are later further divided; cutaneous leishmaniasis (CL), visceral leishmaniasis (VL) and mucocutaneous leishmaniasis (ML) (**Alawieh et al, 2014**).

### **Cutaneous Leishmaniasis**

CL is typically not life threatening and presents as changes in the skin's appearance, such as papules that may ulcerate forming lesions at the site of bite (**Bañuls et al, 2011**) and multiple nodules. This form of leishmaniasis is caused by *Leishmania amazonensis*, *Leishmania mexicana*, *Leishmania braziliensis*, *Leishmania panamensis*, *Leishmania peruviana* and *Leishmania guayanensis* (New World CL) (Figure 2A), *Leishmania infantum*, *Leishmania chagasi* (Mediterranean and Caspian Sea regions) and *Leishmania major*, *Leishmania tropica*, *Leishmania aethiopica* (Old World CL) (Figure 3A) (**Rezvan, Nourain and Navard, 2017**). These ulcers heal spontaneously after 2-10 months dependent on lesion severity, unless a secondary infection occurs at the site of lesion. CL is further subdivided to Anthroponotic CL, Zoonotic CL, and Diffuse CL making CL the most complex form to diagnose (**Bañuls et al, 2011**).

### **Mucocutaneous Leishmaniasis**

ML occurs following chronic CL (**Reithinger et al, 2010**) in a metastatic manner, where CL lesions act as a primary site and dissemination occurs through the lymphatic system or blood vessels (**Bañuls et al, 2011**). This usually causes destruction to the oronasal and pharyngeal cavities in 90% of cases (**Bañuls et al, 2011**), causing eating and breathing problems (**Rezvan, Nourain and Navard, 2017**). ML infections leave life-long disfiguring scars leading to social stigma and in the worst cases leads to mortality. This form of leishmaniasis is mostly caused by *L. braziliensis*, however rare forms have been associated with *L. panamensis*, *L. guyanensis* in the New World and occasionally *L. infantum* and *Leishmania donovani* (**Rezvan, Nourain and Navard, 2017; Bañuls et al, 2011**).

### Visceral Leishmaniasis

VL is the most severe form of leishmaniasis affecting internal organs, leading to systemic infection (Rezvan, Nourain and Navard, 2017) and high fatality (Alvar et al, 2013; Gillespie et al, 2016). It is also known as kala-azar, black fever and Dumdum (Rezvan, Nourain and Navard, 2017). This form of leishmaniasis is caused by *L. donovani* complex which is composed of 3 species; *L. donovani*, *L. infantum* and *L. chagasi*, however the composition of complex has been challenged (Mauricio et al, 1999; Rezvan, Nourain and Navard, 2017; Lukes et al, 2007; Bañuls et al, 2011). The distribution of VL in the Old World and New World is similar to that of CL (Figure 2B & 3B). In VL, the symptoms vary in severity from fever, skin pigmentation, anaemia, hepatosplenomegaly and a depressed immune response.

Clinical presentation does not always occur. Over 90% of *L. donovani* and *L. infantum* human infections are asymptomatic (Rezvan, Nourain and Navard, 2017). This leads to asymptomatic carriers such as dogs in Brazil acting as the ideal reservoirs as they escape culling programmes becoming vital in infection propagation (Bañuls et al, 2011).

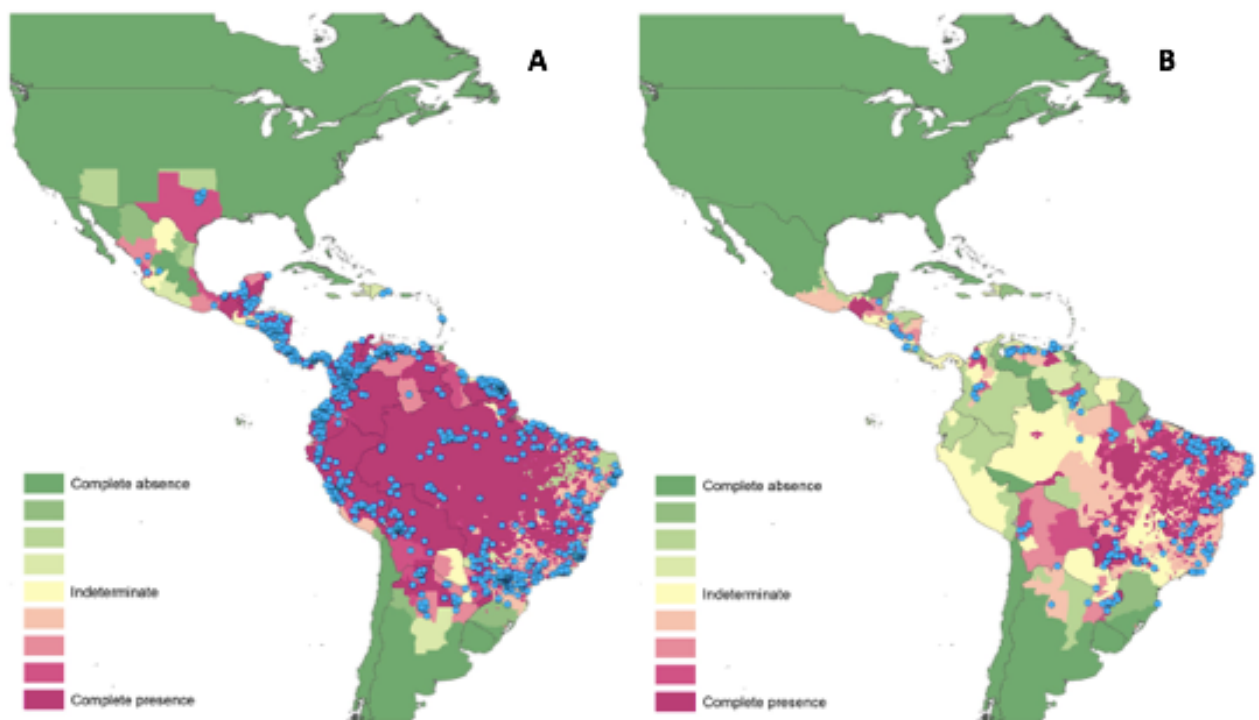
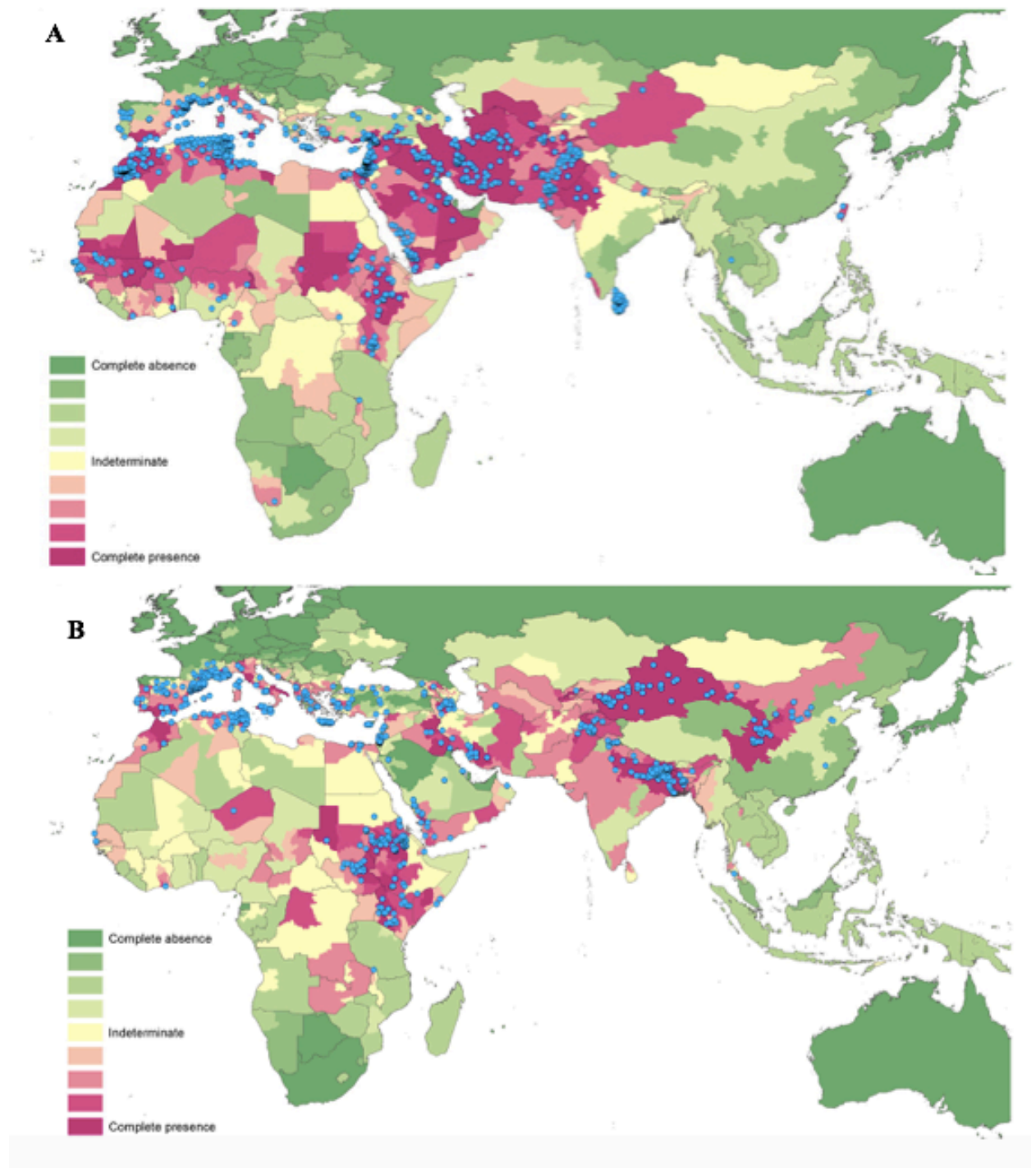


Figure 2. Reported distribution of cutaneous (A) and visceral (B) leishmaniasis in the New World. Evidence consensus for presence of the disease ranging from green (complete consensus on the absence: -100%) to purple (complete consensus on the presence of disease: +100%); blue spots indicate occurrence points or centroids of occurrences within small polygons. Image adapted from Pigott et al, 2014



**Figure 3. Reported distribution of cutaneous (A) and visceral (B) leishmaniasis in the Old World.** Evidence consensus for presence of the disease ranging from green (complete consensus on the absence: -100%) to purple (complete consensus on the presence of disease: +100%); blue spots indicate occurrence points or centroids of occurrences within small polygons. Image adapted from Pigott et al, 2014

### 1.1.3 Causative Agent and Vector

The causative agent of leishmaniasis is the protozoan parasite of the genus *Leishmania* (Gillespie et al, 2016), a kinetoplastid (Spotin et al, 2015) which is transmitted by the bite of an infected female phlebotomine sandfly (Alawieh et al, 2014), its insect vector. There are over 20 *Leishmania* species that are pathogenic to humans (Gillespie et al, 2016; Rezvan, Nourain and Navard, 2017). The correlation between the occurrence of human leishmaniasis and high rates of infected dogs shows the important role dogs play as reservoirs to maintain the propagation of parasites and transmission (Costa et al, 2013; Gillespie et al, 2016). The presence of reservoir hosts depends on the type of *Leishmania* species (Alawieh et al, 2014).

Anthroponotic species such as *L. tropica* in Turkey (Zeyrek et al, 2007) are restricted to human hosts therefore the human population is used as the main reservoir for infection (Reithinger et al, 2010), whereas zoonotic species such as *L. mexicana* in Brazil (Pimentel et al, 2015) have animal hosts (Alawieh et al, 2014). Although *Leishmania* species such as *L. tropica* are known to be anthroponotic in areas such as Kabul in Afghanistan (Reithinger et al, 2010) and Sanliurfa Province in Turkey (Zeyrek et al, 2007), these species can be zoonotic in other areas such as in central and northern Israel where Rock Hyraxes are reservoirs (Talmi-Frank et al, 2010), suggesting that anthroponoticity is dependent on area.

### 1.1.4 Interventions

Controlling the disease is dependent on early diagnosis and treatment (Rezvan, Nourain and Navard, 2017). Diagnosis has advanced over the recent years, however there is a lack of a 'gold standard' test in place for effective control and eradication (Rezvan, Nourain and Navard, 2017). Diagnosis is based on clinical criteria manifested in humans, histopathology of lesions, detection and isolation of parasites from the lesions which can be done by microscopy or culture methods, employment of soluble *Leishmania* protein in enzyme-linked immunosorbent assay (ELISA) method tests, and the analysis of the small subunit ribosomal RNA genes employing the polymerase chain reaction (PCR) (Rezvan and Moafi, 2015). Within diagnosis, the identification of species is necessary for the appropriate treatment and

control of the disease within the community. Using microscopic diagnosis, leishmanial species cannot be distinguished from one another due to their similar morphologies. Therefore, techniques have been employed for the confirmation of species including isozyme analysis and molecular techniques as the kinetoplast DNA is unique to each *Leishmania* species **(Rezvan and Moafi, 2015)**.

With the knowledge of the specific causative *Leishmania* species, the relevant environmental control and treatment can be employed. There are a few approved drug treatments, however no prophylactic drug is available for visceral and cutaneous leishmaniasis due to the biology of the *Leishmania* parasites in the human body. The key aspects to the biology of the *Leishmania* parasites that affect the development of drugs includes the location of the intracellular form of parasite, the varying regional species and the relationship of the parasite to the host immunity resulting in different results **(Croft and Olliaro, 2011)**.

Chemotherapy **(Gillespie et al, 2016; Horn and Duraisingh, 2014)** is the key treatment for all three (3) clinical manifestations of leishmaniasis. As chemotherapy is expensive and requires a long and complicated treatment regime over a period of time, it is not a treatment available to the majority of people affected by the disease. The only preventative methods currently used widely are vector and reservoir control when infection is anthroponotic. This includes the use of methods such as limiting exposure to the vector and reservoir through control: use of insect repellent, culling of infected dogs **(Costa et al, 2013)**, use of insecticide-impregnated collars **(Reithinger et al, 2004)** and use of impregnated bed nets **(Gillespie et al, 2016; Alawieh et al, 2014)**. Despite the implementation of these control mechanisms, a high incidence of leishmaniasis remains in many focal areas such as Latin American countries **(Costa et al, 2013)** and India **(Gomes et al, 2017)**. In Brazil, culling of dogs is the main strategy used however is ineffective **(Costa et al, 2013)** due to culling programmes not being continuous due to a lack of a structured surveillance system, financial problems and the insensitivity of diagnostic testing **(Courtenay et al, 2002)**. This causes the continuous cycle of disease. In India, insect repellent containing the neurotoxin dichlorodiphenyltrichloroethane (DDT) is used as the main strategy for the control of the insect vector, however with continuous use the emergence of DDT resistance has resulted in this strategy being ineffective **(Gomes et al, 2017)**.

Due to the magnitude in mortality and morbidity, an effective preventative measure such as vaccination for leishmaniasis is the most appropriate (**Rezvan, Nourain and Navard, 2017**). Vaccines elicit long lasting immunity which would be ideal in controlling or eliminating leishmaniasis (**Gillespie et al, 2016; Alawieh et al, 2014**) in a cost-effective manner. The argument for vaccine development is that *Leishmania* immunity is present in the majority of people who recover from leishmaniasis. The basis of this was used in the ancient practice of ‘leishmanization’ where an immunized individual used a thorn to introduce live parasite to another (**Gillespie et al, 2016**). Currently there is no licensed vaccine available against human leishmaniasis (**Gillespie et al, 2016**), however there are a number of candidates in various pre-clinical stages in development, such as LEISH-F2 and F3 based on *Leishmania* antigen epitopes (**Rezvan and Moafi, 2015; Gillespie et al, 2016**).

With the interplay between distribution of *Leishmania* species, sandfly species, leishmaniasis disease, control programmes in place, asymptomatic and immunosuppressed persons, and diagnostic tools available, the full understanding of all areas of this NTD is crucial in understanding the disease.

## 1.2 Sandfly – The vector

There are over 800 recognized sand-fly species, which are divided into two (2) main classifications of 464 New World species and 375 Old World species and can be further subdivided (Akhoundi et al, 2016). Of these over 800 species, only 98 have been proven or suspected to transmit *Leishmania* parasites to humans (Maroli et al, 2012; Ready, 2013): 42 *Phlebotomus* species (Old World) and 56 *Lutzomyia* species (New World) (Maroli et al, 2012). Unlike nonhematophagous male sand flies (Lestinova et al, 2017), female *Lutzomyia* and *Phlebotomus* sand flies (Diptera: Psychodidae: Phlebotominae) are hematophagous insects (Telleria et al, 2010). This makes them important in the transmission of *Leishmania* parasites (Lantova and Volf, 2014). They are often considered to be the only natural vectors of *Leishmania*, however midges (Diptera: Ceratopogonidae) have also been shown to play a role in transmission of leishmanial parasites (Kwakye-Nuako et al, 2015; Dougall et al, 2011). Midges are vectors in areas with limited or absent phlebotomine sand flies such as in north Australia (Dougall et al, 2011) and in the Volta region of Ghana (Kwakye-Nnako et al, 2015). *Leishmania* parasites are coinoculated with saliva to the vertebrate host during the process of blood feeding (Lestinova et al, 2017), this makes the act of blood feeding imperative for the successful transmission of *Leishmania* parasites for disease in humans.

### 1.2.1 Life cycle

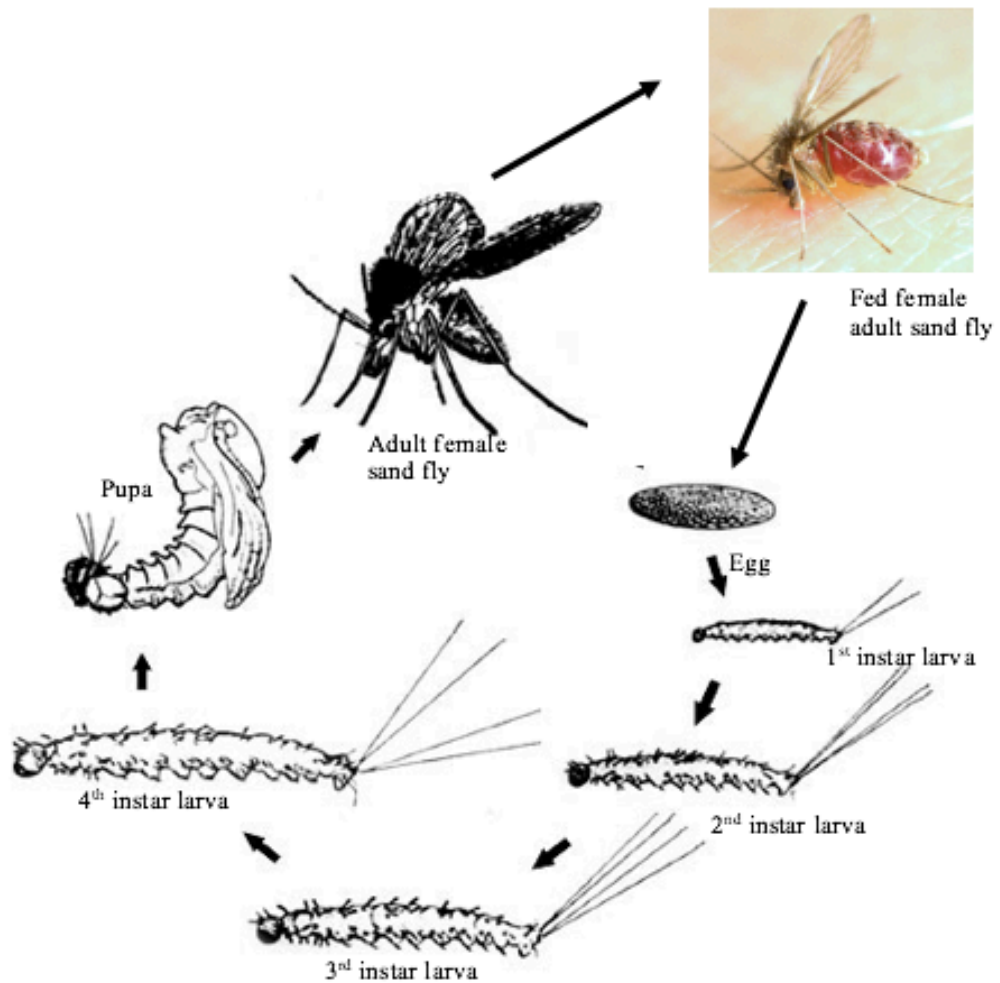


**Figure 4. Sandfly life cycle.** Adapted from European Center for Disease Prevention and Control: Phlebotomine sand flies- Factsheet for experts (<https://ecdc.europa.eu/en/disease-vectors/facts/phlebotomine-sand-flies>) and *Lutzomyia longipalpis* image by Ray Wilson.

The sandfly life cycle has four (4) distinct life stages: egg, larva, pupa and adult fly (Figure 4). Eggs are produced from the adult female sandfly and develop through 4 instars where they scavenge before developing into the pupal stage. The adult sandfly emerges from the pupa, mates and the cycle continues. Aside from mating, feeding is crucial for the development of eggs by the female sandfly therefore only females blood feed. However, autogenous species of sandfly are known (**Chelbi, Kaabi and Zhioua, 2007**). If the sandfly survives oviposition, a new gonotrophic cycle requires another blood feed hence the transmission of *Leishmania* parasites (**Peter J Myler and Nicolas Fasel, 2008**).

## 1.2.2 Structure

Compared to other vector groups, the biology of sandflies is poorly known (Manson, Cooke and Zumla, 2009). Sandfly gut has a slightly more complex structure in which it has compartmentalized regions where specific activities occur (Figure 5). This allows for each region to have a unique function and microenvironment. For the development of *Leishmania* and the factors that may affect migration, focus is given to the gut, malpighian tubules and the ventral diverticulum (crop).

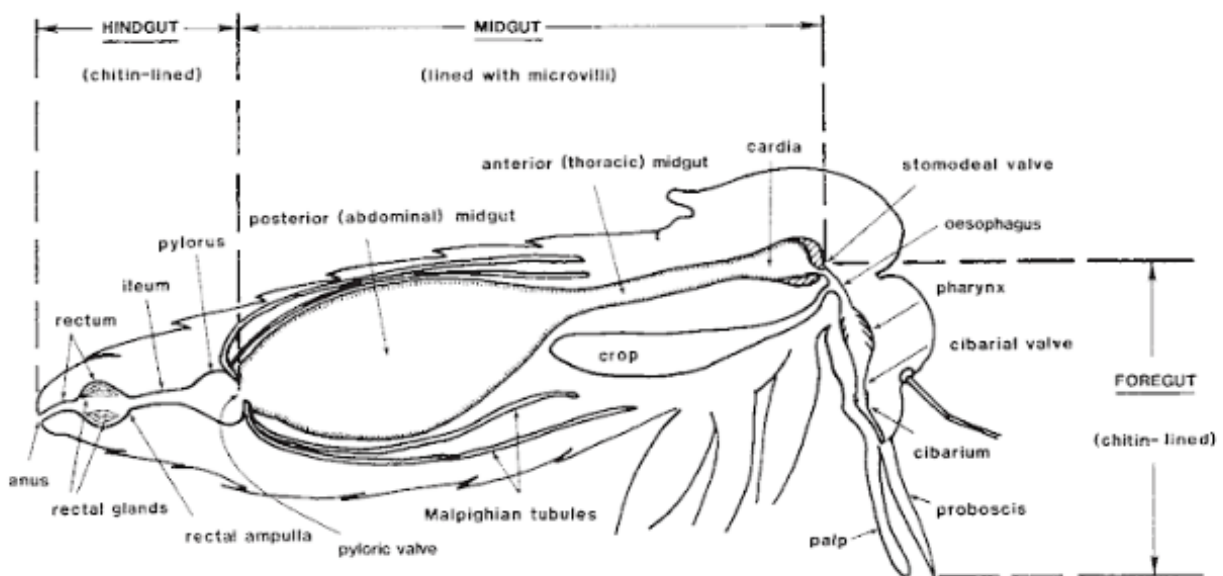


**Figure 5.** The anatomy of the alimentary canal of sandflies, showing the compartmentalized regions of the gut (midgut, hindgut and foregut), ventral diverticulum (crop), and malpighian tubules. Illustration from Manson, Cooke and Zumla, 2009.

Similar to humans, the alimentary canal represents the passage from the mouth to anus functioning primarily to convert food into absorbable particles by the actions of enzymes and muscular movements. The alimentary tube is segmented into 3 primary regions; the foregut, midgut and hindgut which are histologically distinct in terms of their purpose (Richards and Davies, 1977).

Feeding is essential for the survival of the sandfly in addition to the mode of transmission in which disease is spread. The cibarial muscle contraction provides the suction that pulls food in fluid form into the pharynx before passing into the abdominal midgut or crop (Schlein, Jacobson and Messer, 1992). The crop is a foregut organ (Stoffolano and Haselton, 2013) used as a reservoir for carbohydrates.

With a series of pumps and sphincters the flow of fluid into the crop and fluid into the midgut is regulated dependent on hydrostatic pressure (**Thomson, 1975**). The rate of crop emptying of fluid to the midgut for digestion is based on the metabolic rate of the sandfly, temperature (**Moloo and Kutuza, 1971**), growth of the peritrophic membrane (PM) (**Harmsen, 1973**) and composition of the haemolymph (**Stoffolano and Haselton, 2013**).

The two main segments for parasite development is the midgut and hindgut (Figure 5). The midgut is composed of two segments; the narrow anterior (thoracic) midgut which follows from the foregut and the wide posterior (abdominal) midgut (**Adler and Theodor, 1929**). This area is lined with a layer of microvillar epithelium which has a number of functions; it secretes the PM following a blood meal (**Rudin and Hecker, 1982**), secretes and produces the digestive enzymes required, and absorbs nutrients for transport following the digestion process (**Soares and Turco, 2003**). Most of the enzyme produced are proteinases such as trypsins which are more active in the gut alkaline environment (Figure 8). Enzyme levels increases following the bloodmeal and decreases as digestion declines, proportional to the level of protein found in the midgut from the blood (**Lehane, 2005**). The hindgut is cuticle lined similarly to the foregut. The pylorus leads directly from the midgut and contains rows of posteriorly-directed protrusions possibly to aid the removal of remnants from digestion (**Warburg, 2008**).

The malpighian tubules are located between the midgut and the hindgut; playing an important role in insects as the primary excretory system (**Ramsay, 1951**) and perform osmo-regulation (**Littau and Smith, 1960**). They are composed of bundles of tubes made up of 3 different types of cells (Figure 6) (**Littau and Smith, 1960**), the epithelial cells at the distal regions are brush bordered whilst honeycombed at the proximal region of the tubules (**Littau and Smith, 1960**). These narrow tubes infiltrate the haemocoel containing hemolymph from which waste is collected into the distals of the malpighian tubes. Towards the proximal regions, water is reabsorbed back into the haemocoel. The nitrogenous waste remaining in the lumen is converted to urea and later uric acid crystals which is eliminated into the hindgut as excreta.

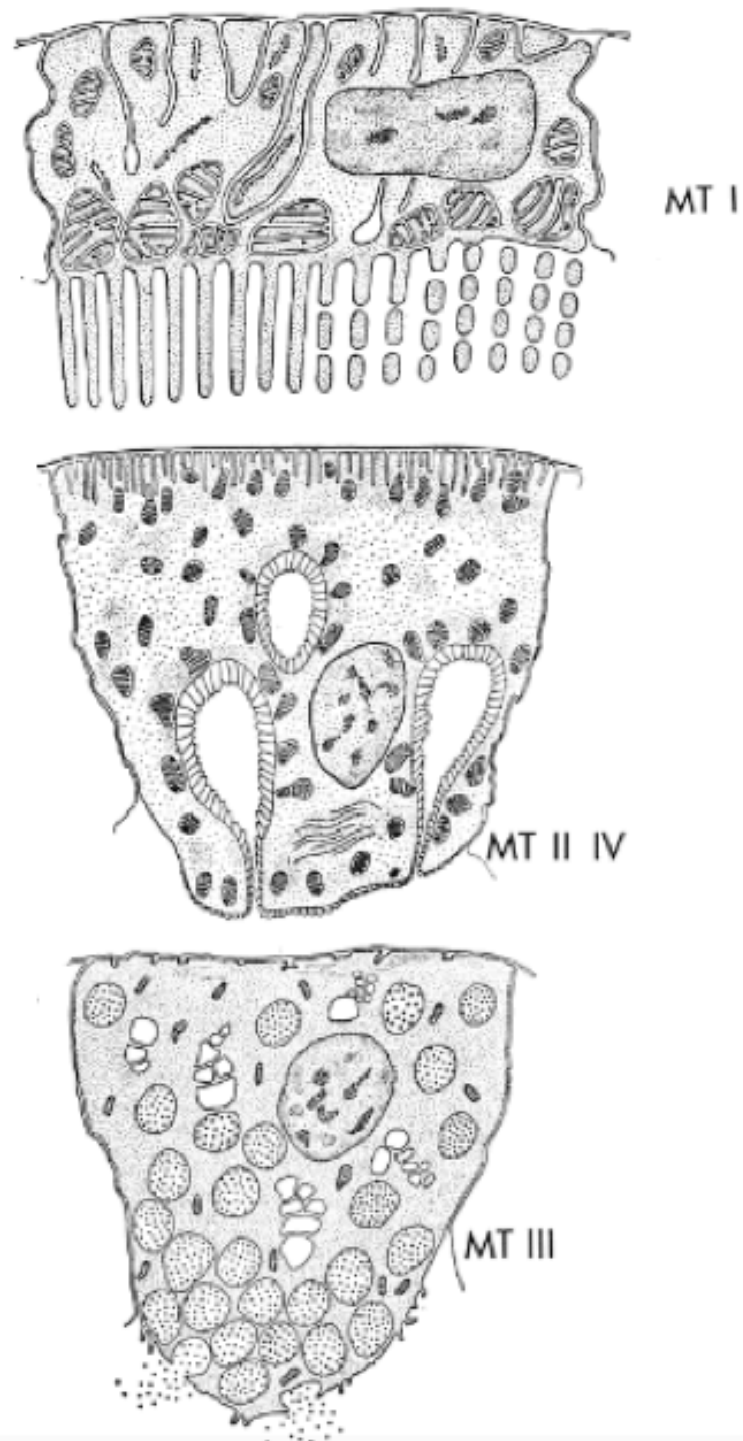


**Figure 6.** Illustration of the 3 cell types in the Malpighian tubules (MT) from I at the distal region in contact with the haemolymph within the haemocoel surrounding the midgut, to IV at the proximal region associated to the hindgut. Region I contain MT I cells have a loosely packed microvilli brush boarder up to 3 $\mu$ l in length and 0.1 - 0.15 $\mu$ l in diameter in contact with the haemolymph with a dense population of granules. Region II and IV contain MT II and IV cells respectively which are structurally similar with numerous randomly distributed mitochondria and shallow infoldings. Region III contain MT III cells containing numerous granular vesicles used for the main role of excretion. Image from (Littau and Smith, 1960)

### 1.2.3 Feeding

Both male and female sandflies require a regular source of carbohydrates for energy acquired from honeydew excreted on plants and plant sap as a 'sugar meal' (Schlein and Jacobson, 1999). Female sandflies require an additional source of protein to support the development of eggs which they acquire from the 'blood meal' (Ready, 1979) known as gonotrophic concordance (Lehane, 2005). Due to the specific need of female sand flies to acquire a 'blood meal', *Leishmania* parasites can pass to and from the sand fly during a blood feed making them an ideal vector (Telleria et al, 2010). The proboscis is used for both feeds, however the blood and sugar have separate destinations due to batch digestion. The blood meal travels through the stomodeal valve and is kept within the midgut where a PM, a sac like structure is secreted by the midgut epithelium within the first couple of hours (Dillon et al, 2006). The sugar meal begins by travelling down the stomodeal valve into the gut, however is quickly diverted into the crop (Tang and Ward, 1998). This separation is important as the sugar meal within the crop may contain proteinases that can inhibit blood digestion (Stoffolano and Haselton, 2013).

#### Sugar meal

The sugar meal is the most important for the survival of the sand fly; in the wild sand flies feed on plants as their source of sugars. Whilst feeding, sandflies can adopt a 'sugar feeding mode' where they have raised palps (Tang and Ward, 1998). This sugar meal is kept completely separate from the blood meal in the crop. Carbohydrate digestion is initiated here due to the presence of salivary glands enzymes before it is slowly released into the gut where digestion by (alpha)-glucosidases continues. This gradual release is possibly to avoid significant body fluid osmolarity fluctuations (Stoffolano and Haselton, 2013). The pH of solely sugar fed sandflies has a slightly acidic pH of 6 which is the optimum pH for (alpha)-glucosidase activity. This enzyme is membrane bound and involved in the breakdown of disaccharides to simple sugars for digestion by hydrolyzing the terminal non-reducing 1-4 bonds.

### **Blood meal**

The blood meal ingested is contained in the midgut surrounded by the PM, confining the early stage development of *Leishmania* to within the PM (**Pruzinova et al, 2015**). For the initial infection of the sandfly, amastigote forms of *Leishmania* are ingested within the blood meal. These parasites multiply and morphologically transform for the establishment of infection. Before the establishment of infection in the midgut, the parasites encounter 3 main handicaps (**Pruzinova et al, 2015; Telleria et al, 2010; Shaden Kamhawi, 2006**); enzymatic activities, midgut peristalsis and the PM.

The first hindrance is the activities of digestive enzymes, particularly the activity of trypsin. Trypsin is the most abundant digestive enzymes within the gut of hematophagous insects, confined to the midgut lumen (**Dillon and Lane, 1993; Telleria et al, 2010**). There are other enzymes that affect *Leishmania* in the midgut such as aminopeptidase found in the midgut wall (**Dillon and Lane, 1993**). These enzymes are produced by the midgut epithelial cells post blood-meal with distinct peak times dependent on sand fly species (**Dillon and Lane, 1993**). Along with digesting the blood serum, the activities of these midgut proteases select for 'compatible' *Leishmania* to sand fly species combination (**Pruzinova et al, 2015**). This is done by the natural vector parasite *Leishmania* species having the ability to modify the midgut environment to favour its development by interfering with trypsin production and subsequently pH and enzyme efficiency (**Santos et al, 2014**). The survival to this proteolytic attack is the first essential step for the parasite development and the establishment of infection within the vector (**Pimenta et al, 1997**).

The second hindrance is the type I PM formed in response to blood feeding (**Lehane, 1997**). Following a blood meal, the PM is developed rapidly and fully formed by 6-24 hours post blood-meal dependent on sand fly species (**Pruzinova et al, 2015**). The PM acts as a physical barrier for the protection of the midgut epithelium to damage from pathogens found in the midgut lumen (**Lehane, 1997**) and conversely protects the *Leishmania* parasites by compartmentalizing them from the hydrolytic activities of the midgut (**Pruzinova et al, 2015; Secundino et al, 2005**). This remains intact until digestion finishes and the disintegration of the PM occurs. The absence of PM is associated to the loss of midgut infections due to the lethal

conditions of the sand fly midgut (**Pimenta et al, 1997**). However, this prevents the escape of the parasites into the ectoperitrophic space and as the remnants of the blood meal is defecated following digestion can lead to the loss of parasites. As intraperitrophic *Leishmania* parasites are not able to traverse the PM prior to its disintegration (**Sádlová and Volf, 2009**), escape from the blood meal occurs in the period between PM disintegration and defecation. *L. major* infections showed sandfly derived chitinases disintegrate the PM from the posterior end, therefore escaping the PM to the ectoperitrophic space requires the high densities of parasite found at the anterior area of the PM to migrate to the posterior end (**Sádlová and Volf, 2009**). This however may be species-specific.

The third hindrance is the action of midgut peristalsis (antegrade)- the motor pattern of the midgut to propel contents in the direction towards the anus for excretion of the blood meal remains following digestion (Figure 7) (**Shaden Kamhawi, 2006**). Here parasites are exposed to possibly being expelled if they have not escaped the PM. Therefore strategies have been employed by *Leishmania* parasite to slow down excretion such as the secretion of a myoinhibitory neuropeptide relaxing the midgut (**Vaidyanathan, 2004**). This leads to the sandfly being less efficient in expelling the blood meal remains, increasing the time period in which parasite can escape the PM.

Following the escape from the PM, parasites can still be removed from the midgut by peristalsis and defecation; they therefore need to colonize and attach to the midgut epithelium to prevent this.

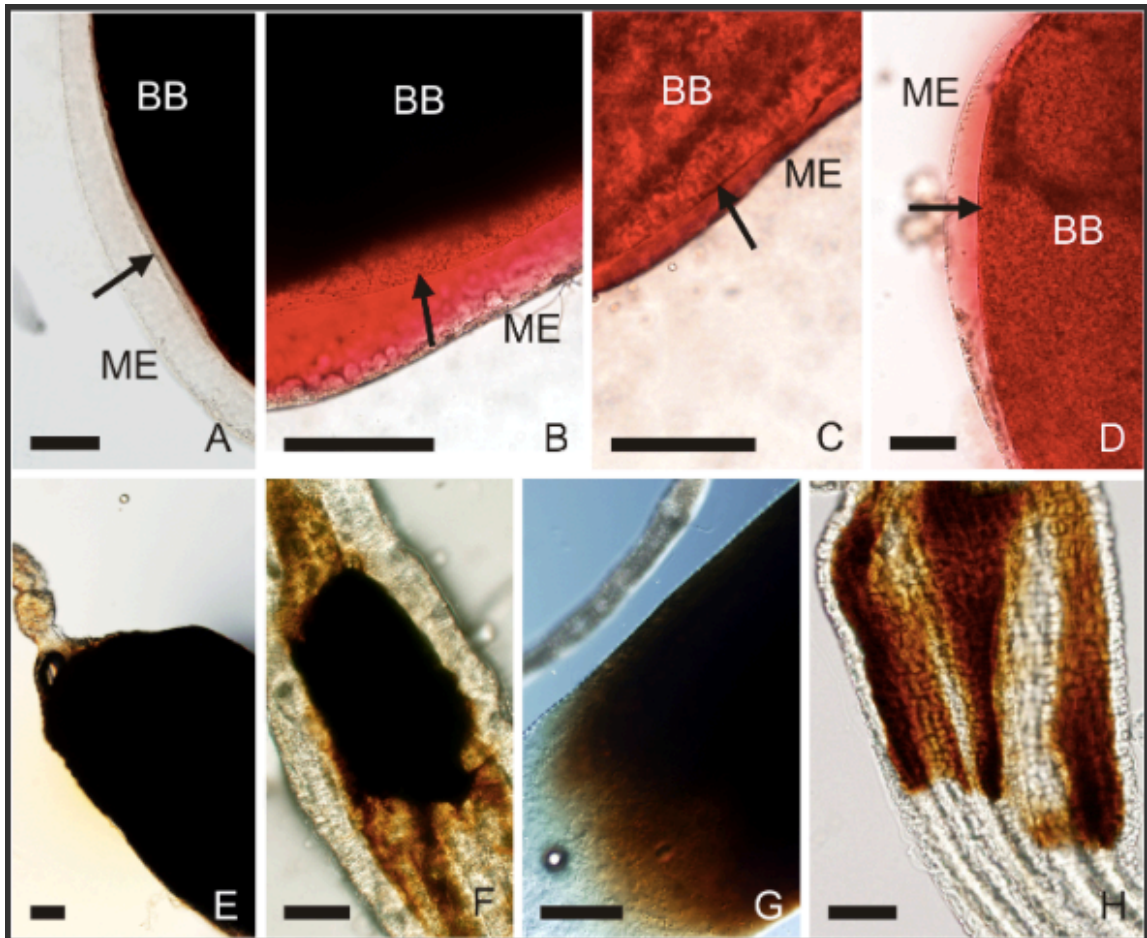


**Figure 7. The digestion of the blood meal within the sandfly midgut.** A-D shows the formation of the PM in *S. schwetzi* (A) and *P. papatasi* (B), *P. orientalis* (C) and in *P. argentipes* (D). The arrow indicates the thin PM separating the blood bolus (BB) from the midgut epithelium (ME). Following digestion, the remnants remain within the PM through its disintegration. E shows the PM intact with no leak of remnants into the ME. F-H shows degradation occurring in the PM causing a leak of remnants into the ME. Image from (Pruzina et al, 2015).

From the changes of diet, the physiology of the midgut of female sandflies modifies to support the digestion of both sugars and blood. These modifications requires the changes of enzymes as well as the changes of pH needed for the appropriate activities (Figure 8) (Santos et al, 2008). Following the blood meal, the slow release of sugars from the crop to the midgut is interrupted by the presence of the blood meal and the modifications (such as changes in enzymes) present for the digestion of blood. These changes: presence of enzymes such as trypsin and chymotrypsin along with the change of acidic pH 6 to alkaline pH 7-8 (Figure 8) allows for protein digestion and potentially favours *Leishmania* development within the gut before an acidic environment is reintroduced post-blood meal.

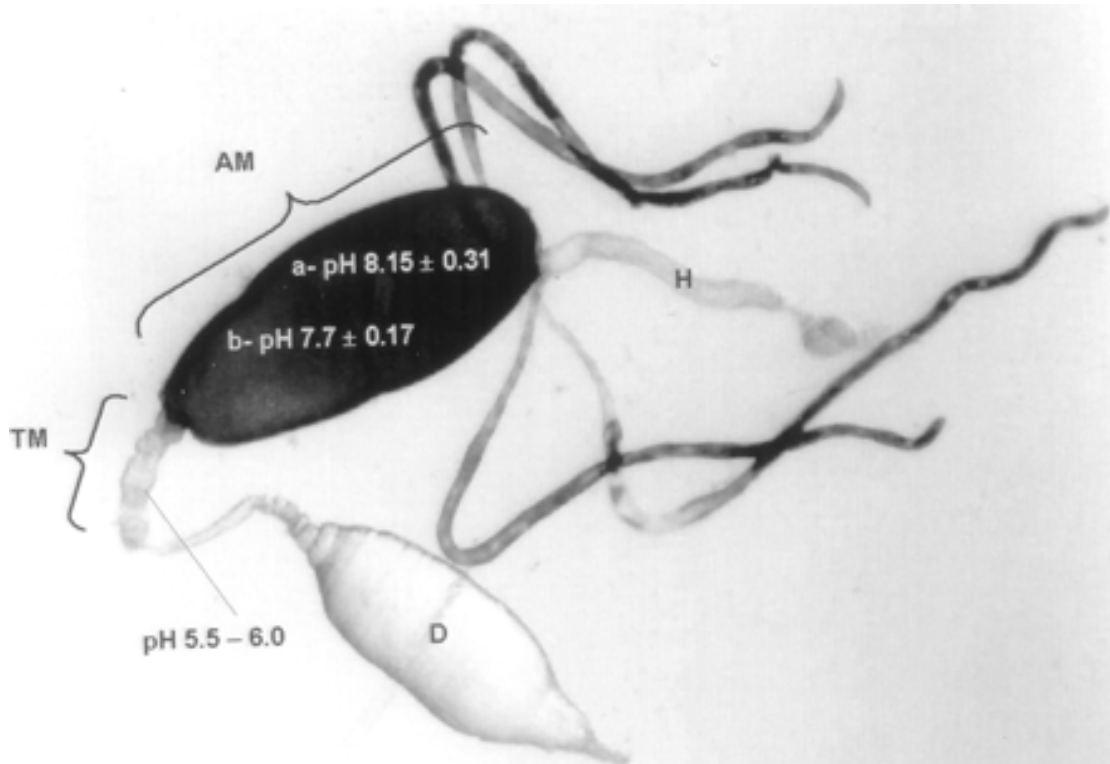


Figure 8. The anatomy of *Lu. longipalpis* gut and the pH of the midgut during the first 10h (a) and 24 hours (b) after blood ingestion shows the returning of an acidic pH from alkaline following the digestion of the blood meal. The thoracic midgut (TM) and diverticulum (D) filled with sugar solution shows an acidic pH (5.5-6). (AM) abdominal midgut. Image from (Santos et al, 2008).

The initial development of *Leishmania* parasites within the gut plays within the fine balance of pH favouring its development along with the hindrances of the presence of the enzymes, midgut peristalsis and the PM development.

#### 1.2.4 Microbiota

Within the gut, *Leishmania* parasites join the symbiotic resident microbial community within the alimentary canal of the sandfly (Pumpuni et al, 1996). The microbiota is said to have a major role influencing the induction, maturation and function of the host immune system (Telleria et al, 2018) along with the development of *Leishmania* parasites (Fraihy et al, 2017); making the interactions between the parasite and sandfly microbiota important in understanding the migration and transmission of *Leishmania*. The life cycle of the sandfly (Figure 4) reflects where resident and pathogenic microbes found in the sandfly's microbiota originates from. This includes disease causing bacteria (Herrer and Christensen, 1975) and viruses (Depaquit et al, 2010).

There is little known about **viruses** found in sandflies (**Depaquit et al, 2010**) however, there are a few phleboviruses transmitted by sandflies that cause disease in humans such as Toscano viruses (TOSV) (**Depaquit et al, 2010**) and Sand fly fever Sicilian Viruses (SFSV) (**Ayhan et al, 2017**). There have been fewer reports of sandflies with the presence of a virus and a *Leishmania* infection. A study using *Phlebotomus papatasi* infected with cytoplasmic polyhedrosis virus (CPV) showed a resistance to the *Leishmania* infection, possibly due to the pathological modifications by the virus preventing the attachment of *Leishmania* to the epithelium and the early exposure to the digestive enzymes found in the gut during blood digestion (**Warburg and Ostrovska, 1987**). Considering other studies of infections of *Leishmania* parasites with various viruses (**Faucher et al, 2014, Ergunay et al, 2014**) it can be determined that there is a complex relationship between the two which differs between *Leishmania* species and specific viruses. Apart from human pathogenic viruses, there are novel viruses of *Lu. longipalpis*; *Lutzomyia Piau*i reovirus 1 (LPRV1), *Lutzomyia Piau*i reovirus 2 (LPRV2), *Lutzomyia Piau*i nodavirus (LPNV) (**Aguiar et al, 2015**).

The life cycle (Figure 4) shows the egg stage and larvae stage from which adult sand flies emerge. Their resident microbiota originates from the diverse and undefined environments in which each stage develop and the food they ingest. This creates a complex network of overlapping bacteria found within the gut of sandflies species which can be seen in Figure 9. This can be dependent on developmental stage and country of origin (**Telleria et al, 2018**).

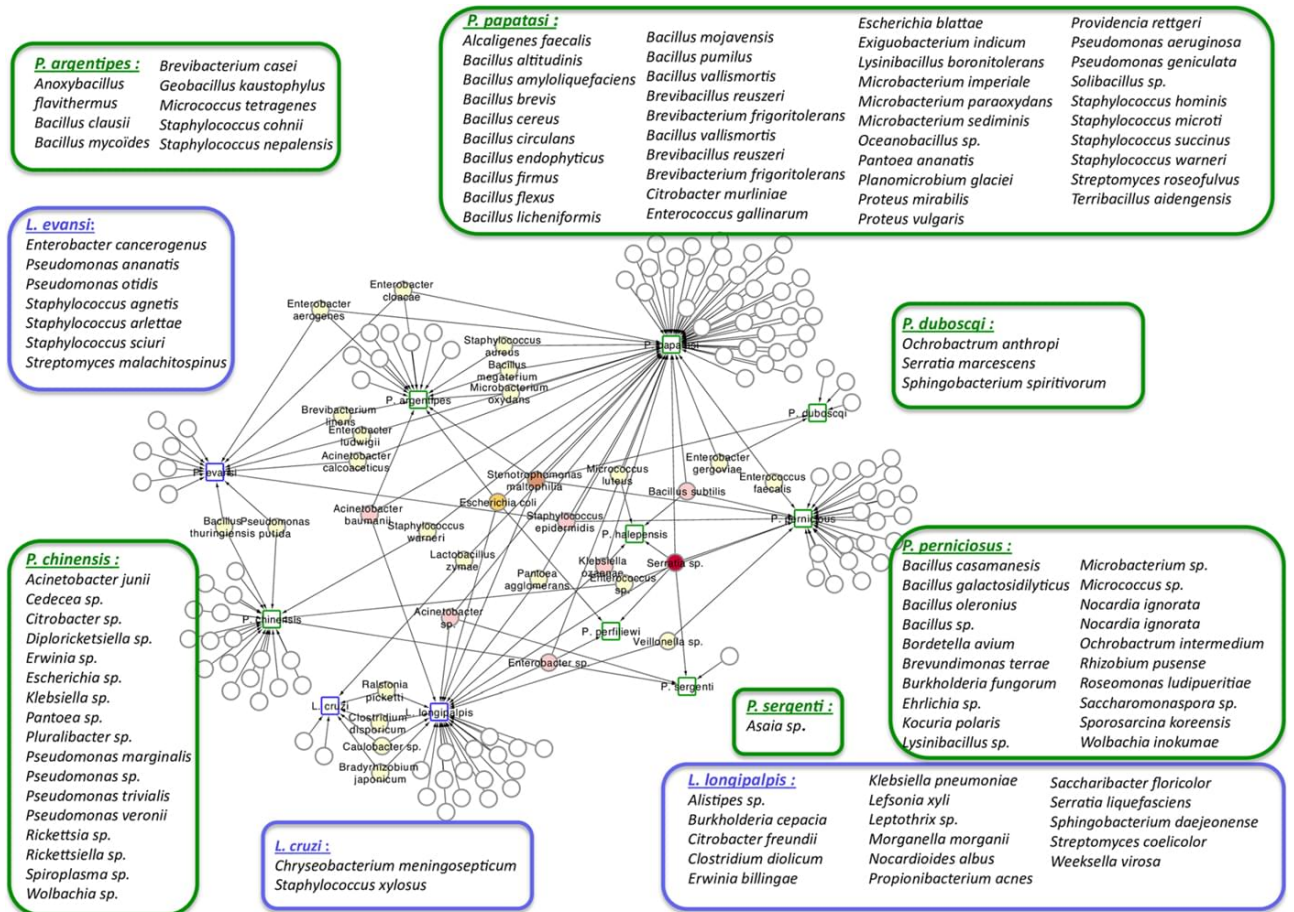


Figure 9. Network analysis showing the shared bacteria species between sandflies species. *Phlebotomus* sand flies are identified by squares surrounded by green and bacteria found in *Lutzomyia* sand flies identified with squares surrounded by blue. Coloured circles represent bacteria species that are shared between sand flies species. White circles represent bacteria species that are unique to each of the sand flies species and are listed inside large rectangles. Image from Fraihi et al, 2017

Ingested food can influence the gut microbiota in both larvae (Vivero et al, 2016) and adult sandflies (Oliveira et al, 2000). The microbial diversity of adult female sandflies changes with blood feeding (Figure 10) with the resident microbiota present in non-blood fed females altering when sandflies are blood fed and return following blood digestion and excreta removed (Endris et al, 1982, Monteiro et al, 2016, Kelly et al, 2017, Pires et al 2017). After a blood meal, bacterial diversity decreases and overall bacteria numbers increase due to the nutrient-rich environment provided by the blood (Volf, Kiewegova and Nemeč, 2002). This shows how substantial a role feeding has on the microbiota of sandflies as *Leishmania* development primarily occurs during blood digestion when the resident microbiota of the gut differs as seen in Figure 10.

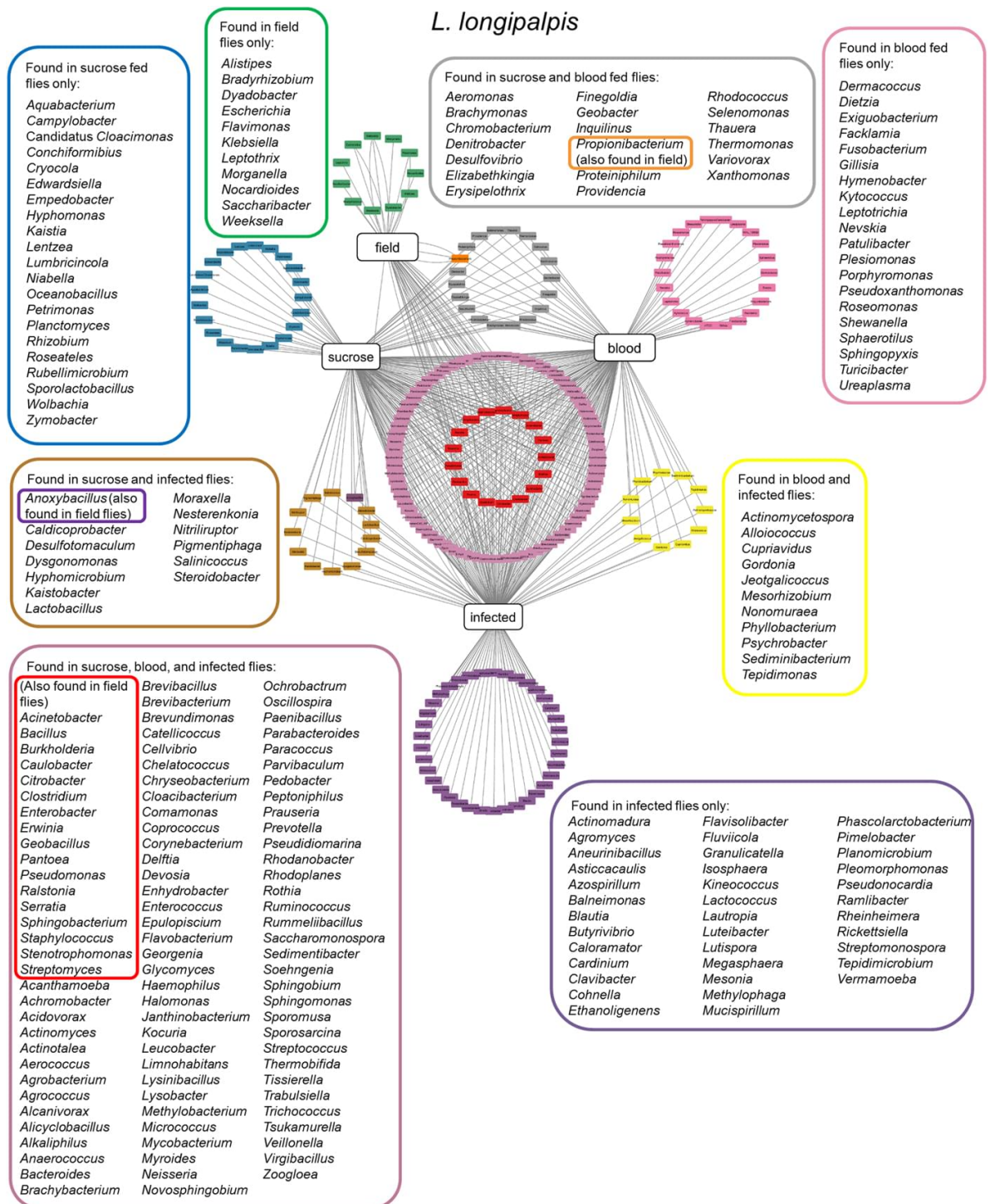


Figure 10. *Lutzomyia longipalpis* gut microbiota. Network analysis showing bacteria found in *Lu. longipalpis* dependent on feeding conditions. Image from Telleria et al, 2018

There is a stark difference in bacteria found in ‘blood and infected flies’ and in ‘blood fed flies only’, however as the data used has been acquired from different publications it represents the wide range of variation of gut microbiota and reflects the conditions of diet and habitat of sandflies globally (Figure 10) (Mukhopadhyay et al,

**2012).** Bacterial diversity of *Leishmania* infected midguts decreases over time post infection to an *Acetobacteraceae* family rich microbiota (**Kelly et al, 2017**). The largest evidence suggesting that the interaction between the microbiota of the sandfly gut and *Leishmania* parasite is important was showed by Kelly et al; antibiotic suppression of gut microbiota resulted in the arrest of parasitic replication and development (metacyclogenesis) without affecting the health of both the sandfly and the *Leishmania* present in the gut showing the huge influence of the microbiota to infection establishment.

The bacteria present in the sandfly gut have not been further compartmentalized into foregut, midgut and hindgut. However, it is understood that quorum sensing will occur in the midgut between bacteria (**Fuqua, Winans and Greenberg, 1994**). During quorum sensing, extracellular signalling molecules are produced to be detected by other bacteria known as autoinducers (AIs). These AIs diffuse producing concentration gradients which can be detected by bacteria via receptors present on their surface. It may be possible for *Leishmania* parasites to also recognise these molecules, producing a response to their presence.

### 1.3 *Leishmania* protozoa - The parasite

There are over 900 species and subspecies of female sandflies from two Phlebotomine genera (*Phlebotomus* and *Lutzomyia*) of which many have been proven to transmit the approximately 40 *Leishmania* protozoa in a zoonotic or anthroponotic manner (Sacks and Kamhawi, 2001). The genus *Leishmania* is made up of protozoa belonging to the Trypanosomatidae family, order Kinetoplastida (Sacks and Kamhawi, 2001). *Leishmania* have a dimorphic life cycle, alternating between two main morphological forms: intracellular amastigotes which are found in the mammalian host and promastigotes which are found in the vector (Figure 11) (Sacks and Kamhawi, 2001). The two forms are significantly different in cell shape and motility, however have a similar organelle organisation (Figure 12).

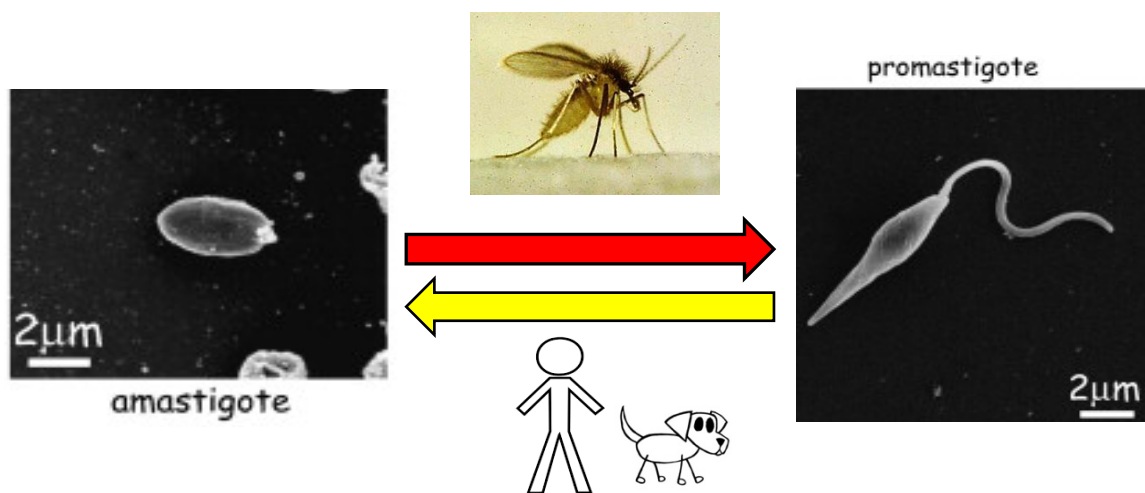


**Figure 11. The two main morphological forms of *Leishmania* spp.** The red arrow shows the amastigote form is ingested by a female sandfly vector during a blood meal, where it undergoes metacyclogenesis through the different forms of promastigotes and transforms into a flagellated metacyclic promastigote. Image in figure shows a procyclic promastigote. The yellow arrow shows this promastigote is transmitted into the mammalian host during the next blood feed where it transforms into the visually aflagellated intracellular amastigote form (amastigotes contain a short flagella which is not visible). Female *Lutzomyia* image from Pete Perkins. Scanning electron microscope images of *L. major* from Besteiro et al, 2007.

The complex transitions that *Leishmania* undergoes within different changes in environment can be stressful. Each developmental form is adapted to cope with environmental stresses, gaining an advantage for survival. These adaptations include nutritional requirements, growth rate, ability to divide, expression of surface molecules and morphology (Besteiro et al, 2007). Amastigotes are well adapted for their intracellular existence within the parasitophorous vacuole in the macrophages:

non-motile as migration is not required, reduced size to exist within a small enclosed space, flagellum length is reduced significantly that it does not emerge from the flagellar pocket (**de Souza and Souto-Padron, 1980**), are acidophiles due to the acidic environment (**Antoine et al, 1990**) and have a different energy metabolism than promastigotes (**Coombs et al, 1982**). Interestingly, from all promastigote forms, metacyclic promastigotes are pre-adapted for the mammalian survival, expressing stage-specific surface molecules and complement-resistant (**Besteiro et al, 2007**). This shows that adaptation occurs not only for the environment they are within but for the next anticipated change in environment.

The morphology of a protozoan is one way to cope with the environmental stresses they may encounter, gaining a competitive advantage for survival. Therefore, observation of the morphology of the cell and their ultrastructures is fundamental to understanding the structure and behaviour of the specific protozoa. The main organelles here are the flagellum, kinetoplast and cell membrane.

### 1.3.1 Flagellum

The immobilisation occurring in the absence of an external flagellum in amastigote forms demonstrates that flagellum is the essential sole means of motility therefore is the key player to migration (**Landfear et al, 2001**). This shows diversity within a singular organism to adapt structure and therefore function for a distinct life cycle stage (**Wheeler, Gluenz and Gull, 2015**). *L. mexicana* can form two distinct flagellum forms; a canonical 9+2 axoneme restricted to motile promastigotes and a 9v axoneme (9+0 axoneme with a collapsed radial symmetry with irregular inward migration of other doublets) restricted to immobile amastigotes used for sensing and signalling (**Silverman and Leroux, 2009, Singla and Reiter, 2006**). The 9+2 axoneme form is present in *Chlamydomonas reinhardtii* a biflagellated green algae that uses its flagella for motility and cell-cell recognition in mating (**Silflow and Lefebvre, 2001**), and the 9+0 axoneme form is present in primary mammalian cilia acting as immobile sensory antennae to coordinate cellular signalling pathways (**Satir and Christensen, 2008**).

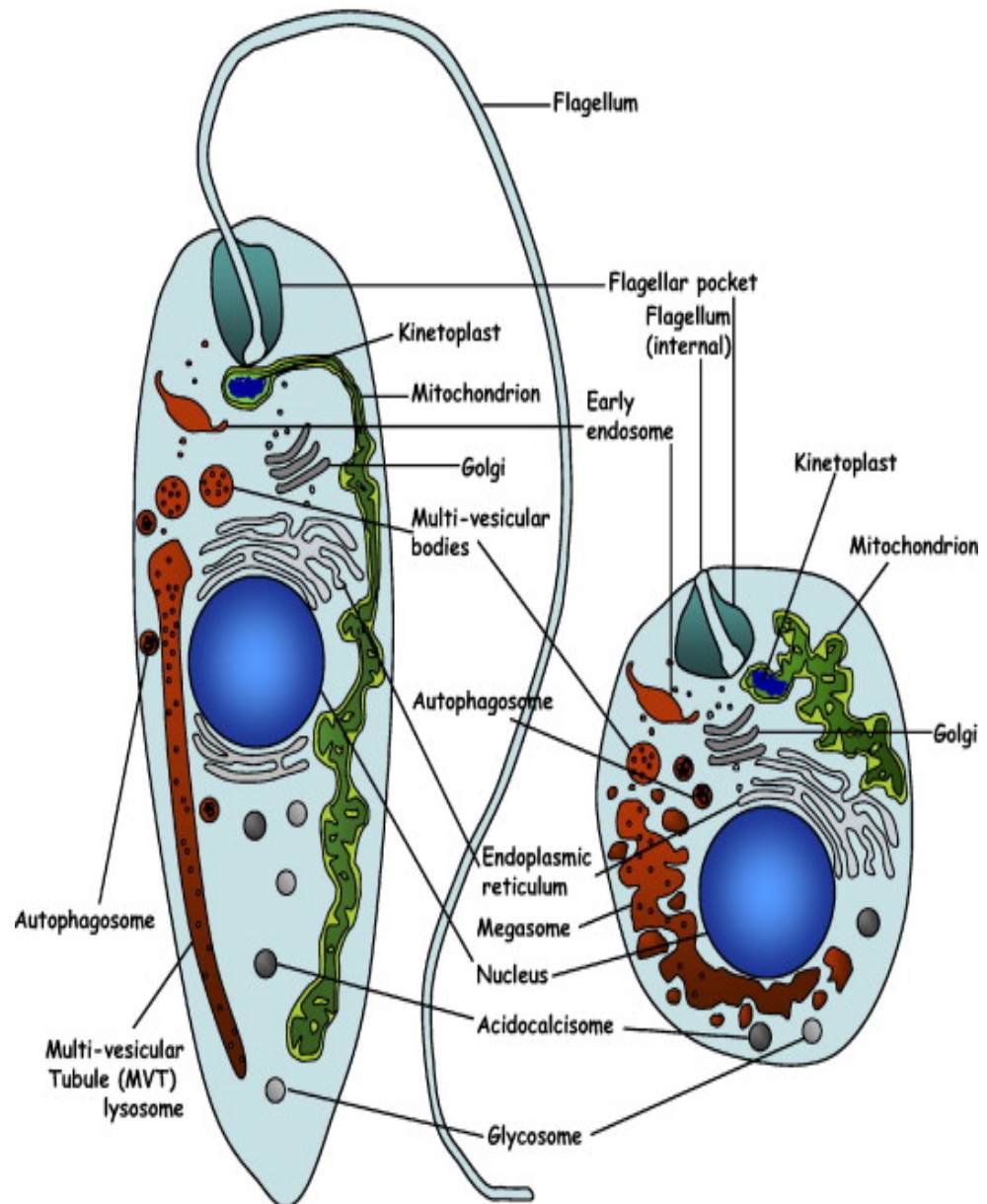


Figure 12. Schematic representation of the main intracellular organelles from *Leshmania* promastigote (left) and amastigote (right) forms. The flagellum pocket represents the anterior end of the cell and migration occurs in a forward motion. Images adapted from Besteiro et al, 2007

The ability to transition between the amastigote and promastigote life stages within a change of environmental factors such as pH and temperature, shows that this transition also occurs with the flagellum axoneme to remodel between the 9+2 and 9+0 forms (**Wheeler, Gluenz and Gull, 2015**). This malleability allows for adaptation needed in different environments; motile parasite transmission or immobile within a macrophage. Ciliogenesis is the process by which the flagellum is built, intraflagellar transport (IFT) increases the flagellar length from the basal body (**Witman, 2003**). IFT decreases during the transition of the 9+2 form to the 9+0 axoneme structure, and the requirement of paraflagellar rod (PFR) (**Langousis and Hill, 2014**) for normal motility suggests that both IFT and PFR play a key role in the flagellum shortening and loss of central pair. For motility, axonemal dynein motors which are attached to the A-tubule of each outer doublet microtubule undergoes structural changes powered ATP-dependently. This causes reversible attachment to B-tubule of the neighbouring doublet, sliding of doublets and resistance causing bending, known as the 'sliding filament' mechanism (**Satir, 1968**) causing movement by wave-like beating of the flagellum. The flagellum pocket is an invaginated site specialized for endocytosis, making it a portal for host-parasite interactions; relaying information about the microenvironment to allow changes in the parasite to reflect the demands of its environment (**Landfear and Ignatushchenko, 2001**).

### 1.3.2 Kinetoplast

As a flagellated protozoa with the presence of a kinetoplast in the mitochondrion, *Leishmania spp* is a kinetoplastid (**Simpson, 1968**). Other parasites in this category such as *Trypanosoma cruzi* and *Trypanosoma brucei* responsible for serious human diseases such as Chagas disease and African sleeping sickness respectively, share the commonality of kinetoplast DNA (kDNA) described by Trager as 'a small spherical or rod-shaped structure lying just posterior to the basal body of the flagellum' (**Trager, 1965**). Kinetoplastids have similar genomic organization and cellular structures, undergoing morphological changes during the progression of their life cycle and having 6,000 orthologs (common ancestral genes) out of 8,000 genes (**Stuart et al, 2008**) in their genome in common. They however have very distinct properties such as their insect vector and the resulting human disease. These

commonalities, allows for the advanced knowledge of kDNA in Trypanosomes spp to support and build on that of *Leishmania* spp.

Along with cell morphological changes observed in development, the kinetoplast is useful for pinpointing the progression within the life cycle of kinetoplastids. It is therefore used to determine differentiated forms due to its positional movement relative to other organelles; particularly the nucleus during cell progression. The morphologic forms of flagellates are defined by the position of the flagellum pocket, nucleus and kinetoplast which varies along the anterior/posterior axis of the cell body. As the kDNA is always posterior to the flagellar pocket and remains closely connected to the basal body (**Vargas-Parada, 2010**), this morphology can simply be defined as the kDNA location relative to the nucleus. This simplistic categorization results in 4 categories where the position of the kinetoplast changes relative to the nucleus; trypomastigote, epimastigote and promastigote having a long/slender body with a protruding flagellum, and amastigote having a round/oval shaped with no protruding flagellum (Figure 13). The flagellum emergence dictates the anterior end of the cell body. In trypomastigotes, the kDNA and flagellar pocket is located at the posterior end of the parasite relative to the nucleus. Epimastigotes have a close centralized kDNA, anterior to the nucleus; and due to the flagellum spanning along the cell body an undulating membrane is formed in a similar manner to that in trypomastigotes. In Trypanosomes spp., the posterior flagellum emerges from the flagellar pocket however is not free as it attaches to the cell body creating morphological forms (trypomastigotes and epimastigotes) with undulating membrane. Promastigotes have the kDNA located furthest anterior to the nucleus resulting in the flagellum being completely free and without an undulating membrane.

The morphologies present for each flagellate life cycle are restricted and dependent on specific species; *Trypanosoma brucei* only having trypomastigote and epimastigote forms (**Field and Carrington, 2009**) and *L. mexicana* only having amastigote and promastigote forms.

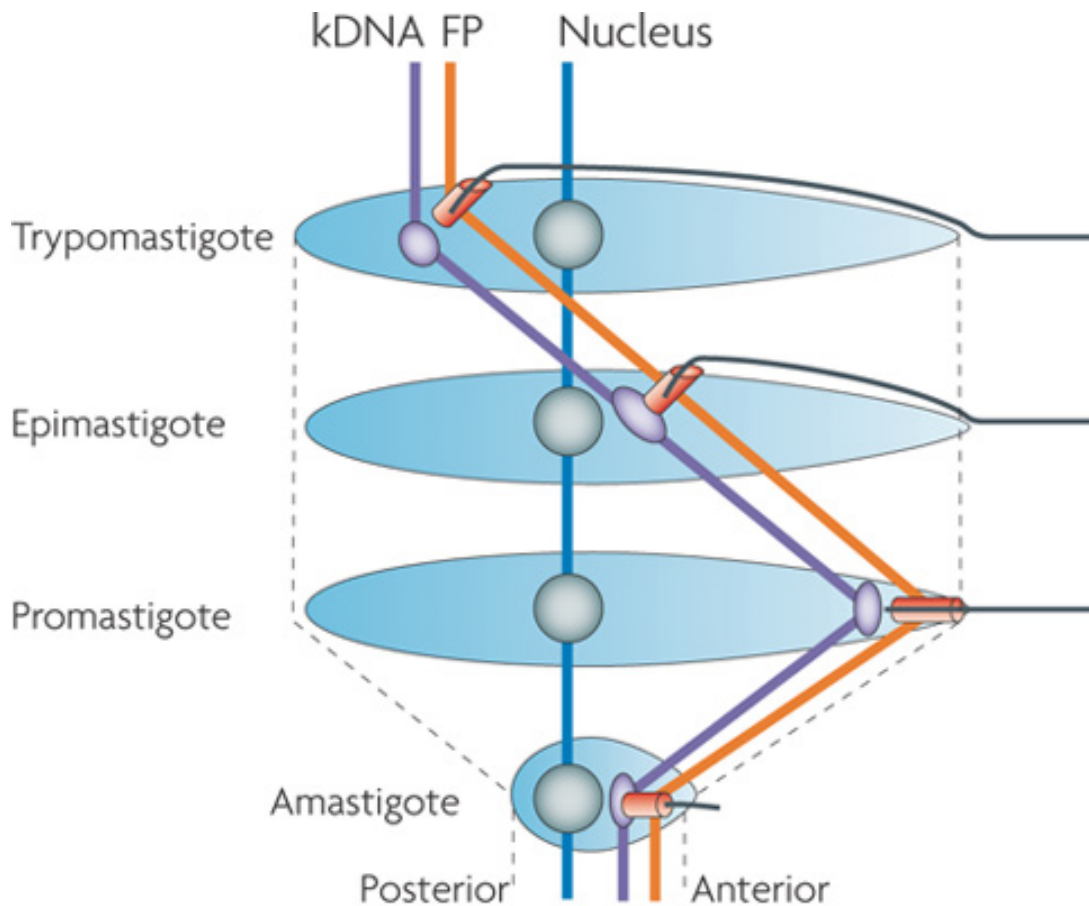


Figure 13. Kinetoplast repositioning in relation to other organelles during the life cycle of a flagellate. FP flagellar pocket, kDNA, kinetoplast DNA. Image from Field and Carrington, 2009.

With the kinetoplast location being one of the key observations to pinpoint progression of life cycle, understanding the kinetoplast movement is important. The kinetoplast is attached to the basal body which is adjacent to the flagellar pocket; the flagellum is formed by extension from the basal body (Wheeler, Gluenz and Gull, 2015). This relation between the three different components (nucleus, flagellar pocket and kDNA) results in differences between the length of unattached flagellum at the anterior end of the cell affecting the motility of the cell.

### 1.3.2.1 Cell cycle

Within an asynchronous population of *Leishmania* promastigotes, dividing cells can be identified through morphological changes by phase contrast microscopy (Ambit et al, 2011). With the use of DAPI (4',6-diamidino-2-phenylindole) staining the nucleus (N) and the kinetoplast (K) with the visualisation of the cell body and the flagellum, the cell cycle position of the individual cell can be given. A cell in G1 phase has the

configuration of 1N1K1F and a cell in cytokinesis has the configuration 2N2K2F configuration.

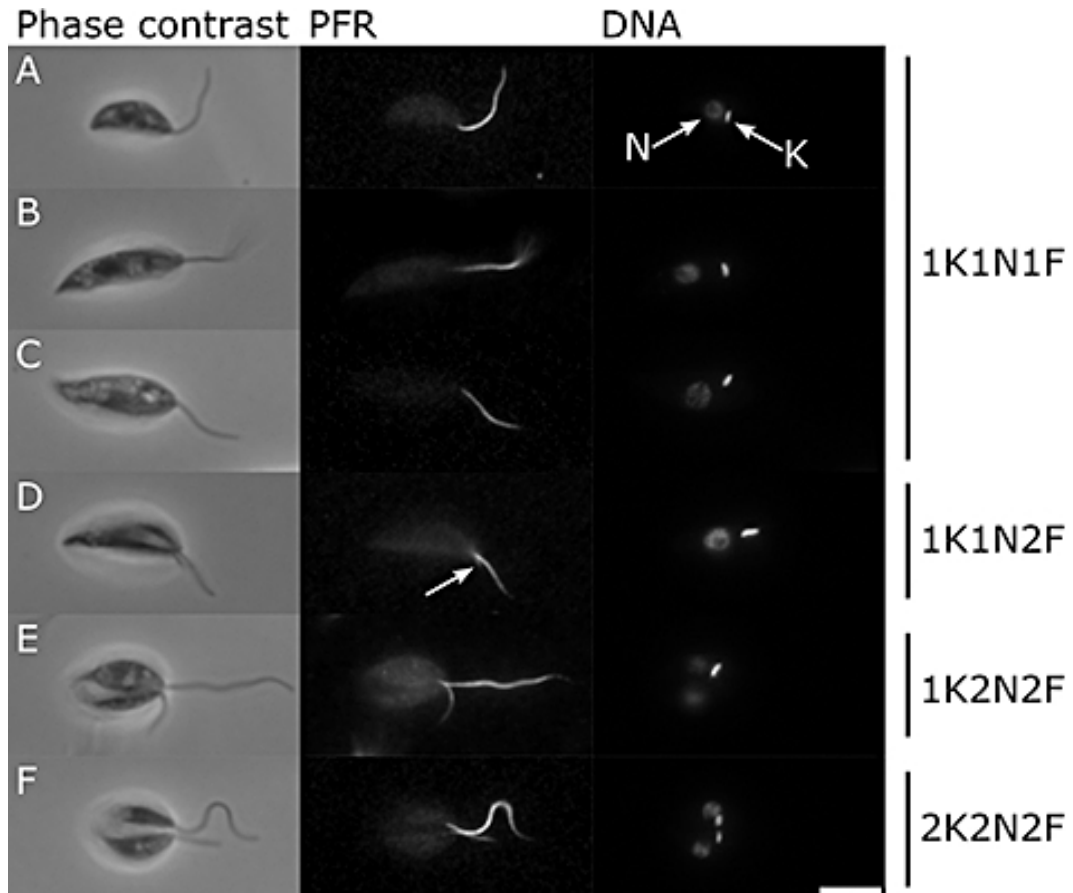


**Figure 14.** The cell cycle of promastigote *L. mexicana* by light microscopy. Micrographs of major cell cycle stages; cells were ordered based on number of kinetoplasts (K), nuclei (N) and flagella (F). The kinetoplast and nucleus are indicated in (A). Arrow in D shows the emergence of the new short flagellum. The scale bar represents 5  $\mu$ m. Image from Wheeler, Gluenz and Gull 2010

During the cell cycle, the *Leishmania* cell initially grows in length with the DNA content remaining constant (Figure 14 A). DNA synthesis begins with the duplication of DNA content while cell length remains constant (S phase) (Figure 14 B and C). Finally, the cell length reduces (G2 phase and mitosis) (Figure 14 D and E) and cytokinesis divides (Figure 14 E and F) the cell from daughter cell, returning to the start of the cell cycle (Wheeler, Gluenz and Gull 2010).

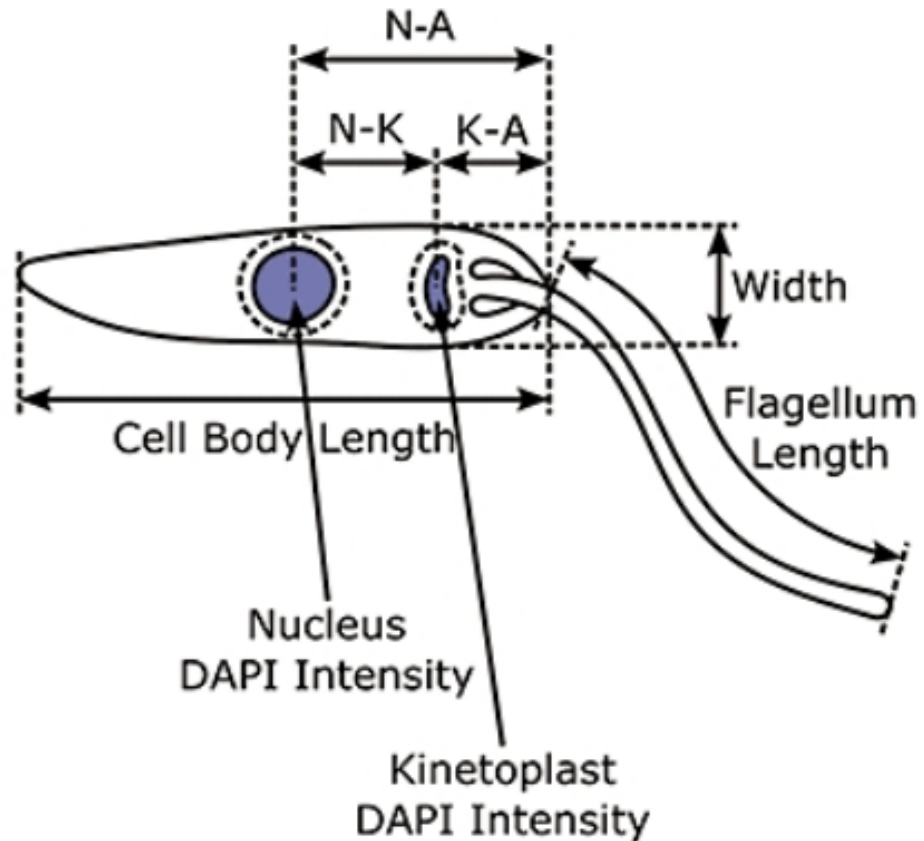


**Figure 15.** Illustrations showing the properties of each cell measurement: cell body length and width, kinetoplast and nucleus DAPI intensity, flagellum length, kinetoplast-anterior (K-A) length, nucleus-kinetoplast (N-K) length, and nucleus-anterior (N-A) length. Image from Wheeler, Gluenz and Gull 2010

The kinetoplast of *L. mexicana* is positioned at a constant distance of approximately 2.5  $\mu\text{m}$  from the anterior end of the cell (Wheeler, Gluenz and Gull 2010). Nuclear position within the cell varies but has a relationship with the cell length defined as  $n \approx 2.5 + 0.2l$  where  $n$  = anterior–nucleus distance and  $l$  = cell length in micrometres (Figure 15) (Wheeler, Gluenz and Gull 2010).

### 1.3.2.2 Morphometrics

There are different morphological changes that promastigotes undergo during metacyclogenesis from the initial procyclic promastigote to the metacyclic promastigotes. These developmental forms are defined according to their cell body length, cell body width and flagellum length (Figure 16) (Rogers et al, 2002):

	<b>Morphological category</b>	<b>Criteria</b>
<b>Promastigote forms</b>	Amastigote	Round body No visible flagellum
	Procyclic	Body length 6.5 - 11.5 $\mu\text{m}$ Flagellum < Body length
	Nectomonad	Body length $\geq 12 \mu\text{m}$
	Leptomonad	Body length 6.5 - 11.5 $\mu\text{m}$ Flagellum $\geq$ body length
	Hptomonad	Expansion of flagellum tip
	Metacyclic	Body length $\leq 8 \mu\text{m}$ Body width $\leq 1 \mu\text{m}$ Flagellum > Body length
	Paramastigotes	Kinetoplast adjacent to nucleus Visible flagellum present

Figure 16. Illustration of promastigote morphologies categorisation. *L. mexicana* morphological categorization (Rogers et al, 2002)

### 1.3.3 Plasma membrane

The contiguous surface membrane (Figure 17) of kinetoplastid protozoa are divided: the flagellar membrane, the flagellar pocket and the pellicular plasma membrane each unique to each other (**Landfear and Ignatushchenko, 2001**).

The flagella pocket is the deep invagination at the base of the flagellum, responsible for uptake of large nutrients by endocytosis and secretion of proteins. L-haemoglobin is seen to be internalised from the flagella pocket membrane (**Landfear and Ignatushchenko, 2001**). Filamentous acid phosphatase (sAP) and filamentous proteophosphoglycan (fPPG) is secreted into the extracellular medium here.

The flagellar membrane covers the flagellum. Specialised membrane proteins are found in the flagella membrane and serve in sensing and signalling such as LmjAQP1 (**Figarella et al, 2007**), ISO1 (**Snapp and Landfear, 1999**), LmGT1

(Burchmore et al, 2003), receptor-adenylate cyclases (Sanchez et al, 1995). LmjAQP1 is a aquaglyceroporin channel involved in detection of extracellular osmotic gradients and osmotaxis (Figarella et al, 2007). LmGT1 is a glucose transporter also found in flagella pocket membrane. Receptor-adenylate cyclases have been expressed and may function as an adenylate cyclase (Sanchez et al, 1995). ISO1 is also found in the flagella pocket (Landfear and Ignatushchenko, 2001). This shows the flagellum pocket and flagellum membrane allows for the detection of signals through the membrane proteins located here.

The pellicular plasma membrane covers the entire of the cell surface and is covered with densely packed microtubules and glycolipid lipophosphoglycan (LPG) coat and contains many permeases for nutrient uptake (Landfear and Ignatushchenko, 2001), such as LmGT2 and LmGT3.

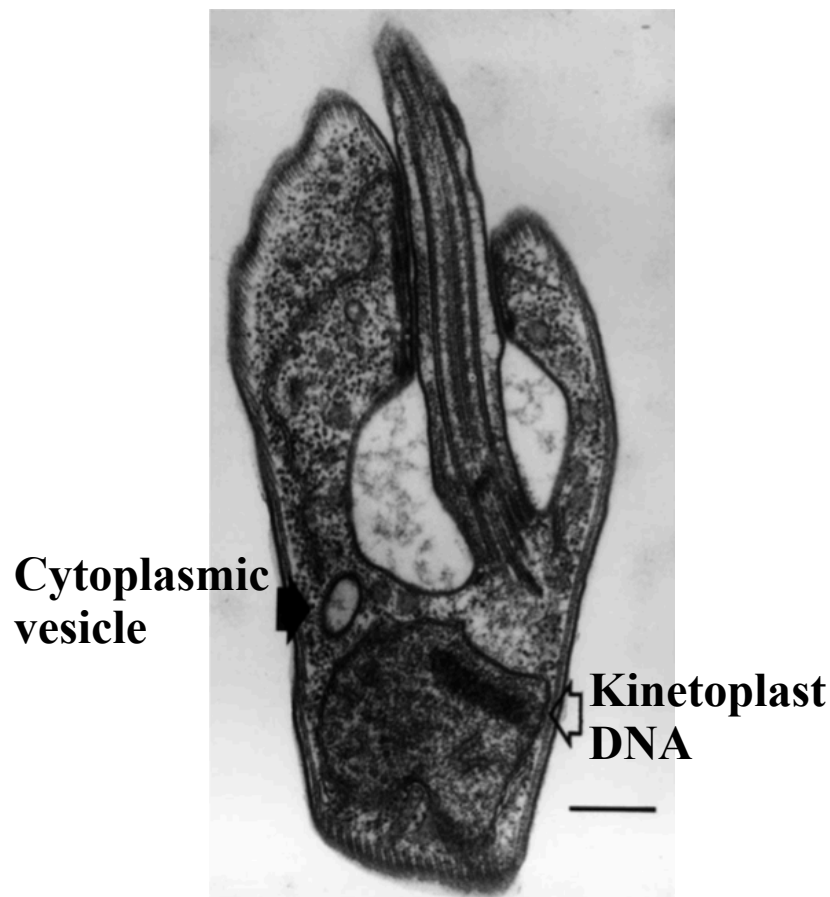


Figure 17. A electron micrograph through the flagellar pocket of a kinetoplastid (*T. brucei*) showing the contiguous surface membrane. Image from Landfear and Ignatushchenko, 2001.

Nutrition of all protozoa is holozoic, therefore they require organic materials **(Johnson, 1941)**. Parasitic protozoa such as *Leishmania*, acquire nutrients from the hosts by using transport proteins located on their plasma membrane known as permeases. Due to the intracellular parasitism nature of the life cycle, there are obstacles that the parasite needs to overcome to acquire the nutrients required for growth **(Landfear, 2011)**. These are described by Landfear as competition with the sandfly and mammalian host for essential nutrients required and the distinct environmental stresses in the sandfly and the macrophages. These distinct environments lead to stresses such pH, temperature and available nutrients found in each of the host. These can be solved by the parasite having an nutrient uptake system which can be modified to accommodate the alternate environment each host; alteration in the uptake in accordance to available nutrient and developmental stage of parasite.

Amastigotes remain within the parasitophorous vacuole (PV) in the macrophage of the mammalian host, there are two main ways in which amastigotes may obtain nutrients; vesicular transport and transporters. Vesicular transport from the macrophage plasma membrane of phagolysosomal degradation products present in the PV lumen or from the host cell cytosol. Nutrients such as hexoses, purines, iron and polyamines are imported through transporters on the cell surface membrane (Table 1) into the amastigote by transporters located in the parasite plasma membrane **(Landfear, 2011)**.

Nutrient (s)	Parasite	Transporters (location)
<b>Hexoses</b>	<i>L. mexicana</i>	LmxGT1 (FM, FPM) LmxGT2 (PPM) LmxGT3 (PPM)
<b>Purines</b>	<i>L. donovani</i> <i>L. major</i>	LdNT1 to LdNT4 LmaNT1 to LmaNT4
<b>Iron</b>	<i>L. amazonensis</i>	LIT1
Polyamines	<i>L. major</i>	LmaPOT1
<b>Amino acids</b>	<i>L. donovani</i>	LdAAP3
Polyols	<i>L. donovani</i>	LdMIT
Folates	<i>Leishmania species</i>	FT1 to FT14
Nucleotide sugars	<i>L. donovani</i> <i>L. major</i>	LPG2 LPG5
Phospholipids	<i>L. donovani</i>	LdMT
Water, glycerol, osmolytes	<i>L. major</i>	LMAQP1
Cations	<i>L. amazonensis</i>	Lmaa1

**Table 1. Transporters in Leishmania species and the nutrients they provide.** FM flagellar membrane PPM Pellicular plasma membrane FPM flagella pocket membrane (Landfear, 2011).

### Hexose transporters

Hexose sugars include glucose, fructose, galactose and mannose. Plant nectar is an important part of sandfly diets. Therefore these sugars are readily found in high concentrations within the thoracic midgut of the sandfly following a sugar meal (**Schlein, 1986**). Hexose transporter genes LmxGT1, LmxGT2 and LmxGT3 are encoded in *L. mexicana* genome by single copy genes that are clustered together at a single locus (**Burchmore and Landfear, 1998**) and homologous to mammalian glucose transporter (GLUT) family. There is a significant downregulation of these genes in amastigotes, reflecting the lower glucose concentration within the macrophage (**Cairns, Collard and Landfear, 1989**). Glucose is metabolised by promastigotes as a source of energy that is readily available, using the glycosome organelle to contain and metabolise the glucose (**Opperdoes, 1987**).

LmGT1, LmGT2 and LmGT3 proteins transport glucose, fructose, galactose and mannose, and LmGT2 and LmGT3 transport ribose (Naula et al, 2010). The LmGT1 membrane protein acts as a glucose sensor, null mutants of LmGT1 growth is rapid without entering stationary phase, therefore may ensure that parasites know when glucose has been exhausted (Burchmore et al, 2003).

### **Purine transporters**

*Leishmania* lack a de novo biosynthetic pathway to synthesize purines, therefore as an essential nutrient these need to be salvaged from host (Hammond and Gutteridge, 1984). In this process preformed purine nucleosides or nucleobases are salvaged and transported into the parasite, followed by interconversion or metabolism to phosphorylated nucleotides which can be used (Landfear, 2011). Identified nucleoside transporters for specific purine includes; LdNT1 (substrates adenosine and the pyrimidine nucleosides) (Vansudevan et al, 1998), LdNT2 (substrates inosine, guanosine, xanthosine) (Carter et al, 2000), LmaNT3 and LmaNT4 (the substrates hypoxanthine, xanthine, adenine, and guanine). These purine transporters are active proton-coupled symporters therefore can use their high affinity to compete with host tissues effectively. Interestingly, NT3 and NT4 have differing transport optimum pH. NT3 has an optimum neutral whilst NT4 has an optimum acidic pH. This suggests that NT3 is designed to function optimally in the insect vector whilst NT4 is designed to function optimally in the phagolysosome (Ortiz et al, 2009). Low levels of purines are detected by *Leishmania* and responded to by the upregulation of mRNA encoding purine transporters for the salvaging (Carter et al, 2010).

### **Iron transporters**

The phagolysosome is kept free of iron by a  $\text{Fe}^{2+}$  pump, therefore *Leishmania* are in an area lacking iron. This is done as  $\text{Fe}^{2+}$  is toxic in high levels, however iron is taken up by *Leishmania* in the form of  $\text{Fe}^{2+}$  (Wilson et al, 2002). Holotransferrin, a complex of two  $\text{Fe}^{3+}$  ions and transferrin protein is however present in phagolysosome. The iron in these complexes are utilised by *Leishmania* however needs to be reduced prior to internalization (Wilson et al, 1994). A membrane-bound NADPH-dependent iron reductase converts  $\text{Fe}^{3+}$  bound to protein to  $\text{Fe}^{2+}$  at the extracellular surface of the parasite (Wilson et al, 2002); *Leishmania* iron transporter

LIT1-1 and LIT1-2. These are however only expressed in environment lacking iron, therefore not expressed in promastigotes (**Landfear, 2011**) and could possibly be a trigger for the differentiation of amastigotes (**Mitra et al, 2013**).

### **Amino Acid transporters**

Amino acids have multiple functions and this is showed by amino acid transporters representing the largest families of permeases (except for ABC transporters) encoded within the genome, with about 35 in *Leishmania major* (**Aslett et al, 2009**). AAP3 arginine carrier from *L. donovani* (LdAAP3) (**Shaked-Mishan et al, 2006**) transport arginine an essential amino acid in protein synthesis and used a s a precursor for polyamines synthesis, and *LdAAP7* transport lysine (**Inbar et al, 2010**).

## CHAPTER TWO: LITERATURE REVIEW

### 2.1 *Leishmania* Sand fly Interactions

*Leishmania* parasites need sand flies to complete their life cycle and to propagate (**Kamhawi, 2006**). Parasites are transmitted by the bite of an infected insect vector. To achieve the status of being a vector, there are criteria that need to be fulfilled. This includes the vector showing anthropophilia, the vector being found in nature infected with the same *Leishmania* species as found within human and reservoir infections in the same area, the vector fully supporting the development of parasite after the digestion of the blood meal and the ability to transmit the parasite by a bite (**Killick-Kendrick, 1990**). Therefore, parasite vector interactions important for the possibility of transmission includes the ability to survive defecation by attaching to the midgut epithelium, and the migration of infective forms of the parasites to the stomodeal valve and anterior midgut (**Maia and Depaquit, 2016**).

#### 2.1.1 Metacyclogenesis of suprapylaria *Leishmania*

Within the sand fly, *Leishmania* parasites undergo a complex development process that occurs exclusively within the alimentary canal. This begins in the midgut where macrophages infected with amastigotes are introduced to the digestive tract with the ingested bloodmeal which goes through the digestion process. During the digestion, parasites multiply and their morphology changes from the amastigote form to the flagellated promastigote motile form. The blood meal arrival to the midgut induces the production of the peritrophic matrix (PM), therefore *Leishmania* present in the blood meal is further confined within the PM. To establish infection, surviving parasites need to escape defecation and successfully attach to the midgut epithelium (**Pruzinova et al, 2015**). This process from introduction to the digestive tract of the sandfly to the establishment of infection in the midgut has many hindrances that need to be overcome for establishment of infection. These includes successful development and morphology changes of parasite, surviving digestion, escaping from the PM and successful attachment to the epithelium before defecation occurs.

### **Surviving digestion and escaping the PM**

Infected blood containing amastigote *Leishmania* passes into the abdominal midgut (**Kamhawi, 2006**) where the PM is secreted by the midgut epithelium within the first couple of hours of blood ingestion (**Dillon et al, 2006**). However before the PM is fully formed, enzymatic activity is the first hinderance that parasites need to overcome for successful infection (**Telleria et al, 2010**). Enzymatic activity includes aminopeptidase, chymotrypsin, carboxypeptidase, alpha-glucosidase and trypsin activity which occurs during the digestion process of sandflies (**Sacks and Kamhawi, 2001**). Aminopeptidase activity is associated with the midgut wall. Trypsins are digestive enzymes abundant in most insects (**Telleria et al, 2010**), with activity associated with the midgut lumen. The blood meal is entirely contained in the PM within 4 hours of ingestion (**Kamhawi, 2006**), here the digestion of the blood meal occurs (**Dillon and Lane, 1993**). The formation of the PM, protects the parasites from the hostile digestive enzymes as the diffusion from the lumen into the space within the PM is slower (**Pimenta et al, 1997**) allowing for differentiation to occur. However this decreases the chance of parasite escape from the blood bolus and being defecated (**Sacks and Kamhawi, 2001**). *Leishmania* parasites differentiate into distinct morphological stages which aids in the migration and therefore survival in the sandfly alimentary canal (**Kamhawi, 2006**).

The first morphological change that occurs following the release of amastigotes from macrophages into the blood is the transformation to a procyclic promastigote form. Most *Leishmania* parasites are killed by the actions of the enzymes early on as the transitional stage between amastigotes and procyclic are susceptible to the proteolytic attack (**Pimenta et al, 1997**). Procyclic promastigote has a small fat ovoid body and a short flagellum limiting its motility (**Sacks and Kamhawi, 2001**). This form is resistant to the initial digestive enzymes in the blood meal and undergoes rapid replication for 24-48 hours. Following this replication period, the procyclic promastigotes undergo the second morphological change to nectomonads which are longer, slender and highly motile (**Sacks and Kamhawi, 2001**). This differentiation occurs concurrently to the degradation of the PM by midgut-secreted chitinase, allowing nectomonads to initiate the escape from within the blood meal to the gut lumen (**Kamhawi, 2006**). Nectomonads accumulate at the

anterior of the blood bolus as the PM degradation initiates from the anterior (**Sacks and Kamhawi, 2001**).

### **Attachment to the matrix wall- hindrance**

Within the gut lumen, nectomonads may attach to the midgut epithelial wall using LPG on the surface of their flagellum to the glycoconjugates on the microvilli in the midgut; this allows parasites to escape defecation. Attachment of *Leishmania* nectomonads to the microvilli on the surface of the midgut epithelium is important for successful development of parasites within the sandfly midgut (**Dillon et al, 2006**).

These nectomonads also initiate migration towards the anterior midgut and some nectomonads undergo another differentiation into leptomonads, a shorter form of nectomonads. Due to migration and rapid replication, both nectomonad and leptomonad forms are found to colonize the thoracic midgut where they undergo the transformation into metacyclic and haptomonad promastigotes (**Rogers et al, 2002**). Within the stomodeal valve, leptomonads secrete parasite secreting gel (PSG) which contains a large number of metacyclic promastigote (**Stierhof et al, 1999**) and the leptomonads that are continuously replicating and differentiating into metacyclics. Metacyclic promastigotes have slender bodies and the longest flagellum advancing their motility and haptomonad promastigotes bind to the cuticle-lined surface of the valve via the insertion of the flagellum into the hemi-desmosome-like structures. The metacyclic promastigote form is known widely as the infective stage parasite (**Kamhawi, 2006**). This whole process which is dependent on the *Leishmania* species, roughly takes 6-9 (**Kamhawi, 2006**) days

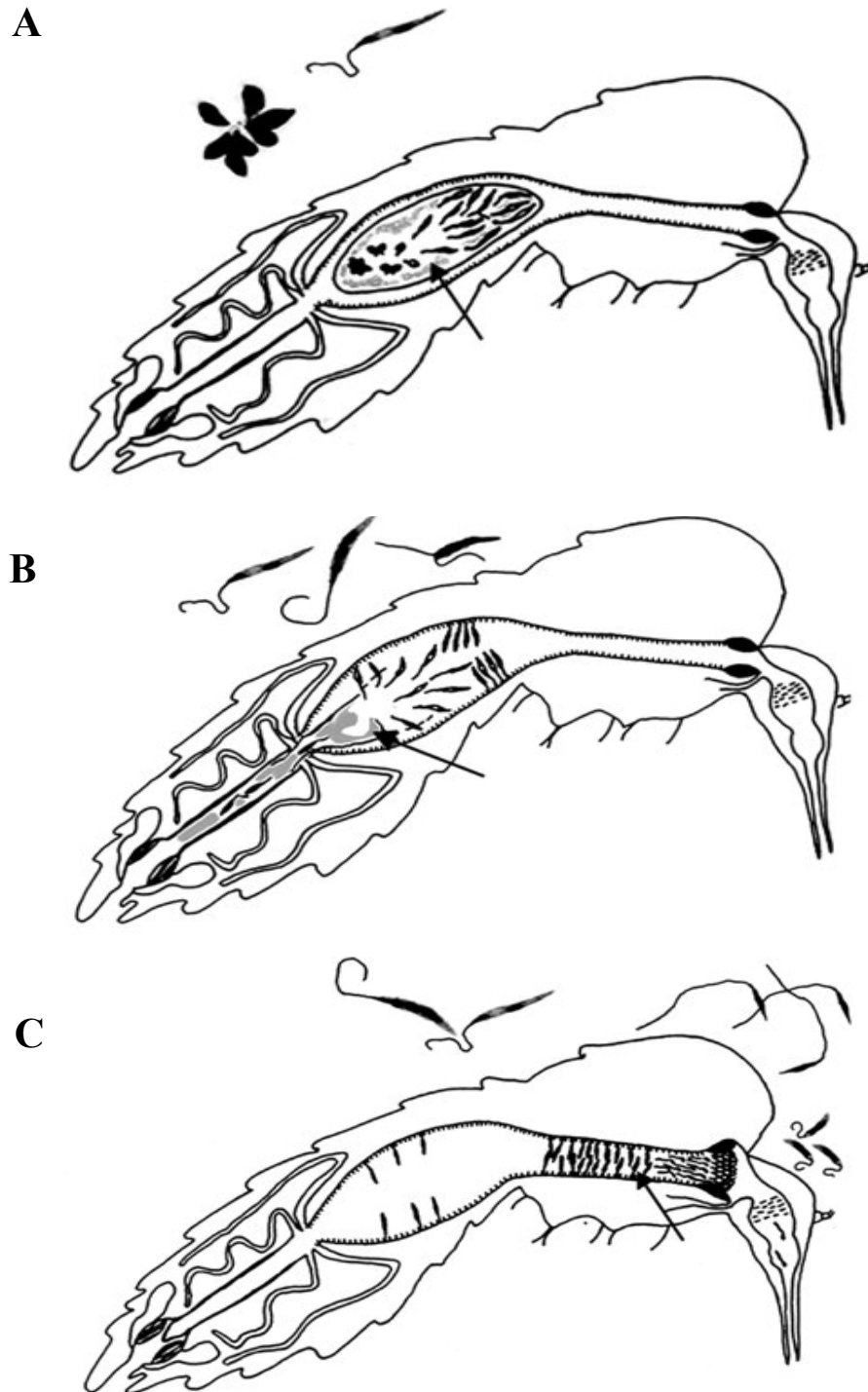


**Figure 18. Metacyclogenesis of suprapylarian *Leishmania*.** The development of *Leishmania* in a permissive vector in a time dependent manner, showing the morphological changes that occurs from procyclics to haptomonads within the sandfly midgut. A) Procyclic promastigotes transform to nectomonad promastigotes which migrate to the anterior of the blood bolus as PM disintegration initiates at the anterior. B) Nectomonads escape from the blood bolus. Digested blood begins to be excreted. Nectomonads attach to the midgut epithelium and transform to leptomonads which rapidly replicate. C) Some nectomonads remain attached to the midgut. Leptomonads migrate to the thoracic midgut where they secrete PSG and transform to motile metacyclics and haptomonads. The PSG damages the cardia and some parasites escape to the foregut. Image from Sacks and Kamhawi, 2001.

### 2.1.2 Developmental cycles in the sand fly

Metacyclogenesis within sand flies can vary depending on the *Leishmania* species. However, in literature, most of the illustrated metacyclogenesis is based on suprapylarian *Leishmania* species such as *L. mexicana*, *L. amazonensis* and *L. chagasi*. Through the section of gut in which development occurs, *Leishmania* species can be divided into 3 groups as suggested by Lainson et al. (**Lainson et al, 1979**): hypopylaria, peripylaria and suprapylaria (Figure 19).

Hypopylarian species develop in the hindgut and are assigned the subgenus *Sauroleishmania* such as *L. tarentolae* (**Lainson et al, 1979**). These species are not transmissible to mammalian hosts but have a lizard host and natural vector *Sergentomyia* sandfly. There is little known about the transmission of *Sauroleishmania*, however it is hypothesized that reptiles get infected by consuming infected sandflies (**Wilson and Southgate, 1979**). Possible reasons for the inability of transmission has been associated to the thicker PM formed around the BB by *Sergentomyia* compared to *Lutzomyia* and *Phlebotomus* sandflies. This does not support anterior migration or metacyclogenesis as parasites cannot escape the thicker PM and development is therefore arrested at procyclic promastigotes (**Lawyer et al, 1990**). However when a *L. tarentolae*, a hypopylarian species develops within *Lutzomyia longipalpis*, development is seen and attachment to the hindgut epithelial is viewed however anterior migration does not occur and parasite is lost (Dillon and Liu, **unpublished work**). Possible reasoning for this includes the inability of metacyclic lipophosphoglycans (LPG) to reattach, flagellum attachment overcome due to abrasion from excreta released from the malpighian tubules and midgut peristalsis, and the possible lack of positive chemoeffectors.

Suprapylaria develop in the midgut and attachment of *Leishmania* nectomonads occurs in the abdominal midgut. Suprapylaria species are assigned the subgenus *Leishmania* such as *L. mexicana*. Peripylarian parasites initially develop in the hindgut where their nectomonads may attach and later migrate anteriorly. Peripylaria species are assigned the subgenus *Viannia* such as *L. braziliensis*. Their ability to migrate further without expulsion similar to hypopylaria species is due a modification in metacyclic LPG, enabling reattachment (**Soares et al, 2005**). Both

suprapylaria and peripylaria migrate to invade the foregut and are therefore able to be transmitted for disease causing.

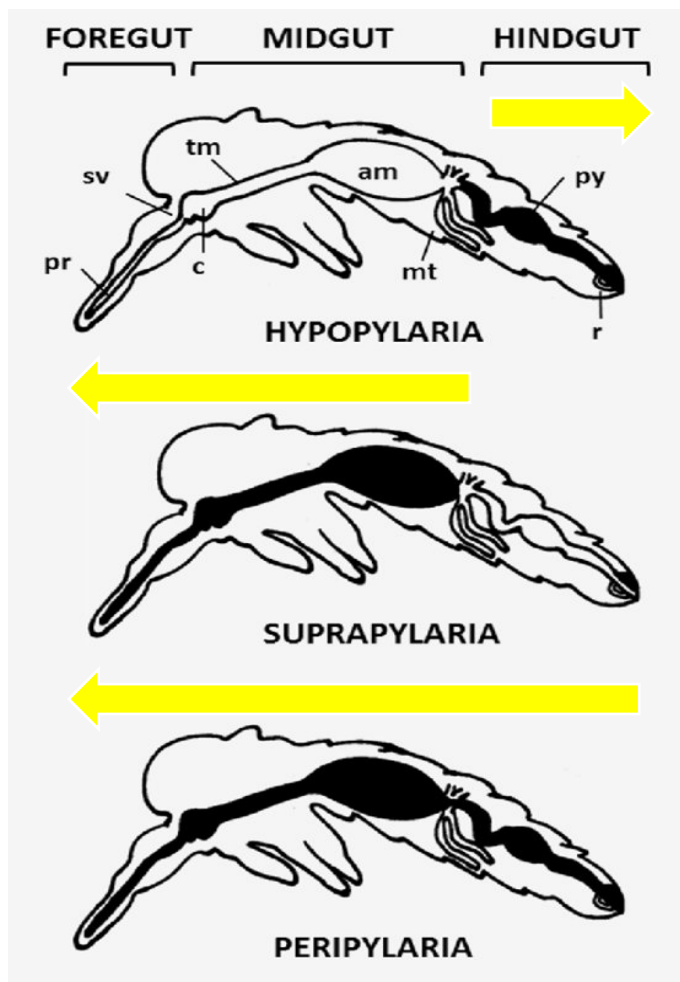


**Figure 19. Diagrammatic representation of *Leishmania* development sections within a sandfly** as proposed by Lainson and Shaw (1979). Structural features of the sand fly includes the proboscis (pr), stomodeal valve (sv), cardia (c), thoracic midgut (tm), abdominal midgut (am), malpighian tubules (mt), pylorus (py) and rectum (r). Figure shows the sections of Hypopylaria (development confined to the hindgut, with the parasites not able to be transmitted due to loss during defecation), Suprapylaria (development confined to the midgut and foregut, with the parasites able to be transmitted) and Peripylaria (development occurs throughout the gut and the parasites can be transmitted). Black shows the sections of *Leishmania* development, with the yellow arrows showing the migration of parasite following metacyclogenesis. Image from Kaufer et al, 2017.

### 2.1.3 *Leishmania* manipulation of the Phlebotomine host interaction

Some species have been shown to manipulate the action of their sandfly vector in order to benefit their survival (**Kamhawi, 2006**). Defecation is the main approach by which sandflies potentially expel parasites. Defeating this is therefore one of the ways in which *Leishmania* manipulates its interaction with sandflies to enhance survival. The PM containing the blood undergoes degradation by chitinases before expulsion occurs. *Leishmania* is shown to secrete chitinases to encourage earlier degradation of the PM to allow nectomonads to escape into the lumen (**Ramalho-Ortigão et al, 2005**). Genes coding secreted chitinases has been identified in many *Leishmania* species with *L. mexicana* showing an overexpression of LmexCht1 (**Joshi et al, 2005**), therefore nectomonads escape the PM quicker, a higher parasite load occurring and infection is established faster (**Rogers et al, 2008**). This chitinase activity may also aid in transmission by damaging the chitin-covered stomodeal valve (**Rogers et al, 2008**). *L. major* secretes a myoinhibitory neuropeptide that successfully inhibits midgut peristalsis, therefore sandfly parasite loss through defecation is reduced (**Vaidyanathan, 2004, Vaidyanathan, 2005**).

Secretion of phosphoglycans by leptomonads causes the build-up of PSG, a filamentous proteophosphoglycan (fPPG)-rich gel that accumulates in the anterior midgut and stomodeal valve leading to blockage in these parts (**Sacks and Kamhawi, 2001**). fPPG is expelled from promastigote flagellar pockets, and can be found in the center of rosettes in culture where flagella aggregate (**Stierhof et al, 1999**). This manipulation causes a change in the nature of the feeding of the sandfly, multiple feeding due to incomplete feeding, and the regurgitation of promastigotes to aid sandfly feeding (**Rogers et al, 2002, Rogers et al, 2004**). This along with the production of chitinases by haptomonads for valve degeneration (**Schlein, Jacobson and Messer, 1992**) impairs feeding for increased efficiency in transmission of metacyclic promastigotes during feeding (**Rogers et al, 2004, Kamhawi, 2006**). This supports for efficient transmission.

*Leishmania* parasites interfere with digestive enzyme activities. Promastigotes inhibit proteolytic activity in the midgut (**Borovsky and Schlein, 1987**) and amastigotes cause delays in trypsin and aminopeptidase activity (**Dillon and Lane, 1993**).

#### 2.1.4 Important features of *Leishmania* for transmission

The main feature of *Leishmania* parasites that allows for transmissibility is the flagellum but the surface receptors and LPGs play a role in transmission.

LPGs are the most abundant glycoconjugates of promastigotes expressed on the entire surface of promastigotes (**Sacks and Kamhawi, 2001**), playing a large role in adhesion to the midgut epithelium via galectin on the sand fly following escape of nectomonads. They play a role in enabling competent *Leishmania* species able to develop within *Phlebotomus* species, known as ‘permissive’ and ‘restricted’ vectors (**Kamhawi et al, 2000**). Permissive vectors allow the survival and/or development of several *Leishmania spp* within them, whereas restricted vectors allow the survival of specific *Leishmania spp*. Change occurs in the LPG during differentiation of the non-infective promastigote form to the infective promastigote form. All LPGs are composed of a conserved glycan core region of Gal( $\alpha$ 1,6) Gal( $\alpha$ 1,3) Gal( $\beta$ 1,3) [Glc( $\alpha$ 1)-PO<sub>4</sub>] Man( $\alpha$ 1,3) Man( $\alpha$ 1,4)-GlcN( $\alpha$ 1) linked to a 1-*O*-alkyl-2-*lyso*-phosphatidylinositol anchor, and a conserved (Gal( $\beta$ 1,4)Man( $\alpha$ 1)-PO<sub>4</sub>) backbone of repeat units and the oligosaccharide cap with a branching variable sugar which is responsible for the polymorphism amongst *Leishmania* species (**Soares and Turco, 2003**).

Metacyclogenesis results in increasingly more sugars getting masked and LPG elongating during promastigote development (**Soares et al, 2002**). In suprapylaria species which develop in the midgut, metacyclic LPG does not bind to the midgut microvilli (**Soares et al, 2002**) due to structural changes caused by metacyclogenesis. This permits the release of infective stage promastigotes during transmission (**Pimenta et al, 1992**). Compared to suprapylaria species, peripylaria species differ in midgut attachment (**Soares et al, 2005**); peripylaria metacyclics make less LPG than procyclics in which glucose residues are added. This is possibly due to their development in the hindgut therefore to avoid defecation, they migrate to the midgut to reattach before migrating further anterior. There are however no studies on LPGs in hypopylarian *Leishmania* species which develop in the hindgut.

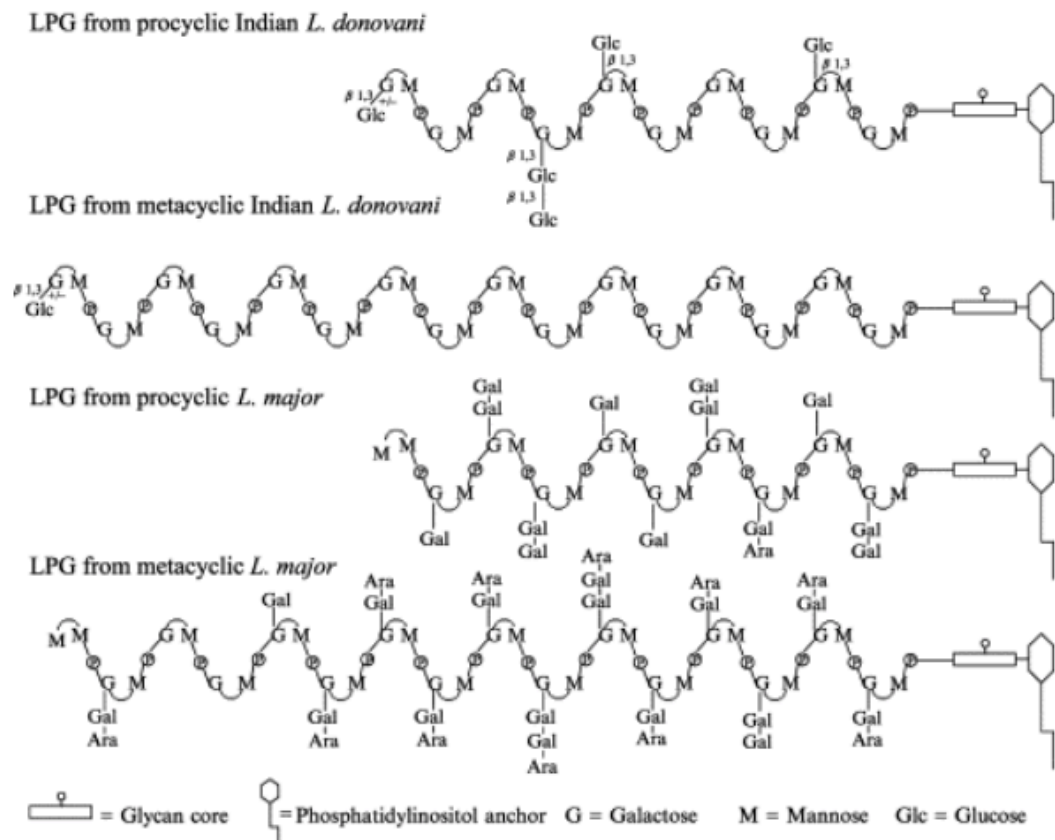


**Figure 20. Schematic diagram of LPGs from representative procyclic and metacyclic *Leishmania* species.** The structure of the glycan core is Gal( $\alpha$ 1,6)Gal( $\alpha$ 1,3)Gal( $\alpha$ 1,3)[Glc( $\alpha$ 1-PO<sub>4</sub>)-6]-Man( $\alpha$ 1,3)Man( $\alpha$ 1,4)GlcN( $\alpha$ 1,6) linked to the 1-*O*-alkyl-2-*lyso*-phosphatidylinositol anchor. The repeat units are 6-Gal( $\beta$ 1,4)Man( $\alpha$ 1)-PO<sub>4</sub>. The diagram shows the result of metacyclogenesis on LPG- elongation and downregulation of glucose resulting in the loss of epitope for binding to midgut epithelium. Arabinosyl (Ara). Image from Turco and Sacks, 2003.

Flagellum is important for motility for escape, allowing the parasite to propel forwards. Due to the position of the flagellum at the anterior of the promastigote, it is the first structure of the promastigote to explore the environment it is moving towards. This allows the opportunity for flagellum to be the main sensory organ through the mitogen-activated protein (MAP) kinases pathway (Rotureau et al, 2009). The length of flagellum continuously increases throughout metacyclogenesis. The length of *Leishmania* has been showed to be important in the adhesion to the midgut, with shorter flagellated promastigotes being more readily excreted due to not binding to the matrix epithelium following escaping the PM (Cuvillier et al, 2003).

### 2.1.5 Transmission

Metacyclogenesis of *Leishmania* ends with highly infective metacyclic promastigotes within the cardia of the sandfly. As pool feeders, sandflies cut the skin of their host damaging dermal capillaries to create a pool of blood on the surface of the skin which they can suck into the pharynx and is later diverted into the midgut through the one way cibarial valve (**Rogers, 2012**). This presence of PSG accumulation and pathology caused by the accumulation such as the damage to the cibarial valve affects the manner in which the sandfly feeds, infected sandflies have multiple feeding attempts by increasing probing, feeding time increases and incomplete blood meal usually occurs (**Beach, Leeuwenburg and Kiilu 1985**) showing that there is difficulty in feeding. This enhances the chances of transmission during feeding (**Killick-Kendrick et al, 1977**).

During the blood meal of an infected sandfly, metacyclic promastigotes can be transmitted to the mammalian host. The mechanism falls within two hypothesis: the regurgitation hypothesis and the inoculation hypothesis. The inoculation model proposed that only promastigotes in the proboscis are involved in transmission due to infection occurring when sandflies were observed to probe skin however no blood feeding taking place (**Killick-Kendrick et al, 1977, Beach, Leeuwenburg and Kiilu, 1985**). The regurgitation model was initially reported by Short and Swaminath 1928. This proposed that the physical obstruction caused by PSG along with the pathology caused by chitinase damage causes a regurgitation of the PSG including promastigotes into the pool of blood before feeding can occur (**Schlein, Jacobson and Messer, 1992**).

Efficient transmission requires the movement of promastigotes to the anterior of the sandfly midgut (**Leslie, Barrett and Burchmore, 2002**), however the exact stimulus that allows this process to occur is not well established. Killick-Kendrick hypothesized the sugar gradient created by the sugar released from the crop provided an stimulus for migration (**Killick-Kendrick, 1978**). This has later been supported by chemotaxic assays.

## 2.2 Chemotaxis

Chemotaxis is the migration of cells directionally when exposed to gradients of chemoeffector molecules (**Englert, Manson and Jayaraman, 2009**). Naturally there will be multiple chemoeffectors in an area, creating multiple coexisting overlapping gradients of specific chemical sensors in which chemotaxis occurs.

For microbes, it is advantageous to move away from unfavourable conditions towards favourable environments such as those containing a source of food (**Adler, 1966**), making chemotaxis important for survival. Cells detect gradients of chemicals in two ways; directly measuring spatial gradients across the cell or indirectly temporally sensing gradients while motile. Motile bacteria randomly change direction regularly however with the detection of a gradient, this behaviour pauses allowing the bacteria to modify its movement dependent on how favourable the gradient is (**Armitage, 1992**).

The first step of chemotaxis is the detection of gradient. Understanding of the detection method of the molecules used for chemotaxis to occur is thought to be through chemoreceptors; chemoeffector molecules binding to the receptors found on the cell surface or the detection of their metabolites (**Adler, 1969**). Ligand molecules bind to their specific membrane chemoreceptors, activating them and triggering signal transduction pathways downstream.

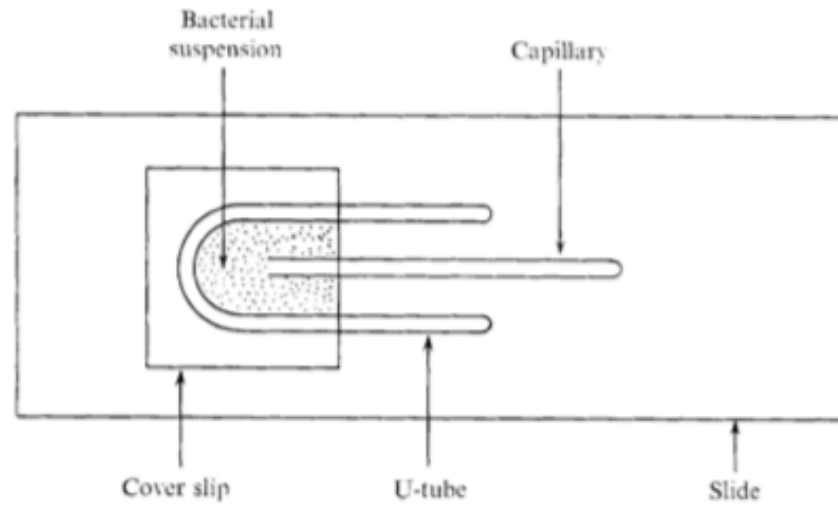
Chemotaxis has been largely studied in *Escherichia coli* by Adler (**Adler, 1972**), acting as the basis for most of the chemotaxis work on other microbes (**Keymer et al, 2006**). Like *E. coli*, motile microbes can be attracted or repelled by specific chemical stimuli (**Adler, 1973**) – positive and negative chemotaxis respectively. Assays describing measuring this chemotaxis were initially discovered in the 1880's by Pfeffer and Englemann (**Adler, 1966**) and continue to be improved upon.

Chemotaxis studies require a way to deliver chemicals to cells in a controlled gradient, for cells to be able to sense and direct their movement according. Earlier work presented a variety of techniques. The first described basic chemotaxic assay is

the Quantitative Pfeffer method (**Adler, 1973**) which involves placing motile *E. coli* at one end of a capillary tube containing a source of energy and oxygen. This allows the migration of *E. coli* into the tube resulting in two visible bands; the first containing *E. coli* that has consumed all the sugars and the second band migrating for the remainder oxygen (**Adler, 1966**). This therefore includes the overlap of osmotaxis and chemotaxis. This method was slightly altered by Adler and Armitage separately resulting in different chemotaxis assays. Adler's method for measuring chemotaxis (**Adler, 1973**) was based on using a capillary tube with a small chamber. A U-shaped tube was bent from a capillary tube, placed on a glass slide and sealed using a cover slip forming the chamber in which 0.2ml of bacterial suspension was added as seen in Figure 21. Another capillary tube was sealed at one end and used to contain the attractant. This was inserted into the chamber containing bacterial suspension. After 1 hour incubation, contents of the capillary tube were removed and plated for colony count the following day (**Adler, 1973**). Armitage developed a method similar to the Boyden Chamber assay (**Boyden, 1962**), by using blind well chemotactic chambers, quantifying the motile bacteria that migrated from the bacterial suspension well through a polycarbonate membrane (2  $\mu\text{m}$ ) into the chemotactic chamber (Figure 21). The migrated bacteria were collected and counted using a Coulter counter (**Armitage, Josey and Smith, 1977**).

Some assays included the use of agar-plates. One such assay uses the PP chamber where there are 2 parallel channels and a connecting channel between the parallel channels with small containers on each side; one will be filled with the cell suspension and the other with the chemoattractant (**Köhidaï, 1995**)

**A**



**B**

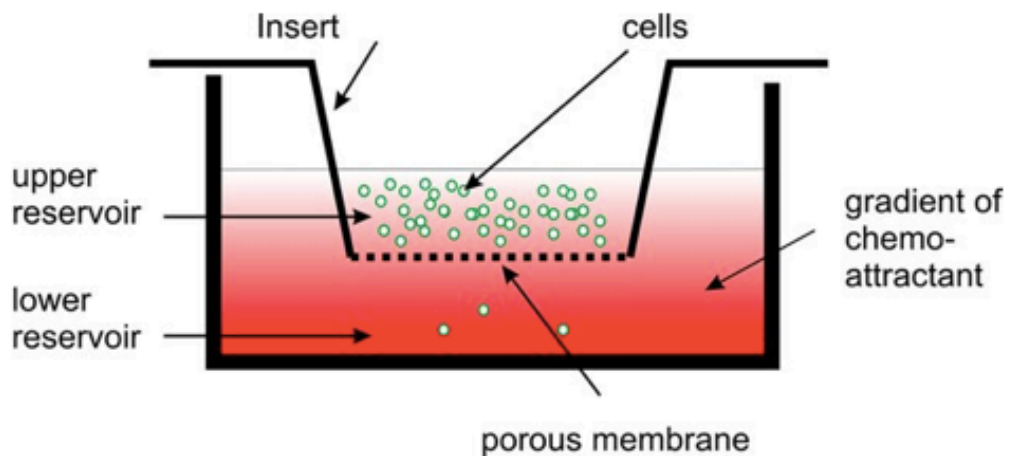


**Figure 21. Apparatus used in early chemotaxis assay. A) Illustration of the chemotaxis assay set up of Adler.** Comprising of a bent capillary tube to a U shape enclosed between a glass slide and a coverslip. This forms a compartment for the bacterial suspension. A second capillary tube is sealed and placed in a solution with chemotactic agent which fills the capillary tube by capillary action. This is placed in the bacterial suspension and diffuses into the suspension to form a gradient to attract bacteria into the capillary tube containing attractant. Counts are done to final the number of migrated cells. **(Image from Adler, 1973).** **B) Illustration of a Boyden chamber assay (Image from Lautenschlaeger, 2011)** The insert containing cells is lowered into a chamber containing the chemotactic agent. These two solutions are separated in their respective compartments by the presence of a porous membrane from which chemoattractant molecules diffuse through forming a gradient to attract the cells to migrate to the area of higher chemotaxis agent. The cells migrated into the chemotaxis agent compartment are counted.

The conditions in these primitive chemotaxis assays does not allow chemotaxis to be considered solo. In Adler's assay, the result included the effect of disturbing *E. coli* prior to plating, the conditions of growth may alter the final counts that are obtained and the processing allows for a lot more human error to affect the result. In Armitage's assay, the vessel was completely sealed allowing outside influences such as oxygen and evaporation to be less of a limiting factor compared to PP chamber assays and Adler's assay. The polycarbonate membrane was meant to allow a slower diffusion of chemical however this is not the case. The membrane may have affected migration of bacteria. PP chamber agar assay would have allowed the diffusion of chemoattractant however bacteria that needed fluid to migrate within would be limited due to evaporation and the absorption of fluid by agar. These main disadvantages make these methods highly insensitive.

### **2.2.1 *Leishmania* chemotaxic assay methods**

Due to the importance of *Leishmania* migration in the transmission of leishmaniasis, chemotaxic studies have been employed for a better understanding of potential chemoeffector molecules that act within the sandfly gut.

Bray (**Bray, 1983**) was the first to study chemotaxis with promastigote *Leishmania* forms. He used an insensitive method (**Oliveira et al, 2000**) which was composed of a disposable syringe filled with promastigote suspension covered at the bottom with 1.2 um pore size Millipore filter and immersed in a solution of chemotaxic fluid (**Oliveira et al, 2000**). This method was recognised as insensitive by Oliveira et al who developed an assay based on Adler's 1973 bacterial chemotaxic method. The similarities were the use of capillary tubes for experimental set up and the use of a defined media which was first done by Adler. Capillary tubes were filled with the defined media washing and incubating solution (WIS) with 0.004% enriched bovine serum albumin (BSA) containing the test chemotaxic agent and 0.2% agarose. Before the solution solidified, modelling clay was used to push the solution to 1cm of the end of the tube and this was covered with Parafilm. To form a gradient, the 1cm unfilled end was filled with WIS. 18 capillary tubes prepared in this manner were placed in a petri dish, positioning them in place using corrugated plastic support. 50ml of WIS was placed in the petri dish for 30 minutes to form a gradient within the 1cm

of the capillary tubes; the tubes were removed and the WIS in the petri dish was replaced with a *Leishmania* promastigote solution of  $5 \times 10^5$  cells  $\text{ml}^{-1}$ . The support and capillary tubes were replaced back in the petri dish horizontally for an incubation of 1 hour after which the capillary tubes were removed. Migrated cells were removed from the WIS 1cm open end and collected for counting using a haemocytometer. This used *L. chagasi* and *L. amazonensis* promastigotes which both showed a chemotactic response to all the carbohydrates tested (glucose, fructose, sucrose, raffinose, mannose, galactose, maltose and melibiose) however the absence of a control substance which was not attractive to the promastigotes suggests the inclusion of osmotactic movement resulting in an overall positive chemotaxis result (Leslie, Barrett and Burchmore, 2002). There was a significant higher chemotactic response in stationary phase promastigotes, this was associated with the greater mobility of metacyclic forms that are in higher numbers in stationary phase growth in culture (Oliveira et al, 2000).

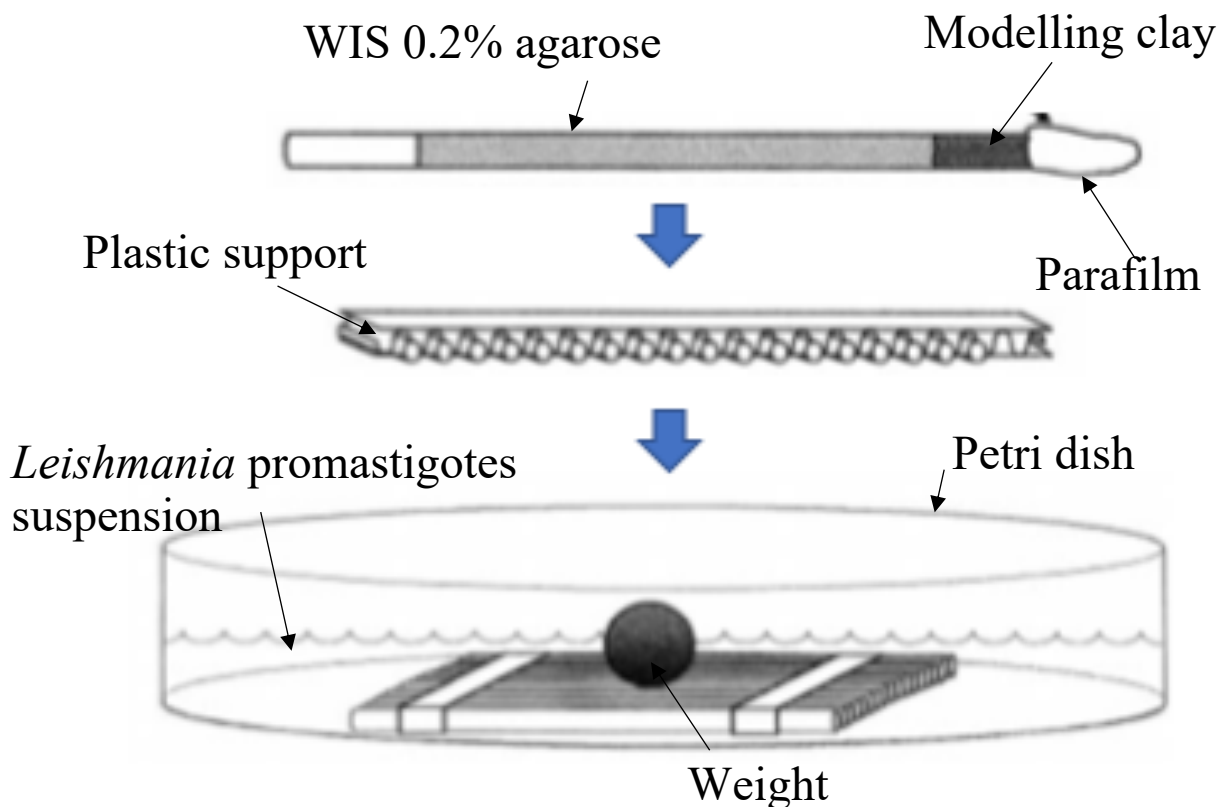


Figure 22. Illustration of the experimental set up used by Oliveira et al, 2000. Image from Oliveira et al, 2000

The capillary assay from Oliveira et al, 2000 was further developed by **Leslie, Barrett and Burchmore, 2002** who establish a reviewed method using a similar experimental set up. The same WIS was used by **Leslie, Barrett and Burchmore** which was used to fill the capillary tubes. WIS with 0.1% agarose and test chemotaxic agent was used to fill the tubes in a similar manner as Oliveira et al, 2000. These capillary tubes were vertically placed in bijou tubes containing late-log *L. mexicana* promastigotes  $2.5 \times 10^7$  cells ml<sup>-1</sup>. This was incubated at room temperature for 1 hour and cells were collected from the 1cm open end and counted with a haemocytometer. This included a control using a capillary tube with no chemotaxic agent included (**Leslie, Barrett and Burchmore, 2002**). Similar to Oliveira et al, 2000, all tested chemotaxic agents showed a chemotaxic response compared to the control. Interestingly, fixed cells were also used in this assay with the test chemotaxic agent of D-glucose. This showed a very low level migration into the capillary tube showing that passive movement into the capillary tubes was not an limiting factor in this assay and the result was from promastigotes actively migrating into the tubes (**Leslie, Barrett and Burchmore, 2002**). However, the idea that motility was based on an osmotic gradient was confirmed in this as in the absence of an osmotic gradient by assaying promastigotes in NaCl no significant movement into the capillary tube occurred (**Leslie, Barrett and Burchmore, 2002**).

This revelation by **Leslie, Barrett and Burchmore, 2002** brought about a study by Barros et al, 2006 which investigated the chemotaxic and osmotaxic responses in promastigotes *Leishmania*. In this study, the experimental set up used *L. amazonensis* in WIS to measure 'time of straight line movement' (TSLM). A mixture of promastigotes in WIS added to WIS containing the chemotaxic agent was mixed and placed on a slide under a coverslip before promastigotes were observed under a microscope. This showed how long promastigotes cultured to the stationary phase travelled in a straight line before chaotic angular motion (tumbling) occurs when added to a new environment which included the testing chemotaxic agent (**Barros et al, 2006**). Although stated that this method allowed chemotaxic responses to be distinguished from osmotaxic responses, the results from this method can only be used to conclude on the length of time it takes for 'adaptation' to occur within a new environment of different concentration of testing chemotaxic agents as the experiment occurs in a zero gradient environment. Adaptation is the process by which cells particularly bacteria detect a difference in environment using a temporal sensing

mechanism representing a form of memory (**Macnab and Koshland, 1972**), therefore TSLM records how long it takes for the cell to stop responding as it has realised the signal as constant.

Relatively recently, deYsasa Pozzo publish two studies utilizing optical tweezers to measure the directional forces exerted on *L. amazonensis* under a glucose gradient (deYsasa **Pozzo et al, 2007**, deYsasa **Pozzo et al, 2009**). The glucose chemical gradient was created using two chambers connected by a duct small enough for the gradient to be kept constant for over ten hours (deYsasa **Pozzo et al, 2007**). Individual *Leishmania* were attached to a 9 µm diameter bead connected to a Nd:YAG laser which recorded optical forces and therefore the forces of the flagellum. This study showed that unlike bacteria which using straight line movement and tumbling to detect gradients, *Leishmania* uses circular movements and tumbling to detect gradients (deYsasa **Pozzo et al, 2009**). With a higher concentration of glucose, *Leishmania* have a clearer sense of direction and move with greater force.

All methods used to study *Leishmania* taxis to date show that there is recorded taxis which includes both chemotaxis and osmotaxis however the effect of osmotaxis is shown to be tiny (**Barros et al 2006**). Earlier studies required a higher concentration of test chemotactic agents to show results making it insensitive (**Oliveira et al, 2000**, deYsasa **Pozzo et al, 2009**, **Leslie, Barrett and Burchmore, 2002**, **Díaz et al, 2011**). deYsasa Pozzo's method used real time observation of the forces exerted and directionality of individual parasites (deYsasa **Pozzo et al, 2009**) whilst allowing direct observation of the behaviour, however did not have a control.

As the capillary assay used by Oliveira and Leslie were easiest and cheapest methods for chemotaxis in *Leishmania*, Díaz explored standardizing this method and found 30 minutes incubation and strict osmolarity of solutions were imperative parameters to record chemotactic rather than chemokinetic responses of the *Leishmania* promastigotes (**Díaz et al, 2011**). Díaz went further to show how chemotaxis may be useful *in vivo* by showing that poly-lysine-methotrexate-conjugate have some chemotactic response, particularly methotrexate conjugates with a terminal serine amino acid. This may therefore improve drug-targeting towards the *Leishmania* parasites (**Díaz et al, 2013**).

With the requirement of a more sensitive methodology, it is apparent from the literature (Table 2) that away from sugars, other avenues have not been explored as chemotactic agents. The environmental habitat of *Leishmania* promastigote within the sandfly is primarily the midgut which has a differing physiochemical nature dependent on the anterior or posterior locations. The migration of some *Leishmania* species towards the anterior region where a sugar gradient emanates from the crop can be explained as osmotactic and chemotactic responses such as that recorded *in vitro* ( **Oliveira et al, 2000**, deYsasa **Pozzo et al, 2009**, Leslie, Barrett and Burchmore, 2002, **Díaz et al, 2011**). However, unlike *Leishmania* promastigotes that migrate anteriorly, some *Leishmania* species escape the PM, attach to the epithelium of the gut and migrate posteriorly therefore not being disease causing species. This brings up questions about what other chemoeffectors particularly chemoattractants could be acting at the posterior of the sandfly alimentary canal.

The importance of motility as well as the presence of chemical sensors forming gradients for chemotaxis allows us to understand that specific chemical stimuli might play a role in the migration of *Leishmania* parasites towards the foregut and not towards the hindgut (Figure 23). Studying chemotaxis quantitatively acts as a method to measuring how effective specific chemicals are as chemoattractants, however the cheaper methods employed are not effective as they do not offer a stable environment away from outside influences and require a high concentration of attractant for chemotaxis to be detected making it insensitive (**Oliveira et al, 2000**). Hence, a more sensitive methodology is required to study *Leishmania* chemotaxis.

<b>Tested agent</b>	<b>Study</b>	<b><i>Leishmania</i> spp.</b>
<i>D-Glucose</i>	Oliveira et al, 2000      deYsasa Pozzo et al, 2009	<i>L. chagasi</i>
	Leslie, Barrett and Burchmore, 2002	<i>L. amazonensis</i>
	Díaz et al, 2011	<i>L. mexicana</i>
<i>Fructose</i>	Oliveira et al, 2000      Díaz et al, 2011	<i>L. chagasi</i>
	Leslie, Barrett and Burchmore, 2002	<i>L. amazonensis</i> <i>L. mexicana</i>
<i>Sucrose</i>	Oliveira et al, 2000      Barros et al, 2006	<i>L. chagasi</i> <i>L. amazonensis</i>
<i>Raffinose</i>	Oliveira et al, 2000	<i>L. chagasi</i> <i>L. amazonensis</i>
<i>Mannose</i>	Oliveira et al, 2000	<i>L. chagasi</i>
	Leslie, Barrett and Burchmore 2002	<i>L. amazonensis</i> <i>L. mexicana</i>
<i>Galactose</i>	Oliveira et al, 2000	<i>L. chagasi</i> <i>L. amazonensis</i>
<i>Maltose</i>	Oliveira et al, 2000	<i>L. chagasi</i> <i>L. amazonensis</i>
<i>Melibiose</i>	Oliveira et al, 2000	<i>L. chagasi</i> <i>L. amazonensis</i>
<i>L-Glucose</i>	Leslie, Barrett and Burchmore, 2002	<i>L. mexicana</i>
<i>Inositol</i>	Leslie, Barrett and Burchmore, 2002	<i>L. mexicana</i>
<i>Guanosine</i>	Barros et al, 2006	<i>L. amazonensis</i>
<i>Glycine</i>	Barros et al, 2006	<i>L. amazonensis</i>
<i>NaCl</i>	Leslie, Barrett and Burchmore, 2002	<i>L. amazonensis</i>
	Barros et al, 2006	
<i>Mannitol</i>	Barros et al, 2006	<i>L. amazonensis</i>

Table 2. All the agents that have been showed to have positive chemotaxic responses from literature.

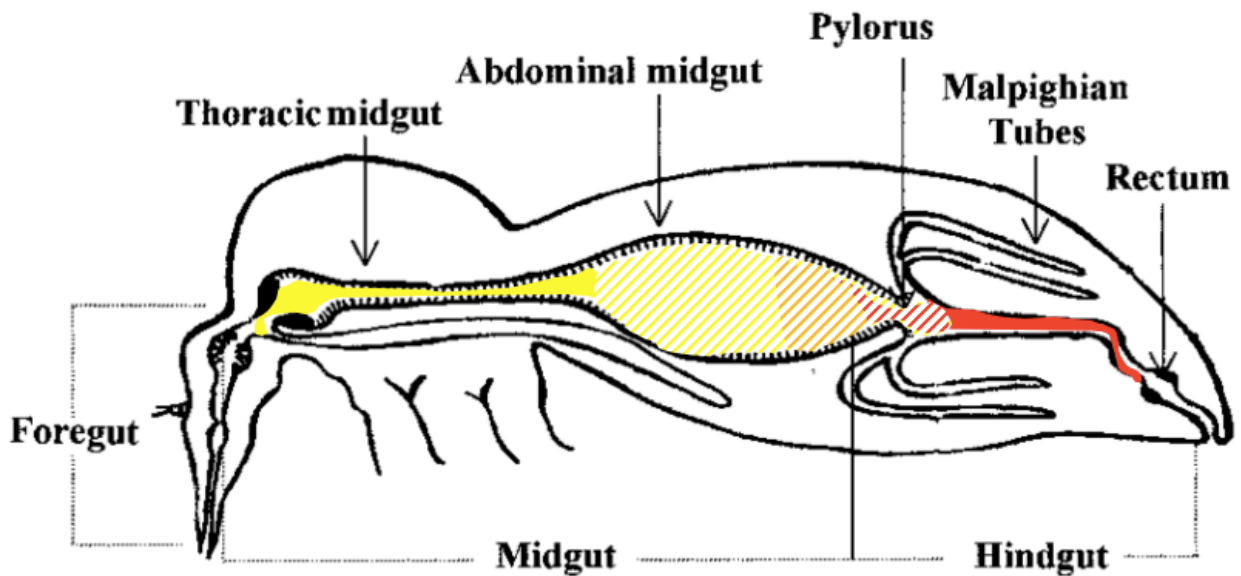


Figure 23. Illustration of the alimentary canal of the sandfly showing areas containing sugars (yellow) and urea (red). The crop contains sugars (yellow) which are slowly released into the abdominal midgut for digestion. As sugars are digested, the gradient of sugar will be continuous yet descending to the hindgut. The malpighian tubules process excreta from the haemolymph which is passed into the hindgut as urate crystals (red). This excreta is removed from the rectum however the presence of urate crystals in the hindgut will allow some to diffuse and be present in the posterior hindgut. With this diffusion gradient, it can be assumed that the posterior midgut will have a similar concentration of urea and sugars. Adapted from Schlein, 1993.

## 2.2.2 Microfluidics for studying *Leishmania* migration

The most-studied model for chemotaxis *E.coli* (Berg, 2004), has been used as a basis to develop methods of chemotaxis studies for *Leishmania* parasites.

Manipulation to result in gradient development constraint in a controlled area with limited flow has been shown in traditional chemotaxis assays such as capillary assays however, precision and reliability in technique is poor.

For gradient development and investigating gradient sensing *in vivo*, microfluidic technology has developed to be an essential technique as it meets all the criteria for precise manipulation (Lin and Levchenko, 2015). Microfluidic devices consist of small chips in which microchannels form precise yet complex structured patterns appropriate for the controlled manipulation of biochemicals and cells for gradient development and gradient sensing (Whitesides et al, 2001). Advances in the application of microfluidic systems have allowed the improvements in studying microbes within a defined environment. This allows for a micrometre scale chemical

gradients to be created by flow or simple diffusion within a common channel known as flow based microfluidic gradient generators and diffusion based microfluidic gradient generators respectively, in which taxis can be studied. Flow based microfluidic gradient generators use two channels with different concentrations merging into a central channel (**Brody and Yager, 1997**) or branching network of serpentine channels (**Jeon et al, 2000**) for the diffusion of biochemical between the streams as they flow together into one channel (**Figure 24(A)**). Diffusion based microfluidic gradient generators use passive diffusion between a source and a sink to generate a gradient (**Figure 24(B)**).

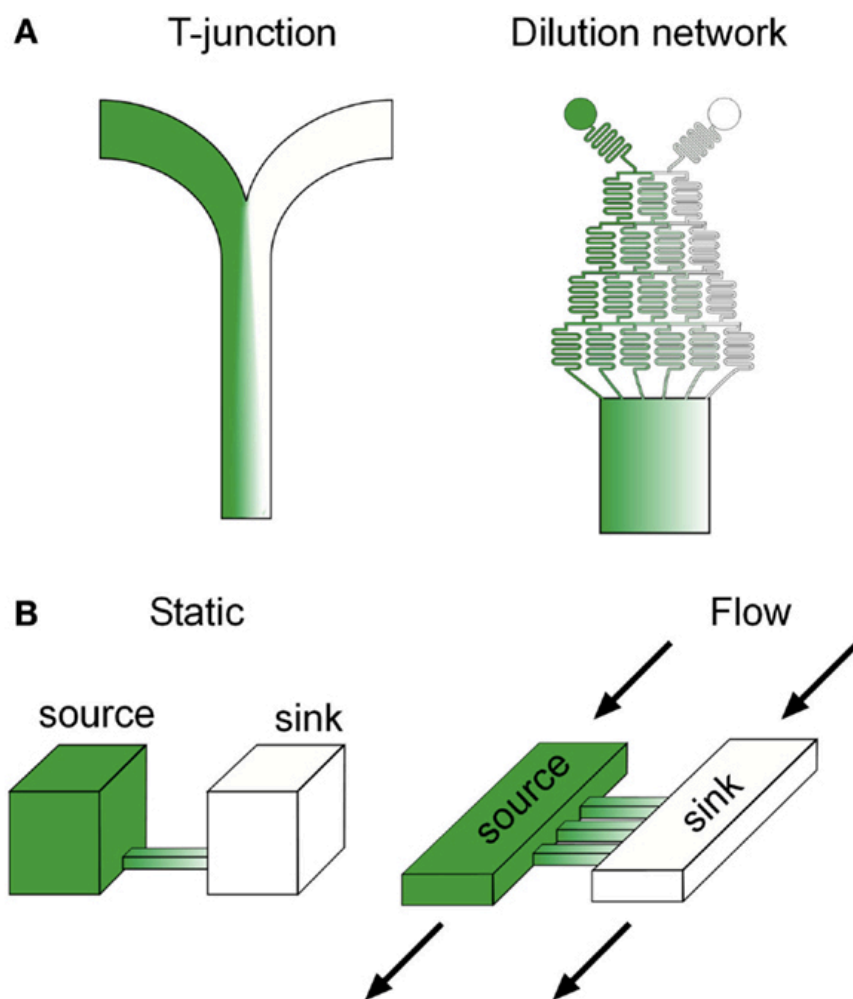


**Figure 24. Microfluidic gradient generation designs.** (A) Flow based and (B) Diffusion based microfluidic gradient generators. The green colour represents the distribution of the biochemical used in each device. Image from (**Lin and Levchenko, 2015**)

Compared to traditional chemotaxis assays, microfluidics allows a high level of control and reproducibility of flows and concentration gradients of volumes similar to that of the microenvironments of the microbes (**Seymour et al, 2008**) with bulk forces like gravity, buoyancy and momentum having little effect on flow . The transparent chip is also advantageous for easy visualisation using microscopy allowing real time assessment.

Microfluidic chemotaxis assays were proposed as sensitive alternatives for *Leishmania* parasites (**Díaz et al, 2011**) and have been used to explore the swimming dynamics of *Trypanosoma brucei* (**Uppaluri et al, 2012**). This showed that by using microfluidic tools, live parasites can be subjected to flow within a defined environment for a range of applications such as chemotaxis, whilst meeting the sensitivity levels that is not possible with the traditional chemotaxis assays.

## 2.3 Aims of the project

For successful parasite transmission from insect vector to mammalian host, the flagellated promastigote forms of the parasite need to migrate from the midgut of the phlebotomine sand fly to the anterior part of the digestive tract. This involves chemotaxis toward nutritional/chemical cues. There are a number of unanswered questions regarding the exact chemical nature of these gradients, how they are established, and the parasitic forms able to detect them.

It was decided to use suprapylarian *Leishmania mexicana* compared to hypopylarian *Leishmania tarentolae* to find out if they differed in their chemotaxis properties.

To address these issues, this project aimed to:

(1) Produce a morphometric analysis (based on cell body length, width, flagellum length, distance kinetoplast- nucleus) of *Leishmania tarentolae* and *Leishmania mexicana* growth in culture conditions, which can be used to identify the forms of promastigotes found in an axenic culture.

(2) Perform a pilot chemical screen (sugars, urea, and salts) using two approaches to measure *Leishmania* chemotaxis. The first experimental approach involves an established capillary assay based on a single endpoint measurement. The second novel approach (in development) would use a microfluidic imaging setup to monitor in real-time individual parasite migration towards the chemical cue.

Results from this study should: (1) establish new technologies to finely measure and screen *Leishmania* behaviour such as chemotactic migration, and (2) provide further insight into the chemicals/metabolites *Leishmania* migratory forms respond to, which could lead to effective chemical strategies to reduce the *Leishmania* vector-host transmission rate.

## CHAPTER THREE: MATERIALS AND METHODS

### 3.1 General Methods

The present project consists of four parts. A) *Leishmania* morphometric studies of *Leishmania tarentolae* and *Leishmania mexicana* in culture. B) Capillary assays studies of both *L. tarentolae* and *L. mexicana* involving the examination of different chemical stimuli. C) The development of a microfluidic method to analyse *Leishmania* chemotaxis in a confined environment. D) Experimental infections of the sandfly *Lutzomyia longipalpis* with *L. tarentolae* and *Crithidia fasciculata* for the examination of PSG formation in the foregut, midgut and hindgut.

#### 3.1.1 Insect rearing

All sand fly experiments used *Lutzomyia longipalpis* reared in a closed laboratory colony that was established (1980's) from individuals caught in Jacobina, Bahia-Brazil and maintained in Lancaster University according to standard laboratory conditions (Modi,1997). The sand flies were kept within incubators (LMS Cool Incubators) maintained at  $26 \pm 2^{\circ}\text{C}$  under an 8 hours light/16 hours dark photoperiod and humid conditions of  $> 80\%$ . All sand flies were offered autoclaved 70% v/v sucrose solution in cotton wool and females fed on sheep blood via a Hemotek membrane feeder (Discovery Workshops-UK) at  $37^{\circ}\text{C}$  using chicken skin. Freezer stored adult chicken skin was prepared by thawing, followed by washing with 70% w/v ethanol and washed with deionized filtered water. Excess fat was removed from the inner surface of the skin using a single edged razor blade and the intact skin was used as the membrane for the Hemotek.

All mosquito experiments used adult *Aedes aegypti* reared in a closed laboratory colony maintained in Lancaster University. For general rearing, mosquitoes were maintained at  $26^{\circ}\text{C}$ , 84% relative humidity, under a 12 hr light and 12 hr dark cycle.

All adult mosquitos were offered autoclaved 10% v/v sucrose solution soaked filter paper and blood fed weekly on anesthetized mice.

### 3.1.2 Parasites

*Leishmania mexicana* (WHO strain MNYX/BZ/62/M379 promastigotes, *Leishmania tarentolae* (Green Florescent Protein, GFP), *Leishmania mexicana* (DSRed), *Leishmania tarentolae* LV101 promastigotes and *Crithidia fasciculata* promastigotes were maintained at 26°C temperature in culture medium prepared as described below.

### 3.1.3 Preparation of culture medium

The culture medium used was dependent on the nutritional requirements of the parasites.

*Leishmania tarentolae* and *Leishmania mexicana* were cultured in medium 199 with Hank's Salts with HEPES, L-glutamine and 1.4 g/L NaHCO<sub>3</sub> (Lonza Cat Number BE12-118F) supplemented with 1x BME vitamins (Sigma Cat Number B 6891), foetal bovine serum (FBS, Hyclone Foetal Bovine Serum SLS Cat number HYC85) heat inactivated at 56°C for 30 minutes and filtered using a 0.2 µm single-use filter unit and 25 µg/ml gentamycin sulphate (Sigma G1272 10 mg/ml stock). The final concentration of FBS was 10% and 20% for *Leishmania tarentolae* and *Leishmania mexicana* respectively.

*Crithidia fasciculata* was cultured in Warrens medium comprised of brain heart infusion broth (OXOID CM1135), hemin solution (50x stock solution prepared by Dr Micheal Ginger and stored at 4°C) and 5% FBS (Hyclone Foetal Bovine Serum SLS Cat number HYC85) heat inactivated at 56°C.

### **3.1.4 Growth of parasites**

Promastigotes in culture were grown using the appropriate culture medium as described above and maintained at culture densities between  $1 \times 10^5$  and  $1 \times 10^7$  cell/ml<sup>-1</sup> by repeated sub-passaging into fresh medium when cultures reached a late-log phase. Passage number remained under 30 for experiments.

The typical cell culture density of each was determined by haemocytometer counting every 24 hours to produce a growth curve. Parasites were prepared for haemocytometer counting using a 1:1 ratio of 2% paraformaldehyde to promastigote medium before counting under a light microscope (MICROTEC LM-1) at 40x magnification.

## **3.2 Part A: *Leishmania* morphological studies of *Leishmania tarentolae* and *Leishmania mexicana* in axenic culture**

### **3.2.1 Slide preparation**

Slides with *Leishmania* promastigotes from the axenic culture was prepared at different time points (approximately 24 hours apart) following sub-passage. A volume of 500µl of culture was centrifuge washed 3 times at 2,000rcf for 5 minutes with sterile phosphate buffer solution (PBS, Sigma 79382). 100µl of solution containing washed promastigotes was smeared on a glass slide, air-dried and fixed with cold methanol. These fixed slides were Giemsa stained using 10% Giemsa solution (Sigma G5637) for 5 minutes before being washed with deionised water and air-dried. For the visualisation of the kinetoplast and nucleus, approximately 300ul DAPI stock solution (VECTASHIELD Antifade Mounting Medium with DAPI, H-1200) was added directly on the Giemsa stained slides. A glass coverslip was used to distribute the dye evenly on the slide and absorbent tissue paper was used to remove excess dye around the coverslip before the edges was sealed with nail polish. The slides were examined under a light microscope at 40x and photomicrographs were taken.

### **3.2.2 Morphological configuration and classification of promastigotes**

For the classification and quantification of morphological configurations using the Image-J software (<https://imagej.nih.gov/ij/>), approximately 100 randomly selected promastigotes from each time point were measured in 3 independent experiments using the following parameters: body length, flagellar length, body width, and the distance between the kinetoplast and nucleus (position of the kinetoplast in relation to the nucleus was also noted). The data for each promastigote was used to categorise each as: procyclic, leptomonad, nectomonad and metacyclic as described by Rogers et al. (2002) and Čiháková and Volf (1997).

## **3.3 Part B: Capillary assays of *Leishmania* challenged with an array of chemical compounds**

75mm long glass capillary tubes (Richardsons of Leicester ltd, C1330) containing chemical stimuli immersed in a suspension of *Leishmania* were used to produce a concentration gradient contained within the central cavity of the tube (method modified from Oliveira et al, 2000). Following an incubation period of 1 hour, migrated promastigotes were collected from the capillary tube for toxic responses of *Leishmania* to the chemical stimulus to be determined.

### **3.3.1 Preparation of Washing and Incubation Solution (WIS) buffer and promastigote suspension**

Washing and incubation solution (WIS) buffer was prepared according to Oliveira et al, (2000) with slight alteration comprised of 30mM sodium  $\beta$ -glycerophosphate, 87mM NaCl, 27mM KCl, 2mM  $\text{CaCl}_2 \cdot 2\text{H}_2\text{O}$ , 2mM  $\text{MgCl}_2$  and 0.004% FBS with the final solution lowered to pH 6.8 with HCl using a pH meter (Hanna instruments HI 2210). WIS buffer was used for both the promastigote suspension and the capillary tube solution to ensure the only differential factor for taxis to occur was the specific chemical stimuli.

*Leishmania* promastigotes from early log phase and late log phase were used to prepare promastigote suspensions from which taxis will occur. Prior to the experiment, a cell count was performed from culture and the volume of cells for  $1 \times 10^7$  cells/ml was centrifuged at 1000g for 5 minutes before washing with WIS buffer 3 times. This promastigote suspension of  $1 \times 10^7$  cells/ml in WIS buffer was kept in 26°C for approximately 30 minutes before aliquoted in 1ml in bijou tubes for capillary assays.

### **3.3.2 Preparation of capillary tube solution**

To the WIS buffer containing 0.004% FBS, agarose (Sigma A9539) was added making the capillary tube solution of 1% agarose. For each experimental condition, specific concentration of substance to be tested was added making the final specific testing substance capillary solution. For controlled experiments, no testing substance was added. The final solution was microwaved to dissolve the agarose and used to fill the capillary tube by capillary action 1cm from the end of the tube. Before the agarose set, modelling clay was added to end of the capillary tube containing the testing substance to prevent evaporation. This is showed in diagrammatic form in Figure 24. An ultra-fine gel loading-tip pipette was used to fill the remaining 1cm open end with WIS buffer with 0.004% FBS avoiding air bubbles. This allowed for the diffusion of testing substance within the capillary tube into the WIS buffer. Capillary tubes were suspended in the bijou tubes containing 1ml of  $1 \times 10^7$  promastigote suspension. Each bijou tube contained 1 capillary tube and was incubated in a 26°C incubator for 30 minutes.

### 3.3.3 Collecting results

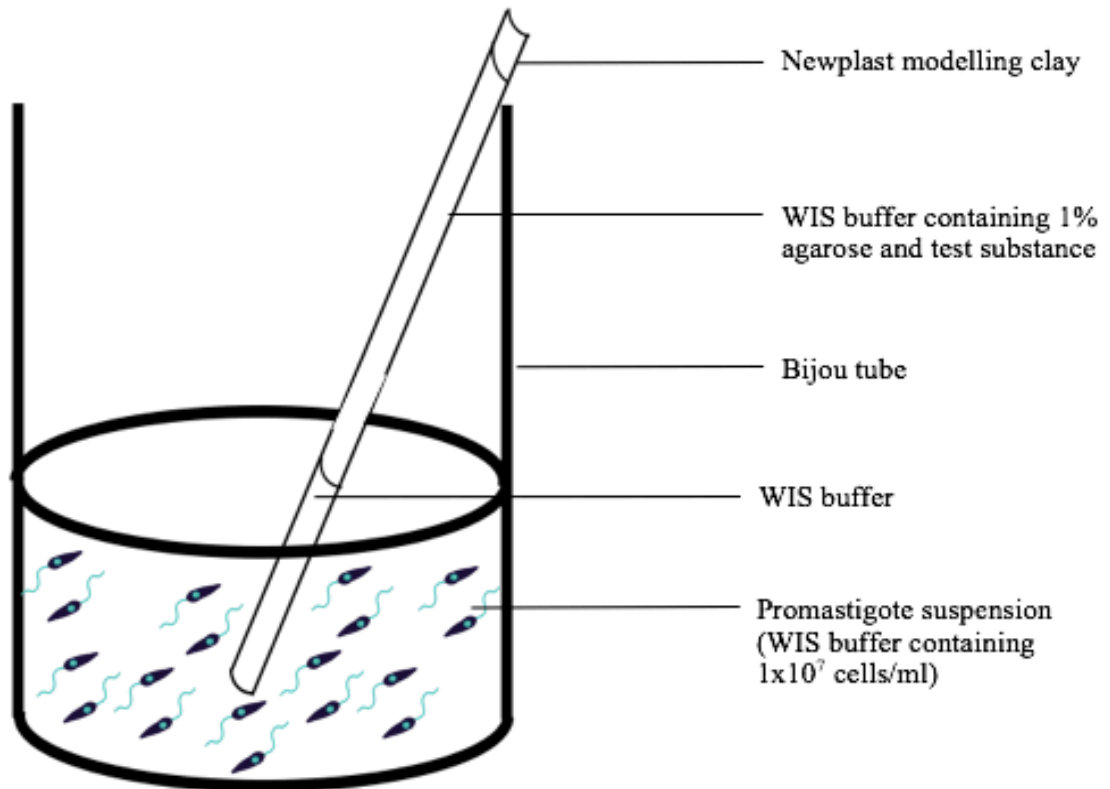


Figure 24. Diagrammatic representation of experimental apparatus used for capillary assay. A glass capillary tube containing WIS buffer with 1% agarose and test substance was placed in a bijou tube containing promastigotes and incubated for 30 minutes.

Following the incubation period of 30 minutes, the capillary tubes were carefully removed from the bijou tube and an ultra-fine gel loading tipped pipette was used to extract  $5\mu\text{l}$  of suspension from the open end of each of the capillary tube. The collected suspension was used for cell counts and slide preparation as explained above (2.2.1). Cell counts using a haemocytometer were performed to calculate the number of migrated cells as cells per ml. Slides were prepared to analyse the population of migrated cells in more detail; the morphology of migrated promastigotes were analysed as above (2.2.2) to classify them as procyclic, leptomonad, nectomonad and metacyclic accordingly.

The results obtained from each repeat were used to produce a mean result of number of migrated *Leishmania tarentolae* and *Leishmania mexicana* and the classification of migrated population for each test substance after 30 minutes incubation period. A chemotaxis index (CI) (equation modified from Oliveira et al. )

was calculated for all results with a positive score indicating attraction towards the test substance and a negative index evidence of repulsion.

$$\text{Migration Chemotaxis Index (MCI)} = \left( \frac{\text{Number of cells migrated in test} - \text{Number of cells migrated in control}}{\text{Total number of cells per ml}} \right)$$

### 3.3.4 Experimental conditions

Substances that were tested were used in specific amounts for the known concentration of substance in the capillary tubes to be calculated and listed in Table 3. L-glutamine, L-leucine, L-methionine, L-cysteine, glycine, L-tyrosine, L-histidine, Uric acid and L-aspartic acid were trialled however required a large volume of Dimethylsulfoxide (DMSO) for solubilisation.

<i>Test substances</i>	<i>Concentrations tested</i>
<i>D-glucose (AnalaR)</i>	1.0M 0.5M 0.1M
<i>Sucrose (Fisher)</i>	0.5M
<i>Urea (Electran)</i>	1.0M 0.5M 0.1M
<i>NaCl (Fisher)</i>	0.5M
<i>Mannose (Sigma)</i>	0.5M
<i>D-sorbitol (Sigma)</i>	0.5M
<i>Fructose (Sigma)</i>	0.5M
<i>Promastigote secretory gel (PSG)</i>	
<i>Copper Sulphate (Sigma)</i>	0.05M

**Table 3. Summary of test substances and concentrations as used for the capillary assay.**

The PSG used was collected from *Lutzomyia longipalpis* infection with *Leishmania mexicana* from the foregut and kept in -4°C in 10µl PBS. For use in the capillary assay, this was homogenised with a pestle before being centrifuged at 3000g for 5 minutes. The supernatant was removed without disturbing the pellet and used to prepare the capillary tube. For the control, capillary tubes containing no substances was used, therefore only 1% agarose, WIS buffer and 0.004% FBS remained in the capillary tube.

### **3.4 Part C: Development of a microfluidic method to analysing *Leishmania* chemotaxis**

#### **3.4.1 Microfabrication**

Computer-aided design of microfluidic chip geometries was done using the AutoCAD 2009 software (Auto-desk). The master fabrication was kindly prepared at the University College London (UCL) generating the master mould containing the central culture chamber and the testing substances channels. For the microfluidic device fabrication at Lancaster University, the mould was cleaned and plasma activated, immersed in 1% tri-decafluoro-1,1,2,2-tetrahydrooctyl-1-dimethylchlorosilane (13F; MCC) in toluene for 30 min, washed, dried, and baked at 55°C for 15 min.

Polydimethyl methylhydrogen siloxane (PDMS) casts were prepared by mixing 1:10 parts of curing agent to base Sylgard 184 elastomer (Dow Corning Corp.). The PDMS mix was degassed and poured onto the 13F-coated patterned wafer and cured at 55°C overnight to harden. The release of the mould obtained a replica of the micro-channels on the PDMS block. Individual devices were cut and stored covered, feature-side up. For the bonding of the microfluidic device to a glass substrate, individual PDMS casts were exposed to plasma for 30s on both side before gentle pressure was applied to bond the device to the glass. The assembled chips were baked for 15 min at 75°C for irreversible bonding.

### 3.4.2 Cell migration in microfluidic device

The test substances were introduced to the peripheral chambers and promastigotes in WIS solution with 0.004% FBS were introduced in the central chamber (Figure 25). Once saturated with cells, the fluid streams adjusted allowing for a linear gradient of substance spanning from the peripheral chamber to the central cells. Upon sensing the substances, cells migrated into transversal channels where they were imaged using fluorescence time-lapsed microscopy effected by a scanning laser confocal microscope.

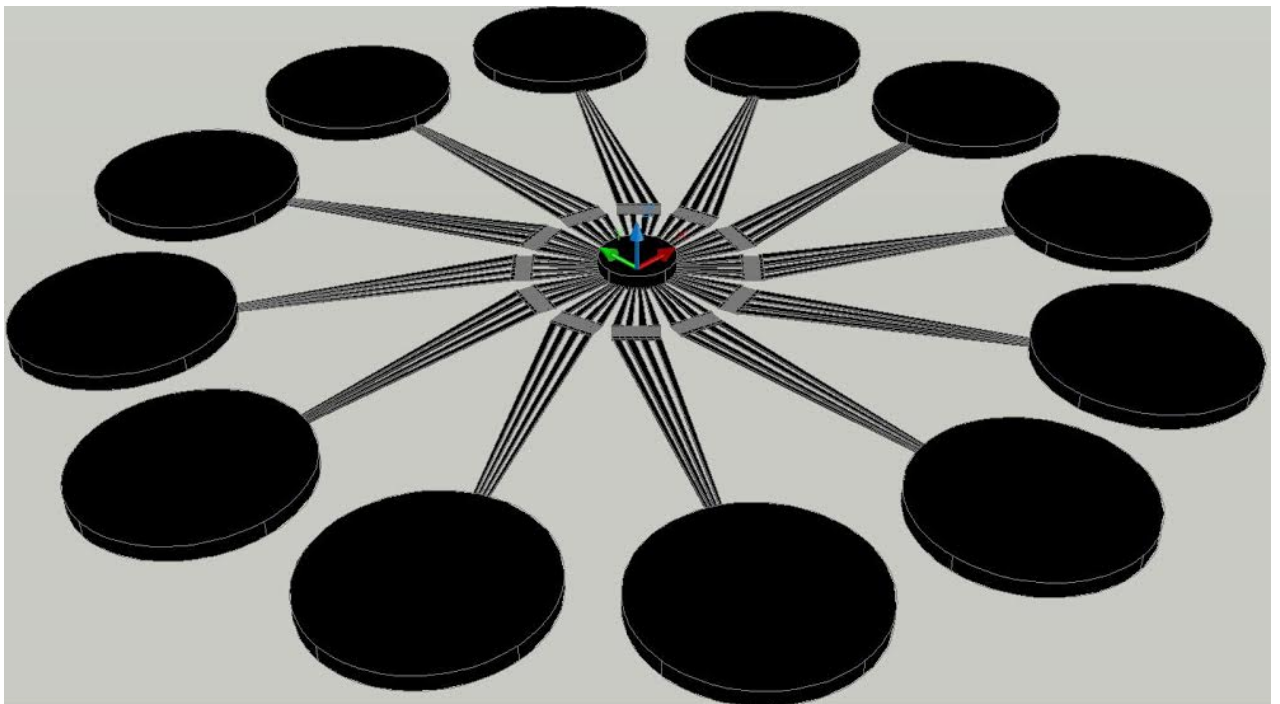


Figure 25: Development of a microfluidic device for *Leishmania taxis* assay. Top view of the radial chip, showing 12 inlets along the outer edge and a singular central reservoir for cell culture.

### **3.5 Part D: Experimental infections of the *Lutzomyia longipalpis* with *Leishmania tarentolae* and *Crithidia fasciculata*, and *Aedes aegypti* with *Crithidia fasciculata***

#### **3.5.1 Heat treatment of sheep blood**

Sheep blood was heat-treated as follows: 5 ml of sheep blood was centrifuged at 3000g for 5 minutes. Serum was removed and incubated at 56 °C for 45 minutes in a water bath. PBS of the same volume as serum removed was added to red cells and centrifuge washed 3 times at 4 °C. Following all washing and given a suitable time to cool down, PBS supernatant was removed and serum was returned to the pellet of red cells for resuspension. This blood was used for the infection protocol.

#### **3.5.2 Infection protocol**

Parasites used for fly infections were cultivated as above (3.1.4). Counts were used to determine the volume of culture to wash and pellet to result in  $2.0 \times 10^7$  cells per ml in 2 ml of either decomplexed sheep as above (3.5.1) blood for *L. mexicana* and *L. tarentolae*, and Warrens medium or 5% autoclaved sucrose solution for *C. fasciculata*. Viability of parasites were checked before and after infection under microscope.

##### *Lutzomyia longipalpis*

4-5 day old female *Lu. longipalpis* were infected with *L. tarentolae*, *L. mexicana* and *C. fasciculata*. For *L. tarentolae* and *L. mexicana* infections, sandflies were fed using infected decomplexed sheep blood containing washed parasites whilst *C. fasciculata* infections used Warrens medium containing washed parasites. For infection, *Lu. longipalpis* fed on the infected blood or medium using the Hemotek and chicken skin membrane feeding method held at 37 °C.

*Aedes aegypti* with *Crithidia fasciculata*

4-5 day old female *A. aegypti* were infected with *L. tarentolae* and *C. fasciculata*. *A. aegypti* was infected with *C. fasciculata* and *L. tarentolae* in a 5% sucrose solution soaked in cotton wool. Feeding with capillary tubes and on a glass slide were also trialled.

### 3.5.3 Dissection

After infecting, visibly fed females were separated to ensure that all dissected insects had ingested parasites during infection. Due to all females normally feeding on a sugar meal, it was assumed that all uninfected insects had fed on sucrose.

To verify successful infections, fed females were dissected in the days following their infection to observe the presence of live parasites within the gut: 1 day, 3 days, 5 days and 7 days post infection. The sandflies and mosquitoes for dissection were collected in a solution with 15ml PBS and one drop of detergent Tween 80 (Sigma) preventing insects using surface tension for escape; solution was kept on ice. Singularly, flies were collected with a tweezer and placed on a glass slide containing a drop of sterile PBS for dissection in which the full gut was removed. Tweezers and needles used in dissections were cleaned with 70% ethanol between each insect dissection to prevent anomalous PSG detection.

The results of the dissection were processed in different ways. The whole gut was examined under a light microscope to determine the location of the infection. The whole gut was later separated into hindgut, midgut, foregut or kept as a whole gut. Roughly 20 insects were dissected for each condition, with separated gut sections kept in 10µl sterile PBS (pH 7.2) on ice before homogenisation. For the later visualisation of parasites, each section was homogenised with a pestle before being used to prepare slides. After air drying, these slides were later fixed and stained for analysis as above (3.2.1). For the analysis of PSG, the section of gut homogenate was centrifuged at 1300g for 10 minutes before the supernatant was removed without disturbing the pellet and placed in a fresh microcentrifuge tube for storage in a freezer for further analysis.

## CHAPTER FOUR: RESULTS

### 4.1 *Leishmania mexicana* morphometric analysis *in vitro*

Prior to the establishment of the development profile of *L. mexicana* promastigotes in culture, a growth curve was constructed to examine the growth rate of the parasite *in vitro*. Growth of parasites in 199 medium with 20% FBS as stated in the Materials and Methods section was monitored over 168.5 hours with cell density calculated using a haemocytometer approximately every 24 hours (27.5, 51.5, 74.5, 101.5, 120.5, 149.0 and 168.5 hours). An average of 10 counts for each time point was used for average results plotted to give the lag, exponential and stationary phases of parasite growth within the environmental conditions mentioned.

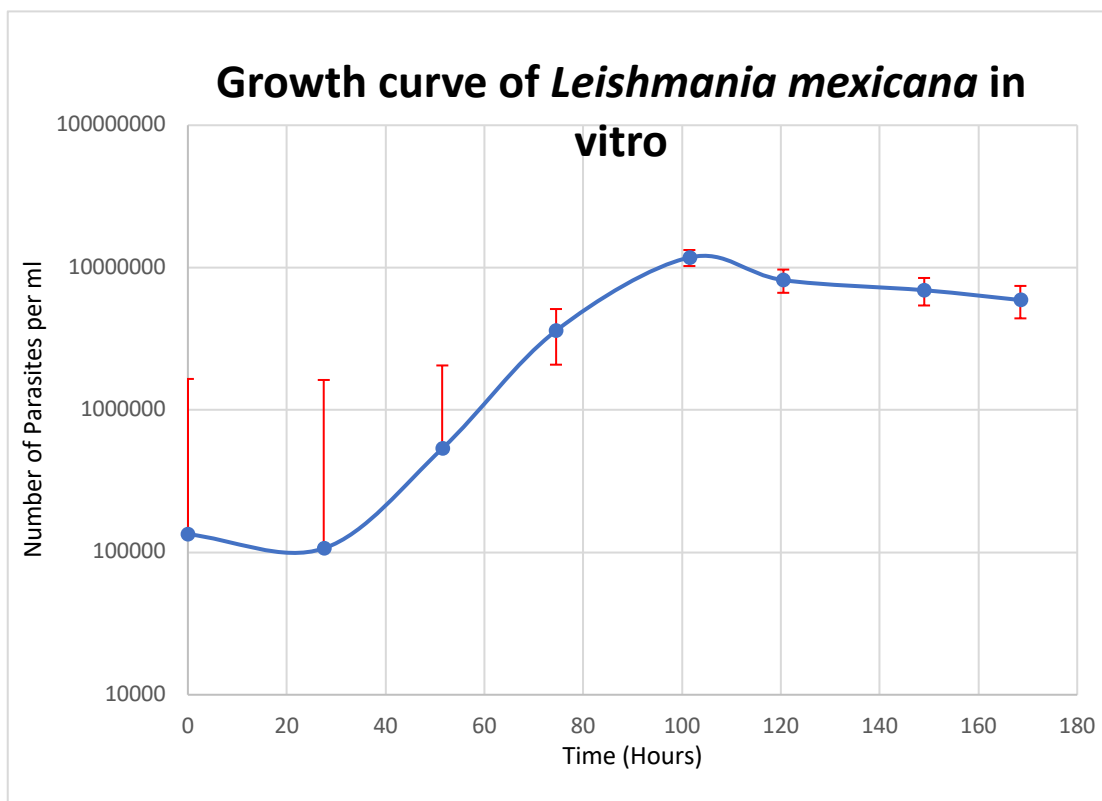


**Figure 26: Growth curve of *Leishmania mexicana* in vitro.** Graph shows the parasite density (y axis) over time (x axis) in 199 medium culture containing 20% FBS and BME vitamins. 0 hours represents the initial density of parasite immediately following passage of late log stage parasites into a new culture flask. Parasite growth was followed for 168.5 hours with the final population density of  $6.0 \times 10^6$  cells  $\text{ml}^{-1}$ . Red line shows the standard error. Data presented was from 3 repeated experiments ( $n=3$ ).

Hours 0 - approximately 25 shows the lag phase with no increase in number of parasites, hours 25- 100 shows an exponential increase in the population density representing the exponential phase of the parasite growth and hours 100- approximately 105 shows a plateau in number of parasites in which cell division and cell death rate is equivalent representing the stationary phase (Figure 26). Following this at 105 hours, there is a steady decline in the number of parasites representing the death phase.

To generate the developmental profile (Figures 27 to 31) of *L. mexicana*, parameters were measured of cells collected daily at the time points (27.5, 51.5, 74.5, 101.5, 120.5, 149.0 and 168.5 hours) from the axenic culture growth for 5 days. The development profile of *L. mexicana* promastigotes used the measured parameters of body length (BL), body width (BW), and flagellum length (FL). However an additional parameter of distance from kinetoplast (K) to nucleus (N) was calculated from only 1N1K cells (2N1K and 2N2K cells were not included in this data) to establish its changes during the development of promastigotes. Using these parameters stated, the morphology of parasite *in vitro* is presented graphically for the variability between parameters to be visualised (Figure 27, 28, 29 and 30).

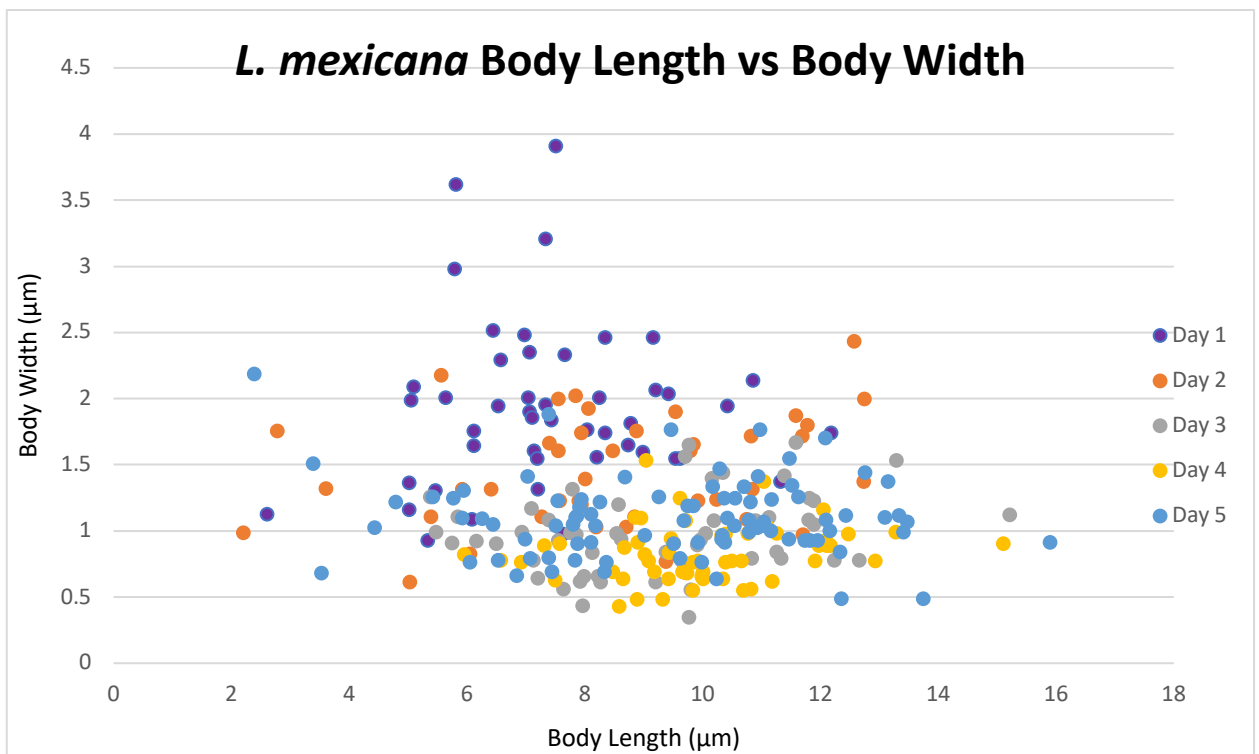


Figure 27: Scatter plot showing *L. mexicana* cell body length (x axis) against cell body width (y axis) measured in μm. Each point represents a singular cell, with the date collected from culture represented by the colour of dot shown in legend. Day 1 n=47, Day 2 n=42, Day 3 n=54, Day 4 n=55, Day 5 n=88. Data presented was from 3 repeated experiments.

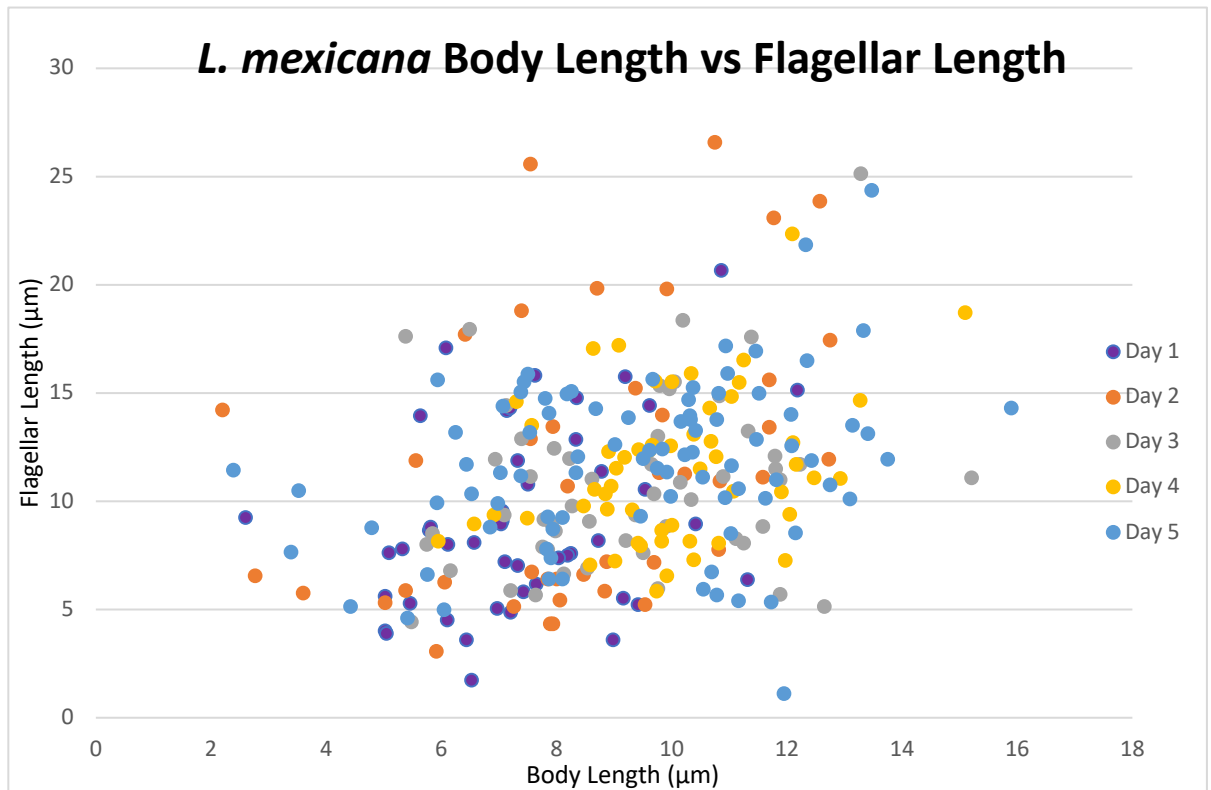


Figure 28: Scatter plot showing *L. mexicana* cell body length (x axis) against cell flagella length (y axis) measured in  $\mu\text{m}$ . Each point represents a singular cell, with the date collected from culture represented by the colour of dot shown in legend. Day 1 n=47, Day 2 n=42, Day 3 n=54, Day 4 n=55, Day 5 n=88. Data presented was from 3 repeated experiments.

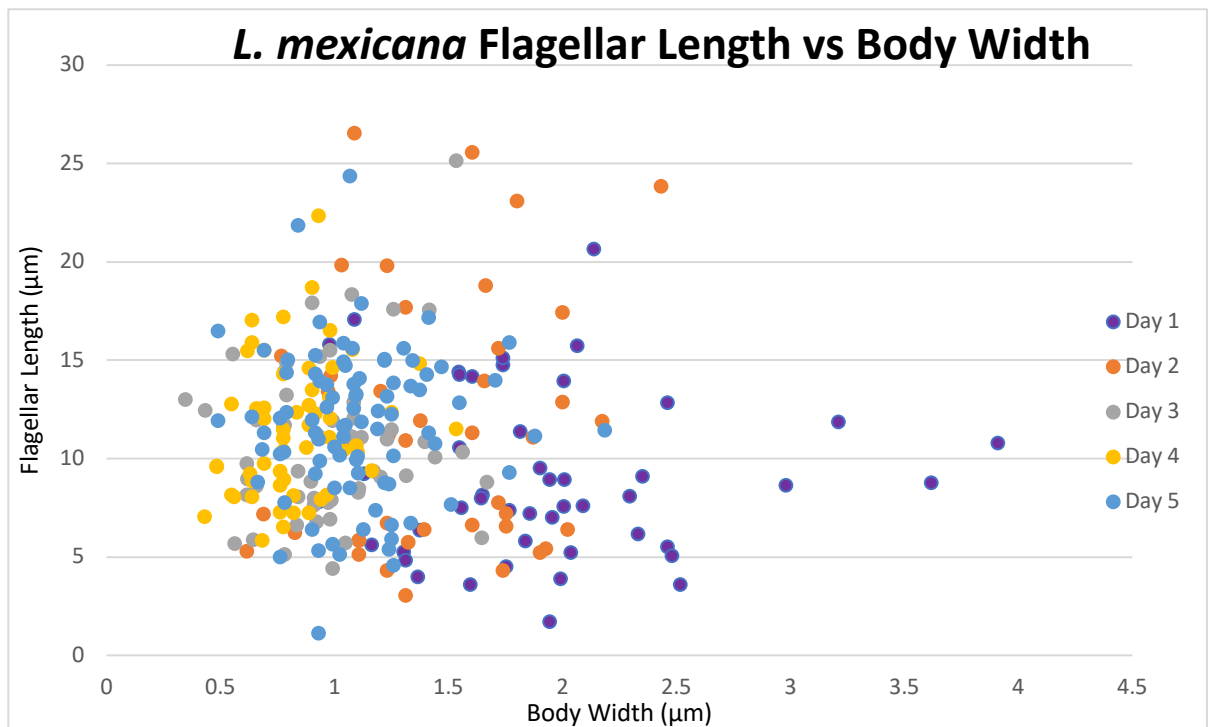


Figure 29: Scatter plot showing *L. mexicana* cell body width (x axis) against cell flagella length (y axis) measured in  $\mu\text{m}$ . Each point represents a singular cell, with the date collected from culture represented by the colour of dot shown in legend. Day 1 n=47, Day 2 n=42, Day 3 n=54, Day 4 n=55, Day 5 n=88. Data presented was from 3 repeated experiments.

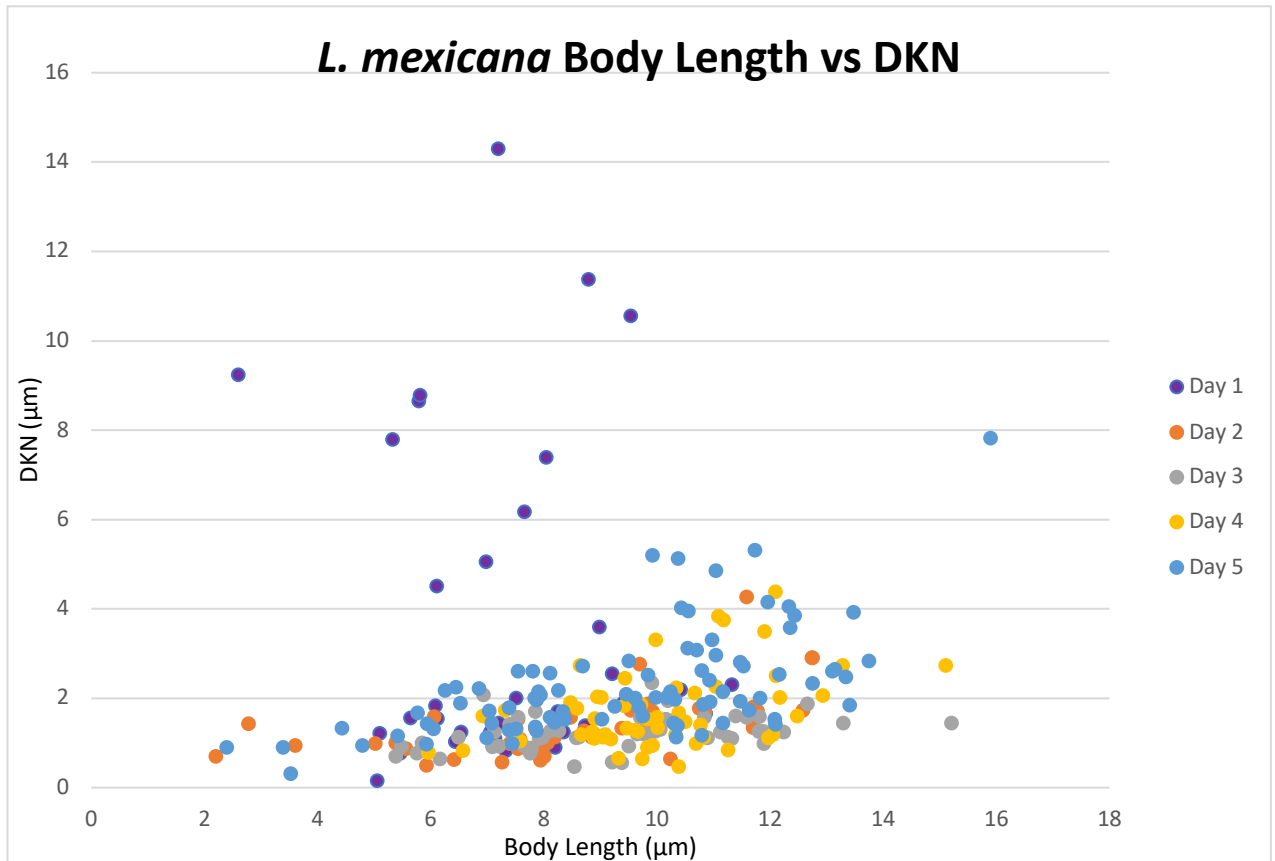
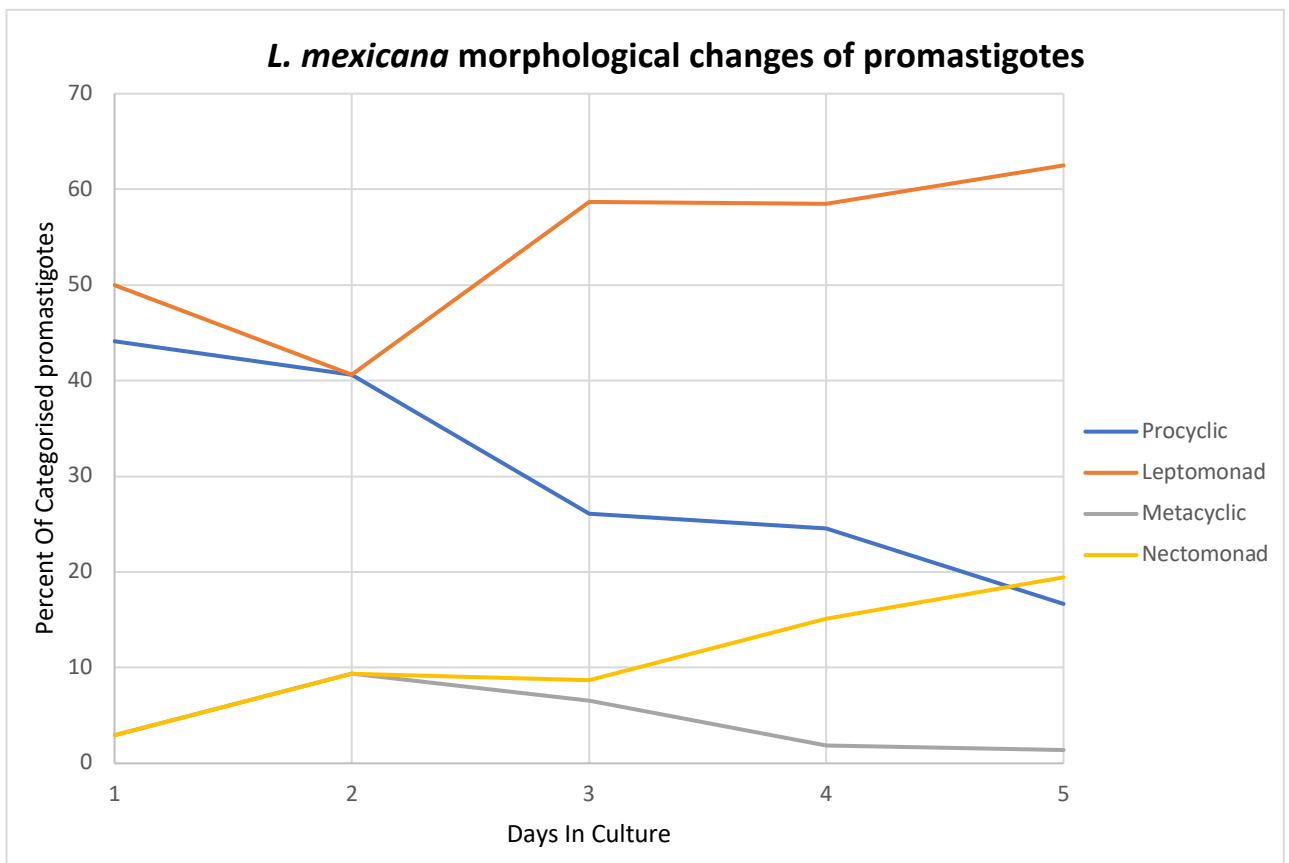


Figure 30: Scatter plot showing *L. mexicana* cell body length (x axis) against distance from kinetoplast to nucleus (y axis) measured in  $\mu\text{m}$ . Each point represents a singular cell, with the date collected from culture represented by the colour of dot shown in legend. Day 1 n=47, Day 2 n=42, Day 3 n=54, Day 4 n=55, Day 5 n=88. Data presented was from 3 repeated experiments.

Figure 27 shows the distribution of cell body length against cell body width of *L. mexicana* promastigotes is variable. Visualising groupings as days collected from the axenic culture, day 1 body length ranges between 5.022  $\mu\text{m}$  and 12.185  $\mu\text{m}$  with the body width ranging between 0.93  $\mu\text{m}$  and 2.982  $\mu\text{m}$ . Day 2 length ranges increases to between 2.773  $\mu\text{m}$  and 12.749  $\mu\text{m}$  with the body width reducing to ranging between 0.615  $\mu\text{m}$  and 2.432  $\mu\text{m}$ . This continues to day 3, with the length range increasing to between 5.381  $\mu\text{m}$  and 15.209  $\mu\text{m}$ , and the body width decreasing to range between 0.347  $\mu\text{m}$  and 1.648  $\mu\text{m}$ . However in day 4, the length range decreases to between 5.954  $\mu\text{m}$  and 12.474  $\mu\text{m}$  with the body width further reducing to range between 0.483  $\mu\text{m}$  and 1.534  $\mu\text{m}$ . Day 5 length ranges increases as normal to between 2.39  $\mu\text{m}$  and 13.749  $\mu\text{m}$  with the body width increasing to range between 0.683  $\mu\text{m}$  and 1.768  $\mu\text{m}$ . These changes in body length and body width are small; however when all the cells are visualised as a whole, a potential trend can be seen in the data. With the increase in cell body length (BL), there is a decrease in the body width (BW).

Figure 28 shows the distribution of cell body length against cell flagella length of *L. mexicana* promastigotes shows a clearer trend than that showed by Figure 27. Generally, the increase of cell body length results in the increase of flagella length. However, when flagella length is compared with the cell body width (Figure 29), the trend is less visible with a variable spread of data.

Figure 30 shows the distribution of cell body length against distance from kinetoplast to nucleus (DKN) of *L. mexicana* promastigotes. This shows a positive correlation of the DKN increase as the body length increases. Therefore as the promastigote increases length due to progressing through the life cycle and the developmental progression of metacyclogenesis.



**Figure 31: *L. mexicana* morphological changes of promastigotes in culture using categorization set by Rogers et al. (2002).** Combining all cells collected in the 3 repeated experiments, Day 1 n=47, Day 2 n=42, Day 3 n=54, Day 4 n=55, Day 5 n=88. Following 1 day in culture, 50% of promastigotes are leptomonad promastigotes, 45% are procyclics and 5% are nectomonads. Overall, the levels of leptomonads increases to 63% at day 5, procyclics decrease to about 16% at day 5, nectomonads increase to 20% and metacyclics start to appear in culture with about 3% in day 5. Data presented was from 3 repeated experiments.

The compilation of these measure parameters from photomicrographs allowed promastigote morphological changes to be presented in a graphical form (Figure 31). The criteria used for promastigote to be categorised into procyclic, nectomonad,

leptomonad, haptomonad and metacyclic promastigotes was dependent on morphology criteria (Figure 16). For *L. mexicana*, criteria set by Rogers et al, (2002) was used. This gave a graph that shows the changes in promastigote forms over 5 days from culture (Figure 31). Day 1 represented 1 day following passage and contained 50% leptomonad promastigotes, 5% nectomonad promastigotes and 45% procyclic promastigotes. Procyclic promastigotes have a body length between 6.5 to 11.5  $\mu\text{m}$ , a flagellum length less than the body length and the body width variable. This form of promastigotes decreased over the days to 16% in day 5. Leptomonad promastigotes have a body length between 6.5 to 11.5  $\mu\text{m}$  with the flagella greater than body length. This form of promastigotes decreased to 40% in day 2, then rapidly increased to 59% in day 3 before steadily increasing over the days to 63% in day 5. Nectomonad promastigotes have a body length greater than 12  $\mu\text{m}$ . This form of promastigotes increased over the days to 20% in day 5. Recovering metacyclics showed the onset of metacyclogenesis. This occurred after day 2, however metacyclic promastigotes did not dominate the culture in day 5 as presumed, with only 3% of cells in day 5 being categorised as metacyclic promastigotes.

## **4.2 *Leishmania tarentolae* morphometric analysis *in vitro***

Prior to the establishment of the development profile of *L. tarentolae* promastigotes in culture, a growth curve was constructed to examine the growth rate of the parasite *in vitro*. Growth of parasites in 199 medium with 10% FBS as stated in the Materials and Methods section was monitored over 175.5 hours with cell density calculated using a haemocytometer approximately every 24 hours (33.3, 56.0, 76.5, 101.0, 124.0, 151.5 and 175.5 hours). An average of 10 counts for each time points was used for average results plotted to give the lag, exponential and stationary phases of parasite growth within the environmental conditions mentioned.

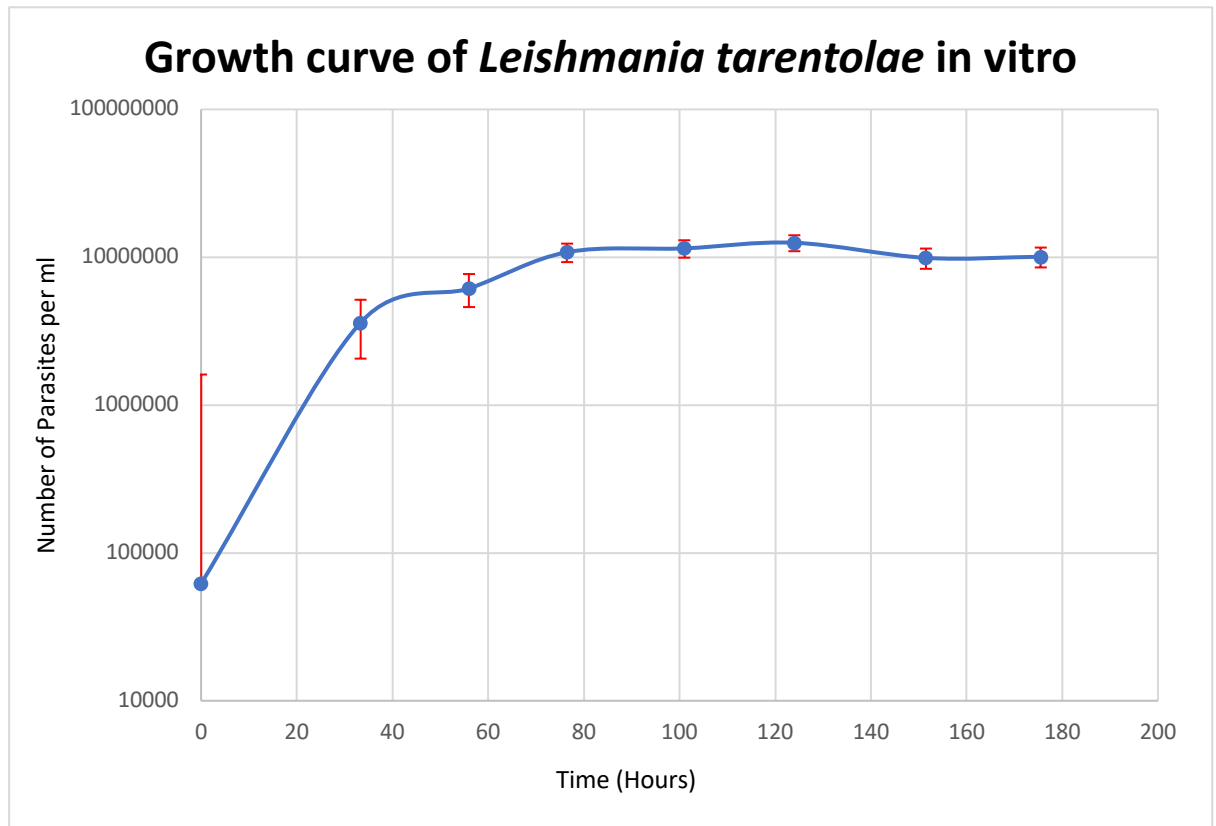


**Figure 32: Growth curve of *Leishmania tarentolae* in vitro.** Graph shows the parasite density (y axis) over time (x axis) in 199 medium culture containing 10% FBS and BME vitamins. 0 hours represents the initial density of parasite immediately following passage of late log stage parasites into a new culture flask. Parasite growth was followed for 175.5 hours with the final population density of  $1.0 \times 10^7 \text{ ml}^{-1}$ . Red line shows the standard error. Data presented was from 3 repeated experiments ( $n=3$ ).

No lag phase is seen as rapid parasite growth occurs. Hours 0- 80 shows an exponential increase in the population density representing the exponential phase of the parasite growth and hours 80- approximately 130 shows a plateau in number of parasites in which cell division and cell death rate is equivalent representing the stationary phase (Figure 32). Following this at 130 hours, there is a steady number of parasites representing the death phase.

To generate the developmental profile of *L. tarentolae*, parameters were measured of cells collected at 24 hour intervals from the axenic culture growth for 5 days. The development profile of *L. tarentolae* promastigotes used the measured parameters of body length (BL), body width (BW), and flagellum length (FL). However an additional parameter of distance from kinetoplast (K) to nucleus (N) was calculated from only 1N1K cells (2N1K and 2N2K cells were not included in this data) establish its changes during the development of promastigotes. Using these parameters stated, the morphology of parasite in vitro is presented graphically for the variability between parameters to be visualised (Figure 33, 34, 35 and 36).

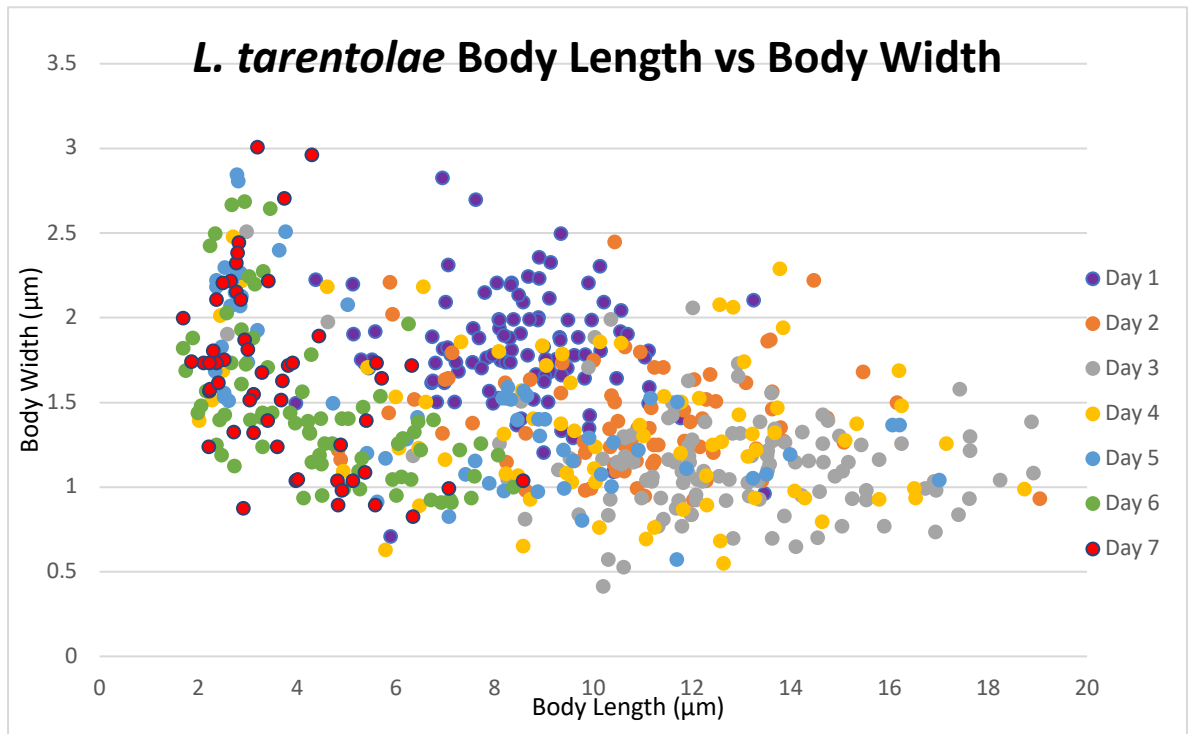


Figure 33: Scatter plot showing *L. tarentolae* cell body length (x axis) against cell body width (y axis) measured in  $\mu\text{m}$ . Each point represents a singular cell, with the date collected from culture represented by the colour of dot shown in legend. Day 1 n=106, Day 2 n=80, Day 3 n=119, Day 4 n=79, Day 5 n=64, Day 6 n=75, Day 7 n=54. Data presented was from 3 repeated experiments.

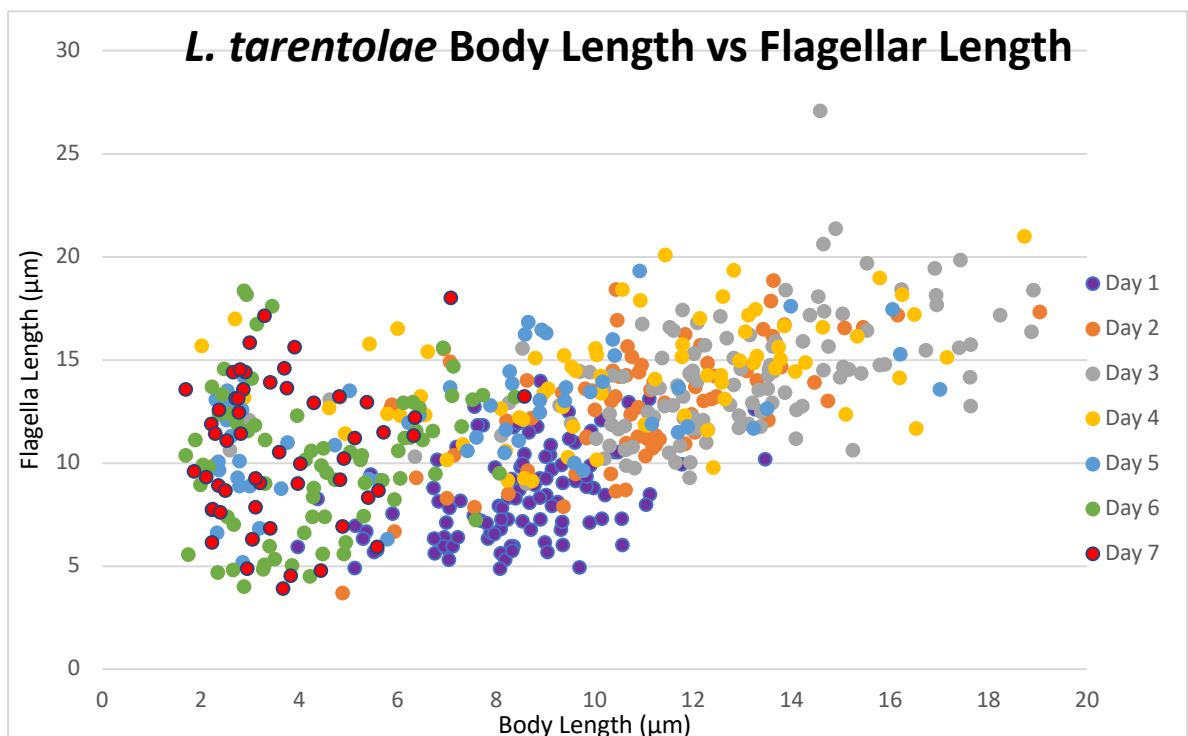


Figure 34: Scatter plot showing *L. tarentolae* cell body length (x axis) against cell flagellar length (y axis) measured in  $\mu\text{m}$ . Each point represents a singular cell, with the date collected from culture represented by the colour of dot shown in legend. Day 1 n=106, Day 2 n=80, Day 3 n=119, Day 4 n=79, Day 5 n=64, Day 6 n=75, Day 7 n=54. Data presented was from 3 repeated experiments.

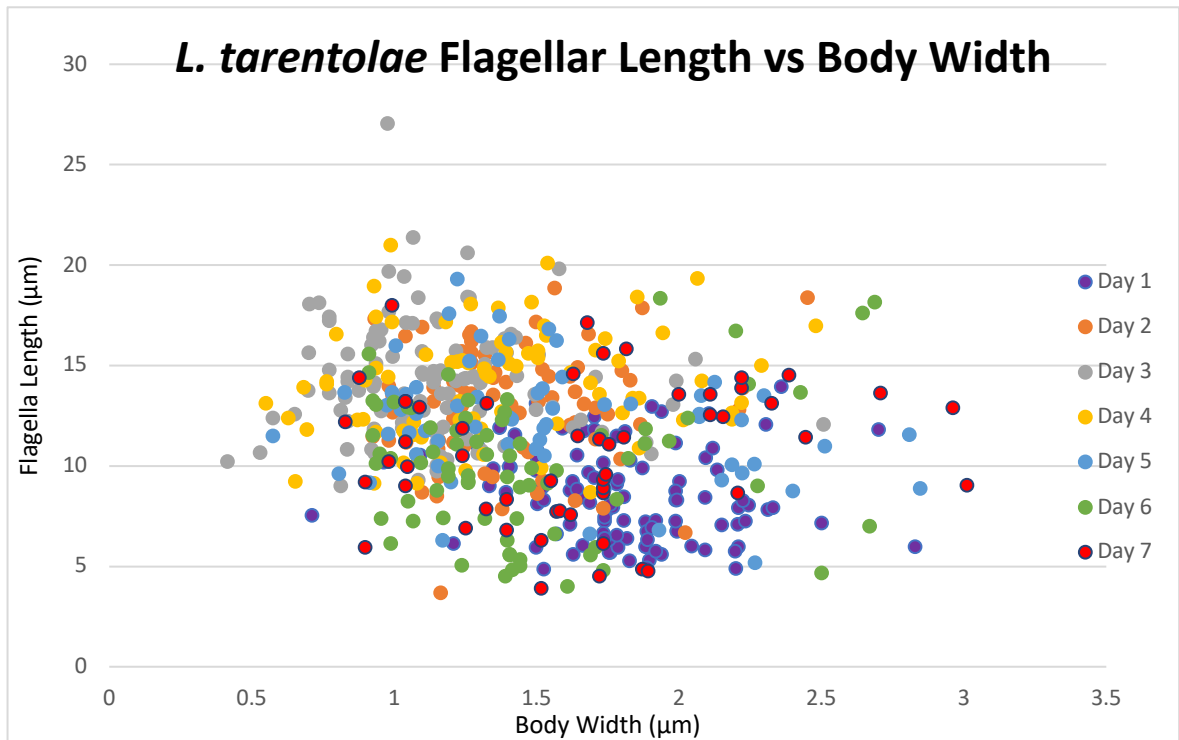


Figure 35: Scatter plot showing *L. tarentolae* cell body width (x axis) against cell flagellar length (y axis) measured in  $\mu\text{m}$ . Each point represents a singular cell, with the date collected from culture represented by the colour of dot shown in legend. Day 1 n=106, Day 2 n=80, Day 3 n=119, Day 4 n=79, Day 5 n=64, Day 6 n=75, Day 7 n=54. Data presented was from 3 repeated experiments.

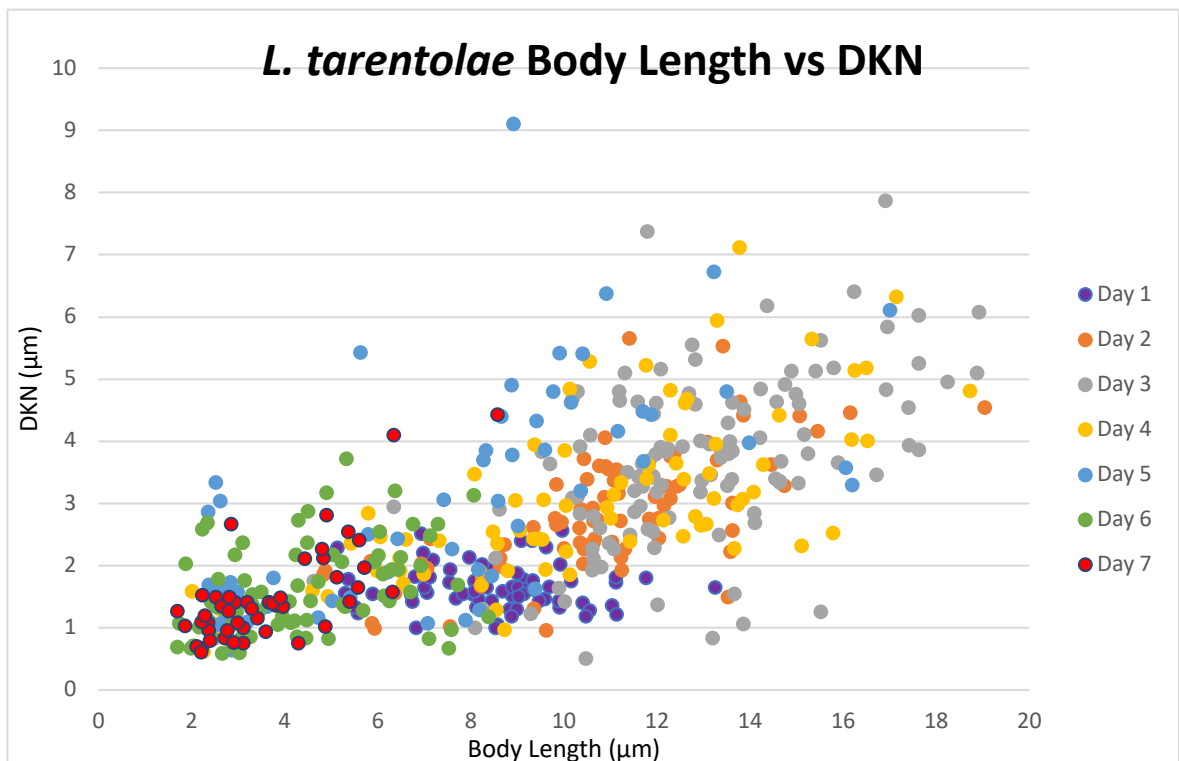
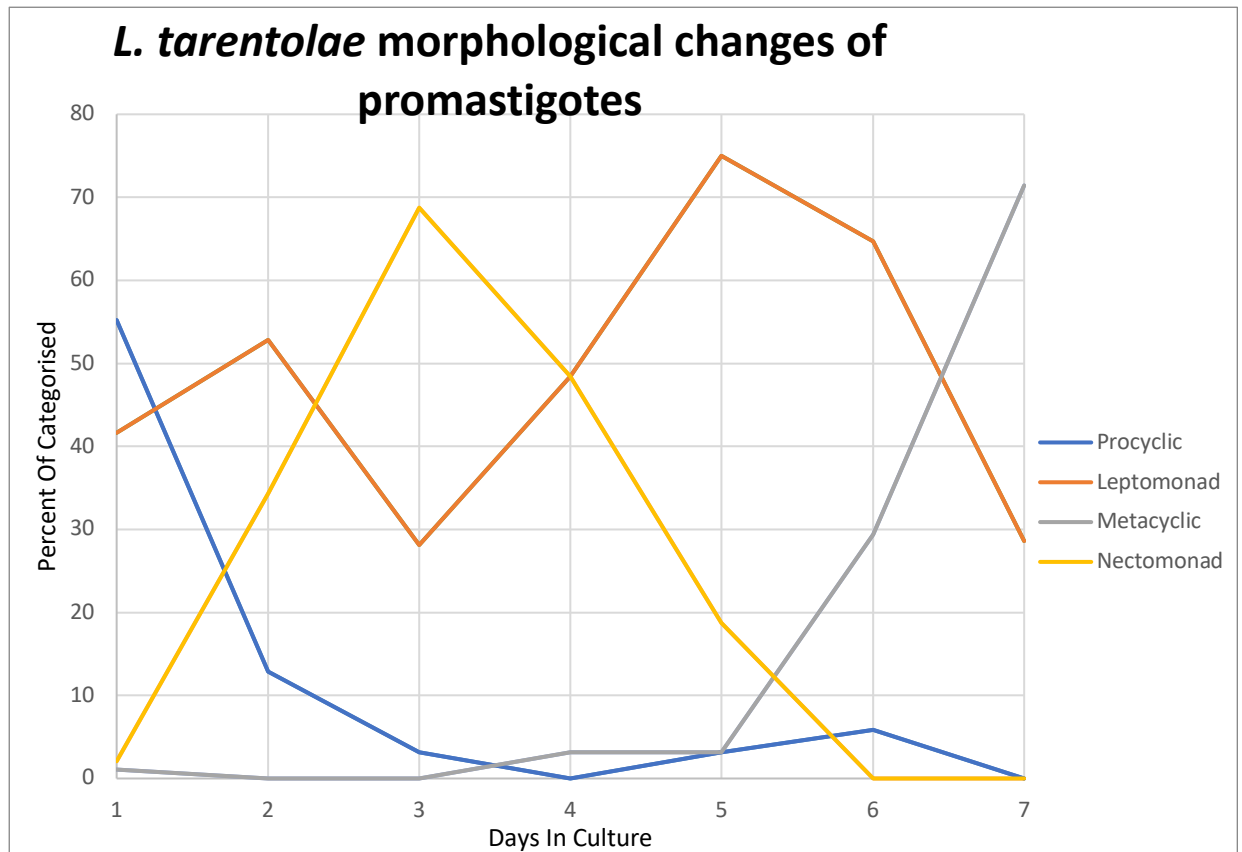


Figure 36: Scatter plot showing *L. tarentolae* cell body length (x axis) against distance from kinetoplast to nucleus (y axis) measured in  $\mu\text{m}$ . Each point represents a singular cell, with the date collected from culture represented by the colour of dot shown in legend. Day 1 n=106, Day 2 n=80, Day 3 n=119, Day 4 n=79, Day 5 n=64, Day 6 n=75, Day 7 n=54. Data presented was from 3 repeated experiments.

Figure 33 shows the distribution of cell body length against cell body width of *L. tarentolae* promastigotes is variable. Visualising groupings as days collected from the axenic culture, day 1 body length ranges between 5.136  $\mu\text{m}$  and 13.466  $\mu\text{m}$  with the body width ranging between 0.711  $\mu\text{m}$  and 2.5  $\mu\text{m}$ . Day 2 length ranges increases to between 6.375  $\mu\text{m}$  and 16.152  $\mu\text{m}$  with the body width ranging between 0.925  $\mu\text{m}$  and 2.45  $\mu\text{m}$ . This continues to day 3, with the length range increasing to between 2.583  $\mu\text{m}$  and 18.913  $\mu\text{m}$ , and the body width ranging between 0.44  $\mu\text{m}$  and 2.508  $\mu\text{m}$ . However in day 4, the length range decreases to between 2.491  $\mu\text{m}$  and 16.496  $\mu\text{m}$  with the body width reducing to range between 0.55  $\mu\text{m}$  and 2.481  $\mu\text{m}$ . Day 5 length ranges increases as normal to between 2.361  $\mu\text{m}$  and 17.007  $\mu\text{m}$  with the body width increasing to range between 0.575  $\mu\text{m}$  and 2.809  $\mu\text{m}$ . Day 6 length ranges decreases rapidly to between 1.69  $\mu\text{m}$  and 7.725  $\mu\text{m}$  with the body width increasing to range between 0.911  $\mu\text{m}$  and 2.688  $\mu\text{m}$ . Day 7 length ranges increases as normal to between 1.692  $\mu\text{m}$  and 8.574  $\mu\text{m}$  with the body width increasing to range between 0.828  $\mu\text{m}$  and 2.962  $\mu\text{m}$ . These changes in body length and body width are small; however when all the cells are visualised as a whole, a slight trend can be seen in the data. With the increase in cell body length (BL), there is a decrease in the body width (BW) similar to *L. mexicana* (Figure 27).

Figure 34 shows the distribution of cell body length against cell flagellar length of *L. tarentolae* promastigotes shows a clearer trend than that showed by Figure 33. Generally, the increase of cell body length results in the increase of flagellar length. However, when flagellar length is compared with the cell body width (Figure 35), the trend is less visible with a variable spread of data.

Figure 36 shows the distribution of cell body length against distance from kinetoplast to nucleus (DKN) of *L. tarentolae* promastigotes. This shows a positive correlation of the DKN increase as the body length increases. Therefore as the promastigote generally increases length due to progressing through the life cycle and the developmental progression of metacyclogenesis similar to that of *L. mexicana* (Figure 30).



**Figure 37: *L. tarentolae* morphological changes of promastigotes in culture using categorization set by Rogers et al. (2002).** Combining all cells collected in the 3 repeated experiments, Day 1 n=106, Day 2 n=80, Day 3 n=119, Day 4 n=79, Day 5 n=64, Day 6 n=75, Day 7 n=54. Following 1 day in culture, 55% of promastigotes are procyclics, 42% leptomonads, 2% nectomonads and 1% metacyclics. Procyclics decreased significantly over the days to 0 found after 7 days. Nectomonads increased rapidly to 68% in day 3 to further decreased to 0 at day 6. Leptomonads increased to 75% in day 5 and later decreased steadily to 28% in day 7. Metacyclics increase steadily to 5% in day 5 and rapidly increase significantly to 72% in day 7. Data presented was from 3 repeated experiments.

The compilation of these measure parameters from photomicrographs allows promastigote morphological changes to be presented in a graphical form (Figure 37). The criteria used for different promastigote stages was based on morphology criteria (Figure 16). To assign promastigote stages in both *Leishmania* species measured (*L. mexicana* and *L. tarentolae*), criteria set by Rogers et al, (2002) developed for *L. mexicana* was used. This gave a graph that shows the changes in promastigote forms over 7 days from culture (Figure 37). Day 1 represents 1 day following passage and contains 55% procyclics, 42% leptomonads, 2% nectomonads and 1% metacyclics. The percentage of promastigotes categorised as procyclics decreases significantly to 13% in day 2 and then remained steadily low for the remainder of the growth in culture. Nectomonads on the other hand increase rapidly to 68% in day 3, later decreasing rapidly to 0% in day 6 and remaining at that level.

Leptomonads increase on day 2 to 53%, decreased to 28% in day 3 before increasing again to 75% in day 5 and decreasing again. Metacyclics increased steadily to 5% in day 5 and rapidly increased to 72% in day 7.

The photomicrographs from which these morphometric analyses were collected from showed some unfamiliar morphologies that could not be explained or properly categorised using the criteria from Rogers et al (2002).

#### **4.2.1 Bulgtomonad promastigotes**

These were first described by Dillon and Liu (unpublished) in which a new criteria was suggested taking these promastigotes into consideration. Bulgtomonads were described as having a body width between 2.3-3.5  $\mu\text{m}$  with the body length roughly 15  $\mu\text{m}$ .

Cells that fit the visual description of bulgtomonads promastigotes were found in the axenic culture of *L. tarentolae* on day 4 (Image 1). These cells made up 20.24% of cells found in day 4. The bulgtomonad promastigotes all had their nucleus contained within the 'bulge' of the cell with the kinetoplast adjacent to the flagella. 11% of promastigotes that visually fit the criteria for bulgtomonad promastigotes did fit within the described morphology of bulgtomonad promastigotes by Dillon and Liu. Due to the low proportion of cells fitting the criteria, the cells that visually fit the description of bulgtomonads from day 4 *L. tarentolae* in culture have been used to give a revised average morphological criteria for bulgtomonad promastigotes (Figure 38).

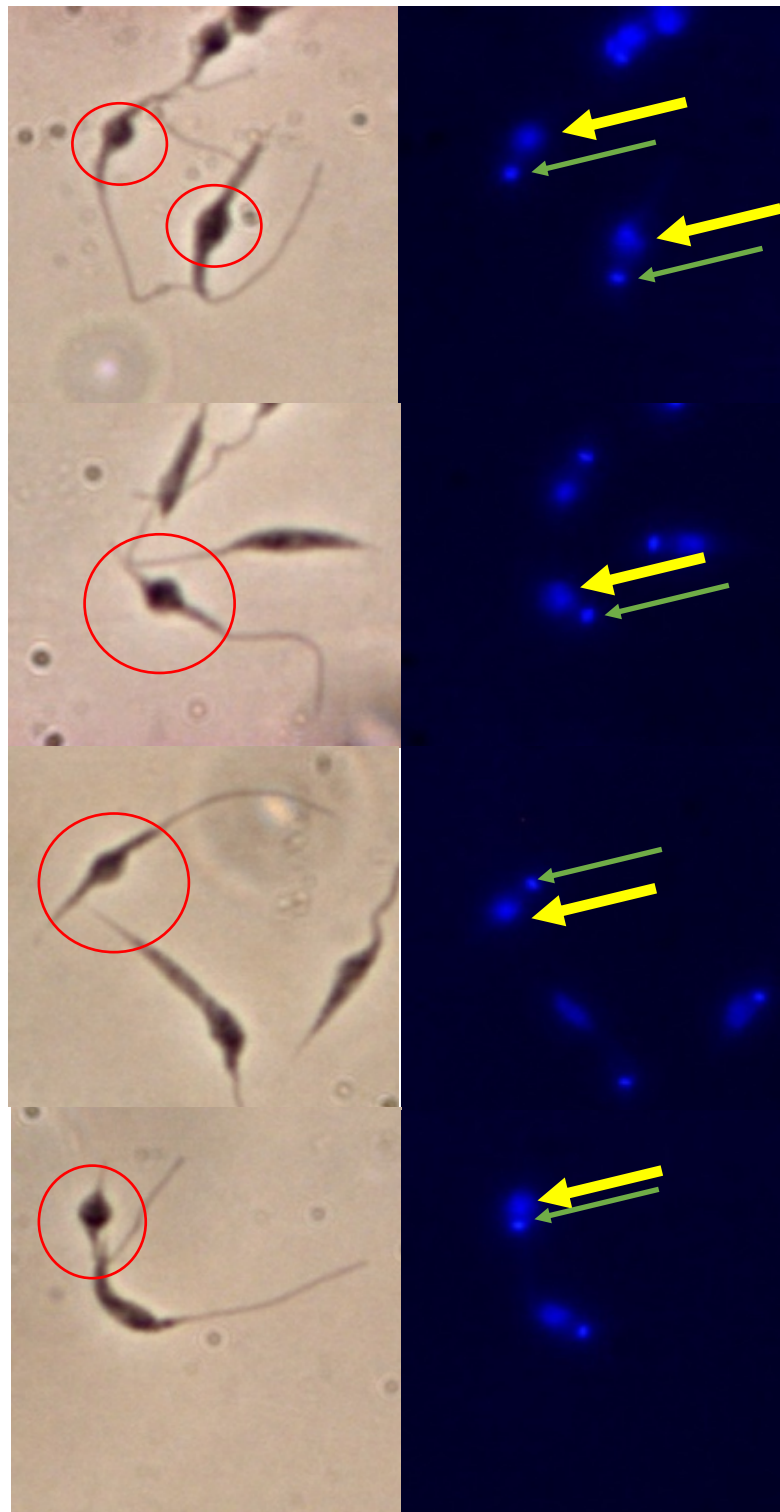


**Image 1:** Image shows *Bulgtomonad* promastigotes from *Leishmania tarentolae* axenic culture day 4. Left images were stained with Giemsa and right images were stained with DAPI. The thick yellow arrow points to the nucleus DNA whilst the thin green arrow points to the kinetoplast DNA. Red circles showing regions of visual bultomonad promastigotes.

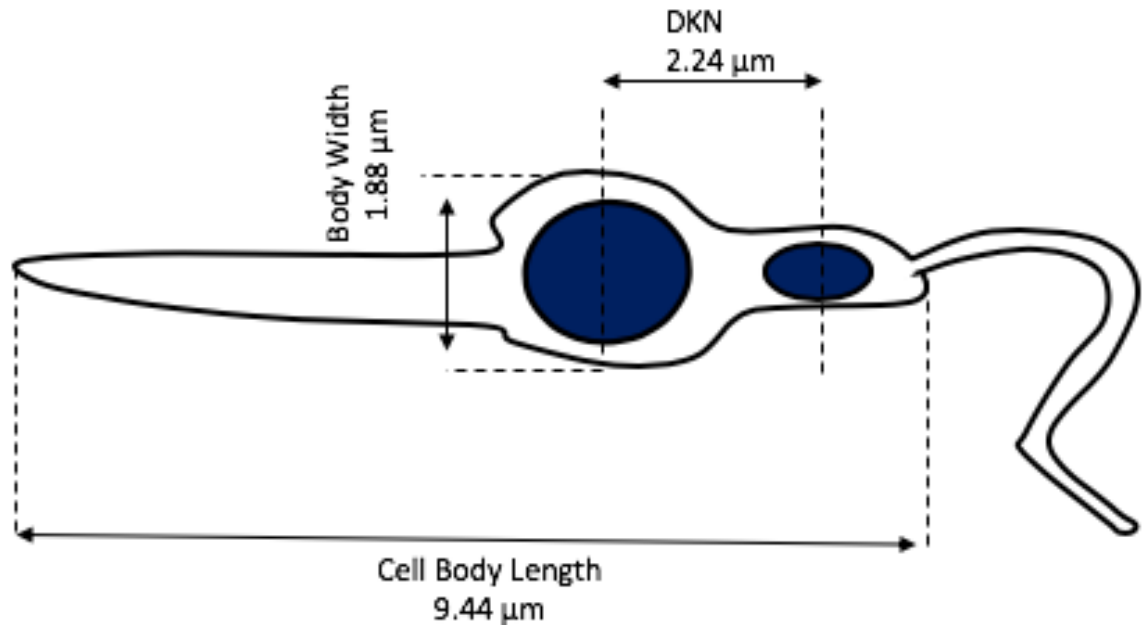


Figure 38: Morphology criteria for *L. tarentolae* Bulgtomonad promastigotes. Body width across bulge of around 1.88μm, distance from nucleus to kinetoplast (DKN) of 2.24μm and cell body length of 9.44μm.

#### 4.2.2 Kinetoplast Nucleus swapping promastigotes

Both the nucleus and kinetoplast is seen under DAPI staining, with the kinetoplast DNA being smaller and brighter when compared to the nucleus DNA. The kinetoplast is seen to be anterior to the nucleus in most promastigotes, however in some promastigotes seen in the death phase of *L. tarentolae* the seems to be a change in its location (Image 2 and 3). These cells were spherical in cell body shape and had a flagellum significantly longer than its cell body. Taking into account all cells that presented this morphology, this cell type was categorized; cell body length was roughly 2 μm, cell body width was roughly 1.7 μm, flagellum length was roughly 10.842 and DKN was roughly 0.7 μm.

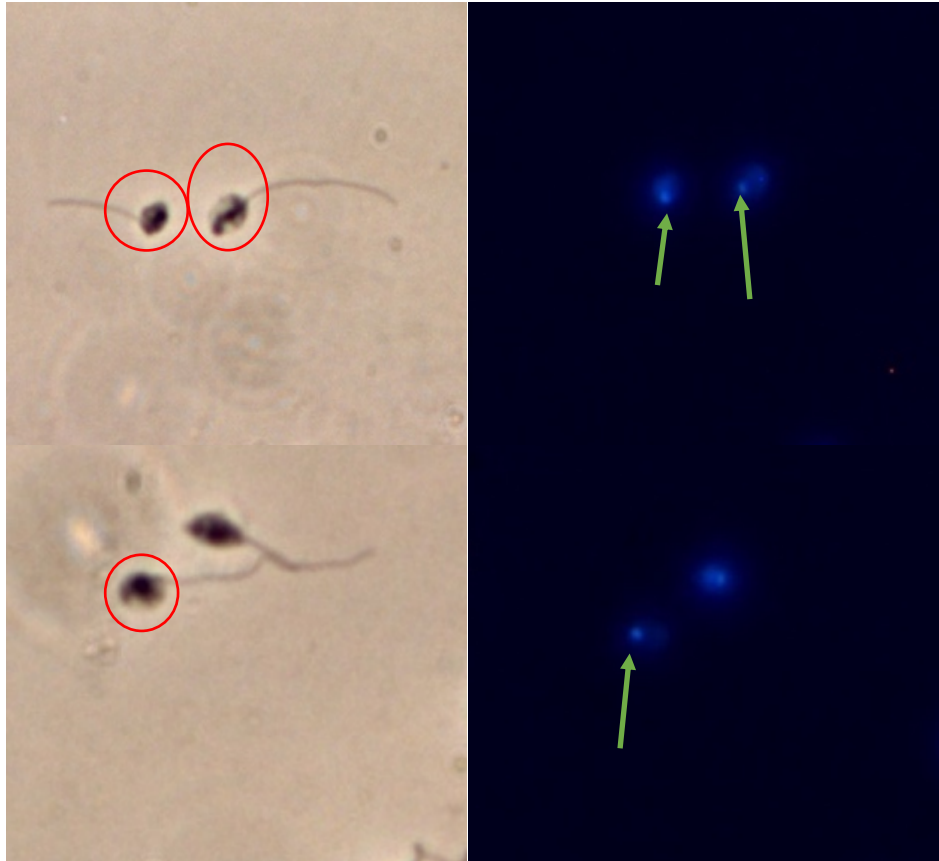


Image 2: Image shows kinetoplast and nucleus swapping promastigotes from *Leishmania tarentolae* axenic culture day 7. Left images were stained with Giemsa and right images were stained with DAPI. The promastigotes of interest are circled, with green arrows showing the kDNA.

### 4.3 Analysing chemotaxic migration

Chemotaxic assay mentioned in Materials and Methods 3.3 was used to produce all the data. Capillary assay was set up using PSG collected in a *L. mexicana* infection with *Lu. longipalpis*, 0.5M glucose, 0.5M fructose, 0.5M urea, 0.5M sorbitol, 0.5M mannose, 0.5M sucrose and 0.05M copper sulphate. Copper sulphate resulted in some migrated cells, however all cells were lysed and therefore could not be used for further analysis.

#### 4.3.1 Capillary assay

Figure 39 shows the migration chemotaxis index (MCI); a positive index showed attraction towards the chemoeffector whereas a negative index shows repulsion. Visualising the graph, generally all chemoeffectors have a positive index for *L. mexicana* and *L. tarentolae* for both days (day 3 and day 5). PSG shows positive chemotaxic index throughout; with *L. mexicana* day 5 having the highest MCI of 2.428, *L. mexicana* day 3 having an MCI of 2.285, *L. tarentolae* day 5 having an MCI of 0.804 and *L. tarentolae* day 3 having an MCI of 0.333. The data shows that *L. mexicana* is more attracted to PSG compared to *L. tarentolae*, with forms found in the late stationary phase/death phase showing higher attraction. Glucose shows a positive MCI to all *L. mexicana* and *L. tarentolae* day 5 promastigotes. *L. tarentolae* day 3 show a slight negative MCI of 0.752. *L. mexicana* and *L. tarentolae* day 5 promastigotes show similar MCIs in fructose between 0.4 to 0.8 and glucose of roughly 1.65 (Figure 39). *L. mexicana* day 3 have the highest MCI to both sugars, followed by *L. mexicana* day 5. Using a 5% two-tailed Mann Whitney U-test (appendix II) for *L. mexicana* day 3 and day 5 glucose recorded cell population of migrated cells result, the p value of 0.006233 was calculated showing that the result was highly significant. *L. mexicana* and *L. tarentolae* day 5 have MCIs below 1.0 towards urea, however *L. tarentolae* day 3 show a high MCI of 2.820. Using a 5% two-tailed Mann Whitney U-test (appendix II) for *L. tarentolae* day 3 and day 5 urea results, the p value of 0.000532 showing that the result was highly significant. Sorbitol and mannose generally have a low MCI between -1.0 and 1.0, however *L. mexicana* day 3 have a MCI of 1.678 towards mannose. Sucrose generally has attractiveness similar to glucose and fructose, with *L. mexicana* day 3 having a MCI of 6.0.

Overall, *L. mexicana* day 3 show a stronger attraction to when compared to *L. mexicana* day 5 towards the sugars glucose, fructose, mannose and sucrose. *L. tarentolae* day 3 show great attraction towards urea, with others not having much of an attraction.

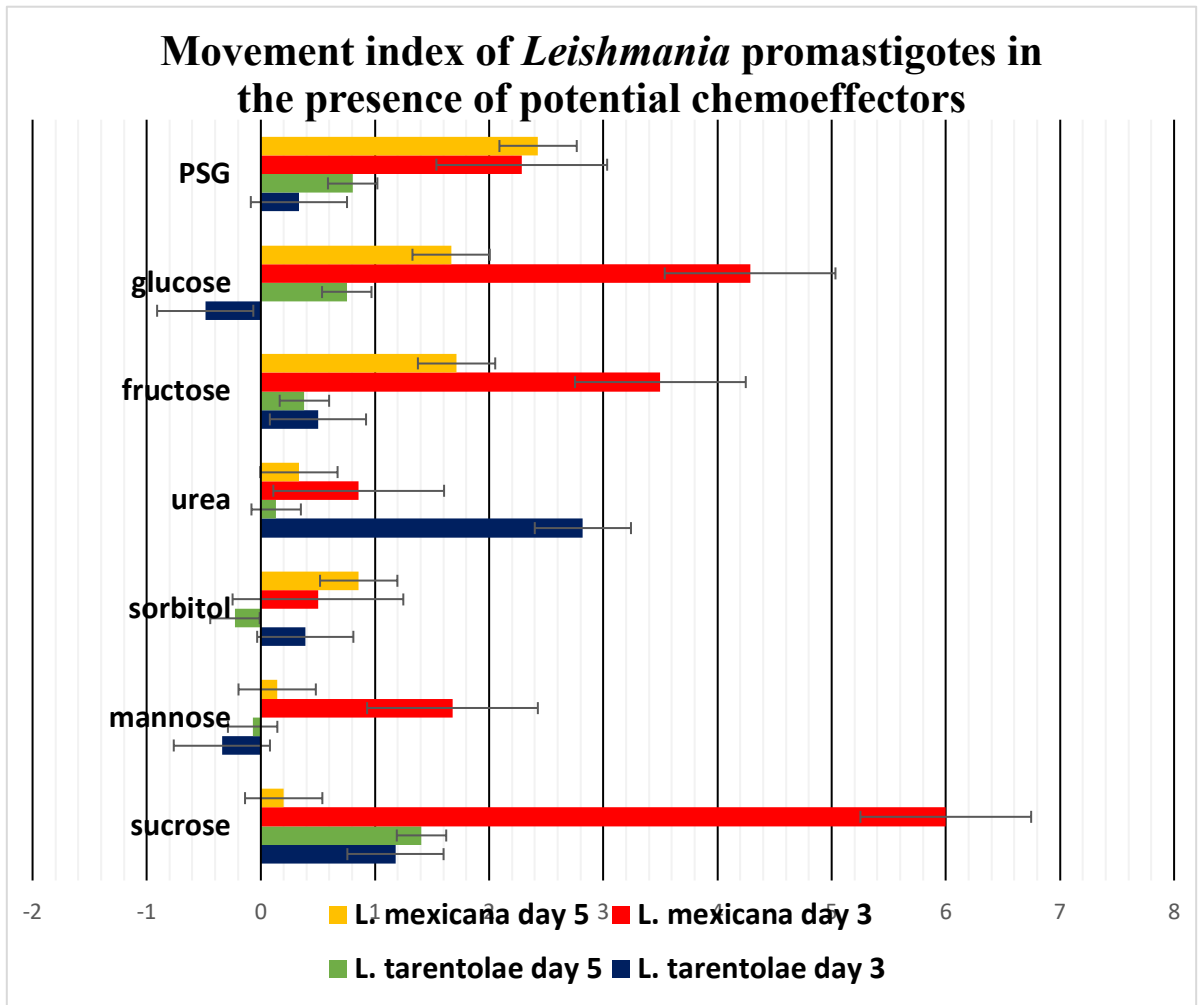


**Figure 39: Movement of *Leishmania* promastigotes in the presence of potential chemoeffectors.** Graph shows the migration chemotaxis index (mentioned in Materials and Methods) of 3 (Exponential growth phase) and 5 (Stationary growth phase) day old culture of *L. mexicana* and *L. tarentolae* towards potential chemoeffectors of PSG, glucose 0.5M, fructose 0.5M, urea 0.5M, sorbitol 0.5M, mannose 0.5M and sucrose 0.5M. Raw data in appendix IV. The date collected from culture represented by the colour of bars shown in legend. Data presented for glucose, fructose, sorbitol, mannose, urea and sucrose was from 3 repeated experiments. Data for PSG was from 1 experiment consisting of 5 capillary tubes for each condition. Standard error showed by error bars.

### 4.3.2 Capillary assay morphometrics

Promastigotes from fructose, urea, sucrose, mannose and PSG capillary assay were used to generate a profile of the morphology of migrated *Leishmania* promastigotes. Parameters measured were body length (BL), body width (BW), and flagellum length (FL), with the additional parameter of distance from kinetoplast (K) to nucleus (N) (DKN). Using these parameters, the morphology of migrated parasite to the chemoeffectors were presented graphically after categorised according to the criteria set by Rogers et al, (2002); Promastigotes were categorised as P (Procyclic), L (Leptomonad), M (Metacyclic), and N (Nectomonad).

#### Sugars

Within the specific species, *L. tarentolae* and *L. mexicana* showed little difference between proportions of promastigote forms that migrated between day 3 and day 5. However, between species there is a variety of differences in the forms that migrate towards specific sugars.

#### Fructose

*L. mexicana* (Figure 40a) shows a high proportion of leptomonad promastigotes to have migrated in both days, with 66.7% migration in day 5 and 58.3% migration in day 3. This is followed by procyclic promastigotes with 16.7% migration in day 5 and 29.1% migration in day 3, and nectomonad promastigotes with 14.4% in day 5 and 12.5% in day 3. The general migration of *L. mexicana* promastigote forms towards a gradient of fructose shows the attraction to be highest in leptomonads, procyclics and lowest in nectomonads, especially within the population from day 5 culture.

*L. tarentolae* (Figure 40b) shows a high proportion of nectomonad promastigotes to have migrated in both days, with 61.5% migration in day 5 and 60% migration in day 3. This is followed by leptomonad promastigotes with 38.5% in day 5 and 40% in day 3. Interestingly there is no migration of procyclics. The general migration of *L. tarentolae* promastigote form towards a gradient of fructose shows the

attraction to be highest with nectomonads followed by leptomonads, however procyclic forms are showed to have no migration towards fructose.

The biggest difference in migration towards a gradient of fructose between *L. tarentolae* and *L. mexicana* is the absence of any migrated procyclic promastigote forms in *L. tarentolae*, and the promastigote form with highest attraction nectomonads in *L. tarentolae* and leptomonads in *L. mexicana*.

### Sucrose

*L. mexicana* (Figure 41a) shows a high proportion of leptomonad promastigotes to have migrated in both days, with 59.6% migration in day 5 and 55.0% migration in day 3. This is followed by procyclic promastigotes with 23.1% migration in day 5 and 30.0% migration in day 3, and nectomonad promastigotes with 15.4% in day 5 and 10.0% in day 3. The general migration of *L. mexicana* promastigote forms towards a gradient of sucrose shows the attraction to be highest in leptomonads, procyclics and lowest in nectomonads, especially within the population from day 5 culture.

*L. tarentolae* (Figure 41b) shows a high proportion of nectomonad promastigotes to have migrated in both days, with 59.0% migration in day 5 and 45.5% migration in day 3. This is followed by 29.5% migration of leptomonad promastigotes in day 5 and 36.4% migration of procyclics in day 3, then a migration of 9.8% in procyclic promastigotes day 5 and 13.6% migration of leptomonads in day 3.

The biggest difference in migration towards a gradient of sucrose between *L. tarentolae* and *L. mexicana* is the procyclic form with highest attraction being nectomonads in *L. tarentolae* and leptomonads in *L. mexicana*.

### Mannose

*L. mexicana* (Figure 42a) shows a high proportion of leptomonad promastigotes to have migrated in both days, with 61.9% migration in day 5 and 45.5% migration in day 3. This is followed by procyclic promastigotes with 30.2%

migration in day 5 and 40.9% migration in day 3, and nectomonad promastigotes with 7.9% in day 5 and 13.6% in day 3. The general migration of *L. mexicana* promastigote forms towards a gradient of mannose shows the attraction to be highest in leptomonads, procyclics and lowest in nectomonads, especially within the population from day 5 culture.

*L. tarentolae* (Figure 42b) shows a high proportion of nectomonad and leptomonad promastigotes to have migrated in both days. However, the promastigote with highest migration differs between age of culture used. Day 5 culture shows a nectomonad migration of 68.2% being the highest migration whereas day 3 culture shows the highest migration to be 50.0% in leptomonads. This is followed by 31.8% leptomonad migration in day 5 culture and 42.9% nectomonad migration in day 3 culture. There is no other forms of promastigotes that are found to migrate in day 5 culture however day 3 show a low migration of 7.1% in procyclics.

The biggest difference in migration towards a gradient of mannose is the promastigote form with highest attraction being leptomonads in *L. mexicana* and differing between leptomonads in day 3 and nectomonads in day 5 *L. tarentolae*. There is also no found procyclic migration in day 5 *tarentolae*.

Between sugars there are similarities as well as a few differences. *L. mexicana* shows the highest migration for both day 3 and day 5 from leptomonad promastigotes, followed by procyclic promastigotes and later nectomonad promastigotes. There are very few migrated metacyclic promastigotes found; sucrose had 5% migration found in day 3 and 1.9% found in day 5, mannose had no metacyclics in either days and fructose had no metacyclics found in day 3 and 2.4% migration found in day 5. *L. tarentolae* shows a different migrated promastigote form profile when compared to *L. mexicana*. *L. tarentolae* from day 5 shows the highest migration from nectomonads, followed by leptomonads and then procyclics. However in response to sucrose mannose and fructose, none of the procyclics or metacyclics from day 5 culture migrate. *L. tarentolae* from day 3 show more of a variation in the forms that migrate; sucrose presents a high migration of nectomonads, followed by procyclics and lowest with leptomonads, mannose presents a high migration of leptomonads, followed by nectomonads and lowest with procyclic, whilst fructose presents a high migration of nectomonads followed by leptomonad with no migration of procyclics.

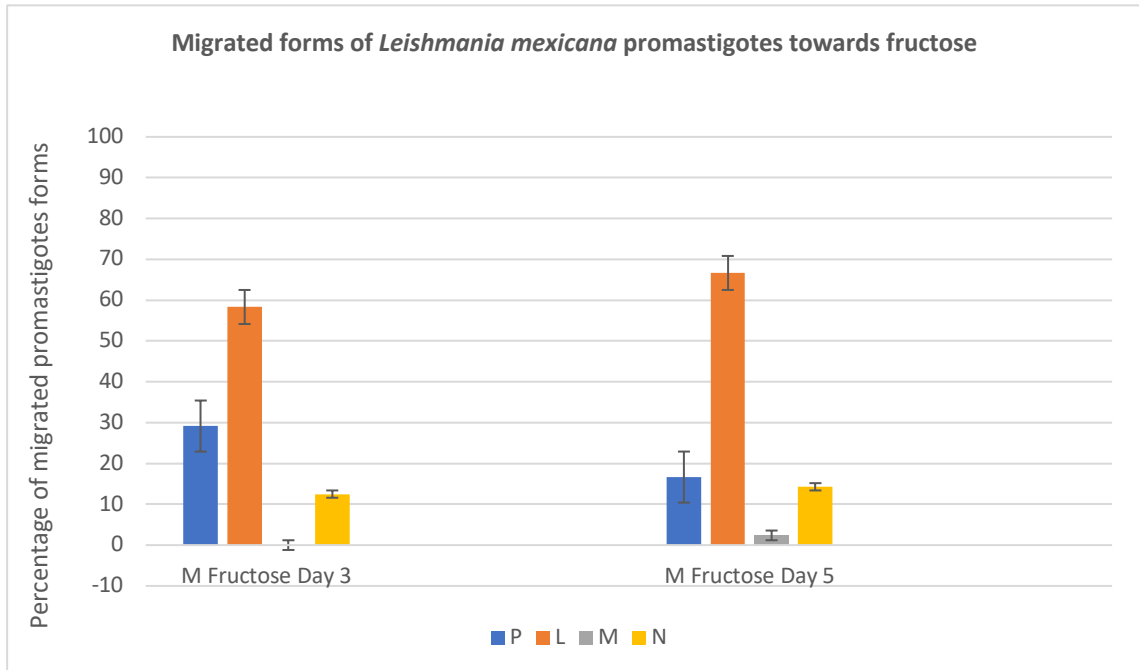


Figure 40a: The percentage of migrated categorised promastigotes of day 3 and 5 old culture of *L. mexicana* towards potential chemoeffectors of fructose 0.5M. Promastigotes were categorised as P (Procyclic), L (Leptomonad), M (Metacyclic), and N (Nectomonad). Raw data in appendix IV. The date collected from culture represented by the colour of bars shown in legend. Data presented was from 3 repeated experiments.

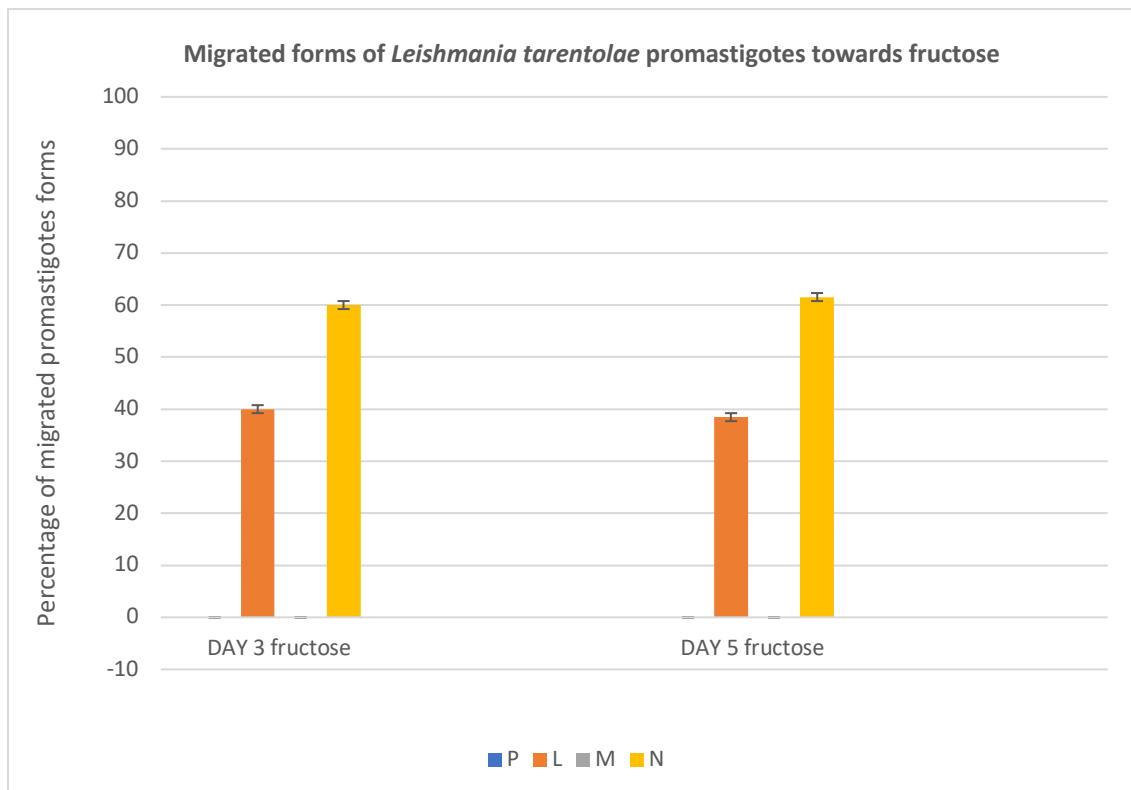
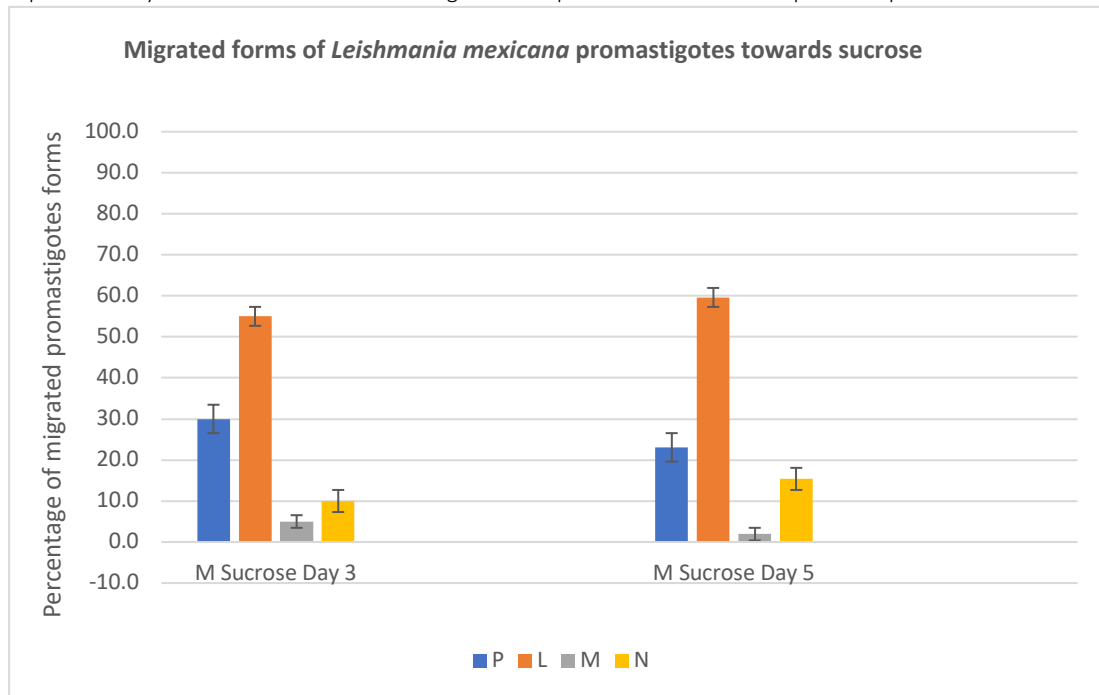
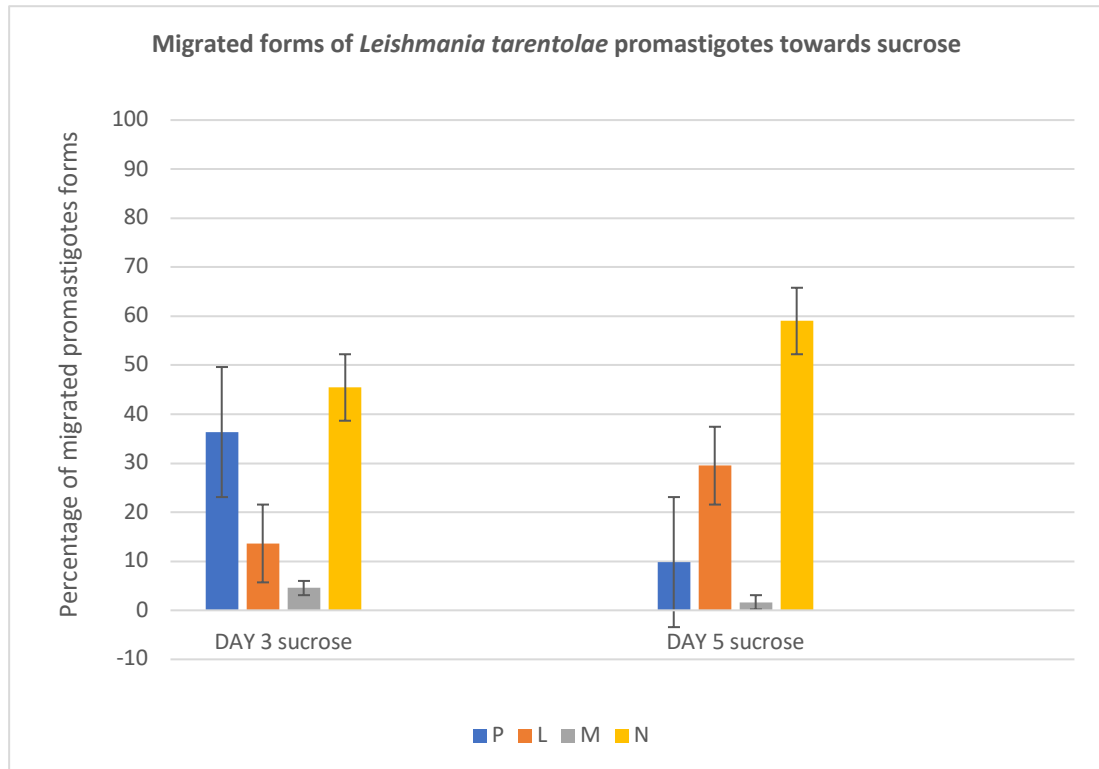


Figure 40b: The percentage of migrated categorised promastigotes of day 3 and 5 old culture of *L. tarentolae* towards potential chemoeffectors of fructose 0.5M. Promastigotes were categorised as P (Procyclic), L

(Leptomonad), M (Metacyclic), and N (Nectomonad). Raw data in appendix IV. The date collected from culture represented by the colour of bars shown in legend. Data presented was from 3 repeated experiments.



**Figure 41a:** The percentage of migrated categorised promastigotes of day 3 and 5 old culture of *L. mexicana* towards potential chemoeffectors of sucrose 0.5M. Promastigotes were categorised as P (Procyclic), L (Leptomonad), M (Metacyclic), and N (Nectomonad). Raw data in appendix IV. The date collected from culture represented by the colour of bars shown in legend. Data presented was from 3 repeated experiments.



**Figure 41b:** The percentage of migrated categorised promastigotes of day 3 and 5 old culture of *L. tarentolae* towards potential chemoeffectors of sucrose 0.5M. Promastigotes were categorised as P (Procyclic), L (Leptomonad), M (Metacyclic), and N (Nectomonad). Raw data in appendix IV. The date collected from culture represented by the colour of bars shown in legend. Data presented was from 3 repeated experiments.

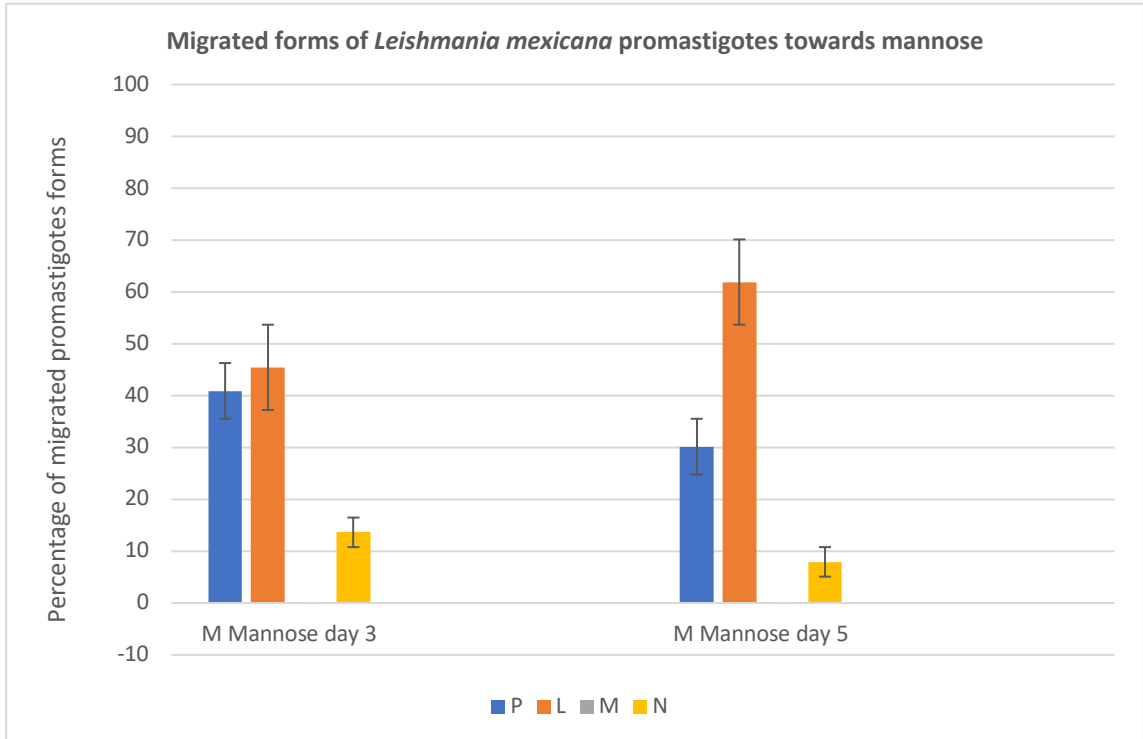


**Figure 42a:** The percentage of migrated categorised promastigotes of day 3 and 5 old culture of *L. mexicana* towards potential chemoeffectors of mannose 0.5M. Promastigotes were categorised as P (Procytic), L (Leptomonad), M (Metacytic), and N (Nectomonad). Raw data in appendix IV. The date collected from culture represented by the colour of bars shown in legend. Data presented was from 3 repeated experiments.

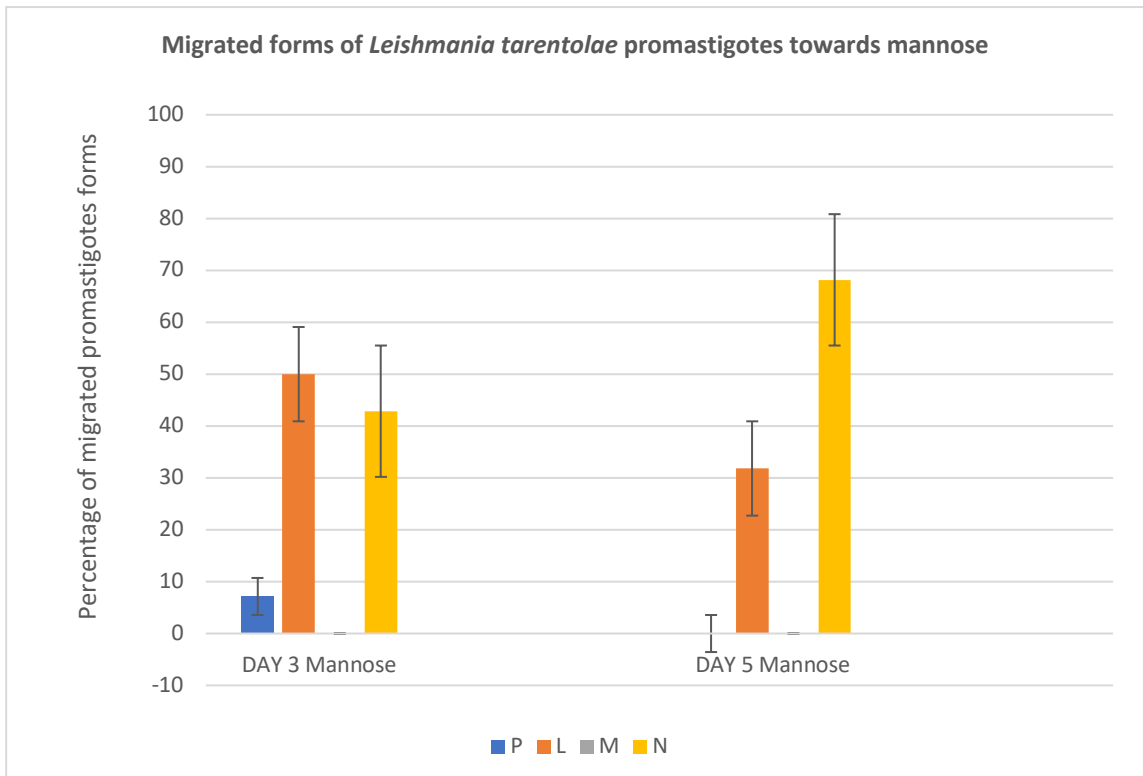


**Figure 42b:** The percentage of migrated categorised promastigotes of day 3 and 5 old culture of *L. tarentolae* towards potential chemoeffectors of mannose 0.5M. Promastigotes were categorised as P (Procytic), L (Leptomonad), M (Metacytic), and N (Nectomonad). Raw data in appendix IV. The date collected from culture represented by the colour of bars shown in legend. Data presented was from 3 repeated experiments.

## **Urea**

Within the specific species, *L. tarentolae* and *L. mexicana* showed little difference between proportions of promastigote forms that migrated between day 3 and day 5. However, between species there is a variety of differences in the forms that migrate towards urea.

*L. mexicana* (Figure 44) shows a high proportion of leptomonad promastigotes to have migrated in both days, with 52.9% migration in day 5 and 35.7% migration in day 3. This is followed by nectomonad promastigotes with 29.4% migration in day 5 and 28.6% migration in day 3, procyclic promastigotes with 11.8% in day 5 and 21.4% in day 3 and metacyclic promastigotes with 5.9% in day 5 and 14.3% in day 3. The general migration of *L. mexicana* promastigote forms towards a gradient of urea shows the attraction to be highest in leptomonads, followed by nectomonads, procyclics and lowest migration in metacyclics.

*L. tarentolae* (Figure 44) shows a high proportion of leptomonad and Nectomonad promastigotes migrated in both days. Day 5 *L. tarentolae* shows nectomonad promastigote to have the highest migration of 56.5% whilst day 3 shows leptomonad promastigote with 60.0% to have the highest migration. This is followed by 39.1% migration of leptomonad in day 5 and 33.3% migration of nectomonads in day 3 cultures. Procyclics shows a very small migration of 6.6% in day 3 and 4.3 in day 5.

The biggest difference in migration towards a gradient of urea between *L. tarentolae* and *L. mexicana* is the absence of *L. tarentolae* metacyclic forms in migration. However, generally similar forms of promastigotes migrate; leptomonad and nectomonads.

## **Promastigote Secreting Gel (PSG)**

Unlike the other chemoeffectors tested, PSG showed the widest variation.

*L. mexicana* day 3 showed procyclics as the most migrated form of 50.0%, followed by leptomonads at 42.9% and nectomonads at 7.14%. *L. mexicana* day 5 showed leptomonads as the most migrated form of 56.0%, followed by nectomonads

Yasmine Precious Kumordzi

at 24.0%, procyclics at 16.0% and metacyclics at 4.0%. Generally, *L. mexicana* had procyclics and leptomonads form of promastigotes migrate towards PSG (Figure 45a)

*L. tarentolae* day 3 showed nectomonads as the most migrated form of 75.0%, followed by leptomonads at 18.75% and procyclics at 6.25%. *L. tarentolae* day 5 showed leptomonads as the most migrated form of 81.8%, followed by procyclics and nectomonads both at 9%. On both days no metacyclics were found to have migrated (Figure 45b)

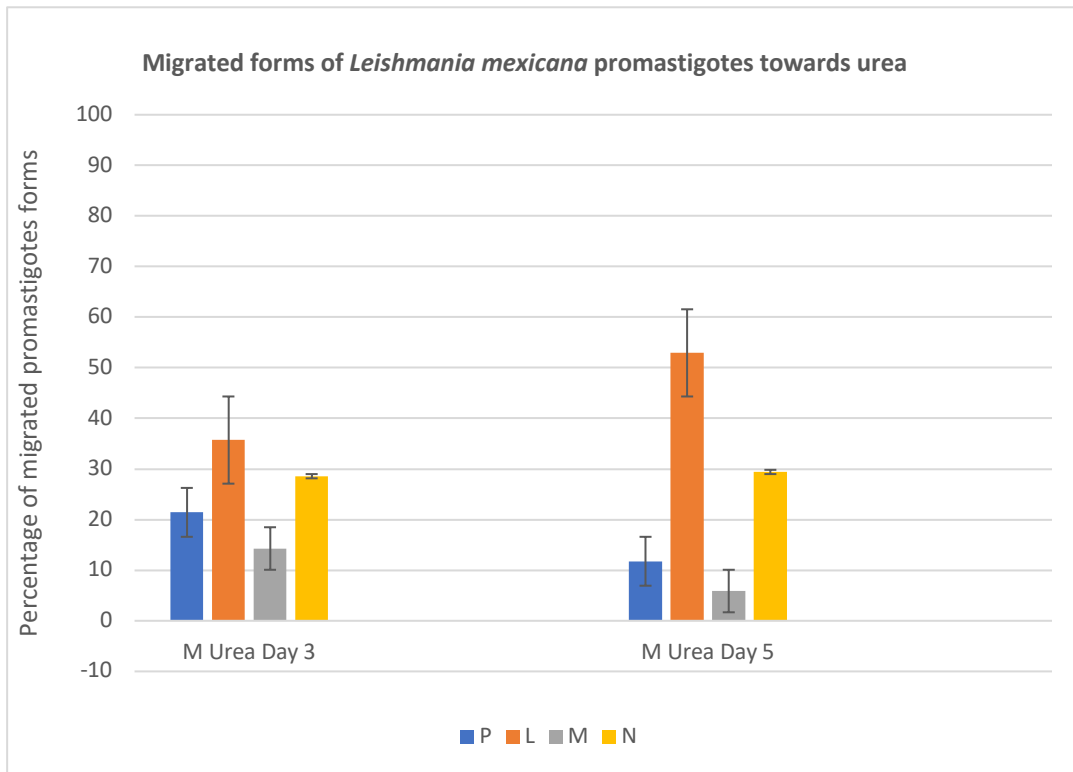


**Figure 43a:** The percentage of migrated categorised promastigotes of day 3 and 5 old culture of *L. mexicana* towards potential chemoeffectors of urea 0.5M. Promastigotes were categorised as P (Procyclic), L (Leptomonad), M (Metacyclic), and N (Nectomonad). Raw data in appendix IV. The date collected from culture represented by the colour of bars shown in legend. Data presented was from 3 repeated experiments.

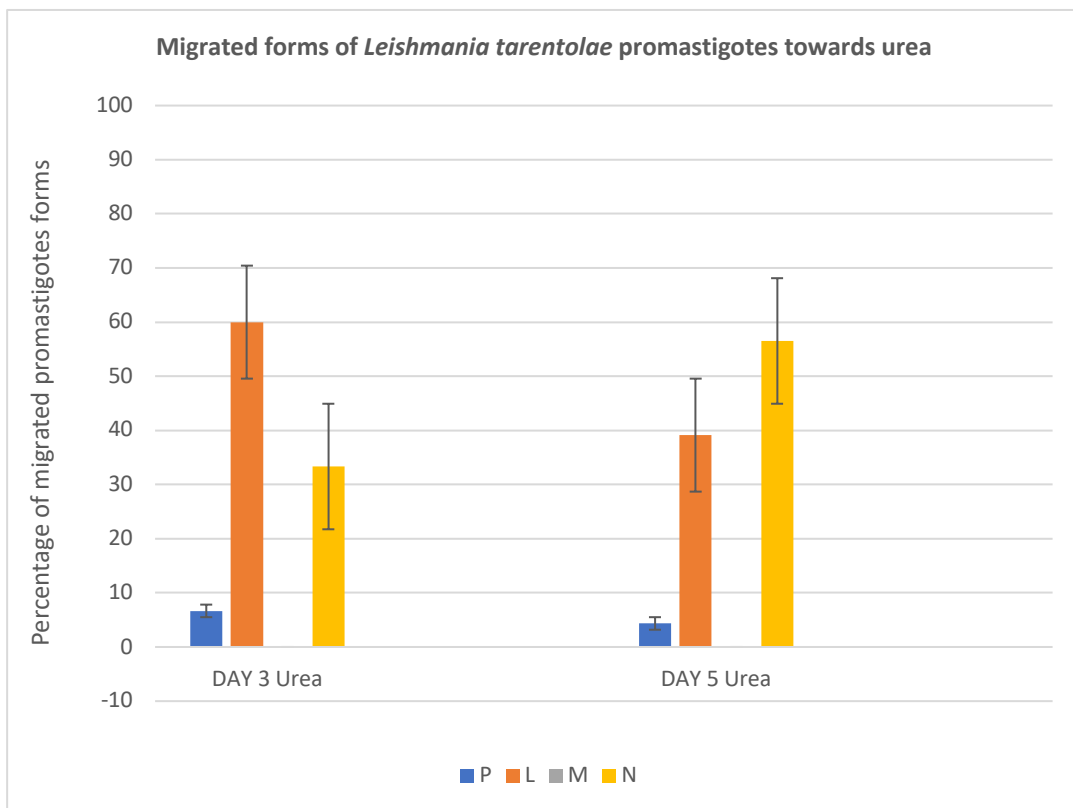


**Figure 44a:** The percentage of migrated categorised promastigotes of day 3 and 5 old culture of *L. tarentolae* towards potential chemoeffectors of urea 0.5M. Promastigotes were categorised as P (Procyclic), L (Leptomonad), M (Metacyclic), and N (Nectomonad). Raw data in appendix IV. The date collected from culture represented by the colour of bars shown in legend. Data presented was from 3 repeated experiments.

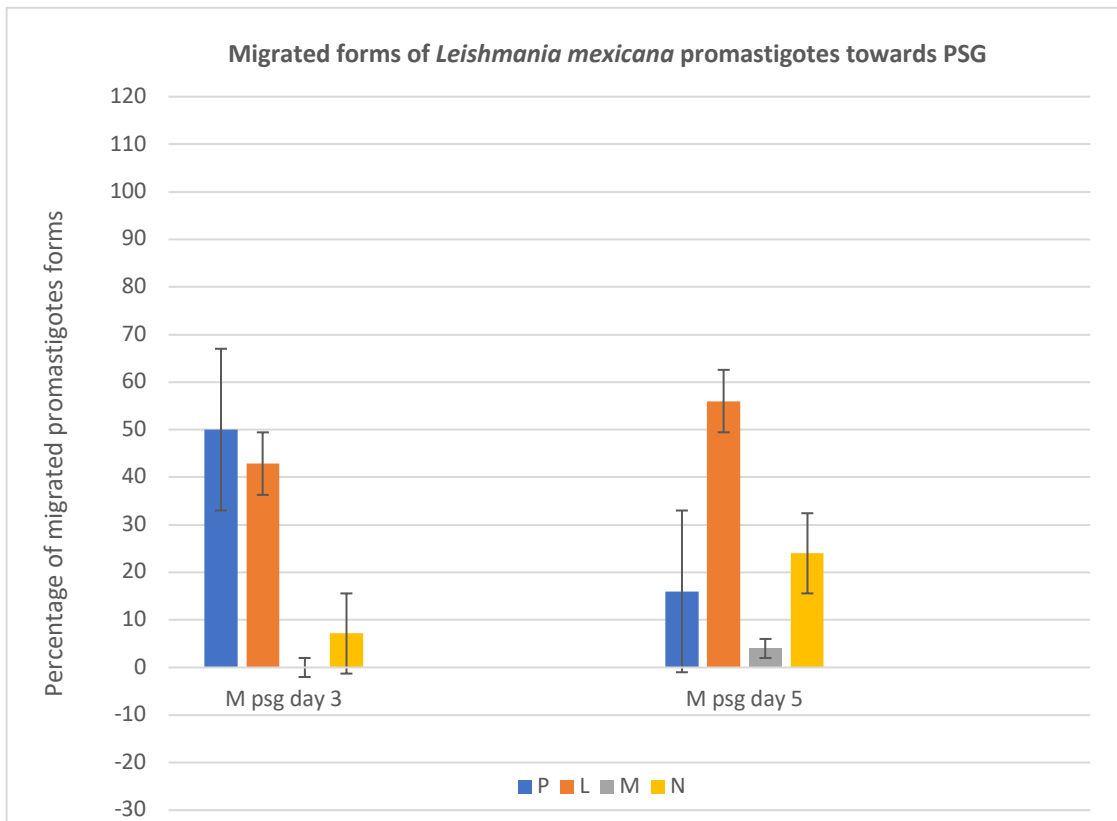


**Figure 45a: The percentage of migrated categorised promastigotes of day 3 and 5 old culture of *L. mexicana* towards potential chemoeffectors of crude PSG** Promastigotes were categorised as P (Procyclic), L (Leptomonad), M (Metacyclic), and N (Nectomonad). Raw data in appendix IV. The date collected from culture represented by the colour of bars shown in legend. Data presented was from 1 experiment.

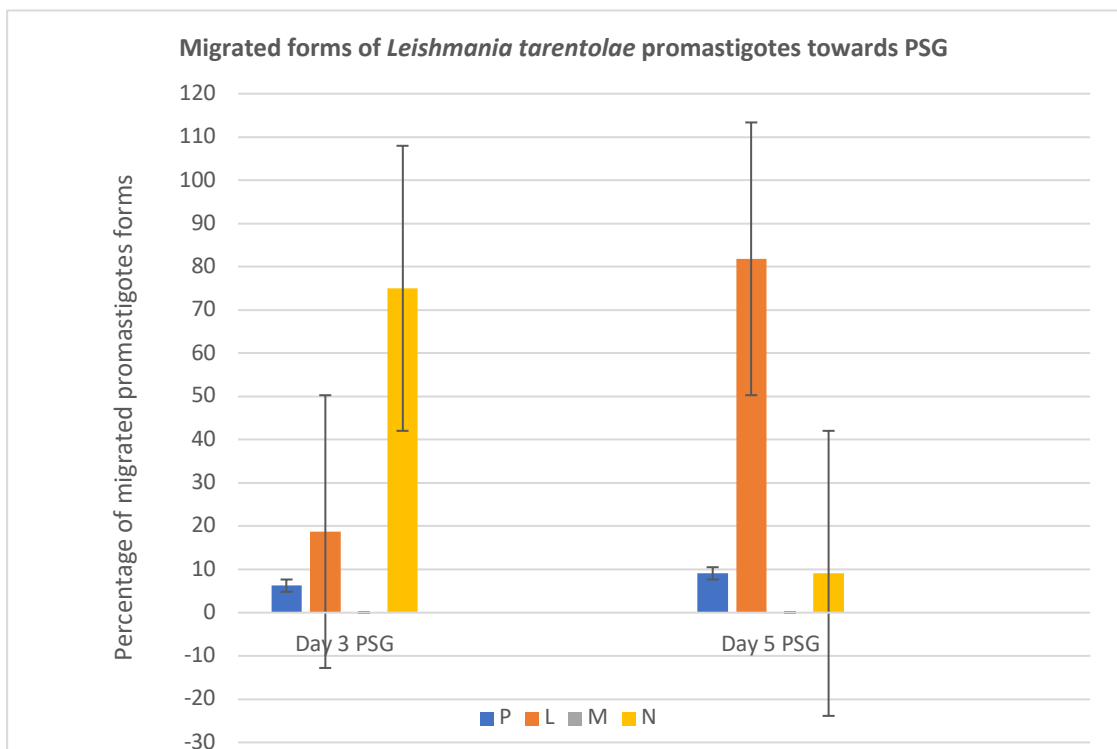


**Figure 45b: The percentage of migrated categorised promastigotes of day 3 and 5 old culture of *L. tarentolae* towards potential chemoeffectors of crude PSG** Promastigotes were categorised as P (Procyclic), L (Leptomonad), M (Metacyclic), and N (Nectomonad). Raw data in appendix IV. The date collected from culture represented by the colour of bars shown in legend. Data presented was from 1 experiment.

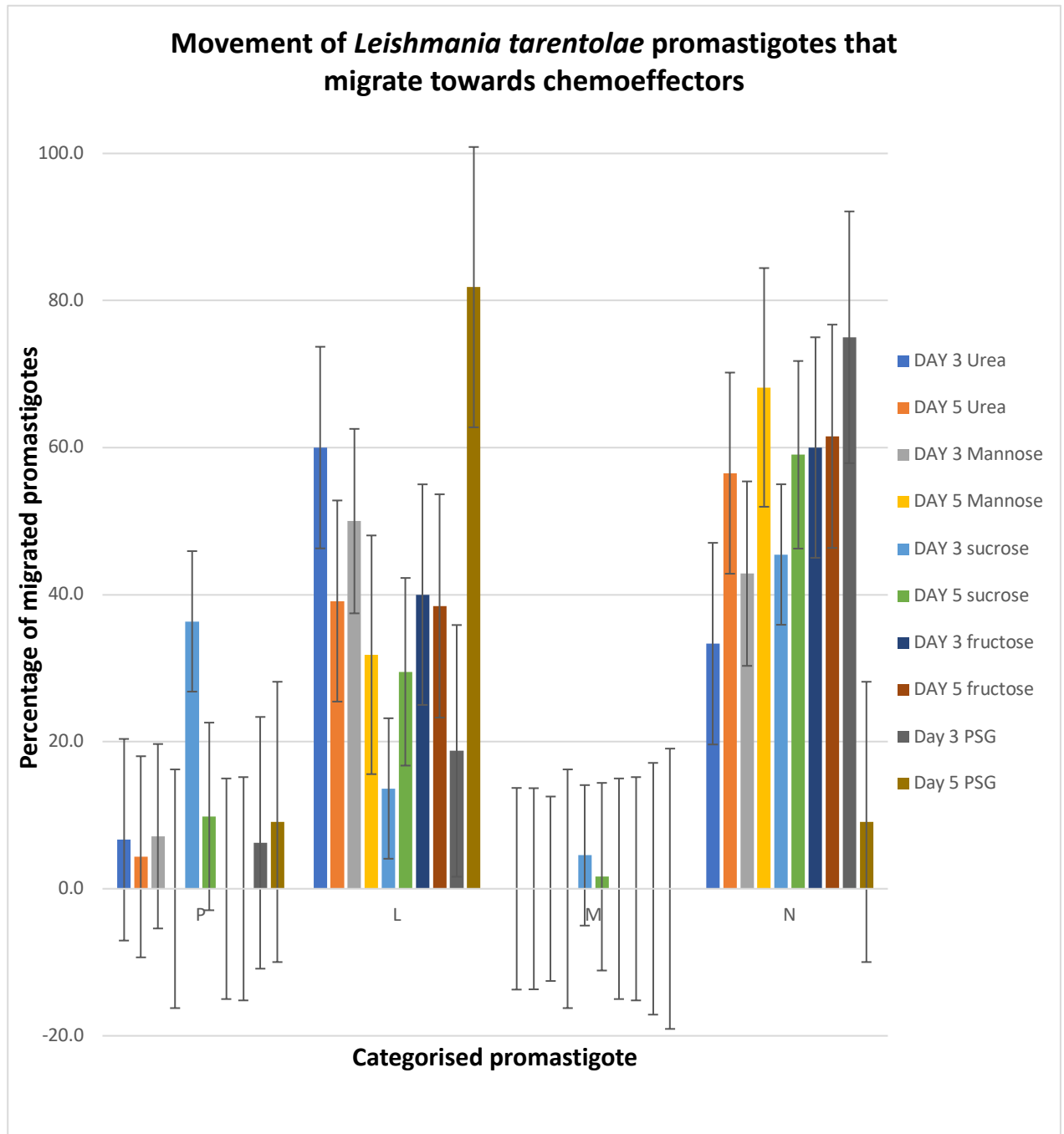


**Figure 46: Overall movement of *Leishmania tarentolae* promastigotes in the presence of chemoeffectors.** Graph shows the percentage of migrated categorised promastigotes of day 3 and 5 old culture of *L. tarentolae* towards potential chemoeffectors of PSG, glucose 0.5M, fructose 0.5M, urea 0.5M, sorbitol 0.5M, mannose 0.5M and sucrose 0.5M. Promastigotes were categorised as P (Procyclic), L (Leptomonad), M (Metacyclic), and N (Nectomonad). Raw data in appendix IV. The date collected from culture represented by the colour of bars shown in legend.

Figure 46 shows the types of *L. tarentolae* promastigotes that migrate towards specific chemoeffectors. Metacyclic promastigotes show the least migration, however the number of metacyclic promastigotes found in day 5 and day 3 culture is very low in *L. tarentolae*. Procyclic promastigotes is the second least migrated form, with less than 10% of migrated cells towards chemoeffectors falling in this category. With 3 day old *L. tarentolae*, 35% of procyclic promastigotes migrate towards sucrose. Leptomonad and nectomonad promastigotes are the most migrated types of *L. tarentolae*. Interestingly when using 5 day old *L. tarentolae* towards PSG, over 80% of migrated cells are leptomonads and under 10% being nectomonads. This shows that *L. tarentolae* nectomonads and leptomonads (particularly nectomonads) play the major role in migration towards chemoeffectors and not metacyclics.

Figure 47 shows the types of *L. mexicana* promastigotes that migrate towards specific chemoeffectors. Similar to *L. tarentolae*, metacyclic promastigotes show the least migration. Nectomonads show the second lowest migration, with high nectomonad promastigotes migration between 20% and 30% towards urea and PSG. More procyclic promastigotes migrate in *L. mexicana* compared to *L. tarentolae*, with migration of procyclics being over 10%. The highest migration of procyclic promastigotes is towards PSG when using 3 day old promastigotes of 50%, second highest is migration towards mannose of 41%. Leptomonad promastigotes are the highest migrated form of promastigotes, showing migration towards all chemoeffectors. This shows that *L. tarentolae* procyclics and leptomonads play the major role in migration towards chemoeffectors and not metacyclics as suggested in literature.

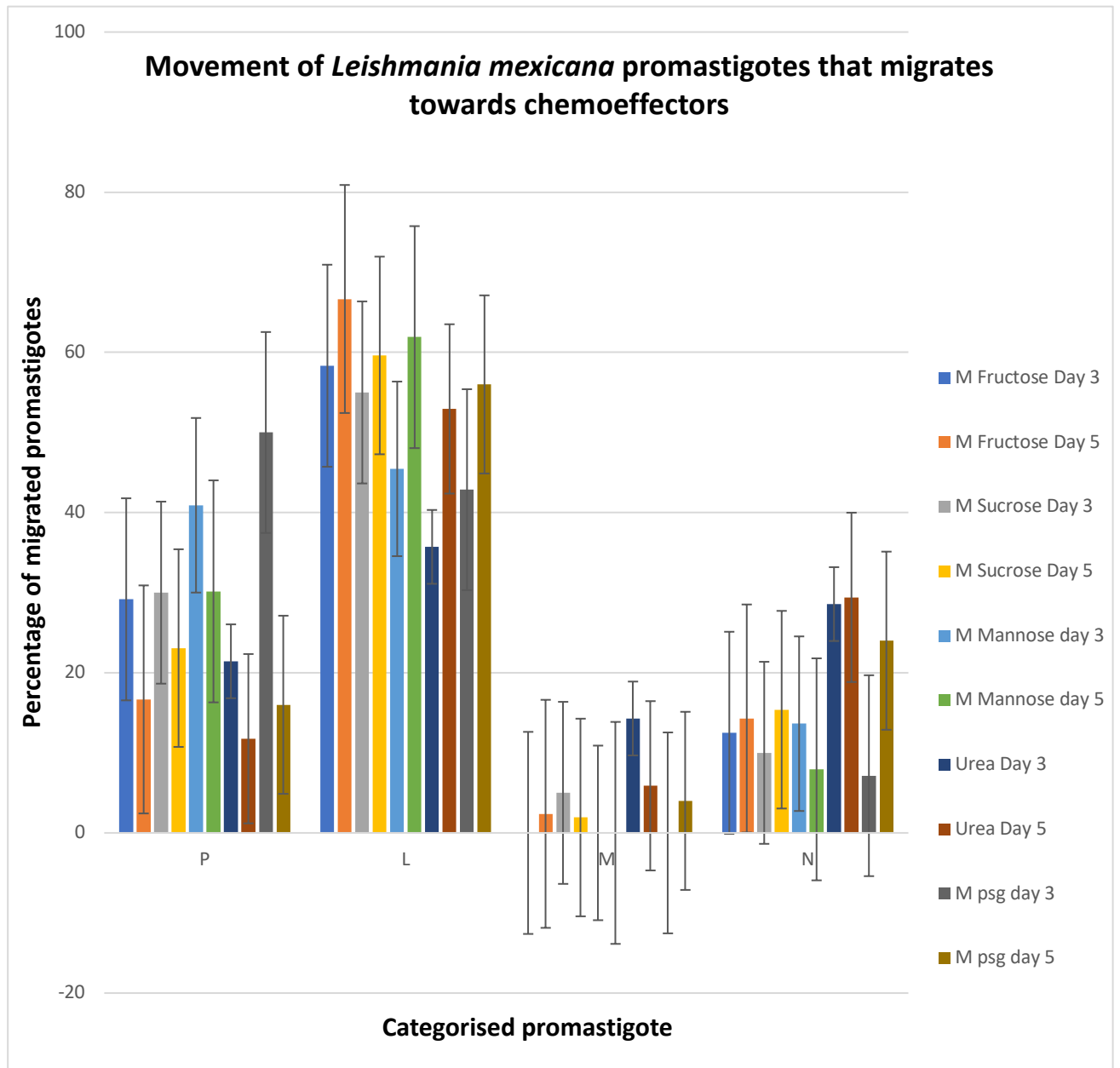


**Figure 47: Overall movement of *Leishmania mexicana* promastigotes in the presence of chemoeffectors.** Graph shows the percentage of migrated categorised promastigotes of day 3 and 5 old culture of *L. mexicana* towards potential chemoeffectors of PSG, glucose 0.5M, fructose 0.5M, urea 0.5M, sorbitol 0.5M, mannose 0.5M and sucrose 0.5M. Promastigotes were categorised as P (Procyclic), L (Leptomonad), M (Metacyclic), and N (Nectomonad). Raw data in appendix IV. The date collected from culture represented by the colour of bars shown in legend.

## 4.4 Microfluidic Chip design

### 4.4.1 Design and operations of the microdevice

To explore the various migration of *Leishmania* to various gradients of chemoeffectors in a controlled and stable manner, we developed a microfluidic device made up of optically transparent PDMS containing one layer as showed in **Figure 48 (A,B)**. The device generated consists of a chip with a diameter of 7 cm. The chip has a 12 chambers along the extremity of the chip with channels connecting them to the central reservoir chamber for parasite culture. This generates a concentration gradient from the chamber at the extremity containing test chemoeffector to the central reservoir chamber containing cells collected from parasite culture. The chambers had a height of 200 $\mu$ m with connecting channels 20 $\mu$ m in height. This type of microfluidic gradient generator has a couple of potential problems such as cross flow occurring between the sink and source (**Paliwal et al, 2007**). This problem was addressed in the design by increasing fluidic resistance between the sink and source by decreasing the height of a part of the connecting channel from 20 $\mu$ m to 6 $\mu$ m for 250 $\mu$ m of the length of channel **Figure 48(C,D)**.

Before the assay, fluorescent *Leishmania* parasites obtained from Dr Paul Bates and Dr Hector Diaz-Albiter were washed with PBS and resuspended in WIS 0.004% FBS. A known volume of parasites was loaded into the central reservoir chamber and potential chemoeffectors such as glucose in WIS 0.004% FBS 0.5M were used loaded into the chambers at the extremities before they were covered with a glass cover slip. Static diffusion based microfluidic gradient generator utilises diffusion between the two chambers to generate gradients across the channel in which can be detected by the parasites for migration to occur.

A confocal laser scanning microscope was used for live imaging of the migrating *Leishmania* parasites. Following the loading of both chambers, a glass coverslip was used to cover the chip, completing the device. Images were taken at a regular interval of 30 seconds of the whole device for an hour and was later stitched to form a video in which migration can be viewed.

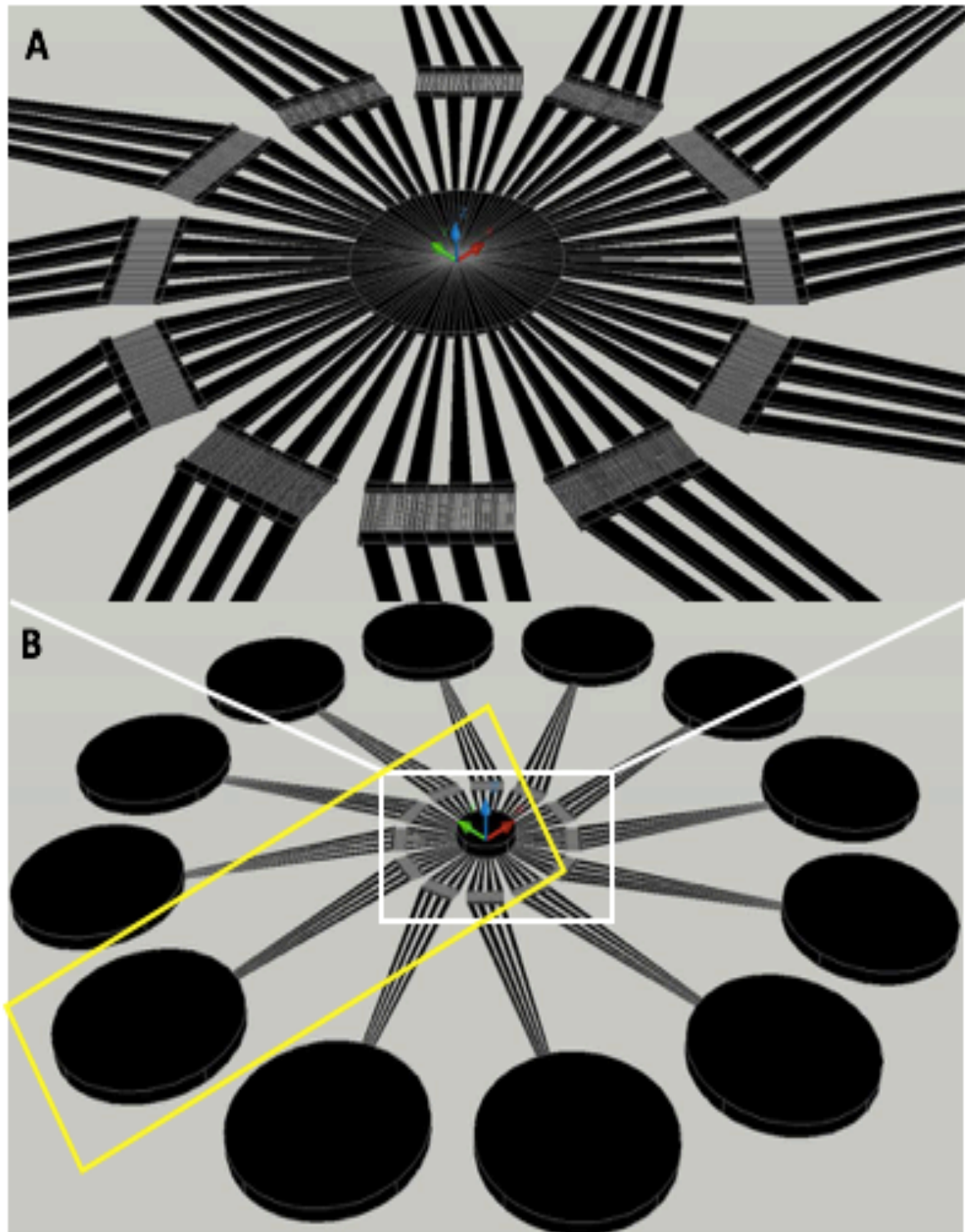


**Figure 48 (A,B): Microfluidic device design.** Top view of the radial chip, showing 12 chambers along the outer edge and a singular central reservoir for the cell culture. The complete design is shown (B) with detailed region shown (A)

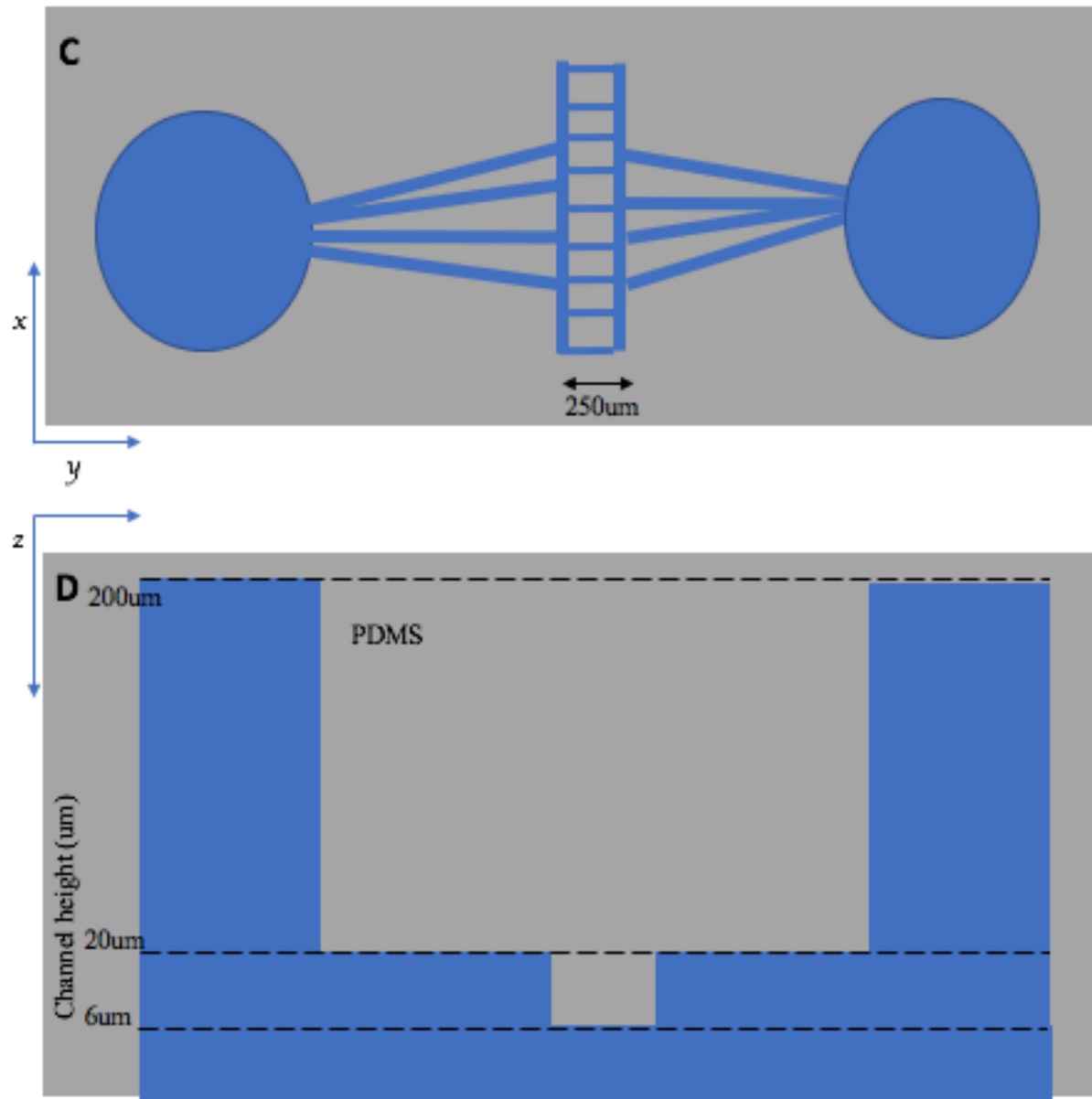


**Figure 48(C,D): Microfluidic device design.** Schematic illustration of the of the microfluidic chip. From a single inlet, four branching channels subject the flow into microchannels (C) with dimensions of channels and wells differing in height (D).

#### 4.4.2 Initial testing of microfluidic device

Initial testing using *Leishmania* parasites in a WIS 0.004% FBS solution placed in the central chamber and WIS 0.004% FBS in the chambers at the extremities showed that the size of the channels and basic design of the device allowed for good stable movement of promastigote *Leishmania* parasites within the channels when viewed under an inverted microscope at x40. However, testing under the correct conditions for microfluidic studies showed outside influence on the migration and fluid diffusion. Placing the cover slip on the loaded chip resulted in some movement of liquid and after about 15 minutes the chip began to dry, this affects both diffusion and the migration of promastigotes. Due to these problems, the experiment was not pursued further.

#### 4.5 Preliminary study of hypopylarian status of *L. tarentolae*

4-5 day old *Lu. longipalpis* and *Aedes. aegypti* were infected with *Leishmania* parasites and *Crithidia fasciculata* to study the establishment and development of successful infections. This was done by using dissections of the full gut and visualisation of the foregut, midgut and hindgut separately to understand the infection.

*Lu. longipalpis* was infected separately with *L. tarentolae*, *L. mexicana* and *C. fasciculata* infections and monitored throughout by analysing the gut throughout the infection. A successful *L. mexicana* infection was established within the first experiment, giving rise to the PSG plug used for the chemotaxis assay. In this initial infection, a suprapylarian infection was seen. Unfortunately *L. mexicana* did not establish infection with the second experiment. Successful *L. tarentolae* infections were established in roughly 60% of sandflies. The parasites within these infections were contained within the hindgut and posterior midgut with heavy infection contained within the hindgut. Attachment to hindgut epithelium was not visualised. A loss of infection occurred 5-10 days following the infection, with *Leishmania* parasites seen within the rectum of the sandfly. It can therefore be assumed that *L. tarentolae* establishes a hypopylarian infection in *Lu. Longipalpis* which is lost

*through excretion. C. fasciculata* infections within the sandfly established similar to *L. tarentolae* in a hypopylarian mode.

*A. aegypti* mosquito infected with *L. tarentolae* and *C. fasciculata* was not the main aspect of this study therefore only one preliminary set of experiment was done. 16% of fed mosquitoes had the presence of parasites in the first day of dissection (day 3). This establishment of infection was quickly lost after day 3 and the presence of parasites were loosely within the midgut and hindgut similar to *L. tarentolae* infection in *Lu. Longipalpis*.

## CHAPTER FIVE: DISCUSSION

### 5.1 Is *Leishmania tarentolae* hypopylarian?

Leptomonad promastigotes are responsible for the production of promastigote secretory gel (PSG) in suprapylarian parasites (Rogers et al, 2002). This developmental stage of promastigote is the precursor of metacyclic promastigotes, the infective stage of promastigote. PSG is known to have a large role in transmission as it is produced at the site of metacyclogenesis. However, this has to date only been investigated in suprapylarian *Leishmania spp.* infections such as *L. mexicana*. From the knowledge of developmental and migration changes of suprapylarian *Leishmania spp* leading to transmission, it is understood that PSG gel plug occurs in the cardia and thoracic midgut. The gel contains predominantly leptomonads from which metacyclic promastigotes are differentiated from. This accumulation of PSG not only allows for metacyclic promastigotes to be produced in an environment promoting transmission during the next blood feed but distorts the stomodeal valve for the regurgitation process to occur for successful blood meal intake and infection. As reported (Vionette, Ginger and Dillon unpublished data) *L. tarentolae* establishes in a hypopylarian manner in *Lutzomyia longipalpis*, successive developmental stages occur within the posterior gut. The reservoir of leptomonads within a successful infection would therefore be located in the hindgut and it was hypothesised that PSG production might occur in this location. Any PSG produced in the hindgut might have a role in preventing premature loss of parasites in the excreta due to partial blockage of the hindgut lumen (Vionette, Ginger and Dillon unpublished). Diaz-Albiter et al, 2018 showed that unlike reported by Vionette, Ginger and Dillon (unpublish data), *L. tarentolae*-GFP infected *Lu. longipalpis* had a distribution that was diffuse with no specific areas of binding to the gut (Diaz-Albiter et al, 2018). Due to the differentiation of leptomonad promastigotes to metacyclic promastigotes being the last stage in metacyclogenesis and the manner in which hypopylarian infection occurs, the discovery of PSG in regions of the gut can be used to determine the location of leptomonads and metacyclics.

A preliminary experiment performed at the end of this study used sectional gut dissection of successfully infected *Lu. longipalpis* to image the morphology of *L. tarentolae* and detect PSG. The intention was to monitor changes that occur in *L. tarentolae* infection and confirm the manner of infection that occurs with *L. tarentolae*. The samples of morphology and PSG were not able to be analysed within the time frame of this study but visualisation of the full gut and gut sections (foregut, midgut and hindgut) from infection showed an hypopylarian infection with leptomonad-type morphology of parasites within the posterior midgut and hindgut. Based purely on visualisation of the infected gut, it can be confirmed that *L. tarentolae* is a hypopylarian *Leishmania* species however no visual PSG formation was seen. This could be due to continuous removal of produced PSG, a low-density infection preventing large amounts of PSG to be produced or alternatively lack of PSG formation by these parasites in the hindgut. Unlike in the foregut where the cardia stops this from occurring, midgut peristalsis and the muscles around the pylorus act to push excreta out for excretion. Further analysis of samples produced would give more insight into the manner of *L. tarentolae* infection.

## **5.2 Morphometric analysis and comparison between *L. mexicana* and *L. tarentolae***

The morphometric analysis follows the development of two species of *Leishmania*; *L. mexicana* a suprapylarian parasite and *L. tarentolae* a hypopylarian parasite, with the results showing the multiplicative promastigotes within the axenic culture and the sequence of morphology changes that occurs in culture. These changes mimic the morphological transformations that occurs within the sand fly during the basic process of metacyclogenesis. There are many published morphometric analysis of *L. mexicana* parasite (Bates et al, 1994) however although a good model kinetoplastid, morphometrics of *L. tarentolae* has not been explored well enough to be published. Comparisons of these two species has provided a morphometric analysis of the metacyclogenesis development that occurs in an axenic culture; cell body length, width, flagellum length and distance between the kinetoplast and nucleus. However using morphology particularly flagellum length to interpret the form of promastigote using Bates et al, 1994 does not take into account the fact that the flagellum length is

continuously growing throughout numerous cell cycles (**Wheeler, Gluenz and Gull 2010**). Therefore many promastigotes that fall within the leptomonad criteria according to morphology may actually be procyclics. Only promastigotes within the multiplicative promastigote stages were found. This was largely due to the continuous passaging and the conditions that the promastigotes were kept in in terms of temperature and pH.

### 5.2.1 *Leishmania mexicana*

The morphologies associated with *L. mexicana* promastigotes within the sandfly and axenic culture (**Rogers et al, 2002**) have all been found. The changes in morphology could be seen to dramatically change throughout development on a daily basis, however using the morphological category stated by Rogers et al, 2002 only the four main developmental forms (procyclic, nectomonad, leptomonad and metacyclic promastigote) were found in culture. These followed a similar pattern of development initiating with high procyclic promastigotes which reduces overtime, an increase of leptomonads and nectomonads, and the emergence of metacyclic promastigotes. However, monitoring of 5 days did not yield a high percentage of metacyclic promastigotes. This was surprising as **Rogers et al, 1993** showed an exponential increase of metacyclic *L. mexicana* in an axenic culture with 20% of total cells in culture being metacyclics at 4 days following passage and roughly 100% of cells in culture 6 days following passage being metacyclics. This differed significantly from the present data produced, with the only difference in methodology being the pH of culture, media used and the passage number of culture. **Bates and Tetley, 1993** reported similar data, explaining that the production of significantly pure cultures of metacyclics is due to the change of pH to a more acidic 5.5 compared to cultivation in an axenic pH 7 culture used which produced a morphologically mixed population.

Looking at the promastigote morphologies present in the first few days (roughly day 3) post infection within a sand fly (**Rogers et al, 1993**), the population is very mixed containing a very low level of procyclic promastigotes, metacyclics and amastigotes, with higher numbers of nectomonad and leptomonad promastigotes. This made stages of promastigotes found in day 5 representative of day 3 post infection of

the sandfly. The promastigotes in this stage are representative of the developmental stage of promastigotes in which they begin the escape and taxis towards the foregut to be the first found in thoracic midgut (**Rogers et al, 1993**). Another realisation from the data produced was the amount of time in which metacyclics took to develop. There is a possibility that with a high number of passages, promastigotes struggle to meet their original developmental cycle, taking significantly longer to develop to the metacyclic stage and therefore were not seen within the 7 days given.

### 5.2.2 *Leishmania tarentolae*

With the lack understanding of a complete developmental cycle of *L. tarentolae* in an axenic culture, it was important that this *Leishmania* species was fully explored to understand the changes they undergo in culture when compared to *L. mexicana* taxis.

The first to be explored was the similarity in the parameters between *L. mexicana* and *L. tarentolae*. These parameters (Body length vs Body Width, Body Length vs Flagellum Length, Flagellum Length vs Body Width and Body Length vs Distance between Kinetoplast and Nucleus (DKN)) was similar showing that the development of *L. tarentolae* was very similar to *L. mexicana* in terms of the progression of morphometrics (**Wheeler, Gluenz and Gull 2010**) and the developmental forms that can be found in an axenic culture. This was as body length increased body width decreased, as body length increased flagellum length increased, as body length increased DKN increased, and body width and flagellum length have few correlations. These correlations are stronger with the *L. tarentolae* data due to the increase of dataset and following the development over a longer period.

Following morphology criteria set by Rogers et al, 2002, the general morphological changes in axenic culture were similar to that of *L. mexicana* studied in sandfly infection (**Rogers et al, 2002**). Day 3 and day 5 were good examples of the developmental stages found in day 3 and day 4 post-infection in *L. mexicana* respectively. Similar to *L. mexicana*, these stages represent the stages in which escape from the PM and initiation of taxis occurred. Surprisingly two unpublished morphologies were found; bulgetomonad and kinetoplast nucleus swapping promastigotes.

An unpublished report by Dillon and Liu, 2014 set a new criterion for *L. tarentolae* in which the new potential morphology of *L. tarentolae* promastigote was found. This described bulgetomonad morphology was visually found in the axenic culture emerging from about day 4 making up 20% of all analysed cells. These cells have a 'bulge' in the cell with the kinetoplast directly adjacent to the flagellum. Although, visually fitting the description stated by Dillon and Liu, only 11% fitted this in morphology parameters and therefore a revised criterion has been set here of a bulge width of roughly 1.88  $\mu\text{m}$ , nucleus within the bulge and the DKN of roughly 2.14 $\mu\text{m}$ .

Wheeler, Gluenz and Gull 2010 showed DAPI stained promastigotes labelling the nucleus and kinetoplast, with the kinetoplast labelled stronger than nucleus. This difference in intensity was used to distinguish between the kinetoplast and the nucleus. Unlike all other *L. mexicana* and early development *L. tarentolae* promastigotes, some *L. tarentolae* showed cells with the less intense DAPI stained organelle closest to the flagellum. These cells were seen in the death phase of culture. The cell shape was spherical with a longer flagellum to cell width length. This suggested that during the death phase, some promastigotes undergo changes that causes the kinetoplast and nucleus to exchange locations. These cells labelled 'Kinetoplast nucleus swapping promastigotes' have not been reported as yet. Due to the location within the growth stage of the cells, it can be assumed that with *L. tarentolae* promastigote a swapping of the kinetoplast and nucleus or the significant shrinkage of nucleus precedes the death of the cell.

### **5.3 Traditional Capillary Chemotaxic Assays**

Traditional capillary assays have been used in many forms for the study of chemotaxis through the delivery of chemicals that can be detected by cells in a controlled gradient manner (Adler, 1973). This technique however has many disadvantages in terms of having influences from outside condition such Brownian

movement and dissolved oxygen changes within solution. Brownian movements affect the movement of the cells within solution and has an effect on the overall migratory potential of the cells. An outside influence that also affects migration within a traditional capillary assay is the amount of dissolved oxygen within the solution, this was seen in earlier assays tested (results not included) using a modified PP chamber. Promastigotes in this assay migrated and accumulated around the channels where the dissolved oxygen was high therefore results using this PP chamber assay did not reflex chemotaxis. Both forms of chemotaxic assay used do not distinguish between osmotaxis and chemotaxis in the proposed assays as there was no salt usage to ensure there was no osmosis occurring within the microfluidic device or the capillary tubes.

The use of the traditional capillary assay as used by Oliveira et al and Barros et al allowed for comparisons between methods and results. However, there was large discrepancy between each. **Leslie, Barrett and Burchmore, 2002** used late-log *L. mexicana*, Oliveira et al, 2000 used *L. chagasi* and *L. amazonensis* at log phase and stationary phase, Barros et al, 2006 used *L. amazonensis* at day 6 and deYsasa Pozzo et al 2009 used *L. amazonensis*. As the developmental form of promastigotes was not investigated prior to experiment and knowledge of only the non-specific growth stage, it is not possible to predict with certainty what morphological forms of promastigotes were used in each of these experiments.

To investigate promastigote migration in the hours following PM disintegration, it is important to investigate using the chemotaxic capillary or microfluidic device using a promastigote population of nectomonad, leptomonad and mostly procyclic. Population of these promastigotes was collected for use from both *L. tarentolae* and *L. mexicana* grown in culture and determined using morphometric analysis as stated by Rogers et al, 2002.

An improvement to the methodology carried out in previous promastigote chemotaxis assays (**Oliveira et al, 2000, deYsasa Pozzo et al, 2009, Leslie, Barrett and Burchmore, 2002, Díaz et al, 2011**) was the collection of cells following migration, and analysing the forms of migratory cells. This not only allowed the determination of the chemotaxic agent but also the determination of the developmental morphological form of promastigotes that was attracted to it.

## 5.4 *Leishmania* promastigote taxis

The main part of the method during the experiment was the collection of the migratory cells. These samples were used to determine the number and morphology of promastigotes that had migrated from the solution into the capillary tubes containing the testing chemotaxic agent. From previous chemotaxic assays (**Oliveira et al, 2000, deYsasa Pozzo et al, 2009, Leslie, Barrett and Burchmore, 2002, Díaz et al, 2011**), everything tested showed a level of taxis towards the test chemoeffectors, however no substance has been used successfully to deter the migration of cells towards it. Copper sulphate is known to be lethal to cells at a high dose (**Davies, 1978**). This was therefore used assuming it would be show negative chemotaxis or a negative chemotaxis index.

Biochemical gradients have been suggested to be used as a mechanism for signalling to *Leishmania* promastigotes within the sandfly alimentary canal (**Killick-Kendrick, 1978**). This mechanism takes advantage of the putative sugar concentration that exists from the crop as sugars are released slowly into the midgut for digestion. This began the numerous adaptations from Bray's initial chemotaxic assays in 1983 (**Bray, 1983**) to the more specialised optical tweezers assay by deYsasa Pozzo. These have all focussed on sugar concentrations and the movement of promastigotes towards a sugar gradient without the presence of a control chemoeffector that showed a negative taxis. No presence of a chemical that deters the migration insinuates a lack of chemotaxic movement but osmotaxic movement. This brings the question, what other chemoeffector are promastigotes attracted to and what type of taxis occurs in the sandfly. The experiment designed to answer this was to perform a pilot chemical screen using more chemoeffectors and to collect the migrated promastigotes to determine which morphological population was attracted to each chemical.

Similar to previous assays, the general movement index of *Leishmania* promastigotes in the presence of potential chemoeffectors all showed a movement toward all chemicals of interest (Figure 39) including copper sulphate. The promastigotes recovered following migration towards copper sulphate microscopically

showed cell lysis, with the cell membrane ruptured. This therefore was not quantifiable and was removed from results reported.

Interestingly, based on the counted number of migrated promastigotes *L. tarentolae* showed a negative movement index towards glucose and mannose with the *L. tarentolae* day 3 population and mannose with the *L. tarentolae* day 5 population (Figure 39). However only the negative movement index towards glucose in the *L. tarentolae* day 3 population is significantly relevant. Generally, *L. mexicana* showed a high positive movement index towards PSG, and the sugars tested whereas *L. tarentolae* showed a lower positive with a few negative movement indexes towards sugars tested and PSG. Urea showed an opposite outcome when compared to *L. mexicana* and *L. tarentolae* movement index with sugars, with a generally low positive movement index and high positive movement index respectively.

Using chi-squared test on a contingency table with SPSS containing all the raw data from the migration assay, there was showed to be no association between promastigote morphology and the chemical cue that migrated towards in *L. mexicana* (Appendix IIIa). This was however the opposite in *L. tarentolae* (Appendix IIIb) where there was a strong association suggesting that specific *L. tarentolae* promastigote forms migrate towards certain chemical cues.

#### **5.4.1 Migration of *Leishmania* within the sand fly alimentary canal**

Sand flies predominantly feed on plant-derived fluids which are composed of sugars. This ‘sugar meal’ is stored in the ventral diverticulum (crop) of the sand fly separate from the abdominal midgut which in an infected sand fly will contain the ‘blood meal’ encapsulated by the PM. Following digestion and the escape of early developmental stage promastigotes such as nectomonads and procyclics, nectomonads attach to the midgut epithelium which is seen in both *L. tarentolae* (Dillon and Liu, unpublished) and *L. mexicana*. Therefore migration following this escape and attachment dictates transmissibility. Sugars from the crop are slowly released into the midgut for carbohydrate digestion, this generates a sugar gradient from the crop, cardia, thoracic midgut and finally the abdominal midgut. This gradient has been used

continuously to support chemotaxis in *Leishmania* promastigotes, however the use of *L. tarentolae* in this study and its attraction to all sugars used suggests another source of gradient which they might have a higher affinity to.

The malpighian tubules are located posterior to the abdominal midgut, excreting their product into the pylorus ready for excretion by the sandfly. The osmo-regulation function of the tubules leads to the proximal regions to have a high concentration similar to the high concentration found in the crop of sugars. The nitrogenous waste of uric acid crystals have a high level of urea. This led to our hypothesis that there is a gradient generated from the pylorus and malpighian tubules towards the abdominal midgut of urea, illustrated in Figure 23 that may be more attractive to hypopylaria *Leishmania* species such as *L. tarentolae* leading to proximal migration. This hypothesis was tested using urea as a chemoeffector within the capillary tubes to analyse the migration of both *L. mexicana* and *L. tarentolae*. Urea showed a movement index of below 1 when using a population of *L. mexicana* at day 3 from culture and day 5 from culture as well as a population of *L. tarentolae* at day 5 from culture. Compared to the movement index showed when using PSG, glucose, fructose and sucrose, this was significantly lower attraction. The day 5 *L. tarentolae* population however showed a movement index of 2.8; the maximum attraction seen from *L. tarentolae* towards any of the tested chemoeffectors. This suggests that compared to sugars such as glucose, fructose, sorbitol, mannose and sucrose, *L. tarentolae* is more attracted to urea and therefore could be the reason to why it migrated towards the urea gradient and therefore pylorus which contains the highest concentration of urea. *L. mexicana* on the other hand had an attraction towards all tested chemoeffectors including the urea. The attraction to sugars however was significantly stronger showing the population from 3 days in culture having the strongest attraction.

The differential attraction between *Leishmania spp.* along with the differential attraction towards each chemoeffector dependent on *Leishmania spp.* shows that migration of *Leishmania spp.* within a sand fly was an interplay between osmotaxis and chemotaxis. Osmotaxis showed by the migration generally towards any sample with higher concentration including copper sulphate which leads to the death of promastigotes. Chemotaxis is showed by the differential attraction towards chemoeffectors.

Looking at the populations of *Leishmania* used, *L. mexicana* showed initial attraction to sugars such as glucose, fructose and sucrose but later the attraction to PSG increases as the promastigotes develop and begin to change to the transmissible form of metacyclic promastigotes. *L. tarentolae* on the other hand begin with the high attraction to urea and later the attraction to sucrose is initiated. This could possibly suggest the manner in which peripylaria *Leishmania spp.* migrate within the sandfly alimentary canal. The question of attachment comes to play here. LPG's present on the surface of promastigotes, allowing the binding to the midgut epithelium. However it is known that procyclic and metacyclic LPG differ, with metacyclics having fewer LPGs when compared to procyclics (Soares et al, 2002) with the level of LPG decreasing through metacyclogenesis. With the development and migration of peripylarian *Leishmania spp.* possibly reaching the metacyclic developmental stage within the hindgut, the attraction to sugars could initiate the migrate to the foregut hence why Diaz-Albiter et al, 2018 viewed *L. tarentolae*-GFP infection as diffuse with no specific areas of binding. The action of the midgut peristalsis and excretion might deter this forward migration leading to no or few *L. tarentolae* found in the foregut and the loss of infection.

#### 5.4.2 Morphology of migrated promastigotes

The study is the first to differentiate chemotaxis of *Leishmania* based on their morphology. When looking at migration, understanding the types of morphological types of promastigotes migrating towards each chemoeffector is important to further understand the sequence in development and migration that occurs in the sandfly. This is well explained in suprapylarian *Leishmania* species such as *L. mexicana* infections (Figure 18) where metacyclogenesis is initiated in the midgut from the transformation of amastigotes to procyclics and later nectomonads which attach to the midgut epithelium to escape the blood bolus. Nectomonads initiate the migration towards the anterior midgut where they transform into leptomonads and haptomonads. As Nectomonad promastigotes initiate the migration towards the anterior midgut (Rogers et al, 2002), it was hypothesised that this form of promastigotes are the most involved in migration.

*L. mexicana* promastigotes (Figure 47) showed leptomonads to be the highest morphological population that were collected from the migrated samples in fructose, sucrose, mannose, urea and PSG, accounting for 50.6% of all migrated forms (Appendix III). The differentiation into the leptomonad form of promastigote occurs at the thoracic midgut (Sunter and Gull, 2017). However from infection studies (Rogers et al, 2002) leptomonads were found in the anterior and posterior midgut. As they do not attach to the midgut epithelium, they are able to migrate. The finding that migration of leptomonads is potentially greater than that of nectomonads towards the chemoattractants is surprising however shows that metacyclogenesis and development might not entirely be limited to a specific compartment within the sandfly alimentary canal. The migration of metacyclics is very limited however this is attributed to the low amounts of metacyclics found in the culture at both day 3 and day 5 populations.

The high attraction of *L. tarentolae* promastigotes to urea suggests that the migration of promastigotes is generally towards the gradient of urea from the uric crystals stored in the pylorus, the data from the types of migrated promastigotes was quite similar to that found in *L. mexicana*. *L. tarentolae* promastigotes (Figure 46) showed nectomonads to be the highest morphological population to be collected from the migrated samples in the sugars (fructose, sucrose and mannose). The day 3 population showed a high level of the migrated promastigotes were leptomonads whereas in day 5, the highest level of promastigotes that migrated were nectomonads. Nectomonads have been suggested to be the morphology of promastigote to initiate migration. This is due to the location in which specific morphologies of *Leishmania* are found within the gut during the development of infection, from the abdominal midgut to the thoracic midgut.

Leptomonads are found in both the posterior abdominal midgut and the anterior abdominal midgut (Rogers et al, 2002). This morphology of promastigote need to migrate to differentiate into metacyclic promastigotes in the thoracic midgut and foregut where metacyclics are required. The seen step by step development in specific regions of the gut could possibly be driven by the increased attraction of promastigotes as they develop to ensure the final infectious metacyclic promastigote is in the cardia gut region.

Therefore compared to nectomonad which are seen in higher levels in the thoracic midgut, leptomonads have a stronger attraction to the sugar cue from the diverticulum for migration to ensure high levels of metacyclic promastigotes are found in the cardia. This supports the assumption that nectomonads are the first to initiate migration however leptomonads react to the sugar cue stronger (Appendix IIIa) to migrate possibly further and faster.

## **5.5 Understanding the taxis of hypopylarian and suprapylarian and parasites.**

This study has brought about a lot of new understanding of the less studied *Leishmania* species, *L. tarentolae*. Previous understanding of sand fly infection has mostly been based upon the infection of *L. mexicana*, a well-studied *Leishmania* species which establishes a suprapylarian infection. This mode of infection leads to the migration and development of promastigotes towards the foregut where metacyclogenesis ends with the production of metacyclic promastigotes. This form of promastigotes produce PSG which aids in their accumulation at the foregut; this build-up of PSG causes the damage of the cibarial valve. Suprapylarian infection not only causes the escape of parasites into the foregut but the need for the infected sandfly to regurgitate the parasites prior to feeding. The main events allowing the establishment and successful transmission of infective parasites are : i) the delays of excretion (**Vaidyanathan, 2005**), ii) the escape from the PM (**Joshi et al, 2005**), iii) the migration of *Leishmania* parasites within the sandfly alimentary canal (**Killick-Kendrick, 1978**), and iv) the attachment to the midgut epithelium (**Warburg, Tesh and McMahon-Pratt, 1989**).

The initial activity that occurs from the arrival of the infected blood meal is the production of the PM compartmentalising the blood bolus from the midgut lumen. Digestion occurs within the PM, which remains intact until digestion finishes. To enhance the number of parasites that can escape from the blood bolus, excretion is delayed. The delays of excretion occurs through the secretion of myoinhibitory neuropeptide. This was shown in *L. major* to act on the sandfly by slowing down the action of midgut peristalsis by relaxing the midgut (**Vaidyanathan, 2005**). Escaping

the PM has to be accomplished by any *Leishmania spp.* to establish infection within the sandfly, unrelated to the location of infection. Chitinases (Joshi et al, 2005) are produced by parasites to encourage early escape from the blood bolus by degrading the PM. This allows nectomonads to escape the blood bolus and escape the actions of midgut peristalsis and excretion by attachment to the midgut epithelium.

The mode of infection of *L. tarentolae* parasites has remained unconfirmed due to conflicting data, however visualising an *L. tarentolae* infection within *Lutzomyia longipalpis* has confirmed a hypopylarian infection. The established hypopylarian infection does not permit the transmission of parasites during blood feed. This could be due to many reasons. The decreased number of successfully infected sandflies seen with *L. tarentolae* when compared to *L. mexicana* in *Lu. longipalpis* confirms that successful development and escape from within the blood bolus is challenging for *L. tarentolae* compared to *L. mexicana*. Unlike in *L. infantum*, *L. panamensis*, *L. mexicana*, *L. braziliensis*, *L. major*, *L. donovani*, *L. mexicana* and *L. guyanensis*, no chitinase protein has been found in *L. tarentolae* to encourage the breakdown of the PM (Data from UniProt, Appendix I). However due to the breakdown of the PM following digestion, a complete loss of all *L. tarentolae* infection does not occur. This along with visualising infections within sandflies confirms that establishment of infection is possible within a sandfly.

Unpublished work by Dillon and Liu showed attachment to the hindgut epithelium where parasites developed (Image 3). This all shows that some of the events required for successful transmission are fulfilled: escaped excretion, escaped from the PM enclosing the blood bolus and attached to the epithelium. As a hypopylarian infection, no migration towards the foregut was observed. Therefore this brings up questions about the migration of *Leishmania* parasites within the alimentary canal of the sandfly.

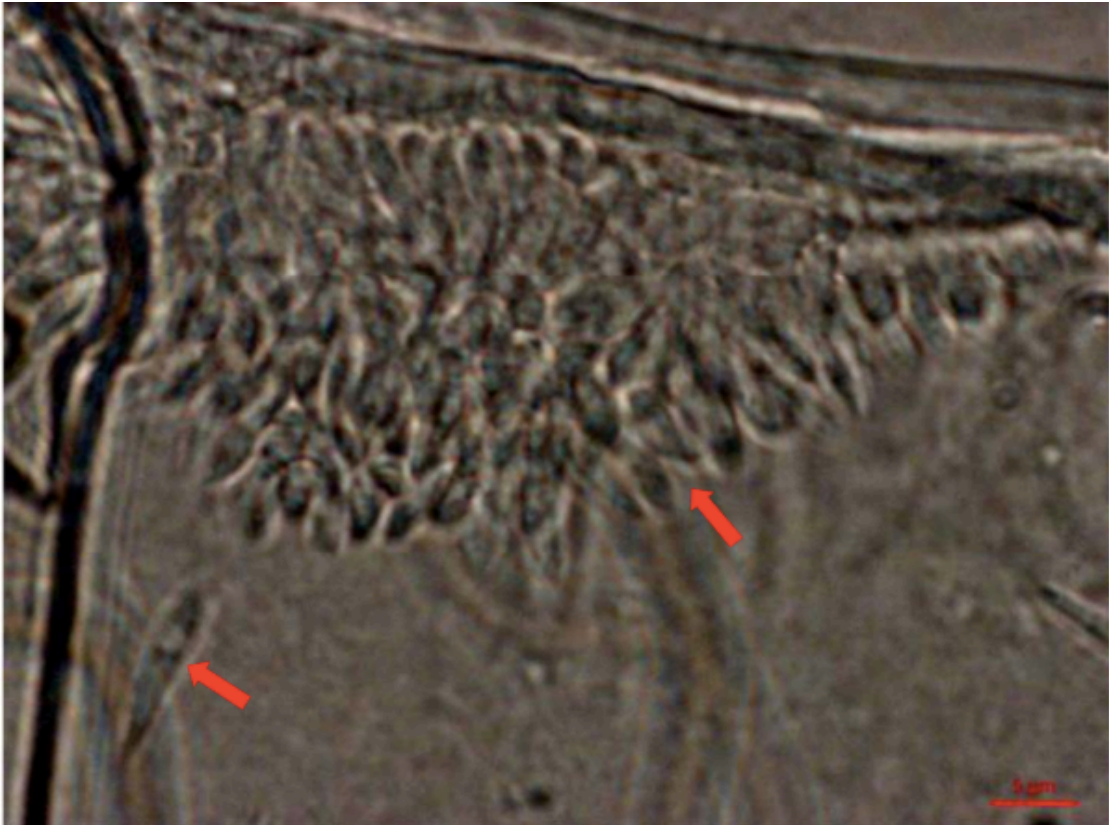


Image 3: Image shows *L. tarentolae* promastigotes found in the hindgut on day 10 of infection in *Lu. longipalpis*. Red arrow shows the parasite attached to the cuticular surface of the hindgut. (Dillon and Liu, unpublished)

Capillary assays showed the migration of both *L. tarentolae* and *L. mexicana* promastigotes which were described as leptomonads by Rogers et al. This confirms that migration is part of the events within the alimentary canal of the sandfly. *L. tarentolae* and *L. mexicana* have different gradient cues which they migrate towards. Following escape from the PM and attachment to the epithelium wall; hindgut epithelium for *L. tarentolae* as described by Dillon and Liu and midgut epithelium for *L. mexicana*, migration via the gradient cues determines the location in which metacyclogenesis ceases. This location contains metacyclic promastigotes with modified LPGs which do not attach to the epithelium. For *L. mexicana* promastigotes, migration towards the cue of sugars results in metacyclogenesis in the anterior midgut and foregut. Metacyclic promastigotes therefore accumulate, produce PSG and chitinase for the blockage and damage of the cibarial valve, and the loss of epithelium attachment due to LPG modifications. This all leads to the transmission of *L. mexicana* metacyclic promastigotes. For *L. tarentolae* on the other hand, migration towards the cue of urea may result in metacyclogenesis in the hindgut. It can be proposed that metacyclic promastigotes are therefore not able to escape excretion as

attachment does not occur due to modifications of the LPG resulting in the loss of infection and the absence of PSG at high levels in the hindgut.

## **5.6 Development of a microfluidic device for the screening of chemoattractants**

The main aim of the project was to develop a microfluidic device capable of precise chemical gradient control to mimic microenvironment in vitro with the sandfly associated with promastigote migration. Promastigotes are reported to migrate successfully towards a glucose gradient within the sandfly alimentary canal during metacyclogenesis in order to aggregate at the foregut ready for infection to occur during the next blood feed. This influence of glucose is therefore very important, however has not been measured well as the methodology was not able to be fully developed in the time available. Microfluidic devices allows concentrations to be controlled to study migration responses as a function of concentration. This alternative methodology to traditional chemotaxis capillary assay is said to be more sensitive, therefore to measure this a microfluidic device was developed along with traditional chemotaxis assays particularly capillary assays being explored to see how much information can be obtained from these avenues of chemotactic assays.

The design of device had several requirements; there were a number of possible chemoeffectors found by the preliminary studies using capillary assays in which would be advantageous to test simultaneously. Using a hypopylarian *L. tarentolae* and suprapylarian *L. mexicana*, being able to use the same chip was important for repeatability. A transparent chip which would allow good optical transparency for parasite visualisation; therefore using the right material for chip fabrication was vital. PDMS was therefore chosen as it met the criteria of transparency, it bonded strongly with glass and had an easier fabrication procedure for complicated design. The design developed for the purpose of visualising the migration of *Leishmania* to a chemical gradient is illustrated in Figure 42. This design aimed to achieve a device in which the promastigotes within the central reservoir had a relatively low shear stress on cell activity and maintain a stable concentration of the inputted chemoeffectors. Here diffusion occurs from one chamber to another via a

channel therefore occurs by passive diffusion in static microfluidic gradient generators, with each chamber containing potential chemoeffectors to the central chamber representing the spatial distribution of a potential biochemical factor of interest from source to sink respectively of the device (Lin and Levchenko, 2015). Although flow based gradient generators are generally aimed for chemotaxis assays, diffusion based microfluidic gradient generators have recently been showed to be successful as chemotaxis assays (Skoge et al, 2010, Smith et al, 2015), showing a trend towards simple designs in which complex fluid automation is not required (Lin and Levchenko, 2015).

This type of diffusion is advantageous in this type of chemotaxis assay as *Leishmania* parasites have a low adhesiveness, are in suspension, not naturally exposed to shear force and reside in a flow free environment within the insect; therefore using a flow based gradient generator offers a flow rate not experienced by parasites within the insect vector as well as introducing a mechanical input which can influence cell behaviour in the assay (Walker et al, 2005, Polacheck, Charest and Kamm, 2011). Another advantage which aids in the preparation for visualisation is the substantial amount of time for a steady gradient to be achieved.

The vast majority of microfluidic design have focused on varying a single biochemical cue, however promastigotes in the sandfly alimentary canal constantly receive inputs from a variety of sources. Therefore to address this, the design of the device allowed for numerous chemical gradients to be created towards one central reservoir of *Leishmania* allowing the parasite to react and migrate according to the most attractive chemoeffector similar to within the alimentary canal of the sandfly where many chemoeffector cues are present.

The design of device solved the problems which were predicted such as such as cross flow by decreasing the height of a part of the connecting channel. It also allowed reproducibility and repetition on experiment by using a stable and strong material that was easy to fabricate, image through and cheap to produce for future work. This device however has further improvements discovered after testing. The design of the device had the correct proportions of channels for the migration of *Leishmania* parasites and the gradient development through passive diffusion as static

microfluidic gradient generators towards the central reservoir for an integrated device for high content screening.

However, during the testing of the chip, problems were encountered such as the movement of liquid following the placement of a cover slip and the drying out of the liquid within the chip. This caused problems for viewing the real chemotactic migration of the promastigotes as these problems would have affected them. A design consideration therefore which is highly recommended for the future work is redesigning the current design in the fabrication to include ports to form convection units and a completely sealed microfluidic chamber where evaporation causing drying out might be reduced significantly. Inlet and outlet ports will allow fluids to travel from an external source such as a syringe pump into the device whilst maintaining the pressure in the device. In this redesign, each of the current 'inlets' seen in Figure 25 will be converted into a convection unit with each unit acting as a source of a given solute balancing the pressure between each unit. This redesign will not be able to hold a stable gradient over a long period of time, therefore sinks may have to be placed between sources. This redesign is based on devices produced for cell-on-a-chip technology such as the device designed by Ye et al, 2007 (Figure 50).

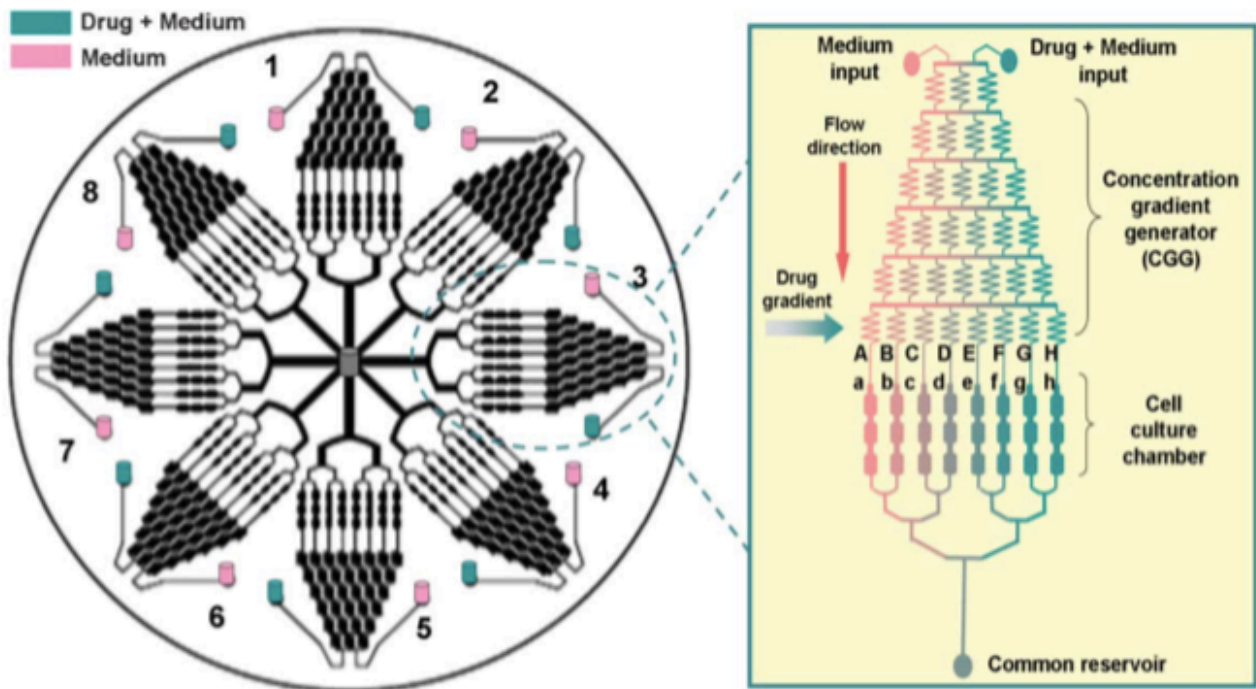


Figure 50: Schematic of the integrated microfluidic device for cell-based High content screening. (a) The device consists of eight uniform structure units and each unit is connected by a common reservoir in the centre of device in which contains the cell culture. (b) Magnified section of the single structure unit containing an upstream concentration gradient generator (CGG) and downstream parallel cell culture chambers (Ye at al, 2007)

## 5.7 Future

The new understanding that has come from this study can be further developed to achieve a better understanding of suprapylarian and hypopylarian migration within the alimentary canal of the sandfly. Due to the problems that arose from the development of the microfluidic device, chemotaxis capillary assays used in prior *Leishmania* taxis assays was adopted and modified for use. An improved device has now been designed and adapted from the device produced to suit *Leishmania* chemotaxis. With further work, this improved design can be used to produce devices minimizing outside influence on the chemotaxis and allow real time visualization of the taxis of promastigotes towards chemoeffectors with easier morphology analysis using ImageJ. Further work may also focus on PSG analysis following the infection and dissection of *Lu. longipalpis*. PSG has been found to be produced by *L. mexicana* promastigotes in the foregut showing the location of promastigote accumulation and end of metacyclogenesis; essentially the main location of infection. Confirmation of

PSG production in the hindgut of an *L. tarentolae* infection would be a highly interesting discovery; it would suggest that PSG has different roles for *Leishmania* with different modes of infection. The study so far has taken into account the gradients that were predicted to be formed at the hindgut originating from the malpighian tubules, and the foregut originating from the crop, however many more gradients will be present in the alimentary canal which could act upon the migration of promastigotes. Other potential chemoeffectors can be based upon many organs, microbial communities etc. therefore for a greater understanding emphasis should be put in the study on other potential chemoeffectors.

## CHAPTER SIX: CONCLUSION

*Leishmania* parasites cause the diseases leishmaniasis, a neglected tropical disease with a wide geographical distribution globally. It is transmitted via the bite of an infected sand fly. An important aspect to understanding transmission of infective stage promastigotes is understanding what differs between the distinct infection of hypopylarian and the forward migrating suprapylarian *Leishmania* species within a sandfly. This work demonstrated a pilot screen of chemoeffectors and the development of a novel technique for a *Leishmania* real time chemotaxis assay to detect chemoeffectors that *Leishmania* promastigotes migrate towards. The development of a microfluidic device for better chemotactic responses and precise control of gradient without outside influence needs future input into the device redesign. This thesis focused on studying *L. tarentolae* a hypopylarian and *L. mexicana* a suprapylarian. This gives the ability to compare results and understand the differences between each mode of infection and transmission.

*Leishmania* promastigotes undergo several morphological changes that have been well studied in *L. mexicana*, giving morphological categories according to criteria. *L. mexicana* fitted this criteria very well, however *L. tarentolae* showed challenges as two new morphologies were found. These findings of new morphology were named bulgetomonad and kinetoplast nucleus swapping promastigotes. This focus on morphometry showed the stage of promastigotes in an axenic culture that was required to replicate the stages of promastigotes in which escaped the PM. This stage of culture was used for further capillary assay as it represented the stage that initiates the migration within the alimentary canal. The migration of promastigotes within the alimentary canal has always been associated with the gradient of sugars emitted from the crop during the slow release of sugars to the midgut for digestion. However this positive taxis did not answer the question of migration of hypopylarian *Leishmania* species as they develop and migrate towards the hindgut. Using capillary assays and urea as a potential chemoeffector showed that compared to sugars, *L. tarentolae* had greater attraction to urea hence the hindgut migration and inability to be transmitted via the bite of an infected sandfly. Interestingly, analysis of migrated

promastigotes showed a higher migration of leptomonad promastigotes. This questions whether or not nectomonads are the primary migratory promastigote morphological stage within a sandfly. As a pilot screen of potential chemoeffectors , this study brings about a lot of new understanding of the less studied species *L. tarentolae*.

## REFERENCES

- Adler, J. (1966). Chemotaxis in Bacteria. *Science*, 153(3737), pp.708-716.
- Adler, J. (1969). Chemoreceptors in Bacteria. *Science*, 166(3913), pp.1588-1597.
- Adler, J. (1973). A Method for Measuring Chemotaxis and Use of the Method to Determine Optimum Conditions for Chemotaxis by *Escherichia coli*. *Journal of General Microbiology*, 74(1), pp.77-91.
- Adler, S. and Theodor, O. (1929). Observations on *leishmania ceramodactyli*. N.SP. *Transactions of the Royal Society of Tropical Medicine and Hygiene*, 22(4), pp.343-356.
- Aguiar, E., Olmo, R., Paro, S., Ferreira, F., de Faria, I., Todjro, Y., Lobo, F., Kroon, E., Meignin, C., Gatherer, D., Imler, J. and Marques, J. (2015). Sequence-independent characterization of viruses based on the pattern of viral small RNAs produced by the host. *Nucleic Acids Research*, 43(13), pp.6191-6206.
- Akhoundi, M., Kuhls, K., Cannet, A., Votýpka, J., Marty, P., Delaunay, P. and Sereno, D. (2016). A Historical Overview of the Classification, Evolution, and Dispersion of *Leishmania* Parasites and Sandflies. *PLOS Neglected Tropical Diseases*, 10(3), p.e0004349.
- Alawieh, A., Musharrafieh, U., Jaber, A., Berry, A., Ghosn, N. and Bizri, A. (2014). Revisiting leishmaniasis in the time of war: the Syrian conflict and the Lebanese outbreak. *International Journal of Infectious Diseases*, 29, pp.115-119.
- Alvar, J., Croft, S., Kaye, P., Khamesipour, A., Sundar, S. and Reed, S. (2013). Case study for a vaccine against leishmaniasis. *Vaccine*, 31, pp.B244-B249.
- Alvar, J., Yactayo, S. and Bern, C. (2006). Leishmaniasis and poverty. *Trends in Parasitology*, 22(12), pp.552-557.

Ambit, A., Woods, K., Cull, B., Coombs, G. and Mottram, J. (2011). Morphological Events during the Cell Cycle of *Leishmania major*. *Eukaryotic Cell*, 10(11), pp.1429-1438.

Antoine JC, Prina E, Jouanne C, Bongrand P. Parasitophorous vacuoles of *Leishmania amazonensis*-infected macrophages maintain an acidic pH. *Infect Immun*. 1990;58(3):779-87.

Armitage, J. (1992). Bacterial motility and chemotaxis. *Sci Prog*, 76(301-302 Pt 3-4), pp.451-77.

Armitage, J., Josey, D. and Smith, D. (1977). A Simple, Quantitative Method for Measuring Chemotaxis and Motility in Bacteria. *Journal of General Microbiology*, 102(1), pp.199-202.

Aslett, M., Aurrecochea, C., Berriman, M., Brestelli, J., Brunk, B., Carrington, M., Depledge, D., Fischer, S., Gajria, B., Gao, X., Gardner, M., Gingle, A., Grant, G., Harb, O., Heiges, M., Hertz-Fowler, C., Houston, R., Innamorato, F., Iodice, J., Kissinger, J., Kraemer, E., Li, W., Logan, F., Miller, J., Mitra, S., Myler, P., Nayak, V., Pennington, C., Phan, I., Pinney, D., Ramasamy, G., Rogers, M., Roos, D., Ross, C., Sivam, D., Smith, D., Srinivasamoorthy, G., Stoeckert, C., Subramanian, S., Thibodeau, R., Tivey, A., Treatman, C., Velarde, G. and Wang, H. (2009). TriTrypDB: a functional genomic resource for the Trypanosomatidae. *Nucleic Acids Research*, 38(suppl\_1), pp.D457-D462.

Ayhan, N., Sherifi, K., Taraku, A., Bërxfholi, K. and Charrel, R. (2017). High Rates of Neutralizing Antibodies to Toscana and Sandfly Fever Sicilian Viruses in Livestock, Kosovo. *Emerging Infectious Diseases*, 23(6), pp.989-992.

Bañuls, A., Bastien, P., Pomares, C., Arevalo, J., Fisa, R. and Hide, M. (2011). Clinical pleiomorphism in human leishmaniasis, with special mention of asymptomatic infection. *Clinical Microbiology and Infection*, 17(10), pp.1451-1461.

Barros, V., Oliveira, J., Melo, M. and Gontijo, N. (2006). *Leishmania amazonensis*: Chemotactic and osmotactic responses in promastigotes and their probable role in

development in the phlebotomine gut. *Experimental Parasitology*, 112(3), pp.152-157.

Bates, P. (1994). Complete developmental cycle of *Leishmania mexicana* in axenic culture. *Parasitology*, 108(01), p.1.

Bates, P. and Tetley, L. (1993). *Leishmania mexicana*: Induction of Metacyclogenesis by Cultivation of Promastigotes at Acidic pH. *Experimental Parasitology*, 76(4), pp.412-423.

Beach, R., Leeuwenburg, J. and Kiilu, G. (1985). Modification of Sand Fly Biting Behavior by *Leishmania* Leads to Increased Parasite Transmission. *The American Journal of Tropical Medicine and Hygiene*, 34(2), pp.278-282.

Berg, H. (2004). E. coli in Motion. *Biological and Medical Physics, Biomedical Engineering*.

Besteiro, S., Williams, R., Coombs, G. and Mottram, J. (2007). Protein turnover and differentiation in *Leishmania*. *International Journal for Parasitology*, 37(10), pp.1063-1075.

Borovsky, D. and Schlein, Y. (1987). Trypsin and chymotrypsin-like enzymes of the sandfly *Phlebotomus papatasi* infected with *Leishmania* and their possible role in vector competence. *Medical and Veterinary Entomology*, 1(3), pp.235-242.

Boyden, S. (1962). The chemotactic effect of mixtures of antibodies and antigen on polymorphonuclear leucocytes. *Journal of Experimental Medicine*, 115(3), pp.453-466.

BRAY, R. (1983). *Leishmania*: Chemotaxic Responses of Promastigotes and Macrophages In Vitro<sup>1</sup>. *The Journal of Protozoology*, 30(2), pp.322-329.

Brody, J. and Yager, P. (1997). Diffusion-based extraction in a microfabricated device. *Sensors and Actuators A: Physical*, 58(1), pp.13-18.

Burchmore, R. and Landfear, S. (1998). Differential Regulation of Multiple Glucose Transporter Genes in *Leishmania mexicana*. *Journal of Biological Chemistry*, 273(44), pp.29118-29126.

Burchmore, R., Rodriguez-Contreras, D., McBride, K., Barrett, M., Modi, G., Sacks, D. and Landfear, S. (2003). Genetic characterization of glucose transporter function in *Leishmania mexicana*. *Proceedings of the National Academy of Sciences*, 100(7), pp.3901-3906.

Cairns, B., Collard, M. and Landfear, S. (1989). Developmentally regulated gene from *Leishmania* encodes a putative membrane transport protein. *Proceedings of the National Academy of Sciences*, 86(20), pp.7682-7686.

Carter, N., Drew, M., Sanchez, M., Vasudevan, G., Landfear, S. and Ullman, B. (2000). Cloning of a Novel Inosine-Guanosine Transporter Gene from *Leishmania donovani* by Functional Rescue of a Transport-deficient Mutant. *Journal of Biological Chemistry*, 275(27), pp.20935-20941.

Carter, N., Yates, P., Gessford, S., Galagan, S., Landfear, S. and Ullman, B. (2010). Adaptive responses to purine starvation in *Leishmania donovani*. *Molecular Microbiology*, p.92-107.

Čiháková, J. and Volf, P. (1997). Development of different *Leishmania major* strains in the vector sandflies *Phlebotomus papatasi* and *P. duboscqi*. *Annals of Tropical Medicine & Parasitology*, 91(3), pp.267-279.

Coombs, G., Craft, J. and Hart, D. (1982). A comparative study of *Leishmania mexicana* amastigotes and promastigotes, enzyme activities and subcellular locations. *Molecular and Biochemical Parasitology*, 5(3), pp.199-211.

Costa, D., Codeço, C., Silva, M. and Werneck, G. (2013). Culling Dogs in Scenarios of Imperfect Control: Realistic Impact on the Prevalence of Canine Visceral Leishmaniasis. *PLoS Neglected Tropical Diseases*, 7(8), p.e2355.

Courtenay, O., Quinnell, R., Garcez, L., Shaw, J. and Dye, C. (2002). Infectiousness in a Cohort of Brazilian Dogs: Why Culling Fails to Control Visceral Leishmaniasis in

Areas of High Transmission. *The Journal of Infectious Diseases*, 186(9), pp.1314-1320.

Croft, S. and Olliaro, P. (2011). Leishmaniasis chemotherapy—challenges and opportunities. *Clinical Microbiology and Infection*, 17(10), pp.1478-1483.

Cuvillier, A., Miranda, J., Ambit, A., Barral, A. and Merlin, G. (2003). Abortive infection of *Lutzomyia longipalpis* insect vectors by aflagellated LdARL-3A-Q70L overexpressing *Leishmania amazonensis* parasites. *Cellular Microbiology*, 5(10), pp.717-728.

Davies, A.G. (1978). Pollution studies with marine plankton. II. Heavy metals. *Adv. Mar. Biol.*, 15: 381-508.

de Souza, W., and Souto-Padron, T. (1980). The Paraxial Structure of the Flagellum of Trypanosomatidae. *The Journal of Parasitology*, 66(2), p.229.

de Ysasa Pozzo, L., Fontes, A., de Thomaz, A., Barbosa, L., Ayres, D., Giorgio, S. and Cesar, C. (2007). *Leishmania amazonensis* chemotaxis under glucose gradient studied by the strength and directionality of forces measured with optical tweezers. *Imaging, Manipulation, and Analysis of Biomolecules, Cells, and Tissues V*.

Depaquit, J., Grandadam, M., Fouque, F., Andry, P. and Peyrefitte, C. (2010). Arthropod-borne viruses transmitted by Phlebotomine sandflies in Europe: a review. *Eurosurveillance*, 15(10), pii:19507.

Diaz-Albiter, H., Regnault, C., Alpizar-Sosa, E., McGuinness, D., Barrett, M. and Dillon, R. (2018). Non-invasive visualisation and identification of fluorescent *Leishmania tarentolae* in infected sand flies. *Wellcome Open Research*, 3, p.160.

Díaz, E., Köhidai, L., Ríos, A., Vanegas, O., Ponte-Sucre, A. (2011). Ensayos de quimiotaxis in vitro en *Leishmania* sp. Evaluación de la técnica de los capilares- dos cámaras en promastigotes. *Rev. Fac. Farm. (UCV)* 74, 31–40.

Díaz, E., Köhidai, L., Ríos, A., Vanegas, O., Silva, A., Szabó, R., Mező, G., Hudecz, F. and Ponte-Sucré, A. (2013). *Leishmania braziliensis*: Cytotoxic, cytostatic and chemotactic effects of poly-lysine–methotrexate-conjugates. *Experimental Parasitology*, 135(1), pp.134-141.

Dillon, R. and Lane, P. (1993). Bloodmeal digestion in the midgut of *Phlebotomus papatasi* and *Phlebotomus langeroni*. *Medical and Veterinary Entomology*, 7(3), pp.225-232.

Dillon, R. and Lane, R. (1993). Influence of *Leishmania* infection on blood-meal digestion in the sandflies *Phlebotomus papatasi* and *P. langeroni*. *Parasitology Research*, 79(6), pp.492-496.

Dillon, R., Ivens, A., Churcher, C., Holroyd, N., Quail, M., Rogers, M., Soares, M., Bonaldo, M., Casavant, T., Lehane, M. and Bates, P. (2006). Analysis of ESTs from *Lutzomyia longipalpis* sand flies and their contribution toward understanding the insect–parasite relationship. *Genomics*, 88(6), pp.831-840.

Docampo, R., de Souza, W., Miranda, K., Rohloff, P. and Moreno, S. (2005). Acidocalcisomes - conserved from bacteria to man. *Nature Reviews Microbiology*, 3(3), pp.251-261.

Dougall, A., Alexander, B., Holt, D., Harris, T., Sultan, A., Bates, P., Rose, K. and Walton, S. (2011). Evidence incriminating midges (Diptera: Ceratopogonidae) as potential vectors of *Leishmania* in Australia. *International Journal for Parasitology*, 41(5), pp.571-579.

Englert, D., Manson, M. and Jayaraman, A. (2009). Flow-Based Microfluidic Device for Quantifying Bacterial Chemotaxis in Stable, Competing Gradients. *Applied and Environmental Microbiology*, 75(13), pp.4557-4564.

Ergunay, K., Kasap, O., Orsten, S., Oter, K., Gunay, F., Yoldar, A., Dincer, E., Alten, B. and Ozkul, A. (2014). Phlebovirus and *Leishmania* detection in sandflies from eastern Thrace and northern Cyprus. *Parasites & Vectors*, 7(1), p.575.

Faucher, B., Piarroux, R., Mary, C., Bichaud, L., Charrel, R., Izri, A. and de Lamballerie, X. (2014). Presence of sandflies infected with *Leishmania infantum* and Massilia virus in the Marseille urban area. *Clinical Microbiology and Infection*, 20(5), pp.O340-O343.

Field, M. and Carrington, M. (2009). The trypanosome flagellar pocket. *Nature Reviews Microbiology*, 7(11), pp.775-786.

Figarella, K., Uzcategui, N., Zhou, Y., LeFurgey, A., Ouellette, M., Bhattacharjee, H. and Mukhopadhyay, R. (2007). Biochemical characterization of *Leishmania major* aquaglyceroporin LmAQP1: possible role in volume regulation and osmotaxis. *Molecular Microbiology*, 65(4), pp.1006-1017.

Fraih, W., Fares, W., Perrin, P., Dorkeld, F., Sereno, D., Barhoumi, W., Sbissi, I., Cherni, S., Chelbi, I., Durvasula, R., Ramalho-Ortigao, M., Gtari, M. and Zhioua, E. (2017). An integrated overview of the midgut bacterial flora composition of *Phlebotomus perniciosus*, a vector of zoonotic visceral leishmaniasis in the Western Mediterranean Basin. *PLOS Neglected Tropical Diseases*, 11(3), p.e0005484.

Fuqua, W., Winans, S. and Greenberg, E. (1994). Quorum sensing in bacteria: the LuxR-LuxI family of cell density-responsive transcriptional regulators. *Journal of Bacteriology*, 176(2), pp.269-275.

Gillespie, P., Beaumier, C., Strych, U., Hayward, T., Hotez, P. and Bottazzi, M. (2016). Status of vaccine research and development of vaccines for leishmaniasis. *Vaccine*, 34(26), pp.2992-2995.

Gomes, B., Purkait, B., Deb, R., Rama, A., Singh, R., Foster, G., Coleman, M., Kumar, V., Paine, M., Das, P. and Weetman, D. (2017). Knockdown resistance mutations predict DDT resistance and pyrethroid tolerance in the visceral leishmaniasis vector *Phlebotomus argentipes*. *PLOS Neglected Tropical Diseases*, 11(4), p.e0005504.

Hammond, D. and Gutteridge, W. (1984). Purine and pyrimidine metabolism in the trypanosomatidae. *Molecular and Biochemical Parasitology*, 13(3), pp.243-261.

Harmsen, R. (1973). The nature of the establishment barrier for *Trypanosoma brucei* in the gut of *Glossina pallidipes*. *Transactions of the Royal Society of Tropical Medicine and Hygiene*, 67(3), pp.364-373.

Herrer, A. and Christensen, H. (1975). Implication of Phlebotomus sand flies as vectors of bartonellosis and leishmaniasis as early as 1764. *Science*, 190(4210), pp.154-155.

Horn, D. and Duraisingh, M. (2014). Antiparasitic Chemotherapy: From Genomes to Mechanisms. *Annual Review of Pharmacology and Toxicology*, 54(1), pp.71-94.

Inbar, E., Canepa, G., Carrillo, C., Glaser, F., Suter Grottemeyer, M., Rentsch, D., Zilberstein, D. and Pereira, C. (2010). Lysine transporters in human trypanosomatid pathogens. *Amino Acids*, 42(1), pp.347-360.

Jeon, N., Dertinger, S., Chiu, D., Choi, I., Stroock, A. and Whitesides, G. (2000). Generation of Solution and Surface Gradients Using Microfluidic Systems. *Langmuir*, 16(22), pp.8311-8316.

Johnson, W. (1941). Nutrition in the Protozoa. *The Quarterly Review of Biology*, 16(3), pp.336-348.

Joshi, M., Rogers, M., Shakarian, A., Yamage, M., Al-Harhi, S., Bates, P. and Dwyer, D. (2004). Molecular Characterization, Expression, and in Vivo Analysis of LmexCht1. *Journal of Biological Chemistry*, 280(5), pp.3847-3861.

Kamhawi, S. (2000). Protection Against Cutaneous Leishmaniasis Resulting from Bites of Uninfected Sand Flies. *Science*, 290(5495), pp.1351-1354.

Kamhawi, S. (2006). Phlebotomine sand flies and *Leishmania* parasites: friends or foes?. *Trends in Parasitology*, 22(9), pp.439-445.

Kaufer, A., Ellis, J., Stark, D. and Barratt, J. (2017). The evolution of trypanosomatid taxonomy. *Parasites & Vectors*, 10(1).

Kelly, P., Bahr, S., Serafim, T., Ajami, N., Petrosino, J., Meneses, C., Kirby, J., Valenzuela, J., Kamhawi, S. and Wilson, M. (2017). The Gut Microbiome of the Vector *Lutzomyia longipalpis* Is Essential for Survival of *Leishmania infantum*. *mBio*, 8(1).

Keymer, J., Endres, R., Skoge, M., Meir, Y. and Wingreen, N. (2006). Chemosensing in *Escherichia coli*: Two regimes of two-state receptors. *Proceedings of the National Academy of Sciences*, 103(6), pp.1786-1791.

Killick-Kendrick, R. (1978). Recent advances and outstanding problems in the biology of phlebotomine sandflies. A review. *Acta Trop*, 35(4), pp.297-313.

Killick-Kendrick, R. (1990). Phlebotomine vectors of the leishmaniasis: a review. *Medical and Veterinary Entomology*, 4(1), pp.1-24.

Killick-Kendrick, R., Leaney, A., Ready, P. and Molyneux, D. (1977). *Leishmania* in phlebotomid sandflies - IV. The transmission of *Leishmania mexicana amazonensis* to hamsters by the bite of experimentally infected *Lutzomyia longipalpis*. *Proceedings of the Royal Society of London. Series B. Biological Sciences*, 196(1122), pp.105-115.

Köhidaï, L. (1995). Method for determination of chemoattraction in *Tetrahymena pyriformis*. *Current Microbiology*, 30(4), pp.251-253.

Kwakye-Nuako, G., Mosore, M., Duplessis, C., Bates, M., Pupilampu, N., Mensah-Attipoe, I., Desewu, K., Afegbe, G., Asmah, R., Jamjoom, M., Ayeh-Kumi, P., Boakye, D. and Bates, P. (2015). First isolation of a new species of *Leishmania* responsible for human cutaneous leishmaniasis in Ghana and classification in the *Leishmania enriettii* complex. *International Journal for Parasitology*, 45(11), pp.679-684.

Lainson, R., Ready, P. and Shaw, J. (1979). *Leishmania* in phlebotomid sandflies. VII. On the taxonomic status of *Leishmania peruviana*, causative agent of Peruvian 'uta', as indicated by its development in the sandfly, *Lutzomyia longipalpis*. *Proceedings of the Royal Society of London. Series B. Biological Sciences*, 206(1164), pp.307-318.

Landfear, S. (2011). Nutrient Transport and Pathogenesis in Selected Parasitic Protozoa. *Eukaryotic Cell*, 10(4), pp.483-493.

Landfear, S. and Ignatushchenko, M. (2001). The flagellum and flagellar pocket of trypanosomatids. *Molecular and Biochemical Parasitology*, 115(1), pp.1-17.

Langousis, G. and Hill, K. (2014). Motility and more: the flagellum of *Trypanosoma brucei*. *Nature Reviews Microbiology*, 12(7), pp.505-518.

Lantova, L. and Volf, P. (2014). Mosquito and sand fly gregarines of the genus *Ascogregarina* and *Psychodiella* (Apicomplexa: Eugregarinorida, Aseptatorina) – Overview of their taxonomy, life cycle, host specificity and pathogenicity. *Infection, Genetics and Evolution*, 28, pp.616-627.

Lautenschlaeger, F. (2011). *Cell compliance: cytoskeletal origin and importance for cellular function*. (Doctoral thesis). <https://doi.org/10.17863/CAM.16575>

Lawyer, P., Githure, J., Roberts, C., Anjili, C., Mebrahtu, Y., Ngumbi, P., Koech, D. and Odongo, S. (1990). Development of *Leishmania major* in *Phlebotomus duboscqi* and *Sergentomyia schwetzi* (Diptera: Psychodidae). *The American Journal of Tropical Medicine and Hygiene*, 43(1), pp.31-43.

Lehane, M. (1997). Peritrophic matrix structure and function. *Annual Review of Entomology*, 42(1), pp.525-550.

Lehane, M. (2005). *The biology of blood-sucking in insects*. Cambridge: Cambridge University Press, p.96.

Leslie, G., Barrett, M. and Burchmore, R. (2002). *Leishmania mexicana*: promastigotes migrate through osmotic gradients. *Experimental Parasitology*, 102(2), pp.117-120.

Lestinova, T., Rohousova, I., Sima, M., de Oliveira, C. and Volf, P. (2017). Insights into the sand fly saliva: Blood-feeding and immune interactions between sand flies, hosts, and *Leishmania*. *PLOS Neglected Tropical Diseases*, 11(7), p.e0005600.

Lin, B. and Levchenko, A. (2015). Spatial Manipulation with Microfluidics. *Frontiers in Bioengineering and Biotechnology*, 3.

Lukes, J., Mauricio, I., Schonian, G., Dujardin, J., Soteriadou, K., Dedet, J., Kuhls, K., Tintaya, K., Jirku, M., Chocholova, E., Haralambous, C., Pratlong, F., Obornik, M., Horak, A., Ayala, F. and Miles, M. (2007). Evolutionary and geographical history of the *Leishmania donovani* complex with a revision of current taxonomy. *Proceedings of the National Academy of Sciences*, 104(22), pp.9375-9380.

Macnab, R. and Koshland, D. (1972). The Gradient-Sensing Mechanism in Bacterial Chemotaxis. *Proceedings of the National Academy of Sciences*, 69(9), pp.2509-2512.

Maia, C. and Depaquit, J. (2016). Can *Sergentomyia* (Diptera, Psychodidae) play a role in the transmission of mammal-infecting *Leishmania*?. *Parasite*, 23, p.55.

Manson, P., Cooke, G. and Zumla, A. (2009). *Manson's tropical diseases*. [Edinburgh]: Saunders Elsevier, p.1715.

Maroli, M., Feliciangeli, M., Bichaud, L., Charrel, R. and Gradoni, L. (2012). Phlebotomine sandflies and the spreading of leishmaniases and other diseases of public health concern. *Medical and Veterinary Entomology*, 27(2), pp.123-147.

Mauricio, I., Howard, M., Stothard, J. and Miles, M. (1999). Genomic diversity in the *Leishmania donovani* complex. *Parasitology*, 119(3), pp.237-246.

Mitra, B., Cortez, M., Haydock, A., Ramasamy, G., Myler, P. and Andrews, N. (2013). Iron uptake controls the generation of *Leishmania* infective forms through regulation of ROS levels. *The Journal of General Physiology*, 141(3), pp.17-17.

Modi G.B. (1997) *Care and maintenance of phlebotomine sandfly colonies*. In: Crampton J.M., Beard C.B., Louis C. (eds) *The Molecular Biology of Insect Disease Vectors*. Springer, Dordrecht

Moloo, S. and Kutuza, S. (1971). Feeding and crop emptying in *Glossina brevipalpis* Newstead. *Transactions of the Royal Society of Tropical Medicine and Hygiene*, 65(2), pp.221-222.

Monteiro, C., Villegas, L., Campolina, T., Pires, A., Miranda, J., Pimenta, P. and Secundino, N. (2016). Bacterial diversity of the American sand fly *Lutzomyia intermedia* using high-throughput metagenomic sequencing. *Parasites & Vectors*, 9(1).

Mukhopadhyay, J., Braig, H., Rowton, E. and Ghosh, K. (2012). Naturally Occurring Culturable Aerobic Gut Flora of Adult *Phlebotomus papatasi*, Vector of *Leishmania major* in the Old World. *PLoS ONE*, 7(5), p.e35748.

Myler, P. and Fasel, N. (2008). *Leishmania: After the Genome*. Norfolk: Caister academic Press, p.209.

Naula, C., Logan, F., Wong, P., Barrett, M. and Burchmore, R. (2010). A Glucose Transporter Can Mediate Ribose Uptake. *Journal of Biological Chemistry*, 285(39), pp.29721-29728.

Oliveira, F., Rowton, E., Aslan, H., Gomes, R., Castrovinci, P., Alvarenga, P., Abdeladhim, M., Teixeira, C., Meneses, C., Kleeman, L., Guimarães-Costa, A., Rowland, T., Gilmore, D., Doumbia, S., Reed, S., Lawyer, P., Andersen, J., Kamhawi, S. and Valenzuela, J. (2015). A sand fly salivary protein vaccine shows efficacy against vector-transmitted cutaneous leishmaniasis in nonhuman primates. *Science Translational Medicine*, 7(290), pp.290ra90-290ra90.

Oliveira, J.S., Melo, M.N., Gontijo, N.F. (2000). A sensitive method for assaying chemotactic responses of *Leishmania* promastigotes. *Experimental Parasitology* 96, 187–189.

Oliveira, S., Moraes, B., Gonçalves, C., Giordano-Dias, C., d'Almeida, J., Asensi, M., Mello, R. and Brazil, R. (2000). Prevalência da microbiota no trato digestivo de fêmeas de *Lutzomyia longipalpis* (Lutz & Neiva, 1912) (Diptera: Psychodidae) provenientes do campo. *Revista da Sociedade Brasileira de Medicina Tropical*, 33(3), pp.319-322.

Opperdoes, F. (1987). Compartmentation Of Carbohydrate Metabolism In Trypanosomes. *Annual Review of Microbiology*, 41(1), pp.127-151.

Ortiz, D., Sanchez, M., Koch, H., Larsson, H. and Landfear, S. (2009). An Acid-activated Nucleobase Transporter from *Leishmania major*. *Journal of Biological Chemistry*, 284(24), pp.16164-16169.

Paliwal, S., Iglesias, P., Campbell, K., Hilioti, Z., Groisman, A. and Levchenko, A. (2007). MAPK-mediated bimodal gene expression and adaptive gradient sensing in yeast. *Nature*, 446(7131), pp.46-51.

Pigott, D. M., Bhatt, S., Golding, N., Duda, K. A., Battle, K. E., Brady, O. J., Messina, J. P., Balard, Y., Bastien, P., Pratlong, F., Brownstein, J. S., Freifeld, C. C., Mekaru, S. R., Gething, P. W., George, D. B., Myers, M. F., Reithinger, R., Hay, S. I. (2014). Global distribution maps of the leishmaniasis. *eLife*, 3, e02851. doi:10.7554/eLife.02851

Pires, A., Villegas, L., Campolina, T., Orfanó, A., Pimenta, P. and Secundino, N. (2017). Bacterial diversity of wild-caught *Lutzomyia longipalpis* (a vector of zoonotic visceral leishmaniasis in Brazil) under distinct physiological conditions by metagenomics analysis. *Parasites & Vectors*, 10(1).

Pimenta, P., Modi, G., Pereira, S., Shahabuddin, M. and Sacks, D. (1997). A novel role for the peritrophic matrix in protecting *Leishmania* from the hydrolytic activities of the sand fly midgut. *Parasitology*, 115(4), pp.359-369.

Pimenta, P., Turco, S., McConville, M., Lawyer, P., Perkins, P. and Sacks, D. (1992). Stage-specific adhesion of *Leishmania* promastigotes to the sandfly midgut. *Science*, 256(5065), pp.1812-1815.

Pimentel, D., Ramos, R., Santana, M., Maia, C., Carvalho, G., Silva, H. and Alves, L. (2015). Prevalence of zoonotic visceral leishmaniasis in dogs in an endemic area of Brazil. *Revista da Sociedade Brasileira de Medicina Tropical*, 48(4), pp.491-493.

Polacheck, W., Charest, J. and Kamm, R. (2011). Interstitial flow influences direction of tumor cell migration through competing mechanisms. *Proceedings of the National Academy of Sciences*, 108(27), pp.11115-11120.

Pozzo, L.Y., Fontes, A., de Thomaz, A.A., Santos, B.B., Farias, P., Ayres, D.C., Giorgio, S., Cesar, C.L., 2009. Studying taxis in real time using optical tweezers: applications for *Leishmania amazonensis* parasites. *Micron* 40, 617–620.

Pruzinova, K., Sadlova, J., Seblova, V., Homola, M., Votypka, J. and Volf, P. (2015). Comparison of Bloodmeal Digestion and the Peritrophic Matrix in Four Sand Fly Species Differing in Susceptibility to *Leishmania donovani*. *PLOS ONE*, 10(6), p.e0128203.

Pumpuni, C., Kent, M., Davis, J., Beier, J. and Demaio, J. (1996). Bacterial Population Dynamics in Three Anopheline Species: The Impact on Plasmodium Sporogonic Development. *The American Journal of Tropical Medicine and Hygiene*, 54(2), pp.214-218.

Ramalho-Ortigão, J., Kamhawi, S., Joshi, M., Reynoso, D., Lawyer, P., Dwyer, D., Sacks, D. and Valenzuela, J. (2005). Characterization of a blood activated chitinolytic system in the midgut of the sand fly vectors *Lutzomyia longipalpis* and *Phlebotomus papatasi*. *Insect Molecular Biology*, 14(6), pp.703-712.

Ramalho-Ortigao, M. (2010). Sand Fly-*Leishmania* Interactions: Long Relationships are Not Necessarily Easy. *The Open Parasitology Journal*, 4(1), pp.195-204.

Ramsay, J. (1951). Osmotic Regulation in Mosquito Larvae: The Role of the Malpighian Tubules. *Journal of Experimental Biology*, 28, pp.62-73.

Ready, P. (1979). Factors Affecting Egg Production of Laboratory-Bred *Lutzomyia longipalpis* (Diptera: Psychodidae)1. *Journal of Medical Entomology*, 16(5), pp.413-423.

Ready, P. (2013). Biology of Phlebotomine Sand Flies as Vectors of Disease Agents. *Annual Review of Entomology*, 58(1), pp.227-250.

Reithinger, R., Coleman, P., Alexander, B., Vieira, E., Assis, G. and Davies, C. (2004). Are insecticide-impregnated dog collars a feasible alternative to dog culling as a strategy for controlling canine visceral leishmaniasis in Brazil?. *International Journal for Parasitology*, 34(1), pp.55-62.

Reithinger, R., Mohsen, M. and Leslie, T. (2010). Risk Factors for Anthroponotic Cutaneous Leishmaniasis at the Household Level in Kabul, Afghanistan. *PLoS Neglected Tropical Diseases*, 4(3), p.e639.

Rezvan, H. and Moafi, M. (2015). An overview on *Leishmania* vaccines: A narrative review article. *Veterinary Research Forum*, 6(1), pp.1-7.

Rezvan, H., Nourian, A. and Navard, S. (2017). An Overview on *Leishmania* Diagnosis. *JoMMID*, 5(1 and 21), pp.1-11.

RG Endris et al. 1982 *Mosquitos News* 42: 400-407

Richards O.W., Davies R.G. (1977) The Alimentary Canal, Nutrition and Digestion. In: IMMS' General Textbook of Entomology. Springer, Dordrecht

Rogers, M. (2012). The Role of *Leishmania* Proteophosphoglycans in Sand Fly Transmission and Infection of the Mammalian Host. *Frontiers in Microbiology*, 3.

Rogers, M., Chance, M. and Bates, P. (2002). The role of promastigote secretory gel in the origin and transmission of the infective stage of *Leishmania mexicana* by the sandfly *Lutzomyia longipalpis*. *Parasitology*, 124(05).

Rogers, M., Hajmová, M., Joshi, M., Sadlova, J., Dwyer, D., Volf, P. and Bates, P. (2008). *Leishmania* chitinase facilitates colonization of sand fly vectors and enhances transmission to mice. *Cellular Microbiology*, 10(6), pp.1363-1372.

Rogers, M., Ilg, T., Nikolaev, A., Ferguson, M. and Bates, P. (2004). Transmission of cutaneous leishmaniasis by sand flies is enhanced by regurgitation of fPPG. *Nature*, 430(6998), pp.463-467.

Rotureau, B., Morales, M., Bastin, P. and Späth, G. (2009). The flagellum-mitogen-activated protein kinase connection in Trypanosomatids: a key sensory role in parasite signalling and development?. *Cellular Microbiology*, 11(5), pp.710-718.

Rudin, W. and Hecker, H. (1982). Functional morphology of the midgut of a sandfly as compared to other hematophagous nematocera. *Tissue and Cell*, 14(4), pp.751-758.

Sacks, D. and Kamhawi, S. (2001). Molecular Aspects of Parasite-Vector and Vector-Host Interactions in Leishmaniasis. *Annual Review of Microbiology*, 55(1), pp.453-483.

Sádlová, J. and Volf, P. (2009). Peritrophic matrix of *Phlebotomus duboscqi* and its kinetics during *Leishmania major* development. *Cell and Tissue Research*, 337(2), pp.313-325.

Sales, K., Costa, P., de Moraes, R., Otranto, D., Brandão-Filho, S., Cavalcanti, M. and Dantas-Torres, F. (2015). Identification of phlebotomine sand fly blood meals by real-time PCR. *Parasites & Vectors*, 8(1).

Sanchez, M., Zeoli, D., Klamo, E., Kavanaugh, M. and Landfear, S. (1995). A Family of Putative Receptor-Adenylate Cyclases from *Leishmania donovani*. *Journal of Biological Chemistry*, 270(29), pp.17551-17558.

Santos, V., Araujo, R., Machado, L., Pereira, M. and Gontijo, N. (2008). The physiology of the midgut of *Lutzomyia longipalpis* (Lutz and Neiva 1912): pH in different physiological conditions and mechanisms involved in its control. *Journal of Experimental Biology*, 211(17), pp.2792-2798.

Santos, V., Vale, V., Silva, S., Nascimento, A., Saab, N., Soares, R., Michalick, M., Araujo, R., Pereira, M., Fujiwara, R. and Gontijo, N. (2014). Host Modulation by a Parasite: How *Leishmania infantum* Modifies the Intestinal Environment of *Lutzomyia longipalpis* to Favor Its Development. *PLoS ONE*, 9(11), p.e111241.

Satir, P. (1968). STUDIES ON CILIA: III. Further Studies on the Cilium Tip and a "Sliding Filament" Model of Ciliary Motility. *The Journal of Cell Biology*, 39(1), pp.77-94.

Satir, P. and Christensen, S. (2008). Structure and function of mammalian cilia. *Histochemistry and Cell Biology*, 129(6), pp.687-693.

Schlein, Y. (1986). Sandfly diet and *Leishmania*. *Parasitology Today*, 2(6), pp.175-177.

Schlein, Y. and Jacobson, R. (1999). Sugar meals and longevity of the sandfly *Phlebotomus papatasi* in an arid focus of *Leishmania major* in the Jordan Valley. *Medical and Veterinary Entomology*, 13(1), pp.65-71.

Schlein, Y., Jacobson, R. and Messer, G. (1992). *Leishmania* infections damage the feeding mechanism of the sandfly vector and impede parasite transmission by bite. *Proceedings of the National Academy of Sciences*, 89(20), pp.9944-9948.

Secundino, N., Eger-Mangrich, I., Braga, E., Santoro, M. and Pimenta, P. (2005). *Lutzomyia longipalpis* Peritrophic Matrix: Formation, Structure, and Chemical Composition. *Journal of Medical Entomology*, 42(6), pp.928–938.

Sevá, A., Ovallos, F., Amaku, M., Carrillo, E., Moreno, J., Galati, E., Lopes, E., Soares, R. and Ferreira, F. (2016). Correction: Canine-Based Strategies for Prevention and Control of Visceral Leishmaniasis in Brazil. *PLOS ONE*, 11(9), p.e0162854.

Seymour, J., Ahmed, T., Marcos and Stocker, R. (2008). A microfluidic chemotaxis assay to study microbial behavior in diffusing nutrient patches. *Limnology and Oceanography: Methods*, 6(9), pp.477-488.

Shaked-Mishan, P., Suter-Grotemeyer, M., Yoel-Almagor, T., Holland, N., Zilberstein, D. and Rentsch, D. (2006). A novel high-affinity arginine transporter from the human parasitic protozoan *Leishmania donovani*. *Molecular Microbiology*, 60(1), pp.30-38.

Sharifi, I., Fekri, A., Aflatonian, M., Khamesipour, A., Nadim, A., Mousavi, M., Momeni, A., Dowlati, Y., Godal, T., Zicker, F., Smith, P. and Modabber, F. (1998). Randomised vaccine trial of single dose of killed *Leishmania major* plus BCG against anthroponotic cutaneous leishmaniasis in Bam, Iran. *The Lancet*, 351(9115), pp.1540-1543.

Silflow, C. and Lefebvre, P. (2001). Assembly and Motility of Eukaryotic Cilia and Flagella. Lessons from *Chlamydomonas reinhardtii*. *PLANT PHYSIOLOGY*, 127(4), pp.1500-1507.

Silverman, M. and Leroux, M. (2009). Intraflagellar transport and the generation of dynamic, structurally and functionally diverse cilia. *Trends in Cell Biology*, 19(7), pp.306-316.

Simpson, L. (1968). Effect of acriflavine on the kinetoplast of *Leishmania tarentolae*: Mode of Action and Physiological Correlates of the Loss of Kinetoplast DNA. *The Journal of Cell Biology*, 37(3), pp.660-682.

Singla, V. and Reiter, J. (2006). The Primary Cilium as the Cell's Antenna: Signaling at a Sensory Organelle. *Science*, 313(5787), pp.629-633.

Skoge, M., Adler, M., Groisman, A., Levine, H., Loomis, W. and Rappel, W. (2010). Gradient sensing in defined chemotactic fields. *Integrative Biology*, 2(11-12), p.659.

Smith, C., Chaichana, K., Lee, Y., Lin, B., Stanko, K., O'Donnell, T., Gupta, S., Shah, S., Wang, J., Wijesekera, O., Delannoy, M., Levchenko, A. and Quiñones-Hinojosa, A. (2015). Pre-Exposure of Human Adipose Mesenchymal Stem Cells to Soluble Factors Enhances Their Homing to Brain Cancer. *STEM CELLS Translational Medicine*, 4(3), pp.239-251.

Smith, D. and Littau, V. (1960). CELLULAR SPECIALIZATION IN THE EXCRETORY EPITHELIA OF AN INSECT, *Macrosteles fascifrons* STAL (HOMOPTERA). *The Journal of Cell Biology*, 8(1), pp.103-133.

Snapp, E. and Landfear, S. (1999). Characterization of a Targeting Motif for a Flagellar Membrane Protein in *Leishmania enriettii*. *Journal of Biological Chemistry*, 274(41), pp.29543-29548.

Soares, R. and Turco, S. (2003). Erratum to "Lutzomyia longipalpis (Diptera: Psychodidae: Phlebotominae): a review". *Anais da Academia Brasileira de Ciências*, 75(4), pp.441-441.

Soares, R., Cardoso, T., Barron, T., Araújo, M., Pimenta, P. and Turco, S. (2005). *Leishmania braziliensis*: a novel mechanism in the lipophosphoglycan regulation during metacyclogenesis. *International Journal for Parasitology*, 35(3), pp.245-253.

Soares, R., Macedo, M., Ropert, C., Gontijo, N., Almeida, I., Gazzinelli, R., Pimenta, P. and Turco, S. (2002). *Leishmania chagasi*: lipophosphoglycan characterization and binding to the midgut of the sand fly vector *Lutzomyia longipalpis*. *Molecular and Biochemical Parasitology*, 121(2), pp.213-224.

Spotin, A., Rouhani, S., Ghaemmaghami, P., Haghighi, A., Zolfaghari, M., Amirkhani, A., Farahmand, M., Bordbar, A. and Parvizi, P. (2015). Different Morphologies of *Leishmania major* Amastigotes with No Molecular Diversity in a Neglected Endemic Area of Zoonotic Cutaneous Leishmaniasis in Iran. *Iranian Biomedical Journal*, 19(3), pp.149–159.

Stierhof, Y., Bates, P., Jacobson, R., Rogers, M., Schlein, Y., Handman, E. and Ilg, T. (1999). Filamentous proteophosphoglycan secreted by *Leishmania* promastigotes forms gel-like three-dimensional networks that obstruct the digestive tract of infected sandfly vectors. *European Journal of Cell Biology*, 78(10), pp.675-689.

Stoffolano, J. and Haselton, A. (2013). The Adult Dipteran Crop: A Unique and Overlooked Organ. *Annual Review of Entomology*, 58(1), pp.205-225.

Stuart, K., Brun, R., Croft, S., Fairlamb, A., Gürtler, R., McKerrow, J., Reed, S. and Tarleton, R. (2008). Kinetoplastids: related protozoan pathogens, different diseases. *Journal of Clinical Investigation*, 118(4), pp.1301-1310.

Sunter, J. and Gull, K. (2019). Shape, form, function and *Leishmania* pathogenicity: from textbook descriptions to biological understanding. *Open Biol*, 7(9)pii: 170165

Talmi-Frank, D., King, R., Warburg, A., Peleg, O., Nasereddin, A., Svobodova, M., Jaffe, C. and Baneth, G. (2010). *Leishmania tropica* in Rock Hyraxes (*Procavia capensis*) in a Focus of Human Cutaneous Leishmaniasis. *The American Journal of Tropical Medicine and Hygiene*, 82(5), pp.814-818.

TANG, Y. and WARD, R. (1998). Sugar feeding and fluid destination control in the phlebotomine sandfly *Lutzomyia longipalpis* (Diptera: Psychodidae). *Medical and Veterinary Entomology*, 12(1), pp.13-19.

Telleria, E., Araújo, A., Secundino, N., d'Avila-Levy, C. and Traub-Csekö, Y. (2010). Trypsin-Like Serine Proteases in *Lutzomyia longipalpis* – Expression, Activity and Possible Modulation by *Leishmania infantum chagasi*. *PLoS ONE*, 5(5), p.e10697.

Telleria, E., Martins-da-Silva, A., Tempone, A. and Traub-Csekö, Y. (2018). *Leishmania*, microbiota and sand fly immunity. *Parasitology*, 145(10), pp.1336-1353.

Thomson, A. (1975). Synchronization of function in the foregut of the blowfly **phormia regina** (Dipteris: Calliphoridae) during the crop-emptying process. *The Canadian Entomologist*, 107(11), pp.1193-1198.

Trager, W. (1965). The Kinetoplast and Differentiation in Certain Parasitic Protozoa. *The American Naturalist*, 99(907), pp.255-266.

Turco, S. and Sacks, D. (2003). Control of *Leishmania*–Sand Fly Interactions by Polymorphisms in Lipophosphoglycan Structure. *Recognition of Carbohydrates in Biological Systems, Part B: Specific Applications*, pp.377-381.

Uppaluri, S., Heddergott, N., Stellamanns, E., Herminghaus, S., Zöttl, A., Stark, H., Engstler, M. and Pfohl, T. (2012). Flow Loading Induces Oscillatory Trajectories in a Bloodstream Parasite. *Biophysical Journal*, 103(6), pp.1162-1169.

Vaidyanathan, R. (2004). *Leishmania parasites* (Kinetoplastida: Trypanosomatidae) reversibly inhibit visceral muscle contractions in hemimetabolous and holometabolous insects. *Journal of Invertebrate Pathology*, 87(2-3), pp.123-128.

Vaidyanathan, R. (2005). Isolation of a Myoinhibitory Peptide from *Leishmania major* (Kinetoplastida: Trypanosomatidae) and Its Function in the Vector Sand Fly *Phlebotomus papatasi* (Diptera: Psychodidae). *Journal of Medical Entomology*, 42(2), pp.142-152.

Vargas-Parada, L. (2010) Kinetoplastids and Their Networks of Interlocked DNA. *Nature Education* 3(9):63

Vasudevan, G., Carter, N., Drew, M., Beverley, S., Sanchez, M., Seyfang, A., Ullman, B. and Landfear, S. (1998). Cloning of *Leishmania* nucleoside transporter genes by rescue of a transport-deficient mutant. *Proceedings of the National Academy of Sciences*, 95(17), pp.9873-9878.

Vivero, R., Jaramillo, N., Cadavid-Restrepo, G., Soto, S. and Herrera, C. (2016). Structural differences in gut bacteria communities in developmental stages of natural populations of *Lutzomyia evansi* from Colombia's Caribbean coast. *Parasites & Vectors*, 9(1).

Volf, P., Kiewegova, A. and Nemeč, A. (2002). Bacterial colonisation in the gut of *Phlebotomus duboscqi* (Diptera: Psychodidae): transtadial passage and the role of female diet. *Folia Parasitologica*, 49(1), pp.73-77.

Walker, G., Sai, J., Richmond, A., Stremler, M., Chung, C. and Wikswo, J. (2005). Effects of flow and diffusion on chemotaxis studies in a microfabricated gradient generator. *Lab on a Chip*, 5(6), p.611.

Warburg, A. (2008). The structure of the female sand fly (*Phlebotomus papatasi*) alimentary canal. *Transactions of the Royal Society of Tropical Medicine and Hygiene*, 102(2), pp.161-166.

Warburg, A. and Ostrovska, K. (1987). Cytoplasmic Polyhedrosis Viruses in *Phlebotomus papatasi* Inhibit Development of *Leishmania major*. *The Journal of Parasitology*, 73(3), p.578.

Warburg, A., Tesh, R. and McMahon-Pratt, D. (1989). Studies on the Attachment of *Leishmania* Flagella to Sand Fly Midgut Epithelium. *The Journal of Protozoology*, 36(6), pp.613-617.

Wheeler, R., Gluenz, E. and Gull, K. (2010). The cell cycle of *Leishmania*: morphogenetic events and their implications for parasite biology. *Molecular Microbiology*, 79(3), pp.647-662.

Wheeler, R., Gluenz, E. and Gull, K. (2015). Basal body multipotency and axonemal remodelling are two pathways to a 9+0 flagellum. *Nature Communications*, 6(1).

Whitesides, G., Ostuni, E., Takayama, S., Jiang, X. and Ingber, D. (2001). Soft Lithography in Biology and Biochemistry. *Annual Review of Biomedical Engineering*, 3(1), pp.335-373.

Wilson V.C.L.C., Southgate B.A. Lizard *Leishmania*. In: Lumsden W.H.R., Evans D.A., editors. vol. 2. Academic Press; London: 1979. pp. 241–268.

Wilson, M. E., Vorhies, R. W., Andersen, K. A., & Britigan, B. E. (1994). Acquisition of iron from transferrin and lactoferrin by the protozoan *Leishmania chagasi*. *Infection and immunity*, 62(8), 3262-9.

Wilson, M., Lewis, T., Miller, M., McCormick, M. and Britigan, B. (2002). *Leishmania chagasi*: uptake of iron bound to lactoferrin or transferrin requires an iron reductase. *Experimental Parasitology*, 100(3), pp.196-207.

Yasmine Precious Kumordzi

Witman, G. (2003). Cell Motility: Deaf Drosophila Keep the Beat. *Current Biology*, 13(20), pp.R796-R798.

Ye, N., Qin, J., Shi, W., Liu, X. and Lin, B. (2007). Cell-based high content screening using an integrated microfluidic device. *Lab on a Chip*, 7(12), p.1696.

Zeyrek, F., Korkmaz, M. and Ozbel, Y. (2007). Serodiagnosis of Anthroponotic Cutaneous Leishmaniasis (ACL) Caused by *Leishmania tropica* in Sanliurfa Province, Turkey, Where ACL Is Highly Endemic. *Clinical and Vaccine Immunology*, 14(11), pp.1409-1415.

Zhioua, E., Kaabi, B. and Chelbi, I. (2007). Entomological investigations following the spread of visceral leishmaniasis in Tunisia. *Journal of Vector Ecology*, 32(2), pp.371-375.

## APPENDICES

**Appendix I:** Table showing the chitinases found in all *Leishmania* species. Data from UniProt

Entry	Entry name	Protein names	Gene names	Organism	Length
A4HWX6	A4HWX6_LEITN	Chitinase	<b>CHI-1</b> LINF_160013400, LINF_16_0790	<i>Leishmania infantum</i>	457
A0A088RM75	A0A088RM75_9TRYP	Chitinase	<b>CHI-1</b> LPMF_160760	<i>Leishmania panamensis</i>	458
A4H8K3	A4H8K3_LEI9R	Chitinase	LBRM_16_0800	<i>Leishmania braziliensis</i>	457
Q4QE00	Q4QE00_LEIMA	Chitinase	<b>CHI-1</b> LMJF_16_0790	<i>Leishmania major</i>	457
Q60994	Q60994_LEIDO	Chitinase	<b>Chi-1</b>	<i>Leishmania donovani</i>	457
Q5SEI6	Q5SEI6_LEIME	Chitinase	<b>CHI1</b>	<i>Leishmania mexicana</i>	457
A0A1E1UT6	A0A1E1UT6_LEIGU	Putative chitinase	<b>LgM4147LRVhigh.20.00911.00200</b> BN36_2025440	<i>Leishmania guyanensis</i>	458
E9AQN8	E9AQN8_LEIMU	Chitinase	LXXM_16_0790	<i>Leishmania mexicana</i> (strain MHOM/GT/2001/U1103)	457
E99CT2	E99CT2_LEID8	Chitinase	LDBPK_160790	<i>Leishmania donovani</i> (strain BPK282A1)	457
Q6R2L9	Q6R2L9_LEITN	Chitinase		<i>Leishmania infantum</i>	343
Q6R2L4	Q6R2L4_LEIDO	Chitinase		<i>Leishmania donovani</i>	343
Q6R2M9	Q6R2M9_LEIDO	Chitinase		<i>Leishmania donovani</i>	343
Q6R2N1	Q6R2N1_LEIDO	Chitinase		<i>Leishmania donovani</i>	343
Q6R2M0	Q6R2M0_LEITN	Chitinase		<i>Leishmania infantum</i>	343
Q6R2M1	Q6R2M1_LEITN	Chitinase		<i>Leishmania infantum</i>	343
Q6R2N2	Q6R2N2_LEIDO	Chitinase		<i>Leishmania donovani</i>	343
Q6R2N8	Q6R2N8_LEIDO	Chitinase		<i>Leishmania donovani</i>	343
Q6R2N7	Q6R2N7_LEIDO	Chitinase		<i>Leishmania donovani</i>	343
Q6R2L3	Q6R2L3_LEIAM	Chitinase		<i>Leishmania amazonensis</i>	343
Q6R2L2	Q6R2L2_LEITR	Chitinase		<i>Leishmania tropica</i>	343
Q6R2P4	Q6R2P4_LEIMA	Chitinase		<i>Leishmania major</i>	343
Q6R2P3	Q6R2P3_LEIMA	Chitinase		<i>Leishmania major</i>	343
Q6R2P0	Q6R2P0_LEITR	Chitinase		<i>Leishmania tropica</i>	343

**Appendix II**

Yasmine Precious Kumordzi

Null hypothesis- there is no significant difference between the two migrated populations (group 1 and group 2).

**Appendix II (a):**

*L. tarentolae* day 3 Urea (group 1) and *L. tarentolae* day 5 Urea (group 2) migration assay used for the Mann Whitney U-test.

For 5% two-tailed level, Critical value of U (from tables) is 15.

As calculated  $U < U$  critical, we reject the Null Hypothesis therefore the result is significant.

z critical (5%, two-tailed) is 1.959964.

p value is 0.000532.

**Appendix II (b):**

*L. mexicana* day 3 Glucose (group 1) and *L. mexicana* day 5 Glucose (group 2) migration assay used for the Mann Whitney U-test

For 5% two-tailed level, Critical value of U (from tables) is 20

As calculated  $U < U$  critical, we reject the Null Hypothesis therefore the result is significant.

z critical (5%, two-tailed) is 1.959964.

p value is 0.006233.

**Appendix III**

H<sub>0</sub>: The data shows an association between promastigote form and the chemical cue it is migrating towards.

H<sub>a</sub>: The data shows NO association between promastigote form and the chemical cue it is migrating towards.

The significance level is 0.05. A P-value measures the strength of evidence in support of a H<sub>0</sub>. If the P-value is less than the significant level, we reject the null hypothesis.

**Appendix III (a): *L. mexicana* chi-squared test on a contingency table with SPSS**

**Case Processing Summary**

	Cases					
	Valid		Missing		Total	
	N	Percent	N	Percent	N	Percent
Chemical cue * Promastigote form	330	100.0%	0	0.0%	330	100.0%

**Chemical cue ^ Promastigote form Crosstabulation**

			Promastigote form					Total
			L	M	N	P		
Chemical cue	Fructose	Count	4	42	1	9	14	70
		% within Chemical cue	5.7%	60.0%	1.4%	12.9%	20.0%	100.0%
		% within Promastigote form	10.8%	25.1%	14.3%	20.9%	18.4%	21.2%
	% of Total	1.2%	12.7%	0.3%	2.7%	4.2%	21.2%	
	Mannose	Count	16	49	0	8	28	101
		% within Chemical cue	15.8%	48.5%	0.0%	7.9%	27.7%	100.0%
		% within Promastigote form	43.2%	29.3%	0.0%	18.6%	36.8%	30.6%
	% of Total	4.8%	14.8%	0.0%	2.4%	8.5%	30.6%	
	PSG	Count	4	20	1	7	11	43
		% within Chemical cue	9.3%	46.5%	2.3%	16.3%	25.6%	100.0%
		% within Promastigote form	10.8%	12.0%	14.3%	16.3%	14.5%	13.0%
	% of Total	1.2%	6.1%	0.3%	2.1%	3.3%	13.0%	
Sucrose	Count	9	42	2	10	18	81	
	% within Chemical cue	11.1%	51.9%	2.5%	12.3%	22.2%	100.0%	
	% within Promastigote form	24.3%	25.1%	28.6%	23.3%	23.7%	24.5%	
% of Total	2.7%	12.7%	0.6%	3.0%	5.5%	24.5%		
Urea	Count	4	14	3	9	5	35	
	% within Chemical cue	11.4%	40.0%	8.6%	25.7%	14.3%	100.0%	
	% within Promastigote form	10.8%	8.4%	42.9%	20.9%	6.6%	10.6%	
% of Total	1.2%	4.2%	0.9%	2.7%	1.5%	10.6%		
Total	Count	37	167	7	43	76	330	
	% within Chemical cue	11.2%	50.6%	2.1%	13.0%	23.0%	100.0%	
	% within Promastigote form	100.0%	100.0%	100.0%	100.0%	100.0%	100.0%	
	% of Total	11.2%	50.6%	2.1%	13.0%	23.0%	100.0%	

**Chi-Square Tests**

	Value	df	Asymp. Sig. (2-sided)
Pearson Chi-Square	24.709 <sup>a</sup>	16	.075
Likelihood Ratio	23.546	16	.100
N of Valid Cases	330		

a. 8 cells (32.0%) have expected count less than 5. The minimum expected count is .74.

Due to over 20% having expected count less than 5, therefore the expectation has been violated. Therefore instead of using the Pearson Chi-Square, the likelihood ratio is to be used. Results show 23.546 statistic, 16 degrees of freedom (df) and the significance value of 0.1.  $0.1 > \text{Level of significance } 0.05$ , therefore accept the the null hypothesis that there is no association between the type of promastigote morphology and the specific chemical cue migrated towards.

**Directional Measures**

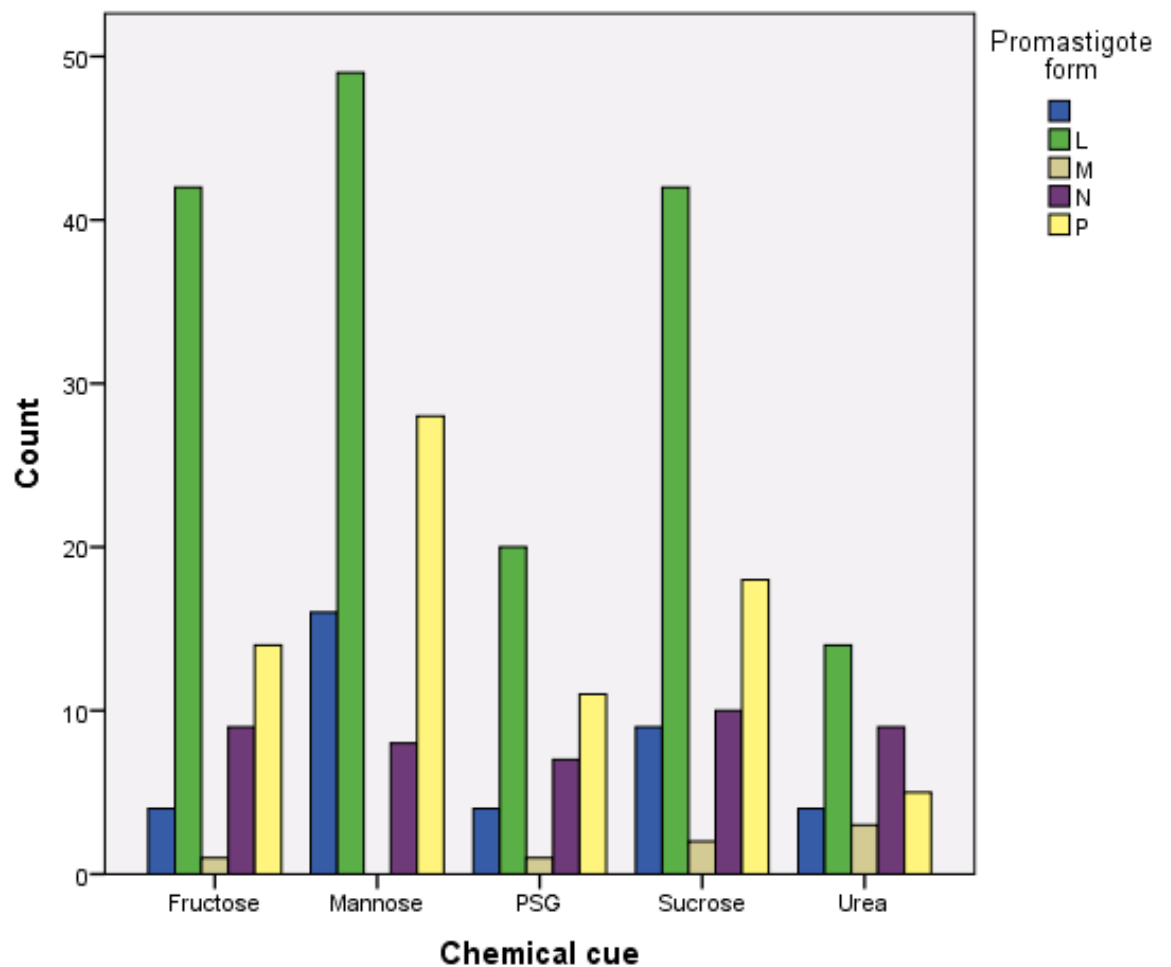
			Value	Asymp. Std. Error <sup>a</sup>	Approx. T <sup>b</sup>	Approx. Sig.
Nominal by Nominal	Lambda	Symmetric	.013	.012	1.093	.274
		Chemical cue Dependent	.022	.020	1.093	.274
		Promastigote form Dependent	.000	.000	. <sup>c</sup>	. <sup>c</sup>
	Goodman and Kruskal tau	Chemical cue Dependent	.017	.007		.113 <sup>d</sup>
		Promastigote form Dependent	.015	.008		.240 <sup>d</sup>

- a. Not assuming the null hypothesis.
- b. Using the asymptotic standard error assuming the null hypothesis.
- c. Cannot be computed because the asymptotic standard error equals zero.
- d. Based on chi-square approximation

**Symmetric Measures**

		Value	Approx. Sig.
Nominal by Nominal	Phi	.274	.075
	Cramer's V	.137	.075
N of Valid Cases		330	

**Bar Chart**



**Appendix III (b): *L. tarentolae* chi-squared test on a contingency table with SPSS**

**Case Processing Summary**

	Cases					
	Valid		Missing		Total	
	N	Percent	N	Percent	N	Percent
Chemical cue * Promastigote form	326	100.0%	0	0.0%	326	100.0%

**Chemical cue \* Promastigote form Crosstabulation**

			Promastigote form					Total
				L	M	N	P	
Chemical cue	Fructose	Count	6	16	0	25	0	47
		% within Chemical cue	12.8%	34.0%	0.0%	53.2%	0.0%	100.0%
		% within Promastigote form	9.5%	17.8%	0.0%	16.6%	0.0%	14.4%
		% of Total	1.8%	4.9%	0.0%	7.7%	0.0%	14.4%
	Mannose	Count	14	20	0	37	1	72
		% within Chemical cue	19.4%	27.8%	0.0%	51.4%	1.4%	100.0%
		% within Promastigote form	22.2%	22.2%	0.0%	24.5%	5.0%	22.1%
		% of Total	4.3%	6.1%	0.0%	11.3%	0.3%	22.1%
	PSG	Count	20	15	0	25	3	63
		% within Chemical cue	31.7%	23.8%	0.0%	39.7%	4.8%	100.0%
		% within Promastigote form	31.7%	16.7%	0.0%	16.6%	15.0%	19.3%
		% of Total	6.1%	4.6%	0.0%	7.7%	0.9%	19.3%
Sucrose	Count	20	21	2	46	14	103	
	% within Chemical cue	19.4%	20.4%	1.9%	44.7%	13.6%	100.0%	
	% within Promastigote form	31.7%	23.3%	100.0%	30.5%	70.0%	31.6%	
	% of Total	6.1%	6.4%	0.6%	14.1%	4.3%	31.6%	
Urea	Count	3	18	0	18	2	41	
	% within Chemical cue	7.3%	43.9%	0.0%	43.9%	4.9%	100.0%	
	% within Promastigote form	4.8%	20.0%	0.0%	11.9%	10.0%	12.6%	
	% of Total	0.9%	5.5%	0.0%	5.5%	0.6%	12.6%	
Total	Count	63	90	2	151	20	326	
	% within Chemical cue	19.3%	27.6%	0.6%	46.3%	6.1%	100.0%	
	% within Promastigote form	100.0%	100.0%	100.0%	100.0%	100.0%	100.0%	
	% of Total	19.3%	27.6%	0.6%	46.3%	6.1%	100.0%	

**Chi-Square Tests**

	Value	df	Asymp. Sig. (2-sided)
Pearson Chi-Square	37.142 <sup>a</sup>	16	.002
Likelihood Ratio	38.956	16	.001
N of Valid Cases	326		

a. 9 cells (36.0%) have expected count less than 5. The minimum expected count is .25.

Due to over 20% having expected count less than 5, therefore the expectation has been violated. Therefore instead of using the Pearson Chi-Square, the likelihood ratio is to be used. Results show 38.956 statistic, 16 degrees of freedom (df) and the significance value of 0.001.  $0.1 > \text{Level of significance } 0.05$ , therefore reject the null hypothesis that there is no association between the type of promastigote morphology and the specific chemical cue migrated towards.

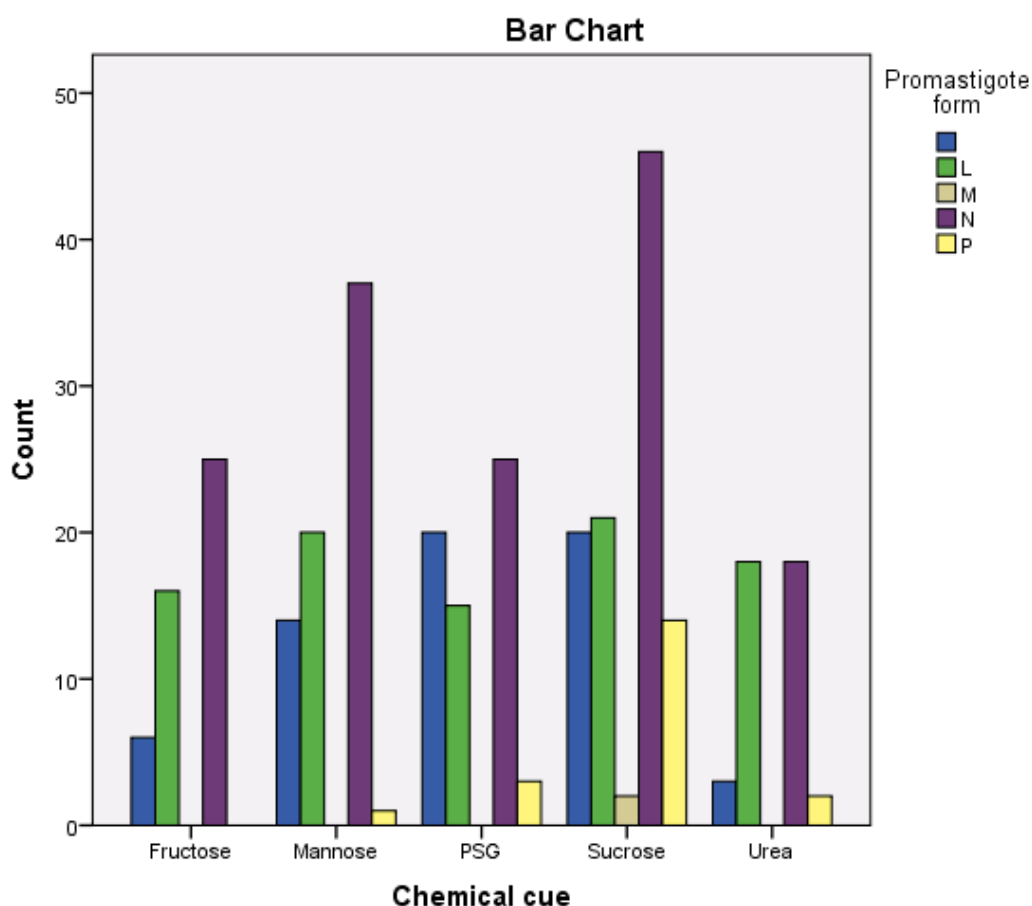
**Directional Measures**

			Value	Asymp. Std. Error <sup>a</sup>	Approx. T <sup>b</sup>	Approx. Sig.
Nominal by Nominal	Lambda	Symmetric	.000	.022	.000	1.000
		Chemical cue Dependent	.000	.028	.000	1.000
		Promastigote form Dependent	.000	.034	.000	1.000
	Goodman and Kruskal tau	Chemical cue Dependent	.033	.009		.000 <sup>c</sup>
		Promastigote form Dependent	.025	.010		.010 <sup>c</sup>

- a. Not assuming the null hypothesis.
- b. Using the asymptotic standard error assuming the null hypothesis.
- c. Based on chi-square approximation

**Symmetric Measures**

		Value	Approx. Sig.
Nominal by Nominal	Phi	.338	.002
	Cramer's V	.169	.002
N of Valid Cases		326	



**Appendix IV: Raw data used for growth curve, promastigote migration, morphological classification and SPSS in CD labelled (MRES RAW RESULTS CD)**